Characterisation of Kaposi's sarcoma-associated herpesvirus (KSHV)-driven pathology and disease outcome in HIV-infected South African patients

Melissa Blumenthal

Thesis presented for the degree of

Doctor of Philosophy

In the Division of

Medical Biochemistry and Structural Biology

Department of Integrative Biomedical Sciences

University of Cape Town

February 2020

Declaration

I, Melissa Jayne Walcott Blumenthal, hereby declare that the work on which this thesis is based is my original work (except where acknowledgements indicate otherwise) and that neither the whole work nor any part of it has been, is being, or is to be submitted for another degree in this or any other university. My MSc thesis, submitted to the University of Cape Town in 2016, is preliminary work relative to the current work and has been included in this thesis and described as such. I am presenting this thesis for academic examination toward the Degree of Doctor of Philosophy in Medical Biochemistry.

I empower the university to reproduce for the purpose of research either the whole or any portion of the contents in any manner whatsoever.

Signed Signed by candidate Date: 09/02/2020

Acknowledgements

My supervisor and mentor, Dr Georgia Schäfer, was instrumental in the successful completion of this thesis. I am very fortunate to have had her consistent encouragement and support through the PhD process. Georgia has offered me a wonderful balance of independence and nurturing in which to develop as a research scientist. Thank you for your genuine interest, insights and exceptionally fast editing!

Thank you to my co-supervisor, Prof Arieh Katz, for his valuable insights and input into my work and his support of my growth as a scientist. I have gained a lot from Prof Katz' experience and greatly appreciate his direction both for my work and career development.

Thank you to the members of the Katz/ Schäfer laboratory for feedback during lab meetings and for the friendly and pleasant atmosphere of our shared space. I would like to acknowledge our technical staff, Graham Christians, Dr Roshan Ebrahim and Xolani Nonzinyana, for their roles in the smooth running of our laboratory. Thank you to Jennifer Baltazaar for kindly and efficiently assisting me by running PCRs.

Part of this work was completed while in the laboratory of Prof Dr Thomas Schulz at the Hannover Medical School, Germany. I am extremely grateful to Prof Schulz for hosting me and for his invaluable guidance and support of the work. Prof Schulz generously provided materials during my research visit and gifted us the materials necessary to set up a number of KSHV assays in our laboratory at UCT that were not previously available in South Africa.

Thank you to Dr Bizunesh Abere for being my laboratory supervisor at Hannover Medical School. At an extremely stressful time in her PhD, she still had patience and time to assist me and I learnt a great deal from her. Thank you to the other members of the Schulz lab, who were very helpful and welcoming.

Thank you to Prof Graeme Meintjes for his collaboration which enabled many aspects of this work and the Khayelitsha Day Hospital Tuberculosis Study staff. Dr Charlotte Schutz deserves special mention not only for her involvement in the recruitment of patients included in this study but also for organising and providing patient data, her assistance in conceptualising, interpreting and analysing data and the study as a whole, all while being an incredibly approachable and lovely person in spite of having a very full plate herself. Thank you to Dr David Barr for advice and assistance with statistical analysis, and Dr Muki Shey for assisting me with the IL-6 ELISA assay setup. Thank you to Dr Michael Locketz, National Health Laboratory Services, for performing the histopathological assessment.

Acknowledgement and thanks to Dr Zainab Mohamed for her contribution to the framing and logistics of this study. Thank you to the staff at the Radiation Oncology Unit, Groote Schuur Hospital for their help with KS patient recruitment which formed the foundation of this work.

I would like to acknowledge Dr Denise Whitby, Vicki Marshall and Wendell Miley for generously sharing the materials and expertise necessary for us to set up KSHV ELISA and KSHV VL assays in our laboratory. Thanks especially to Dr Whitby and Dr Elena Cornejo Castro for their warm encouragement at meetings and helpful critique of our work.

We thank Dr Janina Bruening for engineering the CRISPR/Cas9 vectors and for the kind gift thereof as well as her advice and guidance.

I am grateful to Dr Thomas Uldrick for his assistance in conceptualising and framing our work and for supporting its future development. Dr Uldrick's vision and dedication have been a source of inspiration for me.

Thanks to Dr Alexander Hahn for his interest in our work and unreserved advice which has been extremely appreciated.

This study would not have been possible without the patients who agreed to participate. I would like to acknowledge them not only for their vital contribution to research but also for allowing me the connection between research and the clinic.

We are grateful for the gifts of the RRL.SF.newMCS.i2.Zeo.pre vector from Dr Melanie Galla, Prof Dr Christopher Baum and Prof Dr Axel Schambach, Institute of Experimental Haematology, Hannover Medical School, Germany; the SLK, SLK-KO, LEC and LEC-KO cell lines from Dr Frank Neipel, Institute of Clinical and Molecular Virology, University Clinic, Erlangen; HEK293T, BJAB-rKSHV.219 and HuARTL2 cell lines from Prof Dr Thomas Schulz; the CRISPR/Cas9 vector from Dr Klaus Heger and Dr Marc Supprian, Molecular Immunology and Signal transduction, Max Planck Institute of Biochemistry, Germany; the Lentiviral packaging vectors pCMV-VSV-G and pCMVR8.74 and engineered Scr.pLentiCRISPR v2, G1.pLentiCRISPR v2, G2.pLentiCRISPR v2 and G3.pLentiCRISPR v2 from Dr Janina Bruening and Prof Dr Thomas Pietschmann, Twincore, Hannover Medical School, Germany.

I would like to thank my partner, Vincent Naude, who lived through every day of my PhD with me. Thank you for being there through the highs and lows of this journey and for inspiring me with your passion for your own work. I wouldn't want to be here if you weren't by my side. Thank you to my family: my parents Jenny and Phillip Blumenthal, my sisters Amy Browne and Jessica Blumenthal, my brothers-in-law Mike Browne and Jon Minster, my nephews Elliot and Francis Minster and Ben and Harry Browne and my parents-in-law Su and Edgar Naude for making my life so full and being

continually supportive and interested through the many, many years of postgraduate studies that Vincent and I have slogged through. Thank you to Doris Kana for looking after us with so much heart. Thank you to my Drew, Pan and Indie for bringing me joy.

Finally, the financial assistance of the National Research Foundation (NRF) towards this research is hereby acknowledged. Opinions expressed and conclusions arrived at, are those of the author and are not necessarily to be attributed to the NRF. Additionally, I hereby acknowledge the University of Cape Town, the David and Elaine Potter Foundation, the Ernst and Ethel Erickson Trust, the Struwig-Germeshuysen Kankernavorsingstrust and the Poliomyelitis Research Foundation (PRF) for financial assistance. Furthermore, this work was funded by the Cancer Association of South Africa (CANSA), the NRF and the PRF.

Table of contents

List of figures and tables

Abbreviations

All abbreviated terms are written out in text when first mentioned followed by the abbreviation in parentheses and those used more than once are listed here.

AA	amino acid
AIDS	acquired immunodeficiency syndrome
AR	androgen receptor
ART	antiretroviral therapy
ATP	adenosine triphosphate
BCA	bicinchoninic acid assay
bp	base pair
CD	cluster of differentiation
CI	confidence interval
CRP	C-reactive protein
DC-SIGN	dendritic cell-specific intercellular adhesion molecule-3-grabbing non-integrin
DMEM	Dulbecco's Modified Eagle Medium
DMSO	dimethyl sulfoxide
DNA	deoxyribonucleic acid
EBV	Epstein-Barr virus
EGF-like	epithelial growth factor-like
ELISA	enzyme-linked immunosorbent assay
Eph	erythropoietin-producing hepatocellular carcinoma
EPHA2	Eph receptor A2
Eph-lbd	ephrin ligand binding domain
ephrin	Eph receptor-interacting protein
ERK	extracellular signal-regulated kinase
EV	empty vector
FBS	foetal bovine serum
FcγR	Fc-gamma receptor
Fn-3	fibronectin type-3
GFP	green fluorescent protein
gRNA	guide RNA

GSH	Groote Schuur Hospital
h	hour
HAART	highly active anti-retroviral therapy
HBS	HEPES buffered saline
HEK293	human embryonic kidney 293
HIV	human immunodeficiency virus
HLA	human leukocyte antigen
HPV	human papillomavirus
HREC	Human Research Ethics Committee
HSPG	heparan sulphate proteoglycans
HUVEC	human umbilical vein endothelial cells
IARC	International Agency for Research on Cancer
IgG	immunoglobulin G
IL-6	interleukin-6
IUPAC	International Union of Pure and Applied Chemistry
kb	kilobases
KDHTB	Khayelitsha Day Hospital TB study
KICS	KSHV-inflammatory cytokine syndrome
KIR	killer cell immunoglobulin-like receptor
KS	Kaposi's sarcoma
KSHV	Kaposi's sarcoma-associated herpesvirus
LAM	lipoarabinomannan
LANA	latency-associated nuclear antigen
LB	Luria Bertani
LEC	lymphatic endothelial cells
LMWPTP	low molecular weight protein tyrosine phosphatase
MAF	minor allele frequency
MAPK	mitogen-activated protein kinase
MBL	mannose-binding lectin
MCD	multicentric Castleman disease
MFI	median fluorescence intensity
min	minute

MOI	multiplicity of infection
miRNA	microRNA
mRNA	messenger RNA
MSM	malignant pleural mesothelioma
MTB	*Mycobacterium tuberculosis*
mTOR	mammalian target of rapamycin
MTT	Thiazolyl Blue Tetrazolium Bromide
NCBI	National Center for Biotechnology Information
NFκB	nuclear factor kappa B
NFκBIA	NFκB1 inhibitor alpha
NHLS	National Health Laboratory Service
NIH	National Institute of Health
NK	natural killer
nm	nanometre
NSCLC	non-small cell lung cancer
OD	optical density
ORF	open reading frame
PBMC	peripheral blood mononuclear cells
PBS	phosphate-buffered saline
PCR	polymerase chain reaction
PDB	Protein Data Bank
PEL	primary effusion lymphoma
PI3K	phosphoinositide 3-kinase
Pkinase-Tyr	protein tyrosine kinase
RFP	red fluorescent protein
RIF	rifampicin
rpm	revolutions per minute
rs	reference SNP
RSK	p90 ribosomal S6 kinase 1
RTA	replication and transcription activator
RTK	receptor tyrosine kinase
s	seconds

SAM	sterile alpha motif
SCC	squamous cell carcinoma
SDM	site directed mutagenesis
SDS	sodium dodecyl sulphate
sEPHA2	synthetic EPHA2
SH	Src homology
SNP	single nucleotide polymorphism
SNV	single nucleotide variant
SSA	Sub-Saharan Africa
STAT	signal transducer and activator of transcription
SV40	simian virus 40
TAg	large T antigen
Tat	trans-activator of transcription
TB	tuberculosis
Tm-1	transmembrane domain
UCT	University of Cape Town
USA	United States of America
UTR	untranslated region
UV	ultraviolet
vCCL	viral-encoded C-C chemokine ligands
vCyclin	viral-encoded cyclin
VEGF	vascular endothelial growth factor
vFLIP	viral-encoded FLICE-inhibitory protein
vGPCR	viral-encoded G protein-coupled receptor
vIL-6	viral-encoded interleukin-6
vIRF	viral-encoded interferon response factors
VL	viral load
WHO	World Health Organisation
WT	wild type

Abstract

Kaposi's sarcoma-associated herpesvirus (KSHV), a gamma-herpesvirus with a particularly high seroprevalence in Sub-Saharan Africa (SSA), is the etiological agent of the endothelial tumour Kaposi's sarcoma (KS), the most common acquired immunodeficiency syndrome (AIDS)-related malignancy worldwide and particularly in SSA. It also causes primary effusion lymphoma (PEL), multicentric Castleman disease (MCD) and KSHV inflammatory cytokine syndrome (KICS). AIDS-related deaths have declined, due to global scale-up of antiretroviral therapy (ART). However, the vast majority of these occurred in SSA, where tuberculosis (TB) is the leading cause of mortality among human immunodeficiency virus (HIV)-infected individuals, accounting for a third of all AIDS-related deaths. The exceptionally high burden of suspected TB in SSA causes misdiagnosis or delayed diagnosis of diseases mimicking TB, such as several pathologies associated with KSHV. KSHV infection is essential but insufficient for the development of KS and other KSHV-associated pathologies; precipitating factors, such as HIV-related immune suppression and potentially genetic predisposition, are required. The erythropoietin-producing hepatocellular carcinoma (Eph) receptor A2 protein (EPHA2) tyrosine kinase receptor is a promising candidate for studies on genetic variants as it potentially acts on two levels: susceptibility to KSHV infection (being one of the key receptors utilised by KSHV for cell entry and intracellular trafficking) and susceptibility to KS development (being implicated in oncogenesis).

Despite the high seroprevalence in SSA, the contribution of dysregulated KSHV lytic replication or host KSHV receptor variations to disease outcome in HIV-infected patients is unknown. We hypothesised that KSHV lytic reactivation plays yet unrecognised roles for morbidity and mortality in high HIV settings and to this end, we conducted a cohort study of 682 HIV-positive critically ill patients admitted to Khayelitsha Day Hospital, South Africa, investigated for TB, and followed for 12-weeks to ascertain vital status. We demonstrated that elevated blood KSHV viral load (VL) was a strong predictor of death in hospitalised HIV-infected patients without microbiologically proven TB. Further, we identified and validated variants in the EPHA2 protein tyrosine kinase and sterile alpha motif domains that were significantly associated with susceptibility to infection, KS development and/or KSHV VL in 300 South African HIV-infected patients, by aggregate by-gene analysis. In order to elucidate the functional significance of the identified EPHA2 missense mutations, we knocked out endogenous EPHA2 by CRISPR/Cas9 in the human endothelial cell line, HuARLT2, and reintroduced the wild type and mutant EPHA2 open reading frames by lentiviral transduction. These engineered cells were assessed for baseline EPHA2 phosphorylation levels and susceptibility to KSHV infection utilising recombinant KSHV in binding, internalisation and infection assays. We found that the EPHA2 mutant c.2254T>C (p.Leu700Pro) in the tyrosine kinase domain, associated with KS in our patient

cohort, was deficient in tyrosine phosphorylation and less permissive to rKSHV infection when introduced as a single mutation or as a double mutant together with c.2257A>C (p.Asp701Ala) which was found to be in linkage disequilibrium with it. Another tyrosine kinase domain variant, c.2688G>S (p.Ala845Pro), found to be overrepresented among KS patients, had enhanced baseline tyrosine phosphorylation levels. These findings validated the patient-derived data on the molecular level by assigning functional consequences to some mutants which might have implications for the development of future biomarkers predicting KS susceptibility in high-risk populations.

In summary, this novel research contributes to the understanding of KSHV-associated pathology and disease outcome. It identified KSHV VL as a potential biomarker to predict KSHV-associated diseases and mortality and assessed the contribution of KSHV entry receptor EPHA2 variations to KSHV-associated pathologies, with potential clinical implications, by facilitating the development of novel diagnostic and surveillance tools.

1. Introduction

Kaposi's sarcoma-associated herpesvirus (KSHV, or human herpesvirus-8) is a gamma-herpesvirus with a particularly high seroprevalence (30–50%) in Sub-Saharan Africa (SSA). It is the etiological agent of the most common acquired immunodeficiency syndrome (AIDS)-related malignancy, Kaposi's sarcoma (KS) [1], as well as the rare (although most certainly under-reported [2]) primary effusion lymphoma (PEL), multicentric Castleman disease (MCD) and KSHV inflammatory cytokine syndrome (KICS) which all primarily occur in human immunodeficiency virus (HIV)-infected patients (see 1.3) [3–8]. Exposure to and infection with KSHV is thought to occur early in life via saliva [9], whereupon the virus establishes long-term persistent infection which can, particularly in the context of HIV co-infection, lead to the development of KSHV-associated pathologies (see 1.2.3 and 1.2.4) [10].

The increasing number of HIV-infected individuals on long-term antiretroviral therapy (ART) has led to a global shift in the proportion of deaths from AIDS-defining malignancies, such as KS, and communicable conditions, such as tuberculosis (TB), towards chronic non-communicable conditions, such as cardiomyopathy (see 1.1.1) [11,12]. Yet, in SSA, TB is still the leading cause of mortality among HIV co-infected individuals, claiming more than a third of all AIDS-related deaths [13]. Unsurprisingly, the high number of patients presenting with suspected TB in South Africa has led to overdiagnosis and overtreatment, and associated delay in diagnosis of cancers such as lymphoma and lung cancer given their clinical similarities to TB (see 1.1.2) [14–17]. These include nonspecific symptoms such as lymphadenopathy, fever, weight loss, chest pain and night sweats [15].

KSHV-associated diseases may also mimic TB symptoms. While primary infection among immunocompetent individuals is often asymptomatic, the development of KSHV-related malignancies is generally associated with immunosuppression [1]. KS often presents as cutaneous disease, with KSHV-infected endothelial cells as the predominant cell type [18], but advanced visceral disease with limited or no cutaneous involvement may occur (see 1.3.1) [19]. Both PEL and MCD are lymphoproliferative disorders caused by KSHV-infected B-cells (see 1.3.2 and 1.3.3) [18]. The cell type implicated in KICS is unknown and the syndrome presents with nonspecific and severe inflammatory symptoms characterised by high KSHV viral load (VL) and host and viral interleukin-6 (IL-6) (see 1.3.4) [20]. KSHV can exhibit latent and lytic infection phases which are characterised by distinct viral gene expression patterns in both cell types (see 1.2.3) [21,22]. In KS and PEL, KSHV predominantly expresses a limited number of latent phase genes [18,23,24], and KS patients generally do not have elevated KSHV VL in the blood [8,25]. In contrast, lytically active KSHV in MCD and KICS leads to a broader range of viral gene expression [23] that contributes to pathogenesis [5,8]. Indeed, KSHV VL is significantly higher in MCD and KICS compared to KS patients (see 1.4) [8,25], and both MCD and KICS are

characterised by an overproduction of host IL-6, KSHV-encoded viral IL-6 (vIL-6) and other cytokines, giving rise to severe inflammatory symptoms such as fever, wasting, hypoalbuminemia, cytopenia, hyponatremia and elevated C-reactive protein (CRP) [7,8].

Untreated MCD and KICS have high mortality [6–8,26], and a working case definition of KICS has been proposed that may serve as a surveillance tool for individuals with HIV/KSHV co-infection [6]. While KICS is a proposed clinical diagnosis requiring exclusion of MCD [6] and other serious intercurrent infections [6,8], MCD is diagnosed by histologic confirmation of KSHV-positive staining of plasmablastic cells in the mantle zone of lymph nodes (see 1.3.3.3) [27]. It has been proposed that KICS contributes to the inflammatory symptoms seen in some patients with severe KS or PEL [6]. KICS in the absence of a KSHV-associated malignancy has also been reported [6,8]. Rituximab is a highly effective therapy for MCD, while management of KICS is primarily directed at treating associated malignancies (see 1.3). More research on dysregulated KSHV lytic reactivation is urgently needed in order to better understand these conditions and to identify additional treatments to improve outcomes [2].

Although HIV-related immune suppression is important for the development of KSHV-associated pathologies, not all co-infected individuals develop a disease pointing to a potential underlying genetic predisposition which has been particularly discussed in the context of KS development (see 1.5) [28–30]. While studies have primarily focused on association with immune-modulatory genes [31–33], we recently identified variants in the erythropoietin-producing hepatocellular carcinoma (Eph) receptor A2 protein (EPHA2) receptor tyrosine kinase (RTK) that were associated with KSHV infection and KS development, respectively, in HIV-infected South Africans (see 1.6.6) [34,35]. EPHA2 is a major receptor for KSHV entry and intracellular trafficking (see 1.6.4) [36]. Moreover, EPHA2 signalling plays a role in oncogenesis (see 1.6.3) [36–38], thus potentially acting at the level of both susceptibility to KSHV infection and susceptibility to KS development. Research into altered host factors modulating KSHV infection is still in its infancy, and EPHA2 may be a potential novel biomarker to predict the development of KSHV-associated diseases.

While KS has been well established as an independent risk factor for death in HIV-infected people, a broader range of KSHV-associated diseases with lytic syndromes, particularly in the context of a high-burden HIV/TB setting, may play a yet unrecognised role in HIV-associated morbidity and mortality in SSA. It is therefore important that KSHV research continues, both due to the overlapping clinical features of KSHV-associated diseases with TB as well as their persistent occurrence in the era of ART. Correct diagnosis and identification of patients at risk for development and/or progression of KSHV-associated diseases is critical in order to identify key populations, to provide effective

preventative and therapeutic interventions and to predict the development of clinical disease. Furthermore, it is imperative to identify and evaluate biomarkers for KSHV-associated diseases, in order to accelerate the development of relevant tools for this most at-risk population.

1.1. The HIV epidemic in the age of ART

The burden of the HIV epidemic falls disproportionately on SSA where 63.5% of global new infections occurred in 2018. The World Health Organisation (WHO) estimates that 37.9 million (32.7 million–44.0 million) people are HIV-positive, 15% more than the 33 million estimated a decade ago [39,40]. However, the number of HIV-infected people progressing to AIDS, the most advanced stage of HIV infection defined by the appearance of AIDS-defining diseases (such as toxoplasmosis of the brain, candidiasis of the oesophagus and KS) or a cluster of differentiation (CD)4-positive T-cell count less than 200 cells/µl, has concomitantly decreased [40,41]. This represents the lives saved due to the introduction of ART, and particularly highly active antiretroviral therapy (HAART) [41], which has drastically reduced AIDS-related mortality and shifted HIV from a terminal to a chronic disease [42]. However, the improved HIV survival rate has resulted in increased prevalence of HIV-associated malignancies, other non-communicable diseases and co-infections, again particularly burdening SSA [43–46].

HIV-associated malignancies include the AIDS-defining cancers, KS, non-Hodgkin lymphoma and cervical cancer, caused by KSHV, Epstein-Barr virus (EBV) and human papillomaviruses (HPV), respectively. Other cancers caused by oncogenic infectious agents have additionally increased in prevalence, such as Hodgkin's lymphoma caused by EBV, anogenital, oral and oropharyngeal cancers caused by HPV, hepatitis B virus and hepatitis C virus-related liver cancer and stomach cancer caused by *Helicobacter pylori* infection, in developed countries [43] however this increased risk is less clearly established in studies from Southern Africa [46,47]. HIV co-infection with the mentioned infectious agents likely enhances the risk of cancer as immune suppression is a promoting factor for oncogenesis. Therefore, cancers caused by infectious agents have become an important public health concern in the ART era as a complication of chronic HIV infection [10,43,47–49].

HIV infection, as well as ART, are known to exacerbate a number of non-communicable diseases such as cardiovascular and pulmonary diseases and diabetes in the context of certain lifestyle factors linked to urbanisation and ageing [50,51]. Cardiomyopathy (prevalence of 5–29%) and hypertension (prevalence of 11–28%) are highlighted as the most important cardiovascular diseases in the SSA HIV-positive population in the ART era, although limited data and diagnostic capabilities

have hindered thorough epidemiological assessment of other cardiovascular and pulmonary diseases such as coronary artery disease, stroke, obstructive lung disease and pulmonary arterial hypertension, all of which are proposed to have an increased risk in HIV-positive populations [51]. HIV-positive patients have increased likelihood of dysglycaemia, especially those on efavirenz and protease inhibitors [52,53], and it has been postulated that type 2 diabetes in the context of HIV infection may further increase the risk for the development of pathogen-associated malignancies [12].

The introduction of ART has led to a reduction of risk for all HIV-related opportunistic infections, the key reason for the worldwide decline in HIV-related deaths, but pulmonary and extrapulmonary TB, cryptococcal meningitis and oral candidiasis remain the most common HIV-related opportunistic infectious diseases in SSA in the ART era [54].

1.1.1. Mortality in the context of HIV

Most recent data from The Joint United Nations Programme on HIV and AIDS (UNAIDS) indicates that while AIDS-related deaths have declined from an estimated 1.7 million (1.3 million–2.4 million) in 2004 to 770,000 (570,000–1.1 million) in 2018, due to global scale-up of ART, the vast majority of these (61%) occurred in SSA [40]. In the ART era, TB is still the leading cause of mortality among HIV co-infected individuals, claiming more than a third of all AIDS-related deaths [13,40]. HIV-associated TB case fatality rates in hospitalised patients in high-burden settings are between 11–32% [55–61]. However, diagnosis of HIV-related TB, particularly disseminated TB, remains a challenge despite improved diagnostic assays such as urine Xpert *Mycobacterium tuberculosis* (MTB)/rifampicin (RIF) and urine lipoarabinomannan (LAM) assays [60,61] and approximately 18–25% of patients treated for TB have microbiologically unconfirmed diagnoses (see 1.1.2) [57,62].

1.1.2. Misdiagnosis of TB

In 2017, 10 million people were diagnosed with active TB while about 23% of the global population (1.7 billion) is estimated to have latent TB and 5–10% of those latently infected will develop active TB at some point in their lives. In the context of HIV infection, people living with latent TB are up to 20-times more likely to fall ill [63]. About one-third of the 37.9 million HIV-positive people worldwide are co-infected with TB, the major burden of this falling on SSA: in 2018, the incidence of HIV-positive TB in Africa was 615,000 cases, accounting for 71% of HIV-positive TB incidence globally [64]. Unsurprisingly, the high number of patients presenting with suspected TB and the difficulty of TB

diagnosis has led to overdiagnosis and overtreatment, and associated delay in diagnosis of cancers such as lymphoma and lung cancer given their clinical similarities to TB [14–17]. These include nonspecific symptoms such as lymphadenopathy, fever, weight loss, chest pain and night sweats [15]. Studies conducted in HIV-burdened countries (South Africa, Malawi and Uganda) on misdiagnosis of lymphoma as TB indicate that mean delay in correct diagnosis while on TB treatment is 3.5–5 months [14,15,17] and a significant proportion of patients die without a confirmed diagnosis [55].

1.2. KSHV

1.2.1. Epidemiology

KSHV prevalence varies geographically with the highest prevalence in general adult populations in SSA (seroprevalence 30–50%) and the Mediterranean region (20–30%) and low prevalence in Western and Northern Europe, Asia and North and South America (5–10%) [65–67]. Higher prevalence has been noted in people who have certain behavioural risk factors, such as men who have sex with men (20–40%) in the United States of America (USA) and Northern Europe [68,69], or people of specific ethnicities regardless of HIV infection, such as Uganda (14–86%) and the Ivory Coast (43–100%) where there is risk for endemic KS, and the Mediterranean region (20–30%), at risk for classic KS (see 1.3.1.1) [67,70]. In HIV-infected people in the USA on ART, prevalence was 38% [71].

KSHV prevalence in South Africa has been investigated in only a few epidemiological studies. Sitas *et al*. [72] reported KSHV seroprevalence of 32% among black patients with cancers other than KS and similarly high levels among black blood donors but not white blood donors (5%) in Soweto and Johannesburg. Similarly, another study reported 35% KSHV seroprevalence among a rural black population in Kwa-Zulu Natal province in which adult medical ward patients were found to have extremely elevated KSHV seroprevalence (58%) [73]. Both studies found that KSHV seroprevalence increased with age with as high as a two-fold increase in seroprevalence in the >65 age group compared to the 15–24 age group but did not differ between sexes [72,73].

Of particular public health concern in South Africa are these elevated levels of KSHV together with high HIV prevalence which ranges from 13% in the Western Cape province to 27% in KwaZulu-Natal province [74]. A cross-sectional study in HIV-infected patients initiating ART in Johannesburg reported an even higher incidence (42%) [75]. Our previous study found KSHV seroprevalence among KS-negative HIV-positive patients to be 32% (95% confidence interval (CI): 28–35%) [62].

1.2.2. Structure and classification of KSHV

KSHV is a γ2 herpesvirus of the genus *Rhadinovirus* [76]. KSHV virions, with an average diameter of 100 nm, consist of a double-stranded deoxyribose nucleic acid (DNA) genome encased in a capsid, a tegument and a glycoprotein containing lipid envelope (Figure 1A), resembling the structure of other herpesviruses like EBV [10,77–79]. The KSHV envelope contains unique glycoproteins K8.1A, ORF4, ORF45 and ORF68 in addition to herpesvirus conserved gB, gH, gL, gM and gN [80–83]. In particular, K8.1, gB and a gH-gL complex play essential roles in KSHV entry (see 1.2.3.2) [84–87]. The approximately 140 kb DNA genome encodes 87 open reading frames (ORF), the majority of which are common to herpesviruses while 20 so-called 'K genes' are unique. KSHV encodes at least 14 cellular orthologues pirated from human genes, characteristic of rhadinoviruses, and 17 viral microRNAs (miRNAs) [67,85]. The KSHV episome contains a latency-associated region encoding transcripts that characterise the KSHV latent cycles, while lytic transcripts are encoded on the remainder of the episome (see 1.2.3 and Figure 1B) [67]. A number of latency-associated genes are oncogenes, such as latency-associated nuclear antigen (LANA), viral-encoded Cyclin (vCyclin) and viral FADD-like interleukin-1-converting enzyme (FLICE) inhibitory protein (vFLIP) (see 1.2.4) [67].

Based on variability in the KSHV K1 gene sequence, KSHV has been classified into 7 major subtypes: A, B, C, D, E, F and Z [88]. The different subtypes have been shown to have variable penetrance in various population groups and are distributed along broad geographic and ethnic lines, and it has been proposed that different genotypes may have different pathogenic and tumorigenic properties [89]. Subtypes B and A5 have been suggested to predominate in SSA [88,90,91] while subtypes F and E are found particularly in Uganda and Brazil, respectively. Subtypes A, C and D are found more broadly in the Americas and Northern Europe, the USA and Eurasia and Asia, respectively [89,92,93].

1.2.3. KSHV lifecycle

1.2.3.1. Transmission

KSHV transmission primarily occurs via infection-capable virions shed in saliva with the major routes of infection thought to be from mother to child [9,94–96]. KSHV isolated from throat wash samples is capable of productively infecting oral epithelial cells *in vitro,* likely representing initial infection following exposure [97]. Other body fluids may also contain detectable KSHV, such as blood, breast milk and semen, and KSHV can be transmitted via transfusion or transplant or by sexual contact [97–103].

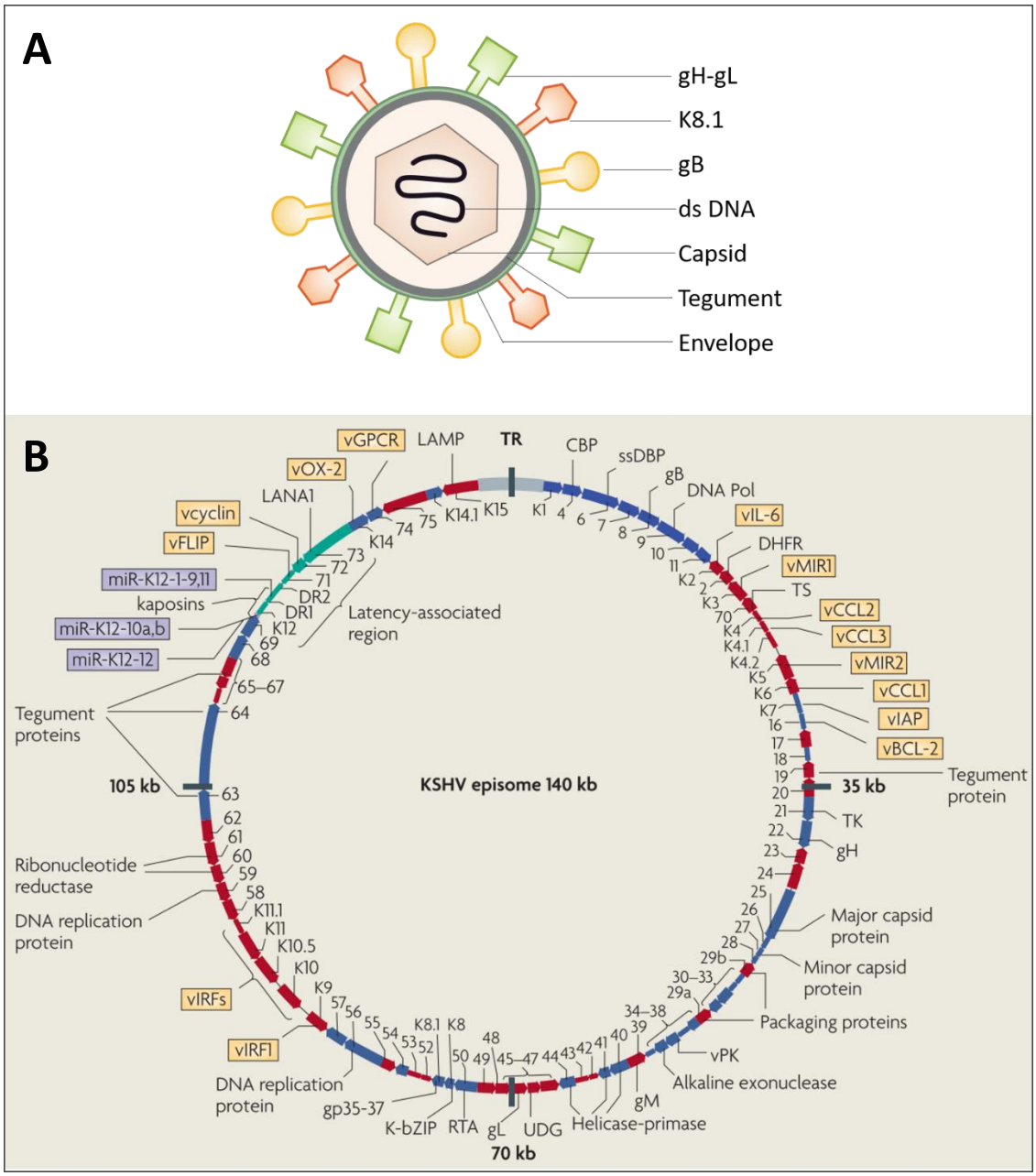

Figure 1: KSHV structure. A) The KSHV virion consists of its linear, double stranded DNA genome, encapsulated by a capsid, tegument and lipid envelope. Glycoproteins are embedded in the envelope and those essential for KSHV entry are depicted here. **B)** In the host nucleus following KSHV infection, the KSHV genome occurs as an episome as depicted. Latent genes are indicated in green, early lytic genes in red, late lytic genes in blue, miRNAs in purple and cellular orthologues in yellow. Figure adapted from [67,132].

1.2.3.2. KSHV entry

KSHV entry is schematically represented in Figure 2. Initially, envelope glycoproteins gB, K8.1A and gH-gL interact with heparan sulphate proteoglycans (HSPG) which occur ubiquitously on the target cell surface [10,86,87,104,105]. This initial attachment facilitates concentration of the virus on the cell surface and is thought to occur in a redundant manner as HSPGs are not essential but do enhance viral entry [105].

Subsequently, KSHV binds to various cellular entry receptors dependent on the target cell type which allows KSHV its wide host cell tropism. There is evidence that KSHV-HSPG binding triggers formation of a lipid raft in the host cell membrane consisting of the cell-dependent combination of entry receptors, including HSPG, various integrins and receptors and the glutamate/cysteine exchange transporter xCT [10,106,107]. KSHV gB binds the integrins α3β1, αVβ3, αVβ5 and αVβ1 [106,108–112] and/or dendritic cell-specific intercellular adhesion molecule-3-grabbing non-integrin (DC-SIGN) [112–114] dependent on target cell type (Table 1). The dimeric complex of viral gH-gL interacts with Eph receptors: EPHA2 on endothelial cells (Figure 2) and fibroblasts [36,115–117]; EPHA2, EPHA4 and EPHA5 on epithelial cells [36,115,116,118,119] and EPHA7 and to a lesser extent EPHA5 on B-cells (Table 1) [120]. Both gH-gL and EPHA2 have been shown to be essential for KSHV entry into endothelial cells while EPHA2 is not necessary for attachment, specifically mediating entry [121,122]. The viral binding partner of xCT is yet unknown [106,123]. Further, an integrin-independent route of infection requiring HSPG and the ectodomain of EPHA2 has been described in endothelial cells [119]. As infection is drastically reduced but not completely abrogated using EPHA2-binding-deficient mutant virus or upon inhibition of any specific binding receptors, it is likely that KSHV may further make use of alternative Eph receptors [107,115,119]. The functions of several glycoproteins have not yet been elucidated, but it is speculated that these have regulatory functions *in vivo* that are undetectable *in vitro* [107].

Following specific binding of KSHV glycoproteins to target cell entry receptors, KSHV binding activates host signalling pathways extracellular signal-regulated kinase (ERK)/mitogen-activated protein kinase (MAPK) and focal adhesion kinase (FAK)/phosphoinositide 3-kinase (PI3K)/protein kinase C (PKC) which facilitate KSHV entry [124–126]. The downstream effector of ERK/MAPK, p90 ribosomal S6 kinase 1 (RSK), has been shown to phosphorylate EPHA2 at Ser897, vital for KSHV infection, and it has been suggested that the androgen receptor (AR), via recruitment of Src, promotes this pathway and enhances KSHV infection [127]. KSHV enters cells utilising diverse endocytic pathways including clathrin- and caveolin-mediated endocytosis, macropinocytosis and undefined endocytic entry pathways (Table 1) [128]. In endothelial cells, EPHA2 coordinates integrin-Casitas B-

lineage lymphoma (c-Cbl) signalling via its tyrosine kinase domain (see 1.6.2.1) enabling endocytosis of KSHV via actin-dependent, dynamin-independent macropinocytosis [129]. Entry into fibroblasts is by clathrin-mediated endocytosis [117,129,130], into monocytes by clathrin- and caveolin-mediated endocytosis [112] while epithelial cell endocytosis is not clathrin-dependent [131] and B-cell endocytosis mechanisms have not been fully defined [114]. Thereafter, the viral envelope fuses with the membrane of the endosome, likely triggered by low pH as in other herpesviruses, and the capsid is released into the perinuclear region. The KSHV genome enters the nucleus via nuclear pores where the linear genome rapidly undergoes circularization into an episome [78,107,132,133].

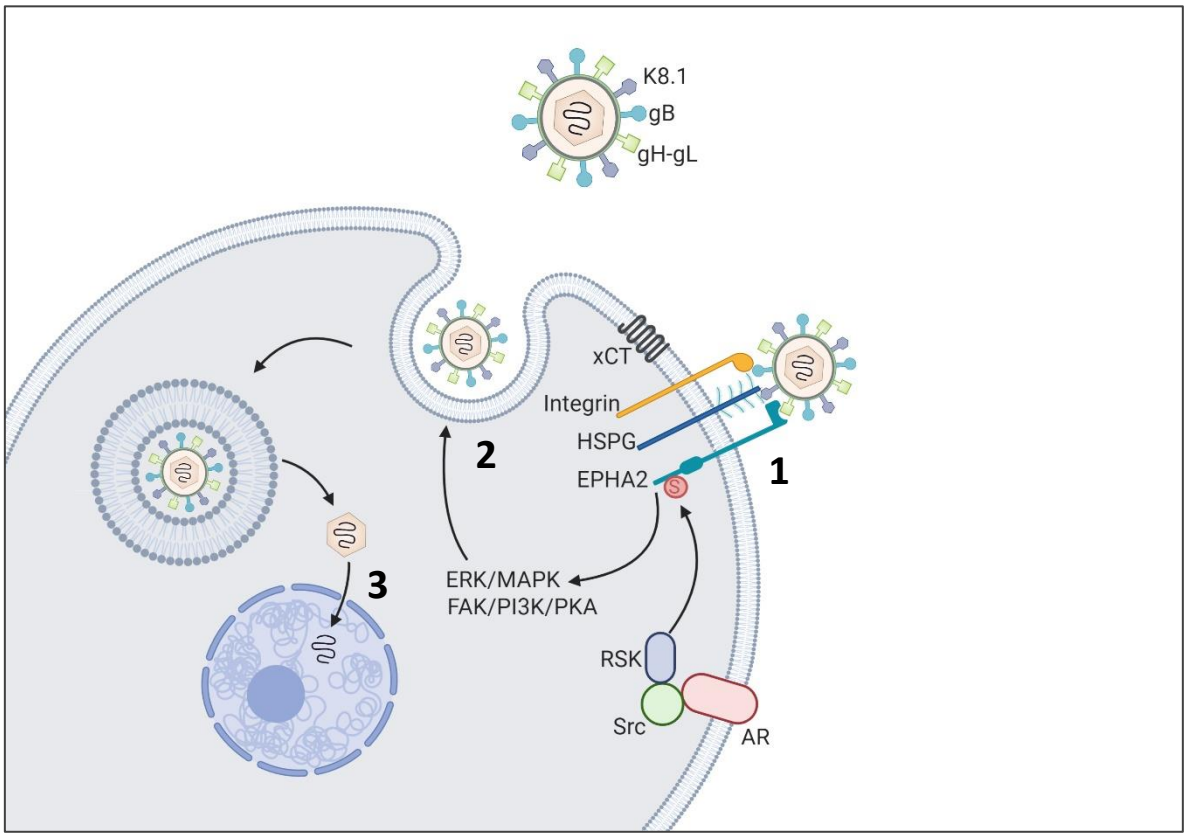

Figure 2: A schematic representation of the entry mechanism of KSHV into endothelial cells. Viral entry consists of three stages. **1)** Binding: initial attachment is mediated by the interaction of K8.1 and gB with heparan sulphate proteoglycans (HSPG). gB binds integrins which associate with xCT in a lipid raft. Subsequently, gH-gL binds EPHA2 which triggers **2)** Entry: KSHV binding to EPHA2 triggers actin-dependent macropinocytosis of the virus into an endosome, the membrane of which subsequently fuses with the viral envelope releasing the capsid into the perinuclear region. This is followed by **3)** Nuclear delivery: via nuclear pores. Adapted from [132].

Table 1: Interaction of KSHV glycoproteins with cellular receptors on KSHV-susceptible cell types. K8.1, gB and gH-gL interact with HSPGs in all cell types (not in table). Adapted from [107]

Cell type	Virion glycoprotein		Entry mechanism
	gB	gH-gL	
Endothelial	α3β1, αVβ3, αVβ5 [106,108]	EPHA2 [36,115,116]	Actin-dependent, dynamin-independent, macropinocytosis [129]
Epithelial	α3β1, αVβ3, αVβ5 [106,109,110] or independent [119]	EPHA2 [36,115,116], EPHA4 [118,119] EPHA5 [119]	Endocytosis (not clathrin-dependent) [131]
Fibroblasts	α3β1, αVβ3, αVβ5 [106,108]	EPHA2 [117]	Clathrin-mediated endocytosis [117,129,130]
Monocytes	α3β1, αVβ3, αVβ5, αVβ1, DC-SIGN [112,113]		Clathrin- and caveolin-mediated endocytosis [112]
Macrophages	DC-SIGN [113]		
Dendritic cells	DC-SIGN [113]		
B-cells	DC-SIGN [114]	EPHA7 [120] EPHA5 [120]	Endocytosis [114]

1.2.3.3. Latent infection

Characteristic of herpesviruses, KSHV soon establishes latency following initial, acute infection which allows KSHV to evade the immune system and establish a viral reservoir. The latency programme prioritizes host cell survival and proliferation. Latent proteins such as LANA, vCyclin, vFLIP, Kaposin A and B and viral miRNAs are expressed from the KSHV episome (Figure 1B) which persists in the host cell nucleus [67]. The episome is replicated during cell division, facilitated by LANA which directly links the KSHV episome to cellular chromosomes during mitosis [22,134]. Latency-associated genes facilitate KSHV persistence and are essential for oncogenesis (see 1.2.4).

1.2.3.4. Lytic infection

Expression of the KSHV lytic switch, replication and transcription activator (RTA), which is encoded by ORF50, triggers KSHV reactivation into the lytic cycle. This can be prompted by various cellular signals,

such as hypoxia, inflammation, oxidative stress and temporary or chronic immune suppression [22,135,136]. The lytic cycle facilitates the production of infectious KSHV virions and as such is cytopathic and no longer hidden from the host immune system. Early lytic transcripts (Figure 1B), such as DNA polymerase, drive KSHV episome replication into a linear, double-stranded DNA molecule that is packaged into a capsid during virion maturation [22,67]. Late lytic transcripts (Figure 1B) encode proteins necessary for structural assembly of the produced virions, such as capsid and tegument proteins [67]. In KS tumours, some spindle cells are lytically infected and express lytic transcripts, such as K1, K15, vIL-6, viral G protein-coupled receptor (vGPCR), viral-encoded B-Cell lymphoma 2 (vBCL-2), viral-encoded interferon response factors (vIRF) 1, 2 and 4 (vIRF3 is latently expressed) and viral-encoded C-C chemokine ligands (vCCL) that promote oncogenesis and thereby KS development (see 1.2.4).

1.2.4. Oncogenesis

KSHV infection in an immune-competent host is insufficient to induce oncogenesis but in the context of HIV infection and immune suppression, the interplay of latent and lytic infection can promote oncogenesis and lead to the development of KS and other KSHV-associated malignancies [21,137,138]. The majority of KS spindle cells express latent genes, but some are lytically infected [139,140]. After acute infection, KSHV establishes latent infection in endothelial cells during which the virus will persist but remain immune silent. Similarly, while cytopathic, lytic infection following a reactivation event will usually be controlled by an immunocompetent host [28]. However, immune suppression favours oncogenesis and results in loss of immune control of lytically infected cells [137]. Expression of lytic transcripts K1 and K15 drives a microenvironment of inflammation and angiogenesis that favours recruitments of target cells for re-infection [28].

Following reactivation, KSHV-infected cells express lytic transcripts in endothelial cells (see 1.2.3.4) leading to genomic instability and inhibition of DNA-damage response pathways. KSHV vIRFs 1–4 inhibit interferon signalling (a vital host immune response to viral infection) and apoptotic pathways and disrupt a number of cell cycle regulatory pathways [141–146]. Importantly, vGPCR induces inflammatory and pro-angiogenic cytokines, IL-6, IL-8, angiopoietin 2 and vascular endothelial growth factor (VEGF) and also inhibits apoptosis via activation of the Akt/TSC/mammalian target of rapamycin (mTOR) pathway, MAPKs and nuclear factor kappa B (NFκB) [147–150]. Growth factors together with KSHV-expressed vIL-6 drive proliferation of latently infected cells in a paracrine manner [67]. In addition to these lytic mechanisms of oncogenesis, latent transcripts further promote

proliferation and angiogenesis, inhibit apoptosis and drive the cancer phenotype. KSHV vCyclin counteracts cyclin-dependent kinase inhibitors, p21 and p27, to override the cell cycle restriction checkpoint before S phase [151]. LANA represses retinoblastoma protein and p53, thereby promoting proliferation and inhibiting apoptosis [152]. Additionally, vFLIP through constitutive activation of NFκB, inhibits apoptosis and induces the characteristic spindle cell morphology in endothelial cells and also leads to the further secretion of chemokines and cytokines [153–155].

Further, HIV-related chronic inflammation promotes KSHV reactivation through inflammatory cytokines and associated pathways (such as Janus kinase (JAK)/signal transducer and activator of transcription (STAT)) [156]. More directly, HIV trans-activator of transcription (tat) protein has been shown to enhance entry of KSHV into endothelial cells and transmission [138]. HIV has also been shown to potently induce lytic replication of KSHV via activation of the KSHV RTA in a tat-independent manner [157]. HIV tat promotes the KS phenotype via secretion of the pro-angiogenic interferon-γ (IFN-γ) and activation of VEGF receptor 2 (VEGFR-2), thereby stimulating the growth of KS lesions [158–160]. Angiogenesis is further enhanced by the synergistic effect of tat and KSHV K1 on NFκB activation via induction of miR-891a-5p [161]. Similarly, HIV negative factor (nef) and K1 synergistically induce miR-718 which inhibits phosphatase and tensin homolog (PTEN) thereby activating the PI3K/AKT/mTOR pathway and enhancing angiogenesis [162]. Tat further enhances cell adhesion via interaction with integrin receptors and via mimicry of matrix proteins which additionally promotes migration and cellular invasion and activation of the basic fibroblast growth factor (bFGF) which has angiogenic properties [163,164]. The effects of KSHV vGPCR are synergistically enhanced by HIV-1 tat which accelerates tumorigenesis in vGPCR transgenic mice [165,166]. Taken together, the oncogenic mechanisms of KSHV promoted by HIV co-infection activate many of the cancer hallmarks and culminate in carcinogenesis [167,168].

1.3. KSHV-associated diseases

Primary KSHV infection, while often silent, may sometimes be associated with nonspecific symptoms including fatigue, rash, diarrhoea and lymphadenopathy [169]. In immunocompetent individuals, the lifelong course of KSHV infection is clinically silent even during intermittent lytic activation, likely controlled by T-cell responses [7,169,170]. However, with a decline in T-cell immunity, most markedly due to HIV immunosuppression, KSHV-infected patients become more likely to develop KSHV-associated diseases [1].

KS was first described by a Hungarian dermatologist, Moritz Kaposi, in 1872 in a case description of six elderly men with angioproliferative tumours [171]. Over a century later, prompted by the peculiar geographic distribution of KS and the massive explosion of KS prevalence during the early AIDS epidemic, KSHV was discovered as the etiological agent of Classic, Endemic, Iatrogenic and AIDS-related KS (see 1.3.1.1) [3]. Soon after, two additional diseases caused by KSHV were identified: PEL, a body-cavity-based B-cell lymphoma [4]; and a KSHV-associated plasmablastic form of MCD (KSHV-MCD) [172]. Recently, an IL-6 related inflammatory syndrome without an MCD diagnosis termed KICS was described [6]. These KSHV-associated diseases often present simultaneously in patients co-infected with KSHV and HIV which has implications for diagnosis and treatment strategies [2,173]. While all of these KSHV-associated diseases have been reported in other immunosuppressed and elderly people [174–176], HIV-related immune suppression (i.e. CD4 count <200 cells/µl) is one of the most important mechanisms that favours KSHV-driven pathogenesis [1].

1.3.1. Kaposi's sarcoma

1.3.1.1. Epidemiology

KS is the most common AIDS-related malignancy globally and incidence rates are still increasing in SSA [177]. Before the AIDS epidemic, KS occurred in particular epidemiological groupings specific to geographical locations. Classic KS primarily occurred in elderly men from the Mediterranean and Eastern European region while Endemic KS was found in Central Africa mostly in younger males [176,178]. Further, Iatrogenic KS was associated with transplant-related immunosuppression and therefore regressed with immune reconstitution [179,180]. With the onset of the AIDS epidemic, the incidence of an AIDS-related or Epidemic KS variant, the most clinically aggressive, burgeoned, driven by HIV/AIDS-related immune suppression and HIV itself (see 1.2.4) [43]. All four epidemiological variants of KS are histologically identical and are all caused by the oncogenic KSHV (see 1.2) [3,181].

The rollout of ART, particularly the HAART strategy, has substantially reduced AIDS-related KS incidence predominantly in resource-rich regions, while this has been less successful in low-income regions [48,182]. KS incidence is the highest in SSA (Figure 3) [177,183]. KS age-standardised incidence rates in South Africa have increased 50-fold in women and 20-fold in men concomitant with the HIV/AIDS epidemic [19,184]. ART coverage in Uganda and South Africa was particularly expanded from 1998 to 2006 but there were no significant declines in KS incidence [48]. On the African continent, there were an estimated 32,446 new cases and a staggering 17,659 deaths in 2018 [185]. Age-standardised incidence rates and mortality rates reported by GLOBOCAN 2018 (schematically

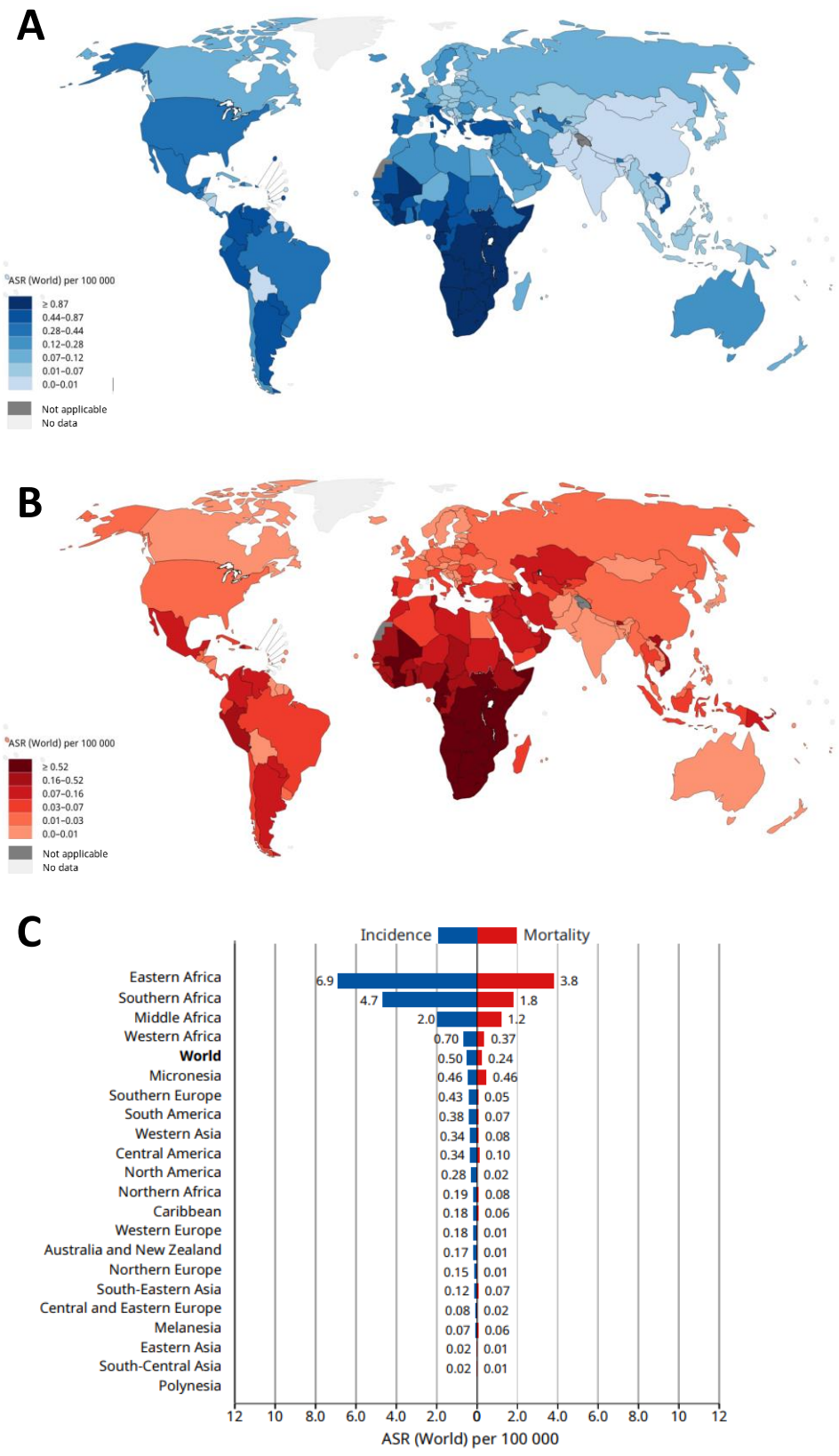

Figure 3: Epidemiology of KS. Geographic representations of **A)** incidence and **B)** mortality of KS are summarised by region in **C)**. Data are from GLOBOCAN 2018 and maps and graph were produced by the IARC, WHO [186].

represented in Figure 3) show that Eastern, Southern and Middle Africa have substantially higher KS incidence rates (>2.0 per 100,000 persons per year) and mortality rates (>1.2 per 100,000 persons per year) compared to the global incidence rate of 0.50 per 100,000 persons per year and global mortality rate of 0.24 per 100,000 persons per year [185,186]. Indeed, the SSA KS incidence in HIV-infected individuals on ART is estimated to be 286/100,000 person-years [187]. Furthermore, a steady increase in the proportions of HIV-infected KS patients with CD4 counts >300 cells/µl has been observed [71]. This might be due to senescence resembling classic (HIV-unrelated) KS as the life expectancy of HIV-infected patients on ART has significantly increased; or due to HIV-related effects independent of T-cell immunosuppression [1].

KS incidence correlates with KSHV seroprevalence [176] and the burden of disease falls predominately on SSA (see 1.2.1). Geographically, high KS-risk areas, such as eastern, central and southern Africa, concomitantly have the highest reported rates of KSHV seroprevalence (>50%) [67,188]. Further, HIV incidence has an overlapping geographical picture. AIDS-related KS is driven by HIV-related immune suppression, and HIV is considered a potent risk factor for KS development following the observation that the incidence of KS in HIV-positive patients is 20,000-fold higher than in the general population in developed countries [138,189–191]. Due to high background of Endemic KS pre-dating the AIDS epidemic, these risks are lower, although still substantial, in Africa [46,192]. Stein *et al.* reported HIV-positive patients aged between 18 and 34 to have 58.6-times greater risk of developing KS than HIV-negative patients [46]. Additionally to HIV-induced immune suppression which creates an environment favourable for carcinogenesis, HIV infection itself supports KSHV-driven pathogenesis beyond just immune suppression; the incidence of KS in HIV-positive patients is 300-fold higher than in patients with alternative forms of immunosuppression (see 1.2.4) [168,191]. Within the context of KS, these numbers clearly show the enormous impact of HIV on clinical outcome in KSHV-infected individuals.

Mortality rates are reported (GLOBOCAN 2018) to be highest in SSA (Figure 3), supported by clinical reports that AIDS-KS is more aggressive than the other KS variants. AIDS-KS is characterised by multifocal presentation and visceral involvement which complicates treatment, resulting in death [193,194]. The introduction of HAART has resulted in decreased KS mortality, but SSA mortality rates are still majorly elevated compared to the rest of the world (Figure 3) [195]. This is postulated to be the result of still limited ART coverage in some parts of SSA, delayed start of ART or non-responsive KS [192,196].

1.3.1.2. KSHV is the etiological agent of KS

Research into an infectious etiological agent of KS was prompted by its peculiar epidemiological presentation leading to the discovery, in 1994, of KSHV in an AIDS-related tumour by representational difference analysis [3]. Since then, polymerase chain reaction (PCR) has been utilised to detect KSHV DNA sequences in blood and tissue of patients with all KS variants [197–203]. The *in vitro* oncogenic properties of KSHV have been well established. KSHV infection was sufficient to induce transformation in primary human endothelial cells and immortalised dermal microvascular endothelial cells (DMVEC), indicated by morphological alteration toward the spindle cell phenotype characteristic of KS, decreased growth factor dependence, loss of contact inhibition and anchorage-independent growth [204–206]. Likewise, KSHV infection of human umbilical vein endothelial cells (HUVEC) inferred a survival advantage under serum-starvation and apoptotic stress conditions via activation of the PI3K/Akt/mTOR pathway [207]. Finally, KSHV-infected immortalised endothelial cells formed tumours in nude mice [208]. As such, these data informed the International Agency for Research on Cancer (IARC) in its classification of KSHV as a class I human carcinogen [209]. Like other oncogenic pathogens, KSHV-induced transformation of endothelial cells is driven by the expression of viral proteins in conjunction with precipitating factors, most importantly HIV infection and related immunosuppression (see 1.2.4) [210].

1.3.1.3. Clinical presentation and diagnosis

KS is a multicentric, highly vascularised tumour comprising of hyperproliferating spindle cells and infiltrating monocytes, T-cells and plasma cells [181,210]. KS commonly presents as a multifocal, flat, red/purple patch of variable size on the skin and progresses to cutaneous plaques and nodules usually on the head, neck or lower limbs [29,210]. Alternative presentation sites are the oral mucosa, the lungs, gastrointestinal tract or the lymph nodes, often accompanied with marked lymphoedema [29,211]. KS spindle cells express endothelial and lymphatic cell markers leading to debate over their lineage [181]. One theory is that transformation of spindle cells results in their evolution from blood vasculature to lymphatic endothelium with loss of cell junctions and the vascular phenotype, resulting in leakage of red blood cells into the stroma giving lesions their florid appearance [181].

Diagnosis of KS skin lesions is made by biopsy. Characteristic microscopic features of KS lesions are spindle-shaped cells and abnormal blood vessels described as vascular slits, often accompanied by fibrosis, inflammatory infiltrates and hemosiderin together with positive immunohistochemical staining for CD31 and KSHV LANA [2,212]. Pulmonary KS is diagnosed by chest X-ray, computerized tomography or visualisation of typical lesions by bronchoscopy, while biopsy of endobronchial lesions is avoided due to risk of bleeding [2]. Gastrointestinal KS is indicated by occult blood loss and/or

microcytic anaemia and, in severe cases (faecal blood loss), is visualised by endoscopy or colonoscopy [2].

1.3.1.4. Treatment

HAART is an effective treatment for KS, and in ART-naïve patients who have limited KS disease, up to 80% of patients may have regression in three to nine months [2,213,214]. However, patients with extensive oral KS, gastrointestinal or non-nodal visceral KS or tumour-associated oedema or ulceration, are considered high-risk and do not show substantial response to HAART [2]. Furthermore, some patients started on HAART develop immune reconstitution inflammatory syndrome (IRIS) and may develop or have an exacerbation of KS [215].

Systemic chemotherapy including doxorubicin, vincristine, vinblastine and bleomycin is used, especially in low-resource settings, in cases where a patient has not responded to HAART or has extensive or advanced KS, but approximately 30% of patients do not have adequate response and long-term use is associated with cumulative toxicity [213].

1.3.2. Primary effusion lymphoma

1.3.2.1. Epidemiology

PEL is considered to be a rare disease, estimated to account for approximately 4–9.8% of AIDS-related lymphomas, and was originally thought to occur in patients with advanced AIDS (CD4 count <200 cells/µl) [4,216,217]. Recent reports, however, suggest that PEL may occur in patients with higher CD4 counts, for example, a median CD4 count of 204 cell/µl was reported in 51 patients with PEL by Guillet *et al.* [4,173,218]. Nonspecific presentation, in the context of high TB prevalence (see 1.1.2), and technically-difficult diagnosis (see 1.3.2.3) likely indicate that PEL is highly underreported, especially in low-resource settings. The prognosis for PEL is poor and median survival, in the era of HAART, is less than a year [173].

1.3.2.2. KSHV is the etiological agent of PEL

Suspecting that body-cavity-based lymphomas in HIV-patients which formed as effusions in the pleural, pericardial and peritoneal cavities may constitute a distinct subgroup with unique clinical, immune and genetic characteristics, Cesarman *et al.* [4] investigated 193 lymphomas from 42 AIDS patients and 151 patients without AIDS and identified the KSHV DNA sequence by Southern blot hybridization, PCR and sequencing in all 8 AIDS-related body-cavity-based lymphomatous effusions in the group. This was soon corroborated in a series of 16 cases of lymphomatous effusion in which KSHV

DNA sequences were detected in and restricted to 4 cases of body-cavity-based effusions [219]. In 2001, PEL was recognized and classified by the WHO as a distinct neoplastic disease [220].

1.3.2.3. Clinical presentation and diagnosis

PEL presents in HIV-infected patients as an effusion in a body cavity — the pleura, peritoneum, or pericardium — together with inflammatory symptoms, such as fever and malaise, and laboratory abnormalities of hypoalbuminemia, thrombocytopenia, anaemia, elevated IL-6 and elevated KSHV VL [218].

Diagnosis of PEL requires pathological examination and identification of tumour cells which have positive expression of CD45, CD138, CD30, CD38 and human leukocyte antigen (HLA)-DR as well as demonstration of KSHV infection (usually latent genes are expressed) and often EBV co-infection [24,221].

1.3.2.4. Treatment

PEL does not have an established therapy but is most commonly treated with anthracycline-based chemotherapy regimens, similarly to other non-Hodgkin lymphomas, along with ART. A CHOP (cyclophosphamide, doxorubicin, vincristine and prednisone)-based regimen in combination with HAART has been shown to achieve remission in 43% of patients [173]. In a series of 20 patients with PEL, treatment with ART and modified EPOCH (etoposide, prednisone, vincristine, cyclophosphamide and doxorubicin) resulted in three-year cancer-specific survival of 47% [218].

1.3.3. Multicentric Castleman disease

1.3.3.1. Epidemiology

KSHV-MCD is considered a rare disorder. In a prospective HIV database (the Chelsea and Westminster HIV cohort) with 56,202 patient-years of follow-up, the incidence of biopsy-proven KSHV-MCD was 4.3/10,000 years of patient follow-up (compared to KS incidence of 210.1/10,000 patient-years) [222]. Unlike KS, MCD patients often display relatively preserved immune functions [26,222]. Indeed, there is evidence that its incidence may have increased in the ART era: when stratified by pre-HAART (1983–1996), early-HAART (1997–2001) and later HAART (2002–2007) eras, KSHV-MCD in the Chelsea and Westminster HIV cohort showed an increase from 2.3 to 2.8 to 8.3/10,000 patient-years [222]. Furthermore, KSHV-MCD is very likely underreported [2]. Despite the high prevalence of HIV and KSHV co-infection in SSA, KSHV-MCD is scarcely reported: a pathology review of 64 reactive lymph nodes from the major pathology laboratory in Uganda demonstrated LANA and vIL-6 positivity in two

specimens that were suggestive of MCD [223], and a single case of MCD was described in a retrospective evaluation of reactive lymphoid tissue specimens from Tanzania [224]. Not only is KSHV-MCD diagnosis technically difficult requiring experienced and vigilant physicians, limited diagnostic pathology in SSA and inadequate surgical capabilities to obtain biopsies for diagnostic assessment further hinders KSHV-MCD diagnosis [2,225]. In Malawi, improved pathology infrastructure led to the first clinical case series of KSHV-MCD being reported from SSA in 2015 and demonstrated late diagnosis and frequent misdiagnosis as lymphadenitis due to HIV or TB [26,225]. Diagnosis of KSHV-MCD in African immigrants in the USA in contrast to few to no diagnoses in Africa is further evidence of underdiagnosis in SSA [2,226,227].

1.3.3.2. KSHV is the etiological agent of MCD

Following the identification of KSHV as the etiological agent of KS and due to the close association of MCD with KS, which were noted to frequently co-occur in the context of HIV, Soulier *et al.* [172] published the first description of KSHV-MCD, in which KSHV sequences were detected in all of 14 HIV-associated MCD cases and in 7/17 HIV-negative MCD cases. Since then, a long list of studies has corroborated that KSHV infection is the cause of MCD in HIV-positive patients [e.g. 173,176–178].

1.3.3.3. Clinical presentation and diagnosis

KSHV-MCD is clinically characterized by inflammatory symptoms including fevers, night sweats, weight loss, cachexia, oedema and effusions with lymphadenopathy and splenomegaly and often, respiratory, dermatologic and neurologic symptoms [2,231]. Laboratory abnormalities include anaemia, decreased albumin, hyponatremia, thrombocytopenia, elevated CRP and elevated KSHV VL in both plasma and peripheral blood mononuclear cells (PBMC) [2,231,232]. The clinical course is characterised by flares during which CRP is highly elevated and has been suggested as a screening marker together with KSHV VL [2,218]. This clinical presentation may mimic plasmablastic leukaemia, lymphoma, TB or bacterial sepsis which may delay diagnosis [2,26,225,232].

MCD is diagnosed by lymph node biopsy and histologic confirmation of KSHV-infected plasmablastic cells (identified by LANA staining) in the mantle zone of lymphoid organs that express IgM and are lambda restricted. KSHV-MCD lymph nodes characteristically have regressed germinal centres with vascularised core and mantle zone expansion [27].

1.3.3.4. Treatment

Rituximab (a monoclonal antibody targeting CD20) is a highly effective therapy for MCD and is now considered the first-line treatment option. It has greatly improved KSHV-MCD outcomes, resulting in survival and resolution of MCD symptoms in >90% of patients [2,227,233,234]. The use of rituximab is

limited in patients with low CD4 counts, organ dysfunction and co-existing KS as rituximab may exacerbate KS [227,233,235]. Severe symptoms or MCD flare-ups require supportive treatment in an intensive care unit [2]. Advanced KSHV-MCD is treated with cytotoxic chemotherapy (liposomal doxorubicin or etoposide) in addition to rituximab and one study found that treating concurrent KSHV-MCD and KS with the combination of rituximab and liposomal doxorubicin resulted in KS improvement in five of six patients and overall survival of 81% [227]. Another study found that virus-activated cytotoxic therapy (high dose zidovudine plus valganciclovir, a pro-drug of ganciclovir) resulted in 86% survival at 12 months [226].

Without treatment, KSHV-MCD is fatal with observed survival of less than two years [231]. In a Malawian study, late diagnosis, inadequate supportive care and inappropriate therapies (neither rituximab, zidovudine nor ganciclovir are available in Malawi) were attributed to poor survival of KSHV-MCD patients (median survival <6 months) [26]. In resource-limited SSA, even chemotherapeutic agents included in the WHO Model Lists of Essential Medicines (which rituximab is not) are limited in their availability [236]. In Malawi and much of SSA, KSHV-MCD is treated with the chemotherapeutics available — etoposide, cyclophosphamide, vincristine and prednisone — with unsatisfactory results [26,236].

1.3.4. KSHV inflammatory cytokine syndrome

1.3.4.1. Epidemiology

KICS is a newly described inflammatory syndrome that was first reported in a retrospective analysis of six patients in the USA [8] and has since been described in a prospective study of ten patients in the USA [6]. Since, a handful of cases have been described: one patient in Italy [174]; seven patients in the USA [237]; and another patient in the USA [238]. While KICS is likely undiagnosed in the majority of cases, it is considered a very rare but serious, high-risk diagnosis [2].

1.3.4.2. KSHV is the etiological agent of KICS

The first description of the syndrome that would be named KICS arose from the observation of patients with KSHV infection and a symptom profile resembling KSHV-MCD in which pathological diagnosis of KSHV-MCD, or any alternative conditions, could not be made [8]. These patients were found to have high KSHV VL and elevated vIL-6 as well as human IL-6, IL-10 and other cytokines and the authors postulated that the syndrome observed was a result of direct or indirect cytokine activation by KSHV [8]. A further series of ten KICS patients were prospectively described by the same group to

characterise the clinical, laboratory, virological and immunological features of KICS, culminating in a working case definition (Table 2 [6,7]).

1.3.4.3. Clinical presentation and diagnosis

KICS is a proposed clinical diagnosis requiring pathological exclusion of MCD [6] and other serious intercurrent infections [6–8]. Like MCD, KSHV is lytically active in KICS and VL is elevated resulting in an overproduction of host and viral IL-6 and other cytokines giving rise to inflammatory symptoms such as fever, wasting, hypoalbuminemia, cytopenia, hyponatremia and elevated CRP [8]. The working case definition for the diagnosis of KICS (Table 2) stipulates that a patient has: at least two clinical manifestations from at least two of the lists of symptoms, laboratory abnormalities and radiographic abnormalities; evidence of systemic inflammation measured by CRP; elevated KSHV VL above 100 copies/10^6 cells; and exclusion of MCD and other serious infections [6,7]. The implicated cell type in KICS is unknown, but it commonly occurs in conjunction with KS or PEL tumours [2]. KICS in the absence of KS or PEL has also been reported [6,8].

Table 2: Working case definition of KICS defined by Polizzotto *et al*. [6,7].

1. Clinical manifestations	
A. Symptoms	**B. Laboratory abnormalities**
Fever	Anaemia
Fatigue	Thrombocytopenia
Oedema	Hypoalbuminemia
Cachexia	Hyponatremia
Respiratory symptoms	**C. Radiographic abnormalities**
Neuropathy with or without pain	Lymphadenopathy
Arthralgia and myalgia	Splenomegaly
Altered mental state	Hepatomegaly
Gastrointestinal disturbance	Body cavity effusions
2. Evidence of systemic inflammation	
Elevated CRP	
3. Evidence of KSHV lytic activity	
Elevated KSHV VL in peripheral blood mononuclear cells (>100 copies/10^6 cells)	
4. No evidence of KSHV-associated MCD	
Exclusion of MCD requires pathologic assessment of lymph node, bone marrow, or spleen.	

1.3.4.4. Treatment

As a recently described syndrome with which there is little clinical experience, it is still unclear how KICS should best be treated. Current management strategies are directed at treating any associated malignancy [2,7]. However, KS in the context of KICS does not respond well to standard therapy, and overall, KICS patients have shown a poor prognosis with high mortality, often from progressive KSHV-related tumours [6–8]. Additionally, approaches developed for KSHV-MCD (high dose zidovudine, valganciclovir and liposomal doxorubicin) showed some promise in the original series of six KICS patients [8]. One case report described treatment of a patient diagnosed with KICS and KS with rituximab and liposomal doxorubicin who died and attributed this to delay in diagnosis due to time spent on differential diagnoses [238], while another describing the first reported case of a KICS-like syndrome in an HIV-negative post-transplant patient had success using rituximab, cidofovir and foscarnet [174].

1.3.5. Clinical management of KSHV infection

Regardless of the individual KSHV-associated pathology, treatment of KSHV infection with anti-herpesvirus therapy to reduce viral replication has been examined in the HIV setting to prevent and treat disease. Prophylactic ganciclovir used to prevent cytomegalovirus retinitis in HIV-positive patients was shown to concomitantly reduce KS incidence [239]. Use of cidofovir in KS patients with KS lesions resistant to ART and chemotherapy treatment led to clinical improvement correlated with reduction in KSHV viremia [240] and similarly, treatment with foscarnet led to a reduction in KSHV DNA in PBMCs to an undetectable level in an HIV-positive patient with disseminated KS [241] and in an HIV-negative patient with primary KSHV infection post-transplant [242]. In a case series of three patients with KSHV-MCD treated with oral and intravenous ganciclovir, reduction in KSHV viral replication was observed along with the resolution of symptoms [243]. Valganciclovir has been successfully used in combination with rituximab [235] or zidovudine [226] to control KSHV viremia.

1.4. KSHV VL as a potential diagnostic and monitoring tool

KSHV DNA levels in peripheral blood differ between KSHV-associated diseases, with highest levels evident in lytically-associated syndromes MCD and KICS and lower levels in PEL and KS [20,25,244]. Further, KSHV VL in blood and oral fluids has been shown to be associated with KS disease status (progressing, stable and regressing) [245,246], severity [7] and KSHV lytic reactivity during KS [247]

and proposed as a clinical tool for assessment of risk of KS progression [7,25,244–247]. KSHV VL has been characterised as a virological parameter, together with vIL-6, to monitor KSHV-MCD treatment progress and outcome in combination with immunological parameters, such as CRP, haemoglobin, albumin, sodium, platelets and host IL-6, to characterise a profile corresponding to best clinical response [25,226,233]. KSHV VL elevated above 100 copies/10^6 cells is included in the working case definition of KICS [6,7]. KSHV VL may be a useful biomarker for KSHV-associated disease risk, to inform diagnosis and to manage KSHV-associated diseases. This study further assessed the applicability of KSHV VL as a surveillance tool for KSHV-associated pathologies in a high HIV/TB setting.

1.5. Host genetic factors in KSHV infection and KS development

KSHV infection is necessary but insufficient for KS development. Precipitating factors such as HIV infection or immune suppression are required for KSHV-associated oncogenesis (see 1.2.4). Even so, HIV-KSHV co-infection does not strictly result in cancer development. Furthermore, exposure to KSHV does not always result in KSHV infection; seroconversion even in areas of high exposure is 30–50% [94]. An epidemiological population-based study on 1,337 individuals of African origin in French Guinea where KSHV is endemic, showed strong correlation of KSHV seroprevalence between mother-child and sibling-sibling pairs, suggestive of familial aggregation, although a plateau in seroprevalence rates with age led the authors to suspect genetic resistance may be present in the population [9]. These observations in addition to the geographic and population-specific incidence of KS suggest a potential role for host genetic factors in KSHV infection following exposure and/or progression to KS [28,29,67,248].

Various groups have investigated host genetic factors in relation to KSHV susceptibility and subsequent KS development. Plancoulaine *et al.* [30] identified, by segregation analysis of KSHV seroprevalence among the aforementioned French Guinean population, the presence of a recessive major gene that affects, in combination with age, susceptibility to KSHV seroconversion in children under ten years of age. This was mapped to chromosome region 3p22 which encodes PDCD6IP, UBP, FBXL2, ARPP-21, LRRFIP2 and CCR4 [249].

Thus far, immune-modulatory genes have been the focus of investigations of candidate susceptibility genes. In particular, published studies have reported significant associations with KS or KSHV-infection of single nucleotide polymorphisms (SNPs) in genes encoding interleukins (IL-6, IL-8 and IL-13) [32,250–252], VEGF [252,253], NFκB [254], mannose-binding lectin (MBL)-2 [255], Fc gamma receptors (FcγR) [33], HLA killer cell immunoglobulin-like receptors (KIR) [248,256,257] and

their HLA ligands and linked genes [31,257–262] and homologues of human genes mimicked by KSHV, namely cyclin D1 (CCND1), IL-6, C-C chemokine ligand 2 (CCL2) and FADD-like apoptosis regulator (CFLAR) [263]. We have conducted a preliminary assessment into the KSHV entry receptor EPHA2 in relation to KSHV infection and KS development [34]. The above-mentioned studies are summarised in Table 3. Further, tumour necrosis factors (TNFα and TNFβ) [32,252], IFN-γ [252], stromal-derived factor 1 (SDF1), C-C chemokine receptor type 5 (CCR5) [32] and caspase 8 (CASP8) [263] have been investigated in relation to KS and KSHV but have not yielded statistically significant results.

From these studies, several notable associations have been identified in genes encoding proteins that are known to be pro-inflammatory (Table 3). A SNP in the IL-6 promoter (c.-174G>C, reference SNP (rs)1800795) which is associated with increased levels of IL-6 was noted in a familial clustering of Classic KS and was further associated with KS in HIV-infected men and renal transplant recipients [32,248,250]. IL-6 potently promotes the growth of KS spindle cells in an autocrine and paracrine manner [264] and is mimicked by KSHV-encoded vIL-6 [67,263]. A SNP in the IL-13 promoter region (c.-1069C>T, rs20541) was associated with Classic KS in patients latently infected with KSHV [252]. Similarly, an IL-8 promoter SNP (c.-251A>T, rs4073), linked to below normal IL-8 expression, was identified in a cohort of patients with Classic KS [252]; however, it was conversely found to decrease the risk of AIDS-KS in HIV-positive patients [251]. The combination of two SNPs (c.1235T>C, rs1126579 and c.-1010G>A**,** rs1126580) in the human homolog to the KSHV-encoded vGPCR, IL-8RB, were found to be protective against the development of Classic KS [252]. The angiogenesis-related VEGF was found to harbour a promotor region SNP (c.-172C>A, rs59260042) associated with KSHV viremia in kidney transplant recipients, and a SNP in the 5' untranslated region (UTR, c.405C>G, rs2010963) was likewise associated with KSHV viremia but in females only [253]. Polymorphisms in the NFκB1 promoter (NFkB1 -94 ins/del ATTG, rs28362491) and the 3'UTR region of the NFκB1 inhibitor alpha (NFκBIA c.2758G>A, rs696) were found to be associated with the presence of antibodies to KSHV lytic antigens [254]. The innate immune system protein MBL haplotype (based on combinations of genotypes of two promoter region SNP (c.-550 H/L and c.-221 Y/X) and three coding SNPs in exon 1 (codon positions 52, 54 and 77)) was associated with intermediate expression of MBL and was found to be associated with lower CD4 count in KSHV co-infected patients compared to HIV mono-infected patients [255].

Immunoregulatory genes have also been implicated in KS development and/or KSHV susceptibility. A polymorphic form of the immunoglobulin G (IgG) binding receptor, FcγRIIIA, was associated with AIDS-KS in a cohort of HIV-positive men and was found to enhance IgG affinity *in vitro* and promote natural killer (NK) cell activation [33,265]. Inflammation mediated by NK cell activation is postulated to promote KS oncogenesis [257,266]. NK cells are regulated by inhibitory KIRs which are

Table 3: Summary of SNPs associated with KS development, KSHV infectivity or KSHV serumpositivity in the studies detailed in 1.5. SNP mRNA position is given where appropriate (a + value indicates a position within the coding region, while a - value indicates a position in the promotor region). Reference SNP identification (rsid) numbers correspond to the SNP database. Alternatively, the haplotype is given where appropriate. HLA haplotypes are named according to the naming convention determined by the WHO Nomenclature Committee for Factors of the HLA System. The base referred to in the corresponding table entry is in bold. Odds ratio (OR), confidence interval (CI) and P values are extracted from papers referenced in the table or calculated from the published data as required. An OR>1 is indicative of increased risk; OR<1 indicates decreased risk. Table is adapted and updated from [35].

Gene	SNP (rsid)/ haplotype	OR (95% CI)	P value	Associated with	Description of study cohort	Cases vs. controls	Ref.
IL-6	**G**-174C (rs1800795)	2.11 (1.2-3.7)	0.0046	AIDS-related KS	HIV+ male patients with or without KS	115 vs. 126	[32]
		5.3 (1.5 to 18.9)	0.008	Iatrogenic KS	Renal transplant recipients with or without KS	15 vs. 40	[250]
IL-8	A-251**T** (rs4073)	0.49 (0.25-0.97)	0.039	AIDS-related KS	HIV+/KSHV+ male patients with or without KS	84 vs. 154	[251]
IL-8RB	T+1235**C** (rs1126579) + G-1010**A** (rs1126580)	0.49 (0.30-0.78)	0.003	Classic KS	HIV-/KSHV+ patients with or without KS	133 vs. 172	[252]
IL-13	C-1069**T** (rs1800925)	1.88 (1.15-3.08)	0.01	Classic KS	HIV- KSHV+ patients with or without KS	133 vs. 172	[252]
VEGF	C-172**A** (rs59260042)	4.8 (1.4-17.1)	0.005	KSHV viremia	Renal transplant recipients, KSHV+ or KSHV- after transplant	44 vs. 128	[253]
	C+405**G** (rs2010963)	3.98 (1.5-11.1)	0.004	KSHV viremia	Female only renal transplant recipients, KSHV+ or KSHV- after transplant	18 vs. 50	[253]
NFκB1	-94 ins/del ATTG (rs28362491)	7.9 (3.3-19.1)	<0.001	KSHV lytic antibody response	HIV+/KSHV+ patients	63 vs. 69	[254]
NFκBIA	G+2758**A** (rs696)	Het: 12.3 (4.3–34.9) Hom: 9.4 (3.2–27.9)	<0.001 <0.001	KSHV lytic antibody response	HIV+/KSHV+ patients	63 vs. 69	[254]
MBL2	HYA/HXA, HYA/ HYO, HYA/LXA, HYA/LYO, LXA/LXA, LYA/LXA and LYA/LYO (intermediate expression haplotypes)	3.1 (1.2-7.6)	0.02	CD4 count response	HIV+ patients who were KSHV+ or KSHV-	124 vs. 213	[255]

HLA Class I	HLA-A*11:01	0.4 (0.2-0.7)	0.002	Classic KS	HIV- patients with or without KS	248 vs. 855	[257]
	HLA-C*07:01	1.6 (1.2-2.1)	0.002	Classic KS	HIV- patients with or without KS	250 vs. 846	[257]
	HLA-B*1401	4.2 (1.1-15.5)	0.03	AIDS-related KS	HIV+/KSHV+ patients with and without KS	348 vs. 318	[31]
		4.27 (1.67-10.91)	0.033	AIDS-related KS	HIV+ patients with or without KS.	157 vs. 523	[258]
	HLA-B*2702/5	0.37 (0.15-0.94)	0.04	AIDS-related KS	HIV+/KSHV+ patients with and without KS	348 vs. 318	[31]
		0.39 (0.16-0.94)	0.04	AIDS-related KS	HIV+ CD4 decline matched patients with or without KS	96 vs. 96	[259]
	HLA-CW4	4.96 (2.9-8.12)	0.03	Iatrogenic KS	HIV- renal transplant recipients with or without KS	44 vs. 15	[260]
	HLA-A30	0.48 (0.25-0.90)	0.48	Classic KS	HIV- patients with or without KS	62 vs. 220	[261]
	HLA-CW5	0..32 (0.16-0.65)	0.0006	Classic KS	HIV- patients with or without KS	62 vs. 220	[261]
	HLA-CW7	2.48 (1.27-4.72)	0.01	Classic KS	HIV- patients with or without KS	62 vs. 220	[261]
	HLA-B58	0.035 (0.002-0.58)	0.00001	Classic KS	HIV- patients with or without KS	62 vs. 220	[261]
HLA Class II	HLA-DRB1*1302-DQB1*0604	6.12 (1.29-28.9)	0.02	AIDS-related KS	HIV+, CD4 decline matched patients with or without KS	96 vs. 96	[259]
	HLA-DRB1*F13	2.24 (1.19-4.20)	0.016	AIDS-related KS	AIDS patients with or without KS	122 vs. 94	[262]
	HLA-DRB1*1104	2.12 (1.05-4.25)	0.047	Classic KS	HIV- patients with or without KS	62 vs. 220	[261]
	HLA-DRB1*1302	5.83 (1.73-19.83)	0.004	Classic KS	HIV- patients with or without KS	62 vs. 220	[261]
	HLA-DRB1*1601	0.50 (0.26-1.0)	0.043	Classic KS	HIV- patients with or without KS	62 vs. 220	[261]
	HLA-DQA1*0302	11.97 (1.27-103.36)	0.019	Classic KS	HIV- patients with or without KS	62 vs. 220	[261]
	HLA-DQB1*0502	0.52 (0.27-0.97)	0.047	Classic KS	HIV- patients with or without KS	62 vs. 220	[261]
	HLA-DQB1*0604	7.75 (2.02-29.70)	0.0017	Classic KS	HIV- patients with or without KS	62 vs. 220	[261]
HLA-DMB	A>G (rs6902982)	4.09 (1.90-8.80)	0.0003	AIDS-related KS	HIV+/KSHV+ patients with and without KS	348 vs. 318	[31]
TAP1	A+ 2090**G** (rs1135216)	1.54 (1.09-2.18)	0.014	AIDS-related KS	HIV+/KSHV+ patients with and without KS	348 vs. 318	[31]
	A+ 1177**G** (rs1057141)	1.45 (1.05-1.99)	0.024	AIDS-related KS	HIV+/KSHV+ patients with and without KS	348 vs. 318	[31]

TAP1/ TAPSAR1	A-127**G** (rs2071541)	1.6 (1.11-2.32)	0.012	AIDS-related KS	HIV+/KSHV+ patients with and without KS	348 vs. 318	[31]
GPANK1	A+1846G (rs7029)	1.55 (1.17-2.05)	0.002	AIDS-related KS	HIV+/KSHV+ patients with and without KS	348 vs. 318	[31]
TRIM31	G+1261**A** (rs1116221)	0.74 (0.56-0.96)	0.033	AIDS-related KS	HIV+/KSHV+ patients with and without KS	348 vs. 318	[31]
LT-α	A-90**G** (rs909253)	0.75 (0.58-0.96)	0.022	AIDS-related KS	HIV+/KSHV+ patients with and without KS	348 vs. 318	[31]
LY6G6C	G+298A (rs1065356)	1.60 (1.18-2.16)	0.002	AIDS-related KS	HIV+/KSHV+ patients with and without KS	348 vs. 318	[31]
KIR	KIR3DS1	4.0 (1.4-11.4)	0.006	Classic KS	Patients with or without KS (those without KS were KSHV+ or KSHV-)	32 vs 51	[256]
HLA and KIR	HLA-B Bw4-80I + KIR3DS1	0.6 (0.4-0.9)	0.01	KSHV viremia	HIV-/KSHV+ or KSHV- patients	277 vs. 562	[257]
		2.1 (1.3-3.4)	0.002	Classic KS	HIV-/KSHV+ patients with or without KS	248 vs. 277	
FcγR	T+559**G** (rs396991)	2.47 (1.46 - 4.16)	0.0063	AIDS-related KS	HIV-infected males with or without KS	112 vs. 128	[33]
EPHA2	T+2254C G+2990T	1.2 (1.1–1.3) 1.2 (1.1–1.4)	0.04 0.02	AIDS-related KS	HIV+/KSHV+ patients with or without KS	50 vs. 50	[34]
	C+2727T	6.4 (1.4-28.4)	0.03	KSHV serumpositivity	HIV+/KSHV+ or HIV+/KSHV- patients	100 vs. 50	[34]

activated by interaction with HLA molecules. Goedert *et al.* [257] reported that the combination of KIR3DS1 (an activating haplotype of KIR) and HLA-B Bw4-80I (the Bw4 haplotype with an isoleucine at position 80) was protective against KSHV viremia but increased the risk of Classic KS among KSHV-positive patients in a cohort of HIV-negative patients without KS although this was not corroborated in a smaller cohort of Italian Classic KS patients [256]. Additionally, the KIR3DS1 haplotype was found to be associated with Classic KS [256].

Several HLA class I and II haplotypes have been thoroughly investigated. KS development post kidney transplant was associated with HLA-CW4 in a small study [260]. In a study of Classic KS in a Sardinian population (high risk for Classic KS), a number of Class I and Class II HLA haplotypes were identified as increasing (Class I: HLA-CW7; Class II: HLA-DRB1*1104, HLA-DRB1*1302, HLA-DQA1*0302, HLA-DQB1*0604) or decreasing (Class I: HLA-A30, HLA-CW5, HLA-B58; Class II: HLA-DRB1601, HLA-DQB1*0502) risk of Classic KS [261]. HLA-C*07:01 has also been associated with Classic KS, while HLA-A*11:01 was found to decrease risk [257]. HLA-B*1401 is a risk allele for AIDS-related KS [31,258] and HLA-B*2705 is protective [31,259]. HLA-DRB1*1302 in linkage disequilibrium with DQB1*0604 was identified as a risk haplotype for AIDS-related KS [259] as were HLA-DRB1 alleles with a phenylalanine residue at position 13 [262]. Several variants identified in a SNP screening of the HLA-DMB gene region were found to increase AIDS-KS risk. Most significantly, a SNP in the HLA-DMB intronic region (rs6902982) was associated with a four-times higher risk of AIDS-KS in HIV-KSHV coinfected men [31]. Non-synonymous SNPs in TRIM31 and LT-α were observed to be protective whereas SNPs within HLA-DMB linked genes, TAP1, TAPSAR1 microRNA, GPANK and LY6G6C, were associated with increased risk of AIDS-KS [31]. While certainly indicative of an association with KS, particularly in Class I and II HLA types, the heterogeneity of studied populations and different HLA genotyping techniques used has led to numerous but inconsistent reports that require validation [258].

Recently, human genes that are mimicked by KSHV have been investigated hypothesising that virally expressed homologues, which promote immune-silent proliferation, may be advantaged by genetic SNPs in their cellular homologues [263]. A SNP screening in AIDS-KS patients including several cellular homologues identified SNPs in CCND1, IL-6, CCL2 and CFLAR (homologues of KSHV-encoded vCyclin, vIL-6, vFLIP and vCCL, respectively). Various combinations of these SNPs (but not the SNPs alone) were associated with AIDS-KS [263].

Key molecules involved in the initial stages of KSHV entry (see 1.2.3.2) are interesting candidate genes for KSHV and KS association studies. We investigated sequence variants in the KSHV entry receptor, EPHA2 (see 1.6), in relation to KSHV infection and/or KS development. Mutation

analysis revealed two novel, non-synonymous heterozygous variants (c.2254T>C and c.2990G>T) significantly associated with KS and a novel heterozygous transition (c.2727C>T) associated with KSHV in a cohort of HIV-infected South African patients stratified by KS and KSHV status (see 1.6.6) [34,35].

1.6. The KSHV entry receptor EPHA2

Eph receptors are important in KSHV entry processes through their direct binding with the KSHV glycoprotein complex gH-gL (see 1.2.3.2, Table 1). EPHA2, in particular, is essential for KSHV entry into endothelial cells (see 1.2.3.2, Figure 2), facilitating KSHV infection (see 1.6.4) and subsequent KS development through oncogenic mechanisms (see 1.6.3).

1.6.1. The Eph and ephrin families

The family of Eph receptors, which bind Eph receptor-interacting proteins (ephrins), are classified as RTKs. The generally conserved structure of Eph receptors consists of an intracellular kinase domain at the C-terminal end, adjacent to a region for binding of interacting proteins, and an extracellular region containing a ligand binding domain, a cysteine-rich domain and two fibronectin type-3 (Fn-3) repeats at the amino-terminal end [267]. Eph receptors, like classical RTKs, are monomeric and dimerize upon ligand binding. Eph receptors are classified based on homology of the extracellular domain either as EphA receptors that bind ephrin A (1–5) ligands or EphB receptors that bind ephrin B (1–3) ligands [268,269]. Unique among RTK ligands, ephrins are situated in the cell membrane and on binding to Eph receptors, elicit both 'forward signalling' in the Eph-expressing cell through activation of the Eph receptor and 'reverse signalling' through the ephrin in the cells on which they are expressed [270–272]. This signalling functions in developmental tissue organization, for example in vasculature organisation and axon guidance via contact adhesion or repulsion, and therefore Ephs and ephrins are expressed at high levels during development [273]. In adult tissue, Ephs and ephrins are expressed in a wide variety of tissues at low levels and function in regulating cell proliferation, dynamics and angiogenesis via signalling cascades [269,273,274]. Eph receptors, additionally, regulate oncogenesis [275] and have been found to be expressed aberrantly in various tumour tissues, correlating with increased invasiveness, angiogenesis and metastatic potential [269].

1.6.2. The EPHA2 receptor

1.6.2.1. Gene and protein structure

The EPHA2 RTK is a transmembrane receptor consisting of 976 amino acids (AA) encoded by a 31,773 base pair (bp) gene (chromosome 1p36, National Center for Biotechnology Information (NCBI) Accession number NG_021396) [276]. EPHA2 is comprised of 17 exons and several domains conserved among the Eph receptor family (Figure 4).

The extracellular region consists of an ephrin ligand-binding domain (Eph-lbd, AA position 28–201); a cysteine-rich epithelial growth factor-like (EGF-like) domain (AA position 260–273); and two Fn-3 domains (AA positions 329–424 and 436–519). The G-H loop (a 15 AA loop region) on Ephrin-A ligands binds EPHA2 promiscuously at the Eph-lbd [277].

The transmembrane domain (Tm-1, AA positions 536–558) connects the extracellular domain to the intracellular region, comprised of the functionally important juxtamembrane region, protein tyrosine kinase (Pkinase-Tyr) domain (AA position 613–871) and sterile alpha motif (SAM) domain (position 902–966) [278,279]. The juxtamembrane region and the Pkinase-Tyr domain are important in activation of the EPHA2 receptor, containing multiple tyrosine, serine and threonine residues that are phosphorylated upon receptor activation thereby creating binding sites for signalling proteins that contain Src homology (SH)2/SH3 domains such as Src, Ras GTPase activating protein (RasGAP), Phosphoinositide 3-kinase (PI3K), Fyn, Nck, Crk, Grb2, Grb10, Src-like-adaptor protein (SLAP), Vav2, Vav3 and low molecular weight protein tyrosine phosphatase (LMWPTP). Signalling mediated through the recruitment of these signalling proteins to the phosphorylated sites of EPHA2 is functionally important, regulating actin dynamics, cellular adhesion, vascular assembly, angiogenesis and cell migration (see 1.6.2.2) [280–282]. For example, phosphorylated tyrosine residues at positions 587 and 593 bind guanine nucleotide exchange factors Vav2 and Vav3 and phosphorylated Tyr734 binds the p85 regulatory subunit of PI3K, and without these interactions, EPHA2 is defective in Rac1 activation and cell migration, and vascular assembly [282]. Additionally, phosphorylation sites Tyr772 and Ser897 in the intracellular region have been highlighted as key to the EPHA2's oncogenic potential (see 1.6.3) [283–286] and phosphorylation of Ser897 is essential in KSHV entry (see 1.2.3.2) [127]. The SAM domain facilitates functionally important protein-protein interactions to regulate receptor dimerization and is the docking site for a number of interacting proteins that mediate downstream signalling [287,288]. A recent report indicates that the EPHA2 SAM domain is an inhibitor of kinase activity by reducing receptor oligomerization as SAM deletion led to constitutively active EPHA2 [289]. Much of the available insight into EPHA2 structure and function has

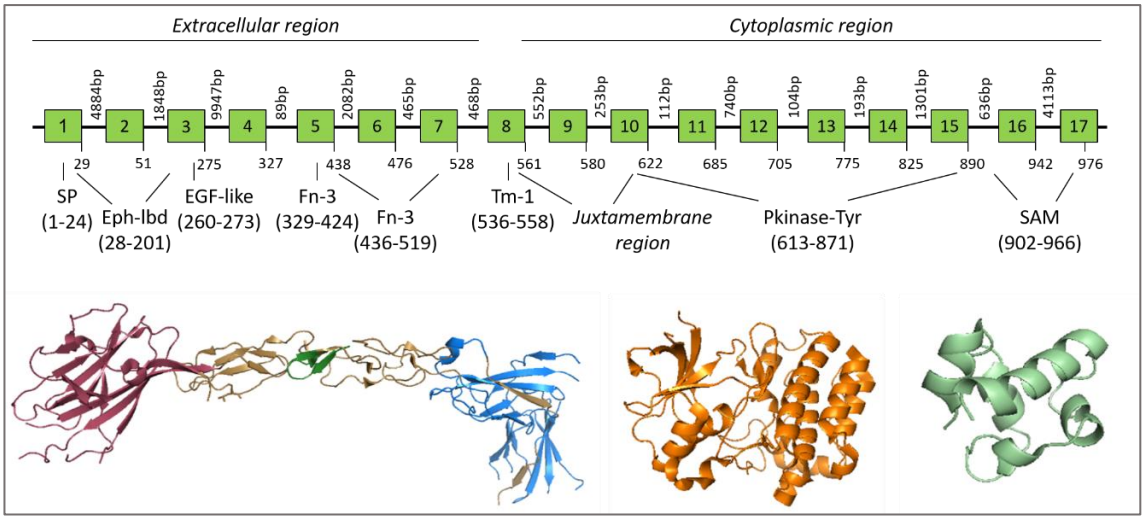

Figure 4: The EPHA2 gene structure showing conserved domains and structural models. Green boxes represent exons and black lines are intronic regions. Depicted as 3D structural models are the ectodomain (PDB ID: 3fl7) including the Eph-lbd (pink), the EGF-like domain (dark green) and the two Fn-3 domains (blue); the Pkinase-Tyr domain (5ek7, orange) and the SAM domain (3kka, light green). Italics indicates regions; non-italics indicates conserved domains. SP, signal peptide; Eph-lbd, Eph-receptor ligand binding domain; EGF-like, epithelial growth factor-like region; Fn-3, Fibronectin type-III domain; Tm-1, transmembrane domain type-I; Pkinase-Tyr, protein tyrosine kinase domain; SAM, sterile-α-motif. Adapted from [279].

been obtained from the crystal structure of the ectodomain (Protein Data Bank (PDB) ID: 3fl7), the Pkinase-Tyr domain (PDB ID: 5ek7) and the SAM (PDB ID: 3kka).

1.6.2.2. Physiological function

EPHA2 is an epithelial and endothelial cell receptor, with mRNA expression detected in tissues with a high turnover of epithelium such as intestinal, bladder, skin and lung tissue, but the extent of protein expression in tissues is not yet known [36,269,290]. Ephrin-A ligands are membrane-bound through glycosylphosphatidylinositol linkage [271,277,291]. All ephrin-A ligands, but in particular ephrin-A1 which is encoded by the *EFNA* gene, bind EPHA2 to trigger canonical contact-dependent signalling in the Eph receptor expressing cell and the ephrin expressing cell [271,272,277]. EPHA2 plays a role in the development processes of the optic lens, inner ear, mammary gland and kidney and in ischemia-reperfusion injury repair in the kidney, angiogenesis, cellular stress response and bone remodelling.

During foetal development, Eph-receptor-ephrin contact-induced attraction and repulsion results in pattern formation, or topographical mapping in tissues. The interaction of EPHA2 and one of its ligands, ephrin-A5, both of which are expressed and co-localised in the pre-natal optic lens, mediates lens transparency and organisation of the refractive fibre cells [292,293]. EPHA2 homozygous knockout animal models demonstrate the importance of this interaction in the prevention of cataracts and EPHA2 mutations have been associated with congenital and age-related

cataract pathogenesis (see 1.6.5) [279,292–298]. EPHA2 is also expressed in the otic placode which likely has an important but currently unknown function in the development of the inner ear [299]. EPHA2 in mammary epithelial tissue is regulated by oestrogen and c-myc, and receptor knockout impaired mammary gland development via reduced proliferation and branching [38,300]. Branching morphogenesis, important for kidney development from the foetal ureteric bud is similarly regulated by EPHA2 [301].

On the level of cellular dynamics, the EPHA2-ephrin-A1 interaction is essential in the regulation of postnatal angiogenesis via cellular migration and vascular assembly facilitated through the EPHA2 canonical pathway [290]. EPHA2 further facilitates the trafficking of T-cells via integrin-mediated adhesion to endothelial cells [302]. Additionally, EPHA2 functions as a regulator of injury and stress response [303], for example, by regulating actin dynamics in the cytoskeleton following renal ischemia-reperfusion injury studied in *in vitro* and *in vivo* models [304]. Furthermore, ultraviolet (UV)-mediated apoptosis is dependent upon EPHA2 upregulation in response to UV in human and mouse melanocytes, keratinocytes and fibroblasts [305]. Remodelling of bone is dependent on the interaction of EPHA2 with ephrin-A2 which drives osteoclastogenesis and suppresses osteoblastogenesis [306]. Canonical signalling through ligand activation of EPHA2 is tumour suppressive while EPHA2 has also been found to induce signalling pathways through a noncanonical ligand-independent pathway that promotes oncogenesis (see 1.6.3 and Figure 5) [285].

1.6.3. Association of EPHA2 with oncogenesis

Several cancer cell lines and cancer tissues have upregulated EPHA2 mRNA and protein expression and EPHA2 signalling has been shown to mediate cellular transformation, angiogenesis and metastasis [267]. EPHA2 was found to be overexpressed in 75.9% of invasive ovarian carcinomas studied by immunohistochemistry [37]. Similarly, EPHA2 was overexpressed in breast cancer tissue compared to normal breast tissue by immunohistochemistry and Western blot and overexpression of *EPHA2* in mammary epithelial cells was sufficient to induce transformation, morphological changes and loss of cell-to-cell contact [307]. Prostate cancer cell lines were also shown to have high levels of EPHA2 expression by Western blot and this was associated with metastatic potential [308], while EPHA2 overexpression in ovarian tumours was linked to advanced disease and poor survival [37]. Moreover, EPHA2 was exclusively expressed in a metastatic melanoma cell line, not in a poorly invasive melanoma cell line [309]. EPHA2 was found to be overexpressed in NSCLC cell lines and tumour samples and this overexpression was associated with worse prognosis [286]. Similarly, Tan *et al.* [310]

showed EPHA2 overexpression in malignant pleural mesothelioma (MPM) cell lines by immunoblotting and in MPM and non-small cell lung cancer (NSCLC)-squamous cell carcinoma (SCC) tumour specimens by immunohistochemistry. Further, the invasive tumour edge and NSCLC metastatic sites had higher EPHA2 expression than the primary tumour [286]. Importantly, EPHA2 protein expression was upregulated in KS skin tissue compared to uninvolved skin by immunohistochemistry [36].

EPHA2 has been shown to exhibit opposing roles in potentiating oncogenesis (Figure 5) via two key phosphorylation sites in its cytoplasmic region (see 1.6.2.1). EPHA2 inhibits cancer cell survival and trans-endothelial migration via a ligand and tyrosine kinase-dependent signalling mechanism (the canonical pathway) reliant on phosphorylation of Tyr772 [274,283,285,310–312]. Ephrin-A1 activation of EPHA2 via Tyr772, concomitant with dephosphorylation of phosphor-Ser897, and subsequent EPHA2 dimerization similarly inhibited cell migration in glioma and prostate cancer cells [311] and cell proliferation in malignant mesothelioma cells [312]. Accordingly, dephosphorylated EPHA2 at position Tyr772 functions as an oncoprotein [283,313,314]. Locard-Paulet *et al.* [283] found that Tyr772 was rapidly dephosphorylated in breast cancer cells upon endothelial cell contact and a comparison of breast cancer cell lines with differing metastatic potential showed dephosphorylated Tyr772 to be selectively associated with higher lung metastatic potential. Kikawa *et al.* [315] identified LMWPTP to be responsible for EPHA2 dephosphorylation in cancer cells. Overexpression of LMWPTP in epithelial cells was sufficient to confer transformation and enhance cellular adherence and proliferation [313,315]. However, in exception to this, sustained Tyr772 phosphorylation was observed upon ephrin-A1 stimulation in a parental breast cancer cell line, indicating that Tyr772 dephosphorylation may act as a molecular switch by which cancer cells can aggressively overcome ligand-dependent EPHA2 inhibition of oncogenesis [283].

Paradoxically, EPHA2 promotes tumour progression via ligand- and tyrosine kinase-independent activation (noncanonical pathway) and phosphorylation, predominantly albeit not exclusively, of Ser897 by Akt, RSK or protein kinase A (PKA)-dependent on the cellular context and induced by inflammatory cytokines and growth factors [285,311,316,317]. Ser897 mutant is sufficient to abolish cell migration [311]. In addition, Tyr772 phosphorylation in association with other tyrosine sites in the EPHA2 juxtamembrane region, such as Tyr588, has been noted in kinase- and ligand-independent mechanisms to modulate trans-endothelial migration [283]. The noncanonical pathway of unliganded activation of EPHA2 explains the enhanced tumorigenesis seen when EPHA2 is overexpressed in malignant cell lines or tissue (as above) which is often accompanied with low ephrin ligand expression [307,318–320]. Zelinski *et al.* [307] showed that failure of overexpressed EPHA2 to interact with its ligand is responsible for its oncogenic capacity.

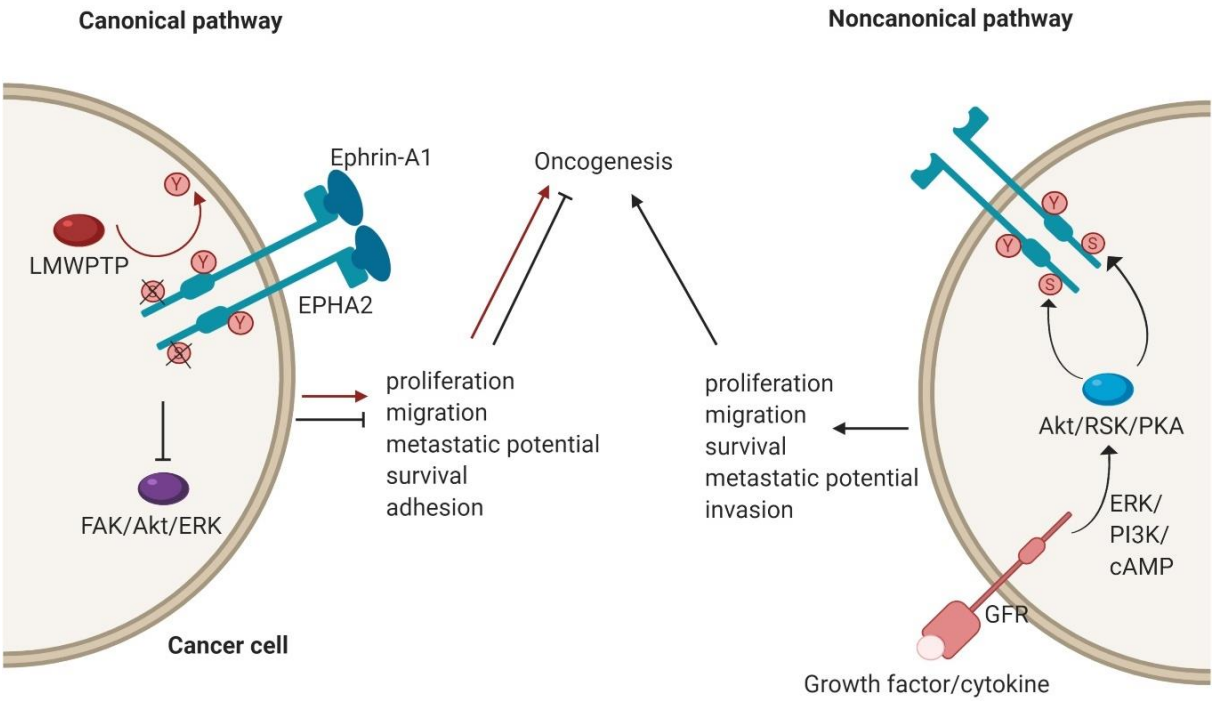

Figure 5: Schematic of the canonical and noncanonical oncogenic mechanisms of EPHA2. Tyrosine dephosphorylation promotes oncogenesis via the canonical pathway when the ligand is bound. In the absence of ligand binding, serine phosphorylation drives oncogenesis via the noncanonical pathway. Red circles indicate phosphorylated residues named by their IUPAC one-letter amino acid codes. Figure created with BioRender.

1.6.4. EPHA2 is a major KSHV entry receptor on endothelial cells

Hahn *et al.* [36] identified EPHA2 as the KSHV entry receptor on endothelial cells with an elegant series of experiments founded on co-precipitation of EPHA2 with KSHV virions and gH-gL. The authors showed that overexpression of EPHA2 proportionally increased KSHV infection (measured by green fluorescent protein (GFP) expression as a proxy for recombinant KSHV (rKSHV) that harboured the GFP gene) which closely correlated with EPHA2 expression levels in several primary cell lines. Conversely, blocking EPHA2 with antibodies or short interfering RNA (siRNA) or pre-treating KSHV with soluble EPHA2 inhibited KSHV infection. These findings were independently corroborated by immunoprecipitation of the lipid raft fraction using antibodies to α3β1 and mass spectrometry to identify EPHA2 in the multi-protein complex composed additionally of c-Cbl and myosin [122]. Similar to Hahn *et al*. [36], Chakraborty *et al*. [122] showed that attenuation of EPHA2 with tyrosine kinase inhibitors, short hairpin RNA (shRNA) or antibodies abolished KSHV entry into dermal endothelial cells. Subsequently, it was discovered that KSHV binds EPHA2 through the gH-gL glycoprotein complex at

the EPHA2 Eph-lbd (bp position 237–756, AA position 28–201), the same binding region as ephrin-A ligands which inhibited the interaction [321]. The intracellular Pkinase-Tyr domain (see 1.6.2.1) is important for KSHV infection, as overexpression of full-length EPHA2 but not a mutant EPHA2 with a deleted intracellular domain, enhanced infection by >70% [36]. This is due to the presence of tyrosine residues in the intracellular domain (see 1.6.2.1) that are phosphorylated upon KSHV treatment and signal activation of the receptor [36]. It has been suggested that phosphorylation of EPHA2 may facilitate KSHV infection by organising cell surface receptors on the membrane, as has been described for hepatitis C virus [36,322]. While EPHA2 is clearly a major KSHV entry receptor in endothelial cells, there is evidence that KSHV may further make use of alternative entry receptors [36,115].

1.6.5. Genetic variation in EPHA2

The majority of studies investigating sequence variants in EPHA2 have been in relation to cataract formation [279,294–298]. Age-related cortical cataract formation has been associated with a missense heterozygous transversion (c.2842G>T, SNP database ID: rs137853199) in an Italian cohort [279], two intronic *EPHA2* variants (rs477558 and rs7548209) in a Han Chinese cohort [296], two variants in the 3' region (rs7543472 and rs11260867) in an Indian cohort [295] and a synonymous variant in the Eph-lbd (c.573G>A, rs6678616) in a meta-analysis of patients from three Caucasian populations [294]. Congenital cataract formation has similarly been linked to EPHA2 sequence variants. A non-synonymous mutation (c.2353G>A, rs766078852) was identified in a consanguineous Pakistani family with autosomal recessive congenital cataracts [297], while autosomal dominant posterior polar congenital cataracts in a Han Chinese family was linked to an EPHA2 missense mutation (c.2819C>T, rs137853200) [298], and a two bp deletion (c.2915delTG) and a splicing variant (c.2826-9G-A) were identified in affected British and Australian families, respectively [298]. Few of these studies have corroborated the others, which may indicate that associations are population group-specific and that EPHA2 is genetically heterogenous amongst different ethnicities.

Few studies have investigated EPHA2 SNPs in relation to cancer. Rare SNPs located in Eph-lbd and Pkinase-Tyr domains were found to be prognostic of worse survival in multiple myeloma, such as c.2080A>G [323]. A non-synonymous EPHA2 mutation (p.Gly391Arg in the Fn-3 domain was detected in a SCC cell line and in 2/28 lung SCC patient samples [286]. Overexpression of this variant resulting in p.Gly391Arg in a human immortalised bronchial epithelial cell line revealed a phenotype of constitutive EPHA2 activation and increased invasiveness, focal adhesions and cell survival mediated by the phosphorylation of Src, cortactin, $p130^{Cas}$ and mTOR [286]. Another study similarly identified p.Gly391Arg in genomic DNA extracted from NSCLC-SCC tumour tissue as well as an Eph-lbd mutant

p.Arg159Gly, a Fn-3 domain mutant p.Pro350Thr, and Pkinase-Tyr domain mutations p.Met631Thr, p.Arg876Cys/His and p.Arg890Gln. Additionally, in MPM tumour tissues, the authors identified p.Thr140Ile, p.Asp184Tyr, p.Arg195Cys and p.Asp232Gly in the Eph-lbd and p.Thr647Met, p.Ala859Asp and p.Arg876His in the Pkinase-Tyr domain [310]. In particular, expression of the Pkinase-Tyr domain mutant p.Ala859Asp, which exhibited low levels of Y772 phosphorylation, in HEK293 cells resulted in increased proliferation and cell migration in wound healing assays mediated by upregulation of the STAT3 and platelet-derived growth factor (PDGF) pathways and suppression of CBL signalling [310]. Additionally, HEK293-EPHA2-p.Ala859Asp showed resistance to doxazosin treatment while BEAS2B cells expressing the EPHA2 Gly391Arg mutation were sensitive to a small molecule tyrosine-protein kinase Met (c-Met) inhibitor, SU11274 [310].

1.6.6. Association of EPHA2 sequence variation with KSHV and KS

Although vital in the uptake mechanism of KSHV [36] and significantly involved in oncogenesis [36,37,307], little was known about the pathological consequences of EPHA2 sequence variants on KSHV infection and/or KS development. We, therefore, performed a retrospective candidate gene association study on 150 HIV-infected South African patients who were grouped according to their KS status and KSHV serodiagnosis [34,35]; namely Group 1: KS+/KSHV+; Group 2: KS-/KSHV+; Group 3: KS-/KSHV-. Mutation analysis revealed two novel, non-synonymous heterozygous single nucleotide variants (SNV) (c.2254T>C and c.2990G>T) in the Pkinase-Tyr and SAM domains, respectively, to be significantly associated with KS; and a novel heterozygous transition (c.2727C>T) in Pkinase-Tyr to be significantly associated with KSHV (Table 3) [34,35]. These variants were designated a 'probably damaging' annotation when assessed for functional impact using the *in silico* PolyPhen-2 prediction tool (see 3.2.1, Table 23), thereby possibly predisposing affected individuals to KSHV infection and KS oncogenesis, respectively [34,35]. To frame the context of the current study, details of this previous association analysis are provided in section 3.2.1. In the present study, these variants were subjected to functional validation.

1.7. Rationale and aims

KSHV has a particularly high seroprevalence in SSA and in the context of HIV co-infection, can lead to the development of KSHV-associated pathologies (see 1.2.1 and 1.3), which likely represent a significant and currently under-recognised public health concern. While therapeutic options exist for

KS, KSHV-MCD and PEL, late and incorrect diagnosis limit the applicability of these in the SSA context where these conditions have high mortality if left untreated (see 1.3). Appropriate implementation of blood KSHV VL testing may offer a potential approach to improving diagnostic accuracy in HIV-infected populations with competing infectious co-morbidities (see 1.4), such as TB which is highly prevalent in South Africa and whose symptoms are often unspecific at presentation and mimic KSHV-associated diseases (see 1.1.2). Since testing for KSHV is not yet included in routine diagnostic workup, research is urgently needed to advance the differential diagnostic capabilities of KSHV-associated pathologies and link results to earlier implementation of appropriate treatments to improve outcomes. Therefore, we aimed to evaluate KSHV VL in the context of KICS-related symptoms and laboratory abnormalities in a cohort of HIV-infected patients presenting with suspected TB and assess the contribution of KSHV and KSHV associated pathologies to mortality in the context of TB and HIV infection.

Peculiar geographical epidemiology of KSHV seroprevalence and population-specific incidence of KS outside the setting of HIV (see 1.2.1 and 1.3.1.1), discrepancies in KSHV exposure and infection and KSHV/HIV co-infection and KS development in addition to evidence of familial aggregation of KSHV seroprevalence add to a growing body of evidence that points to a potential underlying genetic risk of susceptibility to KSHV and KS development (see 1.5). Host factor genetic association studies have primarily focused on immune-modulatory genes as risk factors for KS (see 1.5). The endothelial entry receptor for KSHV, EPHA2 is another promising candidate for investigation not only due to its key role in KSHV entry and intracellular trafficking in endothelial cells (see 1.2.3.2 and 1.6.4) but also its implication in oncogenesis (see 1.6.3), thus potentially acting at the level of both susceptibility to KSHV infection and susceptibility to KS development. Here, we aimed to validate previously identified EPHA2 variants associated with KSHV and KS (see 1.6.6) and further assess the functional consequences of EPHA2 variants on a molecular level in relation to KS oncogenesis and KSHV infection.

2. Materials and methods

2.1. Ethics

Ethics approval was obtained from the Human Research Ethics Committee (HREC), Health Sciences Faculty, University of Cape Town (UCT), for the enrolment of patients and collection of blood samples for the purposes of this study (HREC279/2008, HREC057/2013, HREC729/2014 and HREC136/2013).

2.2. Patient recruitment

Two patient cohorts from two sites were utilised for the purposes of this work: an existing hospitalised HIV-associated TB cohort (n=682), referred to as 'KDHTB cohort', which was recruited at Khayelitsha Day Hospital, Cape Town, South Africa, from January 2014 to October 2016 (UCT HREC Ref: 057/2013)[58]; and a KS cohort (n=100), referred to as 'KS cohort', which was recruited at the Radiation Oncology Unit at Groote Schuur Hospital (GSH, UCT HREC Ref: 279/2008) from December 2014 to February 2018.

2.2.1. KDHTB cohort

2.2.1.1. Study design

We conducted a retrospective analysis of an existing hospitalised HIV-associated TB cohort (n=682) in South Africa. The primary objective was to evaluate whether elevated KSHV VL, defined as >100 copies/10^6 cells, predicted 12-week mortality in the entire cohort, or in a subset that was culture-negative for TB. Secondarily, we evaluated associations of KSHV VL and serologic assays with clinical features in the cohort, as well as the use of clinical parameters that define KICS to predict mortality. Due to the retrospective nature of this study, no prospective sample size calculation was performed.

Dependent on KSHV status determined by enzyme-linked immunosorbent assay (ELISA, see 2.4), KS-negative samples from the KDHTB cohort were randomly selected as KSHV-positive or KSHV-negative controls for validation of EPHA2 SNP analysis (see 2.9).

2.2.1.2. Study cohort

HIV-infected adults presenting with clinical syndromes compatible with pulmonary or extrapulmonary TB were recruited at Khayelitsha Day Hospital, Cape Town, South Africa, from January 2014 to October 2016 in the context of a study entitled "Defining interventions to reduce mortality in severe HIV-associated tuberculosis" lead by Prof Graeme Meintjes (UCT). Emergency room and medical ward patients were screened, eligible patients were enrolled, and written consent was obtained. Eligible patients with a depressed level of consciousness were enrolled and followed up daily until they regained the capacity to consent. If a patient died prior to providing consent, we obtained approval from UCT HREC to use the patient's data. Clinical details, including physical examination with evaluation of skin and oral mucosa, and samples were collected at enrolment. CD4 cell count, HIV VL, CRP, full blood and differential count, and renal and liver function tests were performed by the National Health Laboratory Services (NHLS), as well as serum cryptococcal antigen lateral flow assays (IMMY). Citrate whole blood and plasma were stored at -80°C for KSHV VL and immunologic assays. The standardized TB diagnostic workup included sputum induction if required. TB blood culture in Myco/Flytic bottles (Becton Dickinson Biosciences), sputum Xpert MTB/RIF assay, sputum TB culture, urine lipoarabinomannan (LAM), and urine Xpert MTB/RIF on concentrated urine were performed during enrolment. Bacterial blood cultures were performed in all patients who had not received intravenous antibiotics prior to presentation to hospital. Patients were followed for 12 weeks to ascertain vital status.

2.2.1.3. Definition of patient groups

Patients were grouped into four overlapping categories based on the presence or absence of microbiologically confirmed infections. Group 1 (n=675) consisted of the total patient cohort analysed; Group 2 (n=500) included all patients with microbiologically confirmed MTB (on culture or GeneXpert on any clinical sample or urine LAM-positive); Group 3 (n=175) included the remainder of the total patient cohort without microbiologically confirmed MTB; Group 4 (n=159) consisted of Group 3 patients without another microbiologically confirmed infection (e.g. bacterial bloodstream infection or *Cryptococcus* species), although this group included some patients who were treated for TB despite negative microbiology. These groups are not mutually exclusive.

2.2.1.4. Definition of "possible KICS"

We evaluated Group 4 patients for KICS. The working case definition of KICS requires at least two clinical manifestations from at least two of three categories (Table 2 [6]): A) symptoms (including fever, fatigue, oedema, cachexia, respiratory symptoms, gastrointestinal disturbance, arthralgia and myalgia, altered mental state, and neuropathy); B) laboratory abnormalities (anaemia,

thrombocytopenia, hypoalbuminemia, and hyponatremia); and C) radiographic abnormalities (lymphadenopathy, splenomegaly, hepatomegaly, and body cavity effusions), together with evidence of systemic inflammation (elevated CRP), evidence of KSHV lytic activity (elevated [>100 copies/10^6 cells] KSHV VL in peripheral blood), and exclusion of MCD. As this analysis was done retrospectively, MCD could not be excluded for all patients, hence the designation "possible KICS" patients.

2.2.2. KS cohort

2.2.2.1. Study design

Further to our previous study [34,35], in which we identified significant associations of EPHA2 variants with KS development or KSHV seroprevalence with a sample size of n=150 powered to detect variants with minor allele frequency (MAF) >3%, we recruited a validation cohort of the same sample size (n=150) to supplement and validate the original cohort. Statistical association testing was designed as three analyses: 1) to assess susceptibility to KSHV infection by comparing KSHV seropositive cases to KSHV seronegative controls; 2) to assess KS development by comparing KS cases to KS-negative controls; and 3) to assess detectable KSHV VL in the blood by comparing KSHV seropositive patients with detectable KSHV VL to those with no detectable VL.

2.2.2.2. Study cohort

Patients with KS were recruited from the Radiation Oncology Unit, GSH, where they were receiving treatment for KS, under the supervision of radiation oncologist, Dr Zainab Mohamed. Patients with no KS were identified within the KDHTB study (see 2.2.1) in collaboration with Prof Graeme Meintjes [58] and KSHV serostatus was determined by ELISA (see 2.4). HIV-positive males and females over the age of 18 who were living in South Africa, irrespective of population group, were recruited to the study. Clinical diagnosis of KS was recorded in addition to demographic information (sex, age and population group) and appropriate clinical information (HIV status, latest CD4 count and ART treatment status) was sourced from patient records. KS treatment was recorded but not used as an exclusion criterion.

Enrolment was contingent on the patient giving their informed consent. Recorded patient information and collected samples were anonymised with numerical labelling that did not disclose patient identity. Information was recorded only if necessary for the study purposes and stored on a password-protected computer and in a locked office in accordance with the *Protection of Personal Information Act, No. 4* (2013).

2.2.2.3. Definition of patient groups

Patients were recruited into three groups determined by KS diagnosis and KSHV serostatus. The newly recruited validation cohort (n=150, 50 patients per group as below) was recruited from the same clinics as the original cohort (n=150, 50 patients per group [34]) to supplement the sample sizes:

Group 1 (KS+/KSHV+): patients with KS who were KSHV seropositive (n=100)

Group 2 (KS-/KSHV+): patients without KS who were KSHV seropositive (n=100)

Group 3 (KS-/KSHV-): patients without KS who were KSHV seronegative (n=100)

All patients had a thorough clinical examination by experienced clinicians to document the occurrence of typical KS cutaneous lesions, mucosal lesions and lymphoedema. When indicated, skin biopsy and chest X-ray supported the diagnosis of KS. KSHV serostatus was determined by KSHV ELISA (see 2.4).

2.3. Sample collection, preparation and storage

2.3.1. Sample collection

A nurse practitioner drew 10 ml of peripheral blood from the arm of each patient during their routine visit and, when possible, at the same time as drawing blood for medical purposes to reduce the patient's discomfort. Samples obtained for the KS cohort were collected in ethylenediaminetetraacetic acid (EDTA)-tubes and initially stored at room temperature preceding plasma preparation (see 2.3.2); then at 4°C prior to DNA extraction (see 2.3.3); and thereafter at -20°C at the Institute for Infectious Diseases and Molecular Medicine (IDM), UCT. KDHTB study samples were stored at -20°C after being allowed to settle.

2.3.2. Plasma preparation and storage

Plasma was prepared as soon as possible and within 4 hours (h) after collection of KS cohort samples (see 2.3.1) by centrifugation (Eppendorf 5810 R, 2237 x g for 10 minutes (min) at room temperature) to separate plasma from blood cells. Stored samples from the KDHTB cohort that had been allowed to settle before storage (see 2.3.1) were thawed at 4°C. Following centrifugation or thawing, tubes

were opened in a Biosafety Level 2 laboratory safety cabinet. Plasma was pipetted off the top layer of the separated blood and used immediately or stored in 500 µl aliquots at -20°C to avoid freeze-thawing.

2.3.3. DNA extraction, quality assessment and storage

Following removal of plasma, blood samples containing a leukocyte enriched buffy coat fraction and an erythrocyte fraction were immediately used for genomic DNA extraction using the QIAamp DNA Blood Mini or Midi kits (Qiagen) according to the manufacturer's protocol for DNA purification from blood (spin protocol). Following DNA isolation, DNA quantity and quality were assessed by nanodrop analysis and eluted DNA of good quality (ratio of absorbance at 260 nm to absorbance at 280 nm in the range 1.8–2.0) was stored in Buffer AE (Qiagen) at -20°C.

2.4. KSHV K8.1 and LANA ELISAs

KSHV ELISAs were performed for all patients to determine KSHV serostatus. Cryopreserved plasma (see 2.3.2) was tested by ELISA kits generously provided by Dr Denise Whitby (Frederick National Laboratory for Cancer Research, USA) [324] for antibodies against LANA (ORF73) and K8.1, following established specifications [324]. Briefly, ELISA plates coated either with recombinant K8.1 or LANA and stored at -80°C were thawed in a 37°C incubator. Once thawed, the plates were washed three times with at least 350 µl ELISA wash buffer (see Appendix 7.1) per well, inverted and patted dry on paper towel. Plasma samples stored at -20°C were thawed on ice, vortexed and diluted 1:10 with ELISA assay buffer (see Appendix 7.1). Samples were added to the K8.1 plate and the LANA plate at final dilutions of 1:20 and 1:100, respectively, as determined previously [324]. Only ELISA assay buffer was added to wells as blank controls. Ten pooled KS patient samples at a 1:10 dilution in ELISA assay buffer were used as a positive control, while a pool of ten samples from patients without KSHV served as our negative control. Sealed plates were incubated at 37°C for 90 min. Plates were subjected to five washes with ELISA wash buffer to remove unbound plasma components and dried on paper. ReserveAP Goat anti-Human IgG (H+L) phosphatase labelled antibody (KPL) was diluted with ELISA assay buffer (1:5000) and 100 µl per well was added after which the plate was incubated for 30 min at 37°C and then washed five times. Next, 100 µl of 1-step p-nitrophenyl phosphate (PNPP) substrate solution (Pierce Biotechnologies) was added to each well and the plate was incubated at room temperature in the absence of light for 25 min (K8.1 plates) or 30 min (LANA plates) at which point

the reaction was promptly stopped by adding 50 µl ELISA stop solution (see Appendix 7.1). The ELISA plates were flamed briefly with a Bunsen burner to remove any bubbles and read on an ELISA plate reader (Versa max, with the SoftMax Pro 6.3 software) at a wavelength of 405 nm. The raw values were adjusted according to the average optical density (OD) values of the blank controls. The cut-off OD values were calculated using the equation previously determined by Mbisa *et al.* [324]. The cut-off OD for the K8.1 ELISA was determined as:

$$ODcut\ off_{\text{K8.1}} = mean\ of\ negative\ controls_{\text{K8.1}} + 0.95$$

Similarly, the cut-off OD value for the LANA ELISA was:

$$ODcut\ off_{\text{LANA}} = mean\ of\ negative\ controls_{\text{LANA}} + 0.35$$

A sample was considered KSHV seropositive if antibodies to either antigen were detected [324]. The blank, negative and positive controls were assessed in each assay to determine its validity, as summarised in Table 4 below [324].

Table 4: Quality control specifications for the K8.1 and LANA ELISAs.

Control	K8.1 ELISA	LANA ELISA
Blank (raw value)	<0.20	<0.10
Negative control (blank adjusted)	0–0.30	0–0.20
	Mean x 0.5 - mean x 1.5	Mean x 0.5 - mean x 1.5
Positive control (blank adjusted)	>0.30	>1.0

2.5. KSHV viral load assay

KSHV VL was determined from the blood samples by quantitative TaqMan PCR to the K6 gene. The DNA concentration (see 2.3.3) was adjusted to 25 ng/µl, with 10 µl used per PCR reaction (total volume 50 µl) to detect KSHV DNA using 100 pmole K6 gene region forward and reverse primers (Table 5), 5 pmole FAM/TAMRA labelled probe [325] (Table 5), and 2X Universal Master Mix (Applied Biosystems). KSHV DNA was quantified against a K6-plasmid (kindly provided by Dr Denise Whitby, National Institute of Health (NIH)) standard curve of known concentration of K6 DNA on a LightCycler

480II System (Roche) as follows: 2 min at 50°C; 8 min at 95°C; and 45 cycles of 15 seconds (s) at 95°C and 1 min at 60°C. KSHV DNA concentration was normalised to the number of cellular equivalents in the sample, determined using a quantitative assay for human endogenous retrovirus 3 (ERV-3) which occurs at two copies per human cell. ERV-3 was similarly quantified using forward and reverse primers (Table 5) against a standard curve of known concentration of human ERV-3 DNA (kindly provided by Dr Denise Whitby, NIH) [326]. Assays were deemed valid based on several quality controls (Table 6). Samples were tested in triplicate, averaged, and reported as viral DNA copies per million cells.

Table 5: Primers and probes used in quantitative Taqman PCR to determine KSHV VL.

Primer or probe	Sequence 5'–3'
K6 forward primer	CGCCTAATAGCTGCTGCTACGG
K6 reverse primer	TGCATCAGCTGCCTAACCCAG
K6 probe	FAM-CACCCACCGCCCGTCCAAATTC-TAMRA
ERV-3 forward primer	CATGGGAAGCAAGGGAACTAATG
ERV-3 reverse primer	CCCAGCGAGCAATACAGAATTT
ERV-3 probe	FAM-TCTTCCCTCGAACCTGCACCATCAAGTCA-TAMRA

Table 6: Quality control specifications for the KSHV VL assays.

Control	K6 assay	ERV-3 assay
No template control	No amplification	No amplification
Negative control	No amplification	No amplification
Positive control (Mean copy number range)	10–50,000	10 –100,000
Standard curve slope range	-3.2– -3.7	-3.2– -3.7
Standard curve R^2 value	>0.97	>0.97
Standard curve Y-intercept (range)	37–43	37–43
Standard curve average Ct values (range)	10^6: 18.3–19.5	10^6: 19.3–20.5
	10^5: 21.5–23.3	10^5: 22.5–24.0
	10^4: 25.4–27.0	10^4: 26.3–27.6
	10^3: 28.6–30.4	10^3: 29.4–31.0
	10^2: 32.6–34.2	10^2: 33.3–36.0
	10^1: 37.0–39.0	10^1: 37.0–39.7
	10^0: 39.1–45.0	10^0: 38.0–45.0

2.6. IL-6 assays

Plasma IL-6 was measured using the Human IL-6 SimpleStep ELISA kit (Abcam), with a minimum detectable dose of 1.6 pg/ml[1] quantified against a standard curve of human IL-6 recombinant protein. Briefly, standards were prepared by serial dilution of the supplied human IL-6 recombinant protein which was reconstituted at 2,000 pg/ml in Sample Diluent NS (proprietary reagent, ab193972 Abcam). The blank standard contained only Sample Diluent NS. Plasma samples were thawed on ice and vortexed before 50 µl of sample or standard was added undiluted and in duplicate to the provided ELISA plates that were pre-coated with an anti-tag antibody. An antibody cocktail (50 µl) consisting of Human IL-6 tag-labelled capture antibody and a reporter conjugated detector antibody was added to the sample in the ELISA plate and the capture antibody/analyte/detector antibody complex was immobilised during 1 h incubation at room temperature on a plate shaker set to 400 revolutions per minute (rpm). The plate was washed three times to remove unbound material with 350 µl Wash Buffer PT (proprietary reagent supplied with the kit, Abcam) and the plate blotted against paper towel to remove excess liquid. Next, 100 µl 3,3',5,5'-Tetramethylbenzidine (TMB) Substrate (supplied with kit, Abcam) was added to each well and the plate was incubated in the dark for 10 min on a plate shaker set to 400 rpm at which point 100 µl Stop Solution (proprietary reagent supplied with kit, Abcam ab178013) was added to each well. The plate was shaken on a plate shaker for 1 min to ensure thorough mixing and the absorbance at 450 nm was immediately read on a fluorometer (Versa max, with the SoftMax Pro 6.3 software). The average absorbance for the blank controls was subtracted from all absorbance values. A standard curve was constructed by plotting these adjusted standard absorbance values against the known protein concentration and the sample concentrations were calculated by interpolating the absorbance values onto the standard curve. Samples that were found to have absorbance values greater than the highest standard, were diluted and run again and the resultant concentrations corrected by the appropriate dilution factor.

2.7. Post-mortem histology

Post-mortem histology was performed on one patient lymph node to ascertain a diagnosis of MCD or KICS by Michael Locketz of the NHLS. After obtaining consent from the family, an excisional cervical

[1] The reference median for IL-6 in HIV-infected patients is 1.80 pg/ml (interquartile range, 1.20–2.89 pg/ml) [346].

lymph node biopsy was performed two days post-mortem. Tissue was fixed in 10% formal saline for 48 h, processed overnight in a Tissue-Tek Vacuum Infiltration Processor (Sakura Finetek), and embedded in paraffin. Tissue sections were cut at 4 µm thickness and stained with haematoxylin and eosin and ORF73 immunoperoxidase (Cell Marque) using the Benchmark XT automated staining platform with the Ventana ultraView Universal DAB Detection kit (Roche Diagnostics). Immunostaining for kappa and lambda light chains was also performed. Photomicrographs were obtained with an Olympus SC30 3.3 megapixel USB digital colour camera attached to an Olympus BX41 microscope using analySIS getIT 5.1 digital imaging software (Olympus Soft Imaging Solutions).

2.8. Statistical analysis of KDHTB clinical data

KSHV VL was treated both as a categorical variable (elevated >100 copies/10^6 cells vs ≤100 copies/10^6 cells or nondetectable) and a continuous variable and assessed for association with mortality using the $\chi 2$, Fisher exact, or Wilcoxon rank-sum test, as appropriate. The relationship between KSHV VL and mortality was assessed by binomial logistic regression, controlling for age, sex, CD4 cell count, and ART status. Linearity of the continuous variables with respect to the logit of the dependent variable was confirmed via the Box–Tidwell procedure [327], and studentized residuals with values <2.5 standard deviations were accepted. To compare "possible KICS" patients to the remainder of the cohort, associations of categorical variables (sex, receiving ART, KSHV seropositivity, presence of skin KS) and continuous variables (age, weight, HIV VL, CD4 cell count, KSHV VL, K8.1 and ORF73 antibody levels, IL-6, CRP, haemoglobin, white cell count, platelet count, albumin, and sodium) were assessed by Fisher exact or Wilcoxon rank-sum test, respectively. To assess the independent associations of KSHV seropositivity or KSHV antibody levels with mortality, binomial logistic regression or multiple linear regression was performed, respectively. Continuous variables were transformed, where appropriate, to approximate normal distributions. Survival analysis was performed using the Kaplan–Meier method and log-rank sum test. P values were two-tailed and considered significant if <0.05. Statistical testing was performed using SPSS version 25 (IBM Corp, 2017). Performance characteristics of KICS criteria for predicting death were calculated in R (R Core Team, 2019) using a confusion matrix.

2.9. Validation of EPHA2 SNVs associated with KSHV and/or KSHV

Previous work identified potentially important SNVs in the EPHA2 coding DNA sequence, particularly

in exons 12–17, that were significantly associated with KSHV and KS, however, the study was limited by the small sample size of only 50 patients per group. Based on this previous work, additional patients were now recruited (see 2.2) and a combined analysis of this gene region performed to strengthen previous data.

2.9.1. PCR amplification of selected EPHA2 exons

PCR was performed to amplify the Pkinase-Tyr domain (Exons 12–15) and the SAM domain (Exons 16–17) of the EPHA2 gene (Figure 4) using a number of gene-specific primers (Table 7) together with the FastStart Taq DNA Polymerase kit (Roche) according to the manufacturer's instructions. PCR reactions contained final concentrations of the following reagents: 1X PCR buffer with 2 mM $MgCl_2$; 200 µM nucleotide mix; 0.2 µM forward primer; 0.2 µM reverse primer; 1 U FastStart Taq DNA polymerase; and 2 ng/µl DNA to a total volume of 25 µl. PCR reactions were cycled on a thermal cycler (Applied Biosystems GeneAmp® PCR system 2700 or Perkin Elmer GeneAmp® PCR system 2400) as follows: 4 min at 95°C; 35 cycles of 30 s at 95°C, 30 s at 60°C (or 62°C for exon 14) and 45 s at 72°C; and 1 min at 72°C.

Table 7: Primer sequences for PCR of EPHA2 Pkinase-Tyr and SAM domains [34,36]**.** F and R refer to forward and reverse primers, respectively. Amplicon length is calculated based on the EPHA2 NCBI reference sequence (ID: NM_004431.3).

EPHA2 domain	Exon	Primer sequence (5'–3')		Amplicon length (bp)
Pkinase-Tyr	12	F	TGGTGGTGTAGGTGGCCTCG	602
		R	TACCTCTGCCCACTCCTCCG	
	13	F	CGTCGCTGGCAGAGGTGAAC	600
		R	CCCTGGACAAGTTCCTTCGGG	
	14	F	AACTGTCCTCTGCCCAGCCC	455
		R	CGAGGCCACCTACACCACCA	
	15	F	CTGGGCCATCGTGTCCAGTC	517
		R	GGGCAGCTCTGAAGGTTGGG	
SAM	16	F	TGGCGGAGTTCTGCCCTTCT	458
		R	GACTGGGCTTCCCTGTTGCC	
	17.1	F	AGGGACCGCTTTGGGTCTCA	596
		R	CTCTCCCTCTCTCCCTCCCG	

2.9.2. Agarose gel electrophoresis of DNA

Following cycling, PCR amplicons (5 µl) mixed with 1 µl 6X gel loading dye (Thermo Fisher Scientific) alongside a GeneRuler 1 kb DNA ladder (250-10,000 bp, Thermo Fisher Scientific) were electrophoresed on a 1% agarose gel containing SYBRSafe nucleic acid gel stain (Life Technologies, 1:10,000) in 1X tris-acetate-EDTA (TAE) (see Appendix 7.1) for 1 h at 100 V. Following separation, the DNA bands were visualised under UV light to confirm that the individual PCR products were amplified successfully and specifically.

2.9.3. Dideoxy DNA sequencing

PCR products were purified and sequenced using dideoxy sequencing with the gene-specific primers used for PCR (Table 7) at the Stellenbosch Central Analytical Facility. Sequencing was performed in both the forward and reverse direction to ensure reliable sequence determination. Sequence quality was assessed by viewing the sequence chromatograms on the programme BioEdit (version 7.2.5 ©1997–2013).

2.9.4. Bioinformatic processing of sequence data

Computational processing of the sequence data was performed on the UCT Information and Communication Technology Services High Performing Computing Cluster using bioinformatics programmes encompassed in the European Molecular Biology Open Software Suite (EMBOSS) [328], followed by ClustalW2 multiple alignment (EMBL) [329] to compare the sequences to the EPHA2 reference sequence (NM_004431.3). DNA sequence variants that were predicted to be non-synonymous through *in silico* translation were further assessed for predicted functional consequences using the PolyPhen-2 prediction tool [330]. The SNP database was consulted to assess if the identified variants had been previously reported [331].

2.9.5. Statistical analysis of EPHA2 SNV data

Statistical testing of demographic data included Fisher exact tests for categorical variables: sex, population group and ART status; and Mann-Whitney test for continuous variables: age and CD4 count

using in IBM SPSS Statistics (Version 25.0. Armonk, NY: IBM Corp). This analysis was done according to the comparisons used for association testing (see 2.9.5.2).

2.9.5.1. Aggregate analysis of previous data

In order to determine whether less common variation was associated with KSHV infection and KS status, particularly since using a rather small patient cohort of n=150, we performed an aggregate analysis on our original cohort as in previous studies [332,333] in which we considered whether each participant carried ≥1 or 0 EPHA2 SNV with MAF <5%. Aggregate scores were determined for all SNVs across EPHA2 and for missense, synonymous and UTR variants. Additionally, aggregate scores were determined by functional domain (Pkinase-Tyr, SAM, 5`-UTR, 3`-UTR and Fn-3 domains). Associations between aggregate scores and case-control status were determined using logistic regression.

2.9.5.2. Association testing

Identified sequence variants were statistically analysed for association with KSHV serostatus, KS prevalence and KSHV VL detection. Contingency tables (2x2) assessed the occurrence of variants on the genotypic level in cases versus controls and Fisher Exact association tests were performed in IBM SPSS Statistics (Version 25.0. Armonk, NY: IBM Corp), as described [334], using the following comparisons, as appropriate:

Association with KSHV serostatus: Groups 1 and 2 (KSHV+) vs. Group 3 (KSHV-)
Association with KS development: Group 1 (KS+/KSHV+) vs. Group 2 (KS-/KSHV+)
Association with detectable VL: Detectable VL vs. Non-detectable VL within KSHV+ (Groups 1 and 2) patient groups.

A P value <0.05 was considered significant. Fisher exact tests were corrected for multiple comparisons using the Bonferroni-corrected pairwise technique.

2.9.5.3. Logistic regression

With KSHV serostatus, KS status or KSHV VL status as the binomial dependent variable, the relationship of SNVs identified through association testing (see 2.9.5.2) were subjected to binomial logistic regression, controlling for age, sex, CD4 cell count, and ART status as appropriate for the comparison.

2.10. Plasmids used in this study

Plasmids used in this study are detailed in Table 8. The pLentiCRISPR v2 into which the CRISPR/Cas9 guide RNA (gRNA) target sequences (G1, G2 and G3) were cloned (see 2.13.1) was provided by Dr Klaus Heger and Dr Marc Supprian (Max Planck Institute of Biochemistry, Germany) and engineered by Dr Janina Bruening, Institute for Experimental Virology, Twincore, Hannover Medical School, Germany (see 2.13.1). This plasmid contains both puromycin and ampicillin resistance genes. Lentiviral packaging vectors pCMV-VSV-G and pCMVR8.74, containing ampicillin resistance genes, were received from Dr Janina Bruening and Prof Dr Thomas Pietschmann, Institute for Experimental Virology, Twincore, Hannover Medical School, Germany. The lentiviral vector (HIV-1 based) RRL.SF.newMCS.i2.Zeo.pre containing ampicillin and zeocin resistance genes was kindly provided by Dr Melanie Galla, Prof Dr Christopher Baum and Prof Dr Axel Schambach, Institute of Experimental Haematology, Hannover Medical School, Germany. RRL.SF.newMCS.i2.Zeo.pre was engineered to carry the synthetic EPHA2 (sEPHA2) coding DNA sequence (see 2.15.1) and subjected to site-directed mutagenesis (SDM, see 2.14). The plasmid 17ADD7RP_sEPHA2_pMA consisting of sEPHA2 cloned into a pMA backbone with ampicillin resistance was purchased from Geneart, Invitrogen, Thermo Fisher Scientific. The human EPHA2 ORF mammalian expression plasmid pCMV3-EPHA2 and the pCMV3-untagged negative control vector, both containing ampicillin resistance genes, were purchased from Sino Biological Inc. The pCMV3-EPHA2 was subjected to SDM (see 2.14).

Table 8: Plasmids used in this study. Affiliations are indicated: [1]Max Planck Institute of Biochemistry, Germany, [2]Institute for Experimental Virology, Twincore, Hannover Medical School, Germany; [3]Institute of Experimental Haematology, Hannover Medical School, Germany.

Plasmid name	Source	Purpose	Selection marker	Plasmid map
pLentiCRISPR v2	Kindly provided by Klaus Heger and Marc Supprian[1]	Cas9 containing lentiviral backbone into which gRNA sequences can be cloned.		
Scr.pLentiCRISPR v2 G1.pLentiCRISPR v2 G2.pLentiCRISPR v2 G3.pLentiCRISPR v2	Engineered by Janina Bruening[2] (see 2.13.1)	EPHA2-specific gRNA containing CRISPR/Cas9 lentiviral backbone for production of lentiviruses in conjunction with envelope and packaging vectors.	Puromycin/ ampicillin	Supplementary figure 1
pCMV-VSV-G	Kindly provided by Janina Bruening[2]	Envelope protein for the production of lentiviruses in conjunction with packaging vectors.	Ampicillin	Supplementary figure 2
pCMVR8.74	Kindly provided by Janina Bruening[2]	Packaging vector for production of lentiviruses.	Ampicillin	Supplementary figure 3
RRL.SF.newMCS.i2.Zeo.pre	Kindly provided by Melanie Galla, Christopher Baum and Axel Schambach[3]	Lentiviral backbone into which genes of interest can be cloned.		Supplementary figure 4
sEPHA2-RRL.SF.newMCS.i2.Zeo.pre	Engineered by cloning (see 2.15.1)	sEPHA2 containing lentiviral backbone for production of lentiviruses in conjunction with envelope and packaging vectors.	Zeocin/ ampicillin	
sEPHA2-SDM- and sEPHA2-SDM1–8-RRL.SF.newMCS.i2.Zeo.pre	Engineered by SDM (see 2.14)	sEPHA2 (subjected to SDM) containing lentiviral backbone for production of lentiviruses in conjunction with envelope and packaging vectors.		Supplementary figure 5
17ADD7RP_sEPHA2_pMA	Purchased from Geneart, Invitrogen, Thermo Fisher Scientific	Synthetic EPHA2 cloned into standard backbone vector for cloning.	Ampicillin	Supplementary figure 6
pCMV3-untagged	Purchased from Sino Biological Inc.	Empty negative control vector.	Ampicillin	Supplementary figure 7
pCMV3-EPHA2	Purchased from Sino Biological Inc.	EPHA2 expression vector.	Hygromycin/ ampicillin	Supplementary figure 8
pCMV-3 EPHA2 SDM 1–7	Engineered by SDM (see 2.14)	EPHA2 (subjected to SDM) expression vectors.		

2.11. Cell culture

2.11.1. Established cell lines

Human embryonic kidney 293 cells (HEK293; Cellonex, C293-C) and HEK293T (derived from HEK293 cells by stably expressing simian virus 40 (SV40) large T antigen (TAg); DSMZ No.: ACC 305) were maintained in Dulbecco's Modified Eagle Medium (DMEM) supplemented with 10% heat-inactivated foetal bovine serum (FBS; Sigma). BJAB-rKSHV.219 cells [335], SLK (of epithelial cell origin) and SLK EPHA2-KO cells were grown and maintained in Roswell Park Memorial Institute (RPMI) 1640 medium supplemented with 20% heat-inactivated FBS in the presence of 4.2 µg/ml puromycin and expanded in spinner flasks (Lasec, South Africa). These cells were derived from the Burkitt lymphoma-derived B-cell line BJAB (ACC 757) stably infected with a JSC-1 derived recombinant KSHV.219 (hereafter referred to as rKSHV) that expresses both the red fluorescent protein (RFP) under the control of the KSHV lytic gene PAN promoter as well as GFP under the control of the cellular EF-1α promoter in addition to the puromycin resistance gene as a selectable marker [336]. Lymphatic endothelial cells (LEC) and LEC EPHA2-KO cells in addition to HuARLT2 cells which are a derivation of HUVECs conditionally immortalised by expressing doxycycline-inducible transgenes SV40 large TAg and human telomerase reverse transcriptase (hTert) [337], were grown and maintained in endothelial cell growth basal medium (EBM-2, Lonza) containing supplements and growth factors included in the microvascular (MV) endothelial SingleQuots kit (Lonza, complete media called EGM-2MV contained 5% FBS, 0.5 ml human epidermal growth factor (hEGF), 0.2 ml hydrocortisone, 2 ml basic fibroblast growth factor (FGF-B), 0.5 ml VEGF, 0.5 ml arginine 3-insulin-like growth factor (R3-IGF-1), 0.5 ml ascorbic acid and 0.5ml gentamicin-amphotericin-B (GA-1000) per 500 ml EMB-2) in the presence of 1 µg/ml doxycycline (Sigma-Aldrich). HEK293T, BJAB-rKSHV.219 and HuARTL2 cell lines were kindly provided by Prof Thomas Schulz (MHH, Hannover, Germany) and SLK, SLK EPHA2-KO cells, LEC and LEC EPHA2-KO cells were a kind gift from Dr Frank Neipel, Institute of Clinical and Molecular Virology, University Clinic, Erlangen, Germany.

2.11.2. Cell lines engineered in this study

All engineered cell lines generated in this study are summarised in Table 9. The HuARLT2 cell line was subjected to CRISPR/Cas9 knockout (see 2.13) directed towards the EPHA2 gene generating three cell lines, namely Hu-G1, Hu-G2 and Hu-G3 (the latter was further referred to as Hu-KO) which were transduced with CRISPR/Cas9 lentivirus containing gRNA1, gRNA2 or gRNA 3, respectively. Similarly,

CRISPR/Cas9 with lentivirus containing scrambled gRNA was generated as a control cell line. These CRISPR/Cas9 engineered cell lines were maintained in EGM-2MV media containing 1 µg/ml doxycycline. The Hu-KO cell line was further modified by lentiviral transduction (see 2.15) of the RRL.SF.newMCS.i2.Zeo.pre vector alone (empty vector (EV) control) or vector containing wild type (WT) sEPHA2 or sEPHA2 having undergone SDM (see 2.14). These transduced cell lines were maintained in EGM-2MV media containing 1 µg/ml doxycycline and 200 µg/ml zeocin.

2.11.3. Maintaining cell cultures

All cells were maintained in the media specified above at 37°C in a humidified incubator with 5% CO_2.

Table 9: Engineered cell lines transduced with the indicated lentiviruses.

Cell line name	Parent cell line	Lentiviral vector	Modification from parent cell line
Hu-G1	HuARLT2	G1.pLentiCRISPR v2	gRNA 1 targeting EPHA2
Hu-G2	HuARLT2	G2.pLentiCRISPR v2	gRNA 2 targeting EPHA2
Hu-G3/ Hu-KO	HuARLT2	G3.pLentiCRISPR v2	gRNA 3 targeting EPHA2
Hu-Scr	HuARLT2	Scr.pLentiCRISPR v2	scrambled gRNA.
Hu-EV	Hu-KO	RRL.SF.newMCS.i2.Zeo.pre	Empty vector
Hu-WT	Hu-KO	sEPHA2.RRL.SF.newMCS.i2.Zeo.pre	sEPHA2 wildtype
Hu-WT-SDM	Hu-KO	sEPHA2-SDM.RRL.SF.newMCS.i2.Zeo.pre	sEPHA2 wildtype (SDM with control primers)
Hu-SDM1	Hu-KO	sEPHA2-SDM1.RRL.SF.newMCS.i2.Zeo.pre	sEPHA2 C915T
Hu-SDM2	Hu-KO	sEPHA2-SDM2.RRL.SF.newMCS.i2.Zeo.pre	sEPHA2 A2257C
Hu-SDM3	Hu-KO	sEPHA2-SDM3.RRL.SF.newMCS.i2.Zeo.pre	sEPHA2 T2254C
Hu-SDM4	Hu-KO	sEPHA2-SDM4.RRL.SF.newMCS.i2.Zeo.pre	sEPHA2 A2257C and T2254C
Hu-SDM5	Hu-KO	sEPHA2-SDM5.RRL.SF.newMCS.i2.Zeo.pre	sEPHA2 G2688C
Hu-SDM6	Hu-KO	sEPHA2-SDM6.RRL.SF.newMCS.i2.Zeo.pre	sEPHA2 C2727T
Hu-SDM7	Hu-KO	sEPHA2-SDM7.RRL.SF.newMCS.i2.Zeo.pre	sEPHA2 G2990T
Hu-SDM8	Hu-KO	sEPHA2-SDM8.RRL.SF.newMCS.i2.Zeo.pre	sEPHA2 G2844A

2.11.4. Sub-culturing cells

Adherent cell lines were grown in 75 cm^2 cell culture flasks (SPL Life Sciences) until 80–90% confluency before being washed with phosphate-buffered saline (PBS, 1X) and removed from the flask enzymatically with 0.025% trypsin/0.01% EDTA or accutase (Biowest, for HuARLT2 and LEC cells). Cells were pelleted at 400 x g for 3 min and resuspended in fresh media at the appropriate ratio.

2.11.5. Cell counting and plating

To count cells, 10 µl of re-suspended cells were added to 90 µl of a 0.4% trypan blue solution (Sigma), and 10 µl of this was placed on the Neubauer haemocytometer (Marienfeld) on which a coverslip was placed. Trypan blue allows identification of live cells. Using a microscope (Nikon TMS) live cells were counted and cell concentration was determined using the following formula:

$$\frac{number\ of\ cells\ counted\ in\ 4\ squares\ of\ hemocytometer}{4} \times 10\ \times 10{,}000\ = cells/ml$$

Cell suspensions were diluted to the required density in media and added to the appropriate cell culture plate. Cells maintained in selection media were plated in the presence of antibiotics.

2.11.6. Storage of cell lines in liquid nitrogen

Cell lines were cryopreserved in liquid nitrogen for long term storage. To prepare cells for storage in liquid nitrogen, cell pellets were resuspended in media containing 10% dimethyl sulfoxide (DMSO) and transferred to cryovials. Cells were frozen in a Mr Frosty™ freezing container (Thermo Fisher Scientific) containing isopropanol at -80°C for at least 24 h before being transferred to liquid nitrogen storage. To thaw cells after storage in liquid nitrogen, cryotubes were transported on ice before being thawed rapidly in a 37°C water bath. Cells were resuspended in 4 ml pre-warmed media before being pelleted at 400 x g for 3 min. Cells were resuspended in 10 ml media and added to a cell culture flask.

2.11.7. Mycoplasma testing

Cell lines were routinely tested for mycoplasma contamination. Cells were plated on glass coverslips and, 24 h later, fixed and stained with Hoechst fluorescent DNA-binding stain (Sigma), mounted and visualised on a Zeiss Axiovert 200M Fluorescent Microscope (Carl Zeiss, Jena, Germany).

2.12. Transfection of EPHA2 expression constructs into HEK293 cells

HEK293 cells were plated at a density of $2.5x10^5$ cells/well per transfection in 12-well cell culture plates (see 2.11.5). The next day, 1 µg plasmid DNA (pCMV EV control, pCMV-EPHA2-WT or pCMV-EPHA2 SDM variants) was added to 3 µl Fugene Transfection Reagent (Promega) in 100 µl DMEM (without FBS, pre-incubated at room temperature for 5 min) and incubated at room temperature for 15 min. The transfection mixture was added to cells and incubated for 48 h at 37°C in a 5% CO_2 incubator. Cells were lysed for Western blot (see 2.20.1) or further used in infection experiments (see 2.17).

2.13. CRISPR/Cas9 knockout of endogenous EPHA2

2.13.1. CRISPR/Cas9 gRNA design and plasmid construction

CRISPR plasmids were engineered by Dr Janina Bruening (Institute for Experimental Virology, Twincore, Hannover Medical School, Germany). Three gRNA target sequences were designed to knock out EPHA2 using the online tool CHOPCHOP [338,339] targeted to *H. sapiens* (hg38/GRCh38) EPHA2 (NM_004431; isoform 1) and selected using the CHOPCHOP ranking and binding site (Table 10). Binding sites for gRNAs in the 5' region were preferred to avoid generation of a truncated protein rather than knockout (Table 10). Complementary single-stranded oligonucleotides containing the selected gRNA sequences and a scrambled gRNA as a control, appropriate protospacer adjacent motif (PAM, "CACC") sequence and *Bsm*BI restriction sites were synthesised (Institute for Experimental Virology, Twincore, Hannover Medical School, Germany). The pLentiCRISPR v2 plasmid and annealed double-stranded oligonucleotides were cut with *Bsm*BI and ligated with T4 ligase (Thermo Fisher Scientific) as previously described [340,341].

Table 10: Selected gRNA sequences for EPHA2 CRISPR/Cas9 knockout.

Name	CHOPCHOP ranking	Gene-specific gRNA sequence (without PAM and *Bsm*BI site)	Exon	Strand	GC content (%)	Self-complementarity	Off-target sites
G1	1	GTGCGGGTCAGTCCGTGAGG	5	+	70	0	0
G2	6	GAAGGTAACTCCCAGAGGGG	6	-	65	0	0
G3	14	CGCACCAACTGGGTGTACCG	3	-	65	0	0

2.13.2. Transformation and plasmid DNA extraction of CRISPR/Cas9 plasmids

Ligated plasmid DNA (see 2.13.1) was transformed into *E.coli* TG2 competent cells that were thawed on ice following storage at -80°C. Briefly, 1 µl ligation mixture was added to the thawed competent cells and kept on ice for 30 min. Cells were heat-shocked by placing the Eppendorf tubes in a water bath at 42°C for 45 s and then immediately back on ice for 10 min. Luria Bertani (LB) media (see Appendix 7.1) was pre-warmed to 37°C and 700 µl was added to each tube of transformed cells which were incubated at 32°C for 1 h in a shaking incubator. Liquid cultures were centrifuged at 1000 x g for 3 min and 500 µl supernatant removed to concentrate the cells. 100 µl of the remaining culture was spread on agar plates containing ampicillin (75 µg/ml) and incubated at 32°C overnight. The following day, colonies were picked into 3 ml LB containing ampicillin (75 µg/ml) and incubated at 32°C overnight in a shaking incubator before expanding into a 350 ml LB liquid culture (75 µg/ml ampicillin) which was incubated at 32°C overnight in a shaking incubator. Plasmid DNA was isolated from the liquid culture the following day using the Endofree Plasmid Maxi kit (Qiagen) according to the manufacturer's instructions. DNA was quantified by nanodrop (see 2.3.3).

2.13.3. Lentivirus production

HEK293T cells were seeded at a density of $3.5x10^6$ cells per dish in a 10 cm cell culture dish in DMEM. The following day, cells were co-transfected with gRNA containing pLentiCRISPR v2 and packaging vectors, pCMV-VSV-G and pCMVR8.74 (kindly provided by Prof Dr Thomas Pietschmann and Dr Janina Bruening, Institute for Experimental Virology, Twincore, Hannover Medical School, Germany), using Lipofectamine (Invitrogen) according to the manufacturer's instructions. The following day, media containing the transfection mix was replaced with fresh DMEM containing 30% FBS. The following day,

CRISPR/Cas9 lentiviruses were harvested from the cell culture supernatants by filtering the media through 0.45 µm pore size filters and buffered with HEPES (1:50). Polybrene (Sigma-Aldrich, 5 µg/ml) was added to the virus preparations. Viruses were used immediately or stored at -80°C.

2.13.4. Virus transduction

Target cells (HuARLT2) were seeded at a density of $5x10^5$ cells/well in a 6-well plate. One well was seeded as a negative control for selection. Four h later, media was removed, and 1 ml lentivirus and 5 µg/ml polybrene-containing media was added per transduction. Cells were incubated for at least 4 h after which 2 ml fresh media was added. Forty-eight hours later, media was removed and selection media containing puromycin (4.2 µg/ml) was added to the transduced cells as well as the negative control cells. Selection media was changed daily, and cells were expanded once all of the negative control cells were dead. The three knockout cell lines were then assessed for EPHA2 knockout by Western blot (see 2.20) and sequencing with primers designed to amplify the cut site of transduced cells (Table 11).

Table 11: Primers for amplification and sequencing of genomic DNA of CRISPR/Cas9 transduced cells to analyse cut site gRNA. Tm=melting temperature of primer.

Primer name	Primer sequence	Tm (°C)	Amplicon size (bp)
5' gRNA1	AGCACTGACTCCTCCTGTCTGT	60.5	279
3' gRNA1	GTGAAGGTGTAGTTCATGTGGG	59.4	
5' gRNA2	TAGGCAGCTTCTTACCCACTTC	59.9	234
3' gRNA2	GTGATCATCTATGTGACCAGCC	59.4	
5' gRNA3	CATGAATGACATGCCGATCTAC	60.4	261
3' gRNA3	ATGGTGTCAATCTTGGTGAACA	60.3	

2.14. Site-directed mutagenesis

Point mutations (Table 12) were introduced into the EPHA2-CMV expression plasmid (Sino Biological Inc.), the sEPHA2 cloning vector (17ADD7RP_sEPHA2_pMA, Geneart Invitrogen) or the sEPHA2-RRL.SF.newMCS.i2.Zeo.pre lentiviral vector using the Agilent Quick Change II or Agilent Quick Change XL SDM kit. Briefly, thermal cycling was performed with SDM primers (designed using the QuikChange

Primer Design Program (Agilent), synthesised by the UCT Synthetic DNA lab or Inqaba Biotech, South Africa, and PAGE purified, Table 12) to synthesize the mutant strand. Primers SDM1–7 were designed to introduce EPHA2 SNVs previously identified in our clinical association study [34] and SDM8 primers were designed to introduce a previously described serine phosphorylation deficient mutant, c.G2844A [127], (Table 12). As a control, SDM with benign primers identical to the WT sequence (i.e. inducing no mutagenesis) was performed so that the Hu-WT-SDM cell line was subjected to the same experimental steps as the SDM cell lines, removing the possibility that any functional differences seen were due to experimental conditions. This was followed by *Dpn*I digestion of the parental strand. *Dpn*I digested DNA was transformed into E.*coli* XL1-Blue supercompetent cells and spread onto agar plates containing 75 µg/ml ampicillin. Plates were incubated at 37°C (or 32°C for the lentiviral vector) overnight. The following day, colonies were picked into ampicillin containing LB media and incubated

Table 12: Primers used for site directed mutagenesis.

Introduced mutation	Primer name		Primer sequence (5'–3')	Source
C915T	SDM 1	F	CCAATGGGCACCAACCACTCGCCATCC	[34]
		R	GGATGGCGAGTGGTTGGTGCCCATTGG	
A2257C	SDM 2	F	CCCGAAGGAACTTGGCCAGGGCCCCATTC	[34]
		R	GAATGGGGCCCTGGCCAAGTTCCTTCGGG	
T2254C	SDM 3	F	GAAGGAACTTGTCCGGGGCCCCATTCTCC	[34]
		R	GGAGAATGGGGCCCCGGACAAGTTCCTTC	
A2257C + T2254C	SDM 4	F	GGAGAATGGGGCCCCGGCCAAGTTCCTTCGGG	[34]
		R	CCCGAAGGAACTTGGCCGGGGCCCCATTCTCC	
G2688C	SDM 5	F	GCTGGTAGATGGGGGAGGGGCAGTC	[34]
		R	GACTGCCCCTCCCCCATCTACCAGC	
C2727T	SDM 6	F	GCGGCGGGCACACTCCTGCTGCC	[34]
		R	GGCAGCAGGAGTGTGCCCGCCGC	
G2990T	SDM 7	F	GCACCCCAATCCTATTGATGTCGTCGTTGGTC	[34]
		R	GACCAACGACGACATCAATAGGATTGGGGTGC	
G2844A	SDM 8	F	AGCCGCTCGTGTTGGGGAGCCGG	[127]
		R	CCGGCTCCCCAACACGAGCGGCT	
None	Control SDM	F	GCGGCGGGCACGCTCCTGCTGCC	Not applicable
		R	GGCAGCAGGAGCGTGCCCGCCGC	

shaking at 37°C or 32°C for 16 h. Plasmid DNA was extracted from bacterial cultures using the Wizard® Plus SV Miniprep DNA Purification System kit (Promega). DNA quality and quantity were assessed by nanodrop (see 2.3.3) and plasmid DNA was sequenced (see 2.9.3) using primers designed to cover the EPHA2 gene (Table 13).

Table 13: Sequencing primers for EPHA2 cDNA in EPHA2-pCMV, sEPHA2-RRL.SF.newMCS.i2.Zeo.pre lentiviral vector and transduced (and amplified) cell line genomic DNA.

Primer name	Primer sequence (5'–3')	Use/resultant sequences
Reverse BGH	TAGAAGGCACAGTCGAGG	EPHA2.pCMV/ Supplementary figure 9
T7 promotor	TAATACGACTCACTATAGGG	EPHA2.pCMV/ Supplementary figure 9 3'LTR of sEPHA2-RRL.SF.newMCS.i2.Zeo.pre/ Supplementary figure 11
652F	TCTGATGCACCTTCCCTGG	EPHA2.pCMV/ Supplementary figure 9 sEPHA2-RRL.SF.newMCS.i2.Zeo.pre/ Supplementary figure 12 Transduced cell lines/Figure 21B
858R	CTTCTCGTAGCCTGCCTGG	sEPHA2-RRL.SF.newMCS.i2.Zeo.pre/ Supplementary figure 12 Transduced cell lines/Figure 21B
1296F	CAGCATCAACCAGACAGAGC	EPHA2.pCMV/ Supplementary figure 9 sEPHA2-RRL.SF.newMCS.i2.Zeo.pre/ Supplementary figure 12 Transduced cell lines/Figure 21B
2184R	AGTTCATGTTGGCCAGGTAC	EPHA2.pCMV/ Supplementary figure 9 sEPHA2-RRL.SF.newMCS.i2.Zeo.pre/ Supplementary figure 12 Transduced cell lines/Figure 21B
2155F	GACAAGTTCCTTCGGGAGAA	sEPHA2-RRL.SF.newMCS.i2.Zeo.pre/ Supplementary figure 12
5'LTR	TGCCGATTGGTGGAAGTAAG	5'LTR of sEPHA2-RRL.SF.newMCS.i2.Zeo.pre/ Supplementary figure 10
567R	ATGGGTATTCCCACAGTGTTC	Transduced cell lines/Figure 21B
567F	TCCTACCGGAAGTTCACCTCT	Transduced cell lines/Figure 21B

2.15. Lentiviral EPHA2 expression vector construction, production and transduction

2.15.1. Lentiviral vector construction

To reintroduce EPHA2 to the EPHA2 knockout cells, a sEPHA2 construct was designed and constructed by GeneArt, Thermo Fisher Scientific. This sEPHA2 contained silent mutations in the gRNA target site so to avoid detection by the CRISPR/Cas9 system already transduced into the Hu-KO cells, and the *Age*I and *Bam*H1 restriction enzyme sites 5' and 3' of sEPHA2 construct, respectively, in a standard pMA vector (17ADD7RP_sEPHA2_pMA, see 2.10).

To generate the sEPHA2-RRL.SF.newMCS.i2.Zeo.pre lentiviral vector, the sEPHA2 construct (GeneArt, Thermo Fisher Scientific) was first isolated from the expression vector by restriction enzyme digestion using *Age*I and *Bam*HI. The segment was then inserted into the lentiviral vector RRL.SF.newMCS.i2.Zeo.pre which was pre-digested with *Age*I and *Bam*HI restriction enzymes to produce compatible ends. Successful ligation was confirmed by restriction enzyme analysis with *Age*I, *Bam*HI and *Nde*I and sequencing of the cloned plasmid DNA.

2.15.2. Lentivirus production

Lentiviruses containing the WT sEPHA2-RRL.SF.newMCS.i2.Zeo.pre, the mutant-sEPHA2-RRL.SF.newMCS.i2.Zeo.pre or the EV control RRL.SF.newMCS.i2.Zeo.pre were produced in HEK293T cells by transfecting the respective vector constructs and the packaging plasmids using the calcium-phosphate transfection method. Briefly, HEK293T cells were plated at a density of $4x10^6$ cells in a 10 cm dish. Media was removed 24 h later and replaced with transfection media (DMEM + 10% FBS + HEPES (pH 7)) with 0.1 mM chloroquine. In parallel, the packaging vector pCMV-VSV-G, pGag/pol, pRev together with the RRL-vectors were combined in separate Eppendorf tubes per transfection and mixed with 50 µl of 2.5 M $CaCl_2$. The DNA-$CaCl_2$ mix was added to 2X HEPES buffered saline (HBS) buffer dropwise while bubbling air through the HBS. The HBS-DNA-$CaCl_2$ mixture was incubated at room temperature for 20 min before being added to the HEK293T cells slowly while swirling. Transfected cells were incubated at 37°C, 5% CO_2 for 6–12 h before media was removed and replaced with transfection media. Transfection media was refreshed 12 h and 24 h later. At the 36 h time-point, media containing lentiviruses was removed off HEK293 cells and replaced with fresh media. Lentivirus-containing media was filtered through 0.45 µm filters and stored at 4°C. At the 48 h time-

point, media was again removed from the HEK293 cells and filtered before being pooled with the first harvest. Lentiviruses were purified by ultracentrifugation at 7500 x g at 4°C for 10 h in an SW40 swing rotor (Beckman Coulter Inc.). The supernatant was discarded, and the lentivirus pellet was resuspended in the remaining media and stored at -20°C.

2.15.3. Lentivirus titration

The amount of lentivirus used to transduce cells was determined by titration in control cells. Hu-KO cells were plated at a density of $5x10^6$ cells/well in a 6-well plate and transduced with lentiviruses in series (1 µl–40 µl). After selection, transduced cells were assessed for EPHA2 expression by flow cytometry (see 2.21) relative to EV transduced Hu-Scr cells (representative of endogenous expression).

2.15.4. Determining zeocin sensitivity

The minimal concentration of zeocin required to kill untransfected HuARLT2 cells was determined empirically. Cells were plated in a 96-well plate at a density of $2.5x10^4$ cells/well. The following day, media was removed and replaced by fresh media containing zeocin at a range of concentrations (0, 50, 100, 200, 400, 600, 800 and 1,000 µg/ml). Selection media was replenished every three days for ten days at which time live cells were counted. The concentration that killed the majority of cells was used for future selection of cells transduced with the RRL.SF.newMCS.i2.Zeo.pre vector containing the zeocin resistance gene.

2.15.5. Lentivirus transduction of engineered HuARLT2 cell lines

For transduction, HuARLT2 cells were plated ($5x10^5$) in 6-well plates in duplicate. The next day, media was changed to media containing 5 µg/ml of polybrene. The respective lentiviruses (containing constructs or EV) were thawed on ice and added to the media above the cells. Cells were transduced by spinoculation at 450 x g for 30 min at 30°C. At least 4 h later, fresh media was added containing 400 mg/ml zeocin. When all the control cells were dead, selected cells were expanded. These transduced cell lines were designated Hu-WT-SDM, Hu-SDM1, Hu-SDM2, Hu-SDM3, Hu-SDM4, Hu-SDM5, Hu-SDM6, Hu-SDM7 and Hu-SDM8 (Table 9). Transduced cells were maintained in media containing half the zeocin concentration of the selection media (200 mg/ml). Transduced cells were assessed for EPHA2 expression by flow cytometry (see 2.21) and the reintroduced EPHA2 gene was

amplified and sequenced using primers designed to amplify the regions where mutations were introduced (Table 13).

2.16. Recombinant KSHV production

BJAB-rKSHV.219 cells were utilised to produce rKSHV virus, as previously described [335,342]. Briefly, BJAB-rKSHV.219 cells were inoculated at a density of $6x10^5$ cells/ml in a 500 ml spinner flask (Lasec, South Africa) in the presence of 2.5 µg/ml of anti-human IgM antibody (Sigma-Aldrich) to induce the KSHV lytic cycle. Induced cells were incubated for five days at 60 rpm agitation. Cells and debris were separated from the culture supernatant by low-speed centrifugation at 1125 x g for 10 min and discarded. Virus particles in the supernatant were concentrated by ultracentrifugation at 14,000 rpm for 5 h in a JA20 rotor (Beckman Coulter Inc.). The pellet-containing virus was resuspended in serum-free EGM-2MV medium and stored at 4°C for less than one month.

Infectious virus titre was determined by infection of cells with serial dilutions of the virus. HEK293 or HuARLT2 cells were plated at a cell density of $3x10^4$ cells/per well in a 96-well plate and infected (see 2.17). Three days after infection, GFP-positive cells were counted by fluorescent microscopy (see 2.19) and the infectious virus titre was calculated using the dilution factor.

2.17. Recombinant KSHV infection

Cells were plated at $5x10^5$ cells per well of a 6-well plate (for flow cytometry) or $1x10^5$ cells per well of a 24-well plate (for fluorescent microscopy, fluorometry or Western blot) in duplicate and infected with rKSHV (see 2.16) by spinoculation (450 x g for 30 min at 30°C) at a multiplicity of infection (MOI) of 2.5 in the presence of 10 µg/ml polybrene (Sigma-Aldrich) unless otherwise indicated. The culture medium was changed 1 h post infection unless otherwise indicated. The cells were further incubated at 37°C in a 5% CO_2 cell culture incubator for 48 h before infection levels were assessed by fluorometry (see 2.18), fluorescent microscopy (see 2.19), Western blot (see 2.20) or flow cytometry (see 2.21) as indicated.

2.18. Fluorometry

Following KSHV infection as indicated (see 2.17), media was removed from cells. Cells were washed twice with cold PBS and GFP fluorescence was measured on a microplate reader (Glomax, Promega) using an excitation filter of 490 nm and an emission filter of 510–570 nm. Triplicate readings were averaged, and the average of the uninfected wells was subtracted.

2.19. Fluorescent microscopy

Following infection as indicated (see 2.17), media was removed, and cells were washed twice with PBS. Cells were visualised immediately in PBS using phase contrast and the Alexa Fluor 488 filter (for GFP expression) on a Zeiss inverted fluorescent microscope (Axiovert 200M) using the AxioVision software (version 4.8). Photographs were captured using the monochrome Zeiss AxioCam HRm. GFP-positive cells were counted in five fields of view per well (photographed) and these were averaged.

2.20. Western blot analysis

2.20.1. Cell lysate preparation

To analyse protein expression by Western blot, adherent cells were lysed in the cell culture plates after washing with PBS with 1X sodium dodecyl sulphate (SDS) sample buffer (see Appendix 7.1) and centrifuged at 20,000 x g for 10 min at 4°C. Lysates were either stored at -20°C for later use or processed immediately by sonication for 30 s in a frozen block. Sonicated samples were then placed in a heating block set at 100°C for 5 min and then back on ice for 5 min. Protein concentration was determined by nanodrop (see 2.23.4).

2.20.2. SDS-PAGE and protein transfer

Cell lysates (see 2.20.1) were loaded into a 12% SDS polyacrylamide gel and the precision Plus Protein Standard (Biorad) was loaded as a marker. The gel was run at 20 mA in running buffer (see Appendix 7.1) for 40–60 min following standard procedures. Separated proteins were then transferred from the

gel onto 0.45 µm nitrocellulose membranes (Amersham) in transfer buffer (see Appendix 7.1) for 70 min at 350 mA.

2.20.3. Antibodies

The following antibodies were used for Western blotting: mouse anti-Eck/EphA2 Antibody, clone D7 (05-480, 1:500) and mouse anti-β-actin (A5441, 1:1,000) purchased from Sigma Aldrich; rat anti-LANA (1:1,000), produced by the Schulz laboratory (MHH, Germany) [343]; HRP-conjugated rabbit anti-mouse IgG (1:2,000, P0260) secondary antibody purchased from DAKO; and goat anti-rat IgG (1:1,000, #3050–05) purchased from Southern Biotech.

2.20.4. Immunoblotting and chemiluminescent visualisation

Membranes were blocked by incubating them in 5% (w/v) non-fat milk (Carl Roth) in PBS-Tween (see Appendix 7.1) for 1 h followed by incubation with the appropriate primary antibody (see 2.20.3) in milk-PBS-Tween overnight at 4°C on a tube roller. Membranes were washed three times in PBS-Tween for 5 min on a shaker before incubation with the corresponding HRP-conjugated secondary antibody in blocking solution for 45 min at room temperature. The membranes were washed three times again after which they were visualised in a LAS-3000 Imager (Fujifilm) after signal development using an enhanced chemiluminescence (ECL) kit (Thermo Fisher Scientific).

2.21. Flow cytometry analysis

2.21.1. Experimental setup

Each experiment included negative controls of unstained and secondary antibody only cells. Controls and samples were prepared in duplicate.

2.21.2. Antibodies

Antibodies used for flow cytometry were mouse anti-human EPHA2 antibody (1:800, MAB3035) purchased from R&D systems and Alexa Fluor® 647-AffiniPure Fab Fragment Donkey Anti-Mouse IgG

(1:800, AB_2340867) purchased from Jackson ImmunoResearch.

2.21.3. Secondary antibody titration

Hu-Scr (which expresses WT EPHA2) and Hu-KO (which is negative for EPHA2, Table 9) were mixed to generate a cell population that would stain both positive and negative for EPHA2. These cells were stained with primary antibody at the recommended concentration for flow cytometry (0.25 µg/10^6 cells) and a range of concentrations of secondary antibody (recommended range 1:100–1:800). An unstained and secondary only control were included. Cells were acquired on a BD Fortessa using the BD FACSDiva software in the AF647 channel. Histograms of AF647 intensity were gated with a bisector gate to discriminate EPHA2-positive and -negative peaks and the median fluorescent intensity (MFI) of each was calculated. The ratio of the positive to the negative peak MFI was calculated and the secondary antibody concentration which best discriminated between the negative and positive populations was selected for further experiments.

2.21.4. Sample preparation

Following the relevant treatment, engineered HuARLT2 cells were lifted by adding 500 µl accutase (Biowest) at 37°C for 5 min and neutralised with the equal amount of EGM-2MV media which was used to wash the bottom of the well and ensure all cells were lifted. Lifted cells were centrifuged at 450 x g for 2 min in an Eppendorf centrifuge 5702 (Merck), the supernatant removed, and resuspended in 100 µl flow cytometry block solution (see Appendix 7.1) per stain and transferred to a V-shaped 96-well plate. The samples were incubated at 4°C for 30 min. The pellet was resuspended in 100 µl flow cytometry block solution containing primary antibody (1:800, recommended by the manufacturer) by pipetting up and down to mix. Unstained and secondary antibody only controls were resuspended in block solution only. The cells were incubated with primary antibody at 4°C for 1 h. The plate was centrifuged at 450 x g for 2 min at 4°C and the supernatant removed. The cells were then washed three times by resuspending them in 200 µl flow cytometry wash solution (see Appendix 7.1) followed by centrifuging at 450 x g for 2 min at 4°C and removal of the supernatant. The cells were resuspended in 100 µl flow cytometry block solution containing secondary antibody (1:800, determined by titration, see 2.21.3) by pipetting up and down to mix. Unstained control was resuspended in block solution only. The cells were incubated with primary antibody at 4°C for 1 h in the dark. The cells were washed three times and resuspended in 100 µl flow cytometry fix solution

(see Appendix 7.1) and transferred to flow cytometry tubes (BD). Prepared samples were kept at 4°C and protected from light until data acquisition (see 2.21.5).

2.21.5. Data acquisition

Flow cytometry data were acquired on a BD Fortessa using the BD FACSDiva software in the GFP and AF647 channels. Acquisition parameters were set up using an unstained negative control and stained positive control. To ensure that compensation was not required when acquiring data from both GFP and AF647 signals, fluorescence minus one (FMO) controls were included in a pilot experiment. The cell population was defined by setting the threshold for forward scatter at 10,000 to exclude cell debris and 25,000 events were acquired per sample.

2.21.6. Data analysis

Flow cytometry data were analysed using FlowJo™ software (v10.6.1). The cell population was gated using a dot plot of side scatter (SSC) versus forward scatter (FSC) for the WT cells and the gate was applied to all samples. The GFP histogram of stained, uninfected WT cells was used to identify the GFP-positive population and this was gated with a bisector gate. This gating strategy was applied to all acquisitions providing % GFP+ cells. MFI of the GFP and Alexa Fluor 647 histograms was calculated using FlowJo™.

2.22. MTT assays

To determine cell viability, 5 mg/ml Thiazolyl Blue Tetrazolium Bromide (MTT reagent), Sigma (see Appendix 7.1), was added at a 1:10 dilution to the cell culture media covering adherent cells and incubated for 4 h at 37°C 5% CO_2. Media was removed and MTT crystals were solubilised in DMSO for 45 min. MTT absorbance was measured at 600 nm on a microplate reader (GloMax, Promega). Average absorbance of the blank controls was subtracted from all values.

2.23. EPHA2 phosphorylation

2.23.1. Determining baseline phosphorylation levels

Hu-WT-SDM, Hu-SDM 1, Hu-SDM 2, Hu-SDM 3, Hu-SDM 4, Hu-SDM 5, Hu-SDM 6, Hu-SDM 7 and Hu-SDM 8 cells were plated at a density of $2.5x10^5$ cells/well in 12-well plates in duplicate. The following day, cells were lysed (see 2.23.3), protein concentration was quantified (see 2.23.4) and EPHA2 tyrosine phosphorylation levels were assayed (see 2.23.5).

2.23.2. Determining phosphorylation response to rKSHV

2.23.2.1. Determining cell line sensitivity to serum starvation

Hu-WT-SDM cells were plated at a density of $1x10^4$ cells/well in a 96-well plate. The following day, cells were subjected to EGM-2MV media containing 0% FBS in a time course (serum-starved) in triplicate or serum-containing media (control). At the end of the time course, MTT assays (see 2.22) were performed to determine cell viability. Viability of serum-starved cells was expressed as a percentage of unstarved cells of the same time-point. The time-point at which no change in viability was observed was selected for future experiments.

2.23.2.2. Determining optimal treatment time

Hu-WT-SDM cells were plated at a density of $2.5x10^5$ cells/well in 12-well plates in duplicate in the morning. In the afternoon, once cells were adhered to the cell culture plate, media was removed, cells were washed with PBS and serum starvation media was added. Cells were incubated in the absence of serum overnight (16 h, based on sensitivity experiment, see 2.23.2.1). Cells were treated with rKSHV at MOI 10 for 10 min, 20 min or 60 min. Cells were lysed (see 2.23.3), protein concentration was quantified (see 2.23.4) and EPHA2 tyrosine phosphorylation levels were assayed (see 2.23.5). The time-point at which the most pronounced increase in phosphorylation was observed was selected for future experiments.

2.23.2.3. Determining phosphorylation response to rKSHV

Hu-WT-SDM, Hu-SDM 1, Hu-SDM 2, Hu-SDM 3, Hu-SDM 4, Hu-SDM 5, Hu-SDM 6, Hu-SDM 7 and Hu-SDM 8 cells were plated at a density of $2.5x10^5$ cells/well in 12-well plates in duplicate in the morning. In the afternoon, media was removed and replaced with serum-free EGM-2MV and cells were incubated in the absence of serum overnight (16 h). The following morning, media was replaced with fresh serum-free media only (control) or serum-free media containing rKHSV at MOI 10 for 20 min (as

determined under 2.23.2.2). Cells were lysed (see 2.23.3), protein concentration was quantified (see 2.23.4) and EPHA2 tyrosine phosphorylation levels were assayed (see 2.23.5).

2.23.3. Sample preparation

Following the appropriate treatment, media was removed, and the cells were washed twice with PBS. Cells were solubilised in 100 µl Lysis buffer (IC Diluent #12 (1% NP-40 Alternative, 20 mM Tris (pH 8.0), 137 mM NaCl, 10% glycerol, 2 mM EDTA, 1 mM activated sodium orthovanadate (R&D Systems®, Catalogue # DYC002)) containing 1x cOmplete™, EDTA-free Protease Inhibitor Cocktail (Roche)) in the plate and incubated on ice for 15 min. Lysates were centrifuged at 2,000 x g for 5 min at 4°C and the supernatant transferred to a clean Eppendorf tube. Protein concentration was determined using bicinchoninic acid assay (BCA) assay (see 2.23.4). If necessary, lysates were stored at -80°C.

2.23.4. BCA assay

Lysate protein concentration was determined using the Pierce™ BCA Protein Assay Kit (Thermo Fisher Scientific). Protein standards (5 µg/ml–250 µg/ml) were prepared by diluting the provided 2 mg/ml albumin standard in IC Diluent #12; the blank standard consisted of IC Diluent #12 only. BCA working reagent was prepared as required by combining BCA Reagent A with BCA Reagent B in a 50:1 ratio. Each standard and sample (3 µl) was added to 100 µl BCA working reagent and these were incubated in a heating block set to 37°C for 30 min. Tubes were cooled to room temperature. Absorbance at 562 nm was measured on a Nanodrop. Absorbance of the blank standard was subtracted from the other measurements. A standard curve was constructed from the absorbance values of the standards and the protein concentrations of the samples were determined by interpolating the absorbance values in the standard curve.

2.23.5. Human Phospho-EPHA2 ELISA

ELISA microplates were coated with 100 µl Human Phospho-EphA2 Capture Antibody (Human Phospho-EPHA2 kit component, R&D Systems®, part 842422) reconstituted in PBS and diluted to a final concentration of 4 µg/ml, sealed and incubated overnight at room temperature. The coated plates were washed three times with ELISA Wash Buffer (0.05% Tween® 20 in PBS, pH 7.2-7.4, R&D Systems®, #WA126) by aspirating each well and pipetting 300 µl wash buffer forcefully, followed by

inversion of the plate and blotting against paper towel. Plates were blocked by the addition of 300 µl Block Buffer (1% BSA (R&D Systems®, #DY995), 0.05% NaN_3 (see Appendix 7.1) in PBS, pH 7.2-7.4) to each well and incubation at room temperature for 1–2 h. The plate was washed three times, again.

Samples were diluted with IC Diluent #12 to 0.5 µg/µl and 100 µl of each sample and control was added to the plate. The blank control contained only IC Diluent #12. The positive control was Human Phospho-EphA2 Control (Human Phospho-EPHA2 kit component, R&D Systems®, Part 842154) reconstituted with IC Diluent #12 and diluted to a final concentration of 800 pg/ml. The plate was sealed and incubated for 2 h at room temperature after which the plates were washed three times.

Anti-pY-HRP (mouse anti-phospho-tyrosine antibody conjugated to HRP, Human Phospho-EPHA2 kit component, R&D Systems®, Part 841420) was diluted 1:1800 (as recommended by the manufacturers) in IC Diluent #14 (20 mM Tris, 137 mM NaCl, 0.05% Tween® 20, 0.1% BSA (R&D Systems®, #DY995), pH 7.2-7.4) as needed and 100 µl of this working stock was added per well. The plate was sealed and incubated for 2 h in the dark at room temperature after which the plates were washed three times. 100 µl Substrate Solution (1:1 mixture of Colour Reagent A (H_2O_2) and Colour Reagent B (Tetramethylbenzidine), R&D Systems®, #DY999) was added per well. The plate was sealed and incubated for 20 min at room temperature in the dark at which time 50 µl Stop Solution (2 N H_2SO_4, R&D Systems®, #DY994) was used to halt the reaction. Plates were gently tapped to mix the solutions and the absorbance was immediately determined using a microplate reader (GloMax, Promega) set to 450 nm with a wavelength correction of 560 nm. The average OD of the blank control was subtracted from the other samples.

2.24. KSHV binding and internalisation assay

2.24.1. Validation of binding and internalisation infection conditions

RFP is expressed by rKSHV from the KSHV lytic gene PAN promoter [336]. To validate that RFP fluorescence measured on the fluorometer was indeed indicative of binding and internalisation (see 2.24.2), infected cells were visualised using a fluorescent microscope. Cells were plated on sterile coverslips in 12-well plates at a density of $1x10^5$ cells/well. The following day, cells were infected with rKSHV at MOI 10 in the presence of 10 µg/ml polybrene by centrifuging at 450 x g for 30 min at 4°C and either incubated at 4°C (binding) or shifted to 37°C (internalisation) for 1 h. Cells were washed twice to remove unbound virus, and the coverslips were mounted on microscope slides on a drop of PBS. The same procedure was followed in an empty well (no plated cells) to assess potential

background levels of RFP. Cells were visualised immediately using phase contrast and the Cy-3 filter with the 20X objective of a fluorescent microscope (Axiovert 200M) using the AxioVision software.

2.24.2. Quantifying internalisation and binding

Cells were plated at a density of $1x10^4$ cells/well in six repeats in two 96-well sterile black plates in parallel: one to assess binding of rKSHV and the other to assess internalisation. The following day, media was replaced with fresh media (for uninfected wells) or media with rKSHV at MOI 10 together with 10 μg/ml polybrene (in triplicate) and centrifuged at 450 x g for 30 min at 4°C. To assess KSHV binding, one plate was kept at 4°C. To assess internalisation, the other plate was shifted to 37°C for 1 h. Cells were washed twice with cold PBS and RFP fluorescence was measured on a microplate reader (Glomax, Promega) using an excitation filter of 530 nm and an emission filter of 580–640 nm. Triplicate readings were averaged, and the average of the uninfected wells was subtracted.

2.25. Statistical analysis of experimental data

When replicate experiments were combined (as indicated), means and standard errors were pooled. When data were normalised, standard errors were propagated accordingly. Statistical testing of experimental data was conducted by one-way ANOVA with *post hoc* Dunnett's test corrected for multiple comparisons (as indicated) in IBM SPSS Statistics (Version 25.0. Armonk, NY: IBM Corp).

3. Results

Despite the high seroprevalence of KSHV in SSA, the contribution of KSHV infection or host KSHV receptor variations to disease outcome in HIV-infected South African patients is unknown. To further our understanding of KSHV-driven pathology and disease outcome, we first assessed the contribution of KSHV infection and KSHV-associated syndromes to mortality in a clinical cohort of patients presenting with suspected but not microbiologically confirmed TB, the leading cause of death among HIV-positive South Africans. The results presented in 3.1 have recently been published [62]. Secondly, in continuation of previous work from our laboratory which formed my MSc thesis and has been published [34,35], we investigated EPHA2, the KSHV entry receptor, as a potential genetic susceptibility marker for KSHV infection, KS development or KSHV VL (see 3.2). Thirdly, we characterised EPHA2 variants of interest in terms of KS development and KSHV infection (see 3.3).

3.1. The contribution of KSHV to mortality in HIV-infected South African patients presenting with suspected but unconfirmed TB

3.1.1. Assessment of parameters relevant for this study

To assess the role of KSHV and KSHV-associated diseases in HIV-positive patients presenting with syndromes compatible with TB, demographic and clinical information was recorded, vital status was ascertained at 12-week follow-up and KSHV VL, KSHV serostatus and IL-6 levels were measured. Patients were recruited on presentation with a suspected diagnosis of severe HIV-associated TB (n=682). Seven patients were excluded (two withdrew, one was HIV-negative, and four had no blood samples stored for KSHV assays) and 675 were included in this analysis. The median CD4 count was 62 cells/µl (range: 0–526 cells/µl) (Table 14). Twelve patients were lost to follow-up and 146 (22%) died by 12-weeks follow-up. Ten patients had a clinical diagnosis of cutaneous or oral cavity KS at enrolment. All patients were assessed for KSHV seropositivity, of whom 207 (30.7% (95% CI: 27.2, 34.3) tested positive for the presence of either K8.1 or ORF73 antibodies in the plasma by ELISA (Table 14 and Figure 6).

The entire patient cohort was also assessed for KSHV VL by quantitative real-time PCR. Of the 207 KSHV seropositive patients, 39 (18.8%) showed detectable VL in the blood which is in agreement with earlier studies [24,344,345]. VL in the individual seropositive patients displayed a wide range with a median of 199.05 copies/10^6 cells (range: 13.4–2.2x10^6 copies/10^6 cells). Interestingly, 4 (0.85%) of

the 468 KSHV seronegative patients were found to have detectable VL with a median of 1084.29 copies/10^6 cells (range: 141.4–57054 copies/10^6 cells). These patients had a particularly low median CD4 count of 25.5 cells/µl (range: 20–168 cells/µl) and, assuming they only became infected while immunosuppressed, might not have been able to mount a detectable antibody response against KSHV.

Table 14: Baseline demographic and clinical characteristics of the study cohort (n=675). Sex, ART, anaemia diagnosis, detectable IL-6, TB diagnosis, KSHV status, KS diagnosis and survival are given as count and percentage; HIV VL, IL-6 concentration and KSHV VL are given as median and range.

Sex	
Male	320 (47.4%)
Female	355 (52.6%)
Age (years)	36.1 (18.5-80.8)
Weight (kg)	53 (30-104)
Receiving ART	252 (37.3%)
HIV VL (copies/ml)	104 252 (29-1x10^7)
CD4 (cells/µl)	62 (0-526)
Patients with anaemia	622 (92.1%)
Haemoglobin (g/dl)	8.9 (3.9-17.4)
Patients with detectable IL-6	559 (82.8%)
IL-6 concentration (pg/ml)	42.3 (9.8-103.8)
TB/ infection category	
Patients with proven TB	500 (74.1%)
Patients with an alternate microbiologically proven opportunistic infection	16 (2.4%)
Patients without microbiologically proven TB or other co-infections	159 (23.5%)
KSHV status in patients	
Seropositive	207 (30.7%)
Seropositive with detectable VL; copies/10^6 cells	39 (5.8%); 199.05 (13.4-2.2x10^6)
Seropositive with elevated VL (>100 copies/10^6 cells)	29 (4.3%)
Seronegative	468 (69.3%)
Seronegative with detectable VL; copies/10^6 cells	4 (0.6%); 1084.29 (141.4-57 054)
Seronegative with elevated VL (>100 copies/10^6 cells)	4 (0.6%)
Skin or oral Kaposi's Sarcoma	10 (1.5%)
Survival at 12-weeks	
Died	146 (21.6%)
Survived	517 (76.6%)
Lost to follow-up	12 (1.8%)

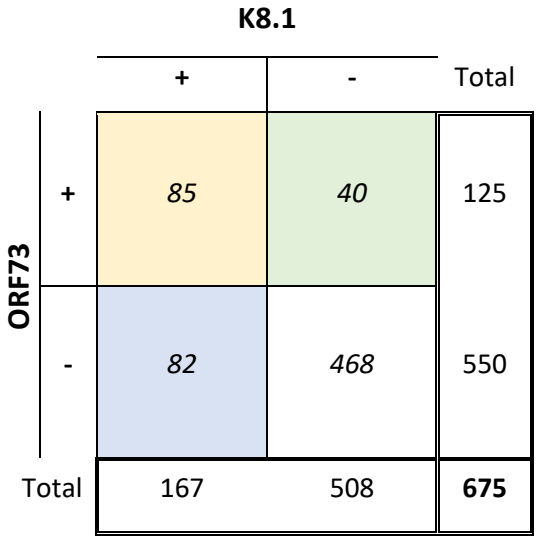

Figure 6: Assessment of KSHV seropositivity in the whole patient cohort (n=675). ELISA results indicating 30.7% KSHV seropositivity (207/675) as defined by the OD values for K8.1 and ORF73 above the cut-off for either ELISA assay (indicated by cells with shaded background).

Importantly, plasma IL-6 was detected in 559 (82.8%) of all patients with a median concentration of 42.3 pg/ml (IQR: 9.8–103.8 pg/ml). This is considered highly elevated compared to a reference population of HIV-positive patients (n=9864, median IL-6: 1.80 pg/ml (IQR: 1.20–2.89) [346]). Finally, when performing a binomial logistic regression predicting KSHV seropositivity or elevated KSHV VL, respectively, by age, sex, CD4 count, haemoglobin levels and ART status, only CD4 count was significantly associated with KSHV seropositivity (p=0.001, adjusted OR= 1.003 (95% CI: 1.001, 1.004), Table 15). Male sex was associated with elevated KSHV VL (p=0.029, adjusted OR=2.367 (95% CI: 1.093, 5.126), Table 16).

3.1.2. Elevated KSHV VL is associated with mortality in critically ill patients with neither MTB nor other microbiologically proven co-infection

Initially, the entire patient cohort (n=675) was assessed for a possible association of elevated KSHV VL (i.e. >100 copies/10^6 cells) with mortality at the end of the 12-weeks study period. We identified 33 patients with elevated KSHV VL of whom 9 (27.3%) did not survive until 12-weeks. Meanwhile, 137 (21.7%) of 630 patients with undetectable KSHV VL or VL <100 copies/10^6 cells had died by the end of the study period. We did not identify a statistical association between elevated KSHV VL and mortality in the whole patient cohort (Group 1, Table 17 and Figure 7A).

Table 15: Multivariate logistic regression of factors assessed for association with KSHV seropositivity in the entire cohort (n=675).

	Unadjusted Odds Ratio	95% CI for Unadjusted OR		Adjusted Odds Ratio	95% CI for Adjusted OR		*P*
		Lower	Upper		Lower	Upper	
Sex[1]	0.969	0.698	1.345	1.009	0.713	1.429	0.960
Haemoglobin[2]	1.034	0.965	1.109	0.998	0.927	1.075	0.958
Age[3]	1.016	1.000	1.033	1.016	1.000	1.033	0.057
CD4 count[4]	1.148	1.063	1.240	1.148	1.059	1.245	0.001
ART status[5]							0.709
Defaulted	0.992	0.649	1.516	1.099	0.713	1.693	0.670
on ART	0.960	0.659	1.397	0.912	0.620	1.341	0.640

[1]Sex is for males compared to females; [2]Haemoglobin levels were mean (9.02g/dl) centred; [3]Age is per 1-year increase; [4]CD4 count is per 50 cells; [5]For ART status, naïve is the reference category. Patients were considered KSHV seropositive if antibodies to either the LANA (or ORF73) or K8.1 were detected. Elevated KSHV VL is >100 copies/10^6 cells.

Table 16: Multivariate logistic regression of factors assessed for association with elevated KSHV VL in the entire cohort (n=675).

	Unadjusted Odds Ratio	95% CI for Unadjusted OR		Adjusted Odds Ratio	95% CI for Adjusted OR		*P*
		Lower	Upper		Lower	Upper	
Sex[1]	2.309	1.101	4.840	2.367	1.093	5.126	0.029
Haemoglobin[2]	1.037	0.895	1.201	0.971	0.833	1.131	0.703
Age[3]	1.029	0.997	1.062	1.024	0.991	1.059	0.151
CD4 count[4]	1.079	0.925	1.258	1.088	0.921	1.286	0.322
ART status[5]							
Naïve							0.108
Defaulted	0.255	0.074	0.879	0.274	0.079	0.954	0.042
on ART	0.675	0.318	1.432	0.669	0.310	1.441	0.306

[1]Sex is for males compared to females; [2]Haemoglobin levels were mean (9.02g/dl) centred; [3]Age is per 1-year increase; [4]CD4 count is per 50 cells; [5]For ART status, naïve is the reference category. Patients were considered KSHV seropositive if antibodies to either the LANA (or ORF73) or K8.1 were detected. Elevated KSHV VL is >100 copies/10^6 cells.

With the rationale that TB illness might be masking an association of KSHV with mortality, four overlapping categories based on the presence or absence of microbiologically confirmed infections were identified. Group 1 (n=675) consisted of the total patient cohort analysed; Group 2 consisted of n=500 patients who had microbiologically proven MTB on a culture or GeneXpert test (on any clinical sample) or tested positive for urine LAM, while of the remaining 175 patients without microbiologically confirmed TB (Group 3), 16 patients had a microbiologically proven alternative opportunistic infection (other than MTB including bacterial bloodstream infection or *Cryptococcus* species). Therefore, 159 patients (Group 4) were defined as patients with neither MTB nor other microbiologically proven co-infection, although this group retained 'clinical' TB patients who were negative for all TB diagnostic tests.

As in the entire patient cohort, proven TB patients (Group 2) showed no significant association of KSHV VL and mortality (Table 17 and Figure 7B). However, in all patients without proven TB (Group 3, n=175) and particularly in patients without proven TB or other co-infections (Group 4, n=159), elevated KSHV VL was detected at a higher frequency, and KSHV VL was significantly higher in patients who had died than in patients who had survived at the end of the 12-weeks study period (Table 17 and Figure 7C and D), indicating an association between KSHV VL and mortality. Binomial logistic regression was performed to assess this relationship while adjusting for the effects of age, sex, CD4 count and ART status in patients without proven TB or proven co-infection (n=159). Of the dependent variables, age, CD4 count and elevated KSHV VL (categorical) were statistically significant (Table 18). The adjusted OR for elevated KSHV VL was 6.467 (95% CI: 1.290, 32.406).

Interestingly, we did not find a significant relationship between KSHV seroprevalence and mortality (Table 19), in contrast to the above-mentioned significant association between KSHV VL and mortality (Table 17). To assess the drivers of KSHV antibody responses among critically ill HIV-positive patients without a proven MTB or alternative diagnosis, KSHV seropositive Group 4 patients (n=60) were analysed indicating that lower haemoglobin levels were associated with higher K8.1 antibody levels (p=0.003, unstandardized coefficient= -0.020) when adjusted for age, sex, CD4 count and ART status by multiple regression; but not with ORF73 levels (Table 20).

Table 17: Association of KSHV VL with 12-weeks mortality. Frequency of mortality among patients with elevated KSHV VL (>100 copies/10^6 cells) versus those with undetectable KSHV VL or VL<100 copies/10^6 cells. Patients were grouped as indicated: Group 1 (n=675, entire patient cohort); Group 2 (n=500, patients with microbiologically proven TB); Group 3 (n=175, patients without a confirmed TB diagnosis); Group 4 (n=159, patients without microbiologically confirmed infections). Twelve patients of the total cohort were lost to follow-up. [1]P value is by [A]Chi-square test for association if expected cell frequencies were >5 or [B]Fisher exact test.

	KSHV Viral load	Died Count (%)	Survived Count (%)	P value[1] OR (95% CI)
Group 1: Entire patient cohort (n=675)	>100 copies/10^6 cells	9 (1.3)	24 (3.6)	p=0.455[A] OR=1.3 (95% CI: 0.6, 3.0)
	<100 copies/10^6 cells or non-detectable	137 (20.3)	493 (73.0)	
Group 2: Patients with proven TB (n=500)	>100 copies/10^6 cells	3 (0.4)	20 (3.0)	p=0.281[A] OR=0.5 (95% CI: 0.2, 1.7)
	<100 copies/10^6 cells or non-detectable	106 (15.7)	363 (53.8)	
Group 3: Patients without proven TB (n=175)	>100 copies/10^6 cells	6 (0.9)	4 (0.6)	p=0.008[B] OR=6.3 (95% CI: 1.7, 23.7)
	<100 copies/10^6 cells or non-detectable	31 (4.6)	130 (19.3)	
Group 4: Patients without microbiologically confirmed infections (n=159)	>100 copies/10^6 cells	5 (0.7)	3 (0.4)	p=0.011[B] OR=7.1 (95% CI: 1.6, 31.7)
	<100 copies/10^6 cells or non-detectable	28 (4.1)	120 (17.8)	

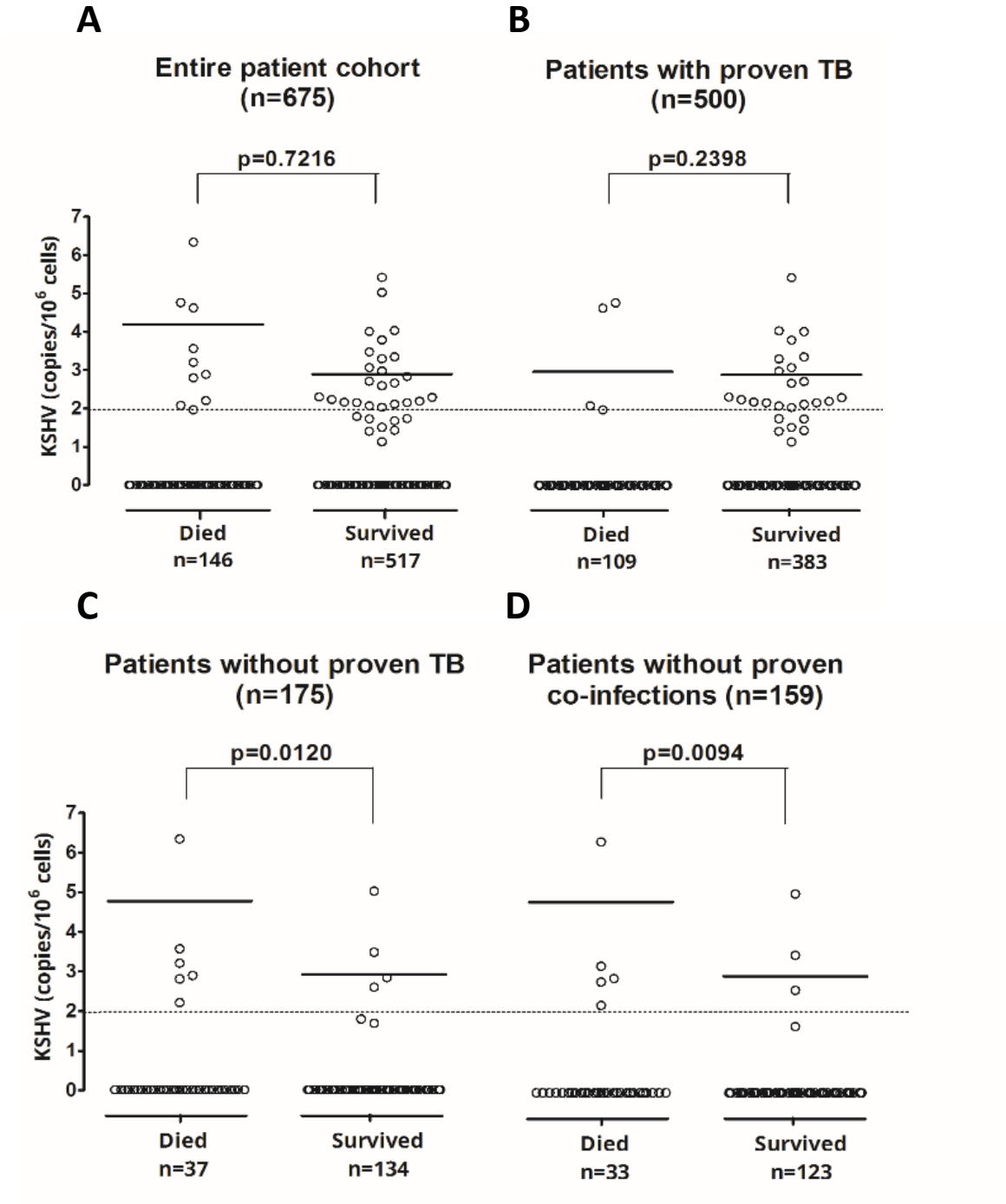

Figure 7: 12-weeks mortality versus KSHV VL in A) the entire patient cohort (Group 1, n=675); **B)** patients with proven TB (Group 2, n=500); **C)** patients without proven TB (Group 3, n=175); **D)** patients without microbiologically proven co-infections (Group 4). Each dot represents a patient.

Table 18: Logistic regression of factors assessed for association with mortality based on elevated KSHV VL among Group 4 patients (n=159).

	Unadjusted Odds Ratio	95% CI for Unadjusted OR		Adjusted Odds Ratio	95% CI for Adjusted OR		*P*
		Lower	Upper		Lower	Upper	
Elevated KSHV VL[1]	7.143	1.611	31.671	6.467	1.290	32.406	0.023
Sex[2]	0.949	0.433	2.082	0.477	0.187	1.214	0.120
Age[3]	1.051	1.014	1.088	1.067	1.022	1.113	0.003
CD4 count[4]	0.892	0.742	1.072	0.777	0.619	0.975	0.029
ART status[5]							0.980
Defaulted	0.790	0.285	2.190	1.067	0.346	3.290	0.910
on ART	0.967	0.395	2.368	1.105	0.417	2.930	0.840

[1]KSHV VL is for elevated (>100 copies/10^6 cells) compared to non-elevated (<100 copies/10^6 cells or non-detectable); [2]Sex is for males compared to females; [3]Age is per 1-year increase; [4]CD4 count is per 50 cell increase; [5]For ART status, naïve is the reference category.

Table 19: Association of KSHV serology with 12-weeks mortality. Frequency of mortality among patients with positive or negative K8.1, ORF73 or overall KSHV seropositivity. Patients were grouped as indicated: n=675 (entire patient cohort); n=500 (patients with microbiologically proven TB); n=175 (patients without a confirmed MTB diagnosis); n=159 (patients without microbiologically confirmed infections). Twelve patients of the total cohort were lost to follow-up. [1]P value is by Chi-square test for association.

	KSHV Serology		Died Count (%)	Survived Count (%)	P value[1] OR (95% CI)
Group 1: Entire patient cohort (n=675)	K8.1	Positive	37 (5.5)	126 (18.7)	p=0.810 OR=1.053 (95% CI: 0.690, 1.609)
		Negative	109 (16.1)	391 (57.9)	
	ORF73	Positive	28 (4.1)	93 (13.8)	p=0.742 OR=1.082 (95% CI: 0.677, 1.729)
		Negative	118 (17.5)	424 (62.8)	
	Overall	Positive	47 (7.0)	156 (23.1)	p=0.640 OR=1.099 (95% CI: 0.740, 1.630)
		Negative	99 (14.7)	361 (53.5)	
Group 2: Patients with proven TB (n=500)	K8.1	Positive	21 (4.2)	85 (17.0)	p=0.512 OR=0.837 (95% CI: 0.491, 1.426)
		Negative	88 (17.6)	298 (59.6)	
	ORF73	Positive	19 (3.8)	64 (12.8)	p=0.859 OR=1.052 (95% CI: 0.599, 1.848)
		Negative	90 (18.0)	319 (63.8)	
	Overall	Positive	29 (5.8)	108 (21.6)	p=0.743 OR=0.923 (95% CI: 0.571, 1.491)
		Negative	80 (16.0)	275 (55.0)	
Group 3: Patients without proven TB (n=175)	K8.1	Positive	16 (9.1)	41 (23.4)	p=0.149 OR=1.728 (95% CI: 0.819, 3.648)
		Negative	21 (12.0)	93 (53.1)	
	ORF73	Positive	9 (5.1)	29 (16.6)	p=0.728 OR=1.164 (95% CI: 0.494, 2.740)
		Negative	28 (16.0)	105 (60.0)	
	Overall	Positive	18 (10.1)	48 (27.4)	p=0.156 OR=1.697 (95% CI: 0.814, 3.540)
		Negative	19 (10.9)	86 (49.1)	
Group 4: Patients without microbiologically proven infection (n=159)	K8.1	Positive	14 (8.8)	37 (23.3)	p=0.180 OR=1.713 (95% CI: 0. 777, 3.776)
		Negative	19 (11.9)	86 (54.1)	
	ORF73	Positive	8 (5.0)	28 (17.6)	p=0.858 OR=1.086 (95% CI: 0.441, 2.673)
		Negative	25 (15.7)	95 (59.7)	
	Overall	Positive	16 (10.1)	44 (27.7)	p=0.183 OR=1.690 (95% CI: 0. 787, 3.671)
		Negative	17 (10.7)	79 (49.7)	

Table 20: Summary of multiple regression analyses for K8.1 and ORF73 OD values in Group 4 patients who were KSHV seropositive (n=60).

	K8.1				ORF73			
	Unstandardized Coefficients	Standard Error	Standardized Coefficients	*P* Value	Unstandardized Coefficients	Standard Error	Standardized Coefficients	*P* Value
Intercept	.293	0.425		0.493	0.099	0.949		0.917
Sex[1]	-0.060	0.065	-0.126	0.357	-0.002	0.144	-0.002	0.987
CD4 count[2]	0.007	0.046	0.020	0.887	0.034	0.102	0.047	0.742
Age[3]	-0.039	0.262	-0.019	0.883	0.060	0.585	0.014	0.919
Haemoglobin levels[4]	-0.033	0.014	-0.307	0.022	-0.017	0.031	-0.075	0.585
ART status[5]	-0.058	0.074	-0.119	0.437	-0.262	0.165	-0.254	0.118

[1]Sex is for males compared to females; [2]CD4 count is per 50 cells; [3]Age is per 1-year increase; [4]Haemoglobin levels were mean (9.02g/dl) centred; [5]ART status is on ART compared to naïve as the reference category.

3.1.3. 'KICS' criteria can be used as a surveillance tool for patient mortality

Since a substantial number of critically ill patients was recruited with suspected TB who, on diagnostic examination, turned out to have neither proven TB nor an alternative microbiologically proven co-infection (n=159, 23.5% of total cohort, Table 14) and who displayed a significant association of KSHV VL with mortality (Table 17, Table 18, Figure 7) we set out to determine whether KSHV-driven KICS might have a currently unrecognised contribution to mortality in patients who present with a suspected diagnosis of TB.

The working case definition of KICS requires at least two clinical manifestations from at least two of three categories (Table 2, [6]): 1) symptoms (including fever, fatigue, oedema, cachexia, respiratory symptoms, gastrointestinal disturbance, arthralgia and myalgia, altered mental state, and neuropathy); 2) laboratory abnormalities (anaemia, thrombocytopenia, hypoalbuminemia, and hyponatremia); and 3) radiographic abnormalities (lymphadenopathy, splenomegaly, hepatomegaly, and body cavity effusions), together with evidence of systemic inflammation (elevated CRP [>10 mg/l]), evidence of KSHV lytic activity (elevated [>100 copies/10^6 cells] KSHV VL in peripheral blood), and exclusion of MCD. As this analysis was done retrospectively, MCD could not be excluded for all patients, hence the designation "possible KICS" patients.

We applied the criteria according to the proposed working case definition for KICS [6,7] and identified six “possible KICS” patients by exclusion of the study subsets with the caveat that we could not exclude MCD in all patients (Figure 8). While most baseline characteristics and selected laboratory abnormalities between “possible KICS” subjects (n=6) compared to the remainder of this patient group (n=153) did not significantly differ (except for age with “possible KICS” patients being slightly older, and platelet count being slightly lower in “possible KICS” patients, Table 21 and Table 22), all “possible KICS” patients (100%) displayed abnormally elevated KSHV VL and abnormally elevated K8.1 OD values compared to 1% and 30%, respectively, in the remainder of this patient group (Table 22 and Figure 9). Abnormally elevated ORF73 OD values were evident in 67% of “possible KICS” patients compared to 22% of the remainder of the group. Median KSHV VL, K8.1 and ORF73 OD values were also significantly higher in the “possible KICS” patients than in the remaining Group 4 patients (Table 22). Interestingly, “possible KICS” patients had significantly higher KSHV VL than a cohort of KS patients (recruited independently n=100 [34,35], see 3.2.1.1) in which elevated KSHV VL levels were not evident (Figure 10).

HIV VL and patient CD4 counts did not differ significantly between “possible KICS” patients and the non-proven TB patients without an alternative microbiologically proven co-infection (Table 21), indicating that HIV infection is not the cause of differences seen between these groups. According to the KICS working case definition (Table 2 [6]), evidence of systemic inflammation (i.e. elevated CRP levels) is among the criteria defining KICS. Moreover, IL-6 and IL-10 have been found to be elevated in KICS patients [6–8]. Although markedly elevated in all (100%) “possible KICS” patients, we found neither IL-6 nor CRP to be significantly different in these patients compared to the non-proven TB patients without an alternative microbiologically proven co-infection (Table 22 and Figure 9). Other laboratory abnormalities reported in KICS subjects such as low haemoglobin and albumin levels [6] were also found to be abnormally low in 83% of the herein reported “possible KICS” patients (Table 22) although not different to the remainder of the group. As mentioned earlier, low haemoglobin was found to be associated with increased K8.1 antibody levels in the entire cohort when adjusted for age, sex, CD4 count and ART status (Table 20); and in the “possible KICS” group, K8.1 antibody levels were significantly higher than in the remainder of the Group 4 patients (Table 22). However, most laboratory abnormalities did not significantly differ among these two patient groups, presumably due to all these patients being critically ill for reasons other than those that had been microbiologically tested for in this study. This is further evidenced by the high proportion of patients in this group with abnormally elevated IL-6 and CRP levels (63% and 85%, respectively) which would not be expected in a healthy cohort (Table 22).

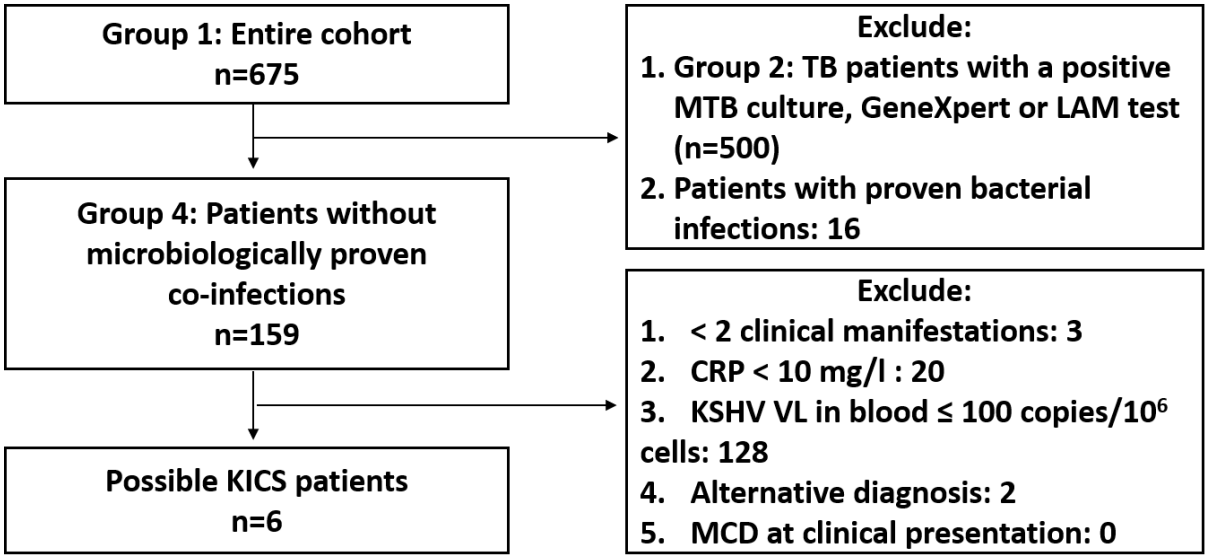

Figure 8: Schematic flow chart showing the diagnosis of "possible KICS" by exclusion in the cohort of critically ill patients investigated for TB. Patients were excluded if they had microbiologically proven TB or other bacterial or fungal infections and those who remained were further evaluated according to the criteria previously described in the KICS working case definition [6]. Two patients were excluded on the basis of alternative diagnoses (TB meningitis and community-acquired pneumonia, respectively). As this analysis was done retrospectively, MCD could not be excluded, hence the designation, "possible KICS".

Table 21: Baseline characteristics of "possible KICS" subjects (n=6) and all other Group 4 patients (n=153). Mortality, sex, ART, KSHV seropositivity and KS diagnosis are given as count and percentage; other characteristics are median and range.

	Possible KICS subjects (n=6)	Remainder of patients without microbiologically proven co-infection (n=153)	P value
Died	5 (83.3%)	28 (18.3%)	0.002
Males	4 (67%)	61 (39.9%)	0.227
Age (years)	47 (26-74)	38 (19-81)	0.049
Weight (kg)	58 (35-71)	53.0 (30-99)	0.912
Receiving ART	3 (50%)	63 (41.2%)	0.290
HIV VL (copies/ml)	81 298 (29-3 507 840)	70 363 (29- 7 934 692)	0.978
CD4 (cells/µl)	106.5 (10-328)	97 (2-519)	0.818
KSHV seropositive	6 (100%)	55 (35.9%)	0.003
Skin KS	1 (16.7%)	4 (2.6%)	0.177

Table 22: Selected laboratory abnormalities in "possible KICS" subjects (n=6) and all other Group 4 patients (n=153).

	Possible KICS subjects (n=6)		Remainder of patients without microbiologically proven co-infection (n=153)		P value
	Abnormal[1] (N, %)	Median, Range	Abnormal[1] (N, %)	Median, Range	
KSHV VL (copies/10^6 cells)	6 (100%)	699.6 (160.7-2 165 641)	2 (1%)	1.00 (1.00-104 664.39)	<0.0001
K8.1 OD	6 (100%)	2.1 (1.3-2.3)	46 (30%)	0.48 (0.10-2.57)	0.001
ORF73 OD	4 (67%)	3.3 (0.32-7.4)	33 (22%)	0.24 (0.03-8.14)	0.003
IL-6 (pg/ml)	5 (83%)	11.5 (1.6-3 307.4)	97 (63%)	12.5 (1.6-1 045.4)	0.978
CRP (mg/l)	6 (100%)	71.4 (11.1-304)	131 (85%)	94.0 (0.38-564.9)	0.767
Haemoglobin (g/dl)	5 (83%)	8.1 (6.9-14.9)	130 (85%)	10 (4.9-17.4)	0.231
White cell count	1 (17%)	7.6 (3.5-21.6)	25 (16.3%)	6.8 (1.0-43.2)	0.783
Platelet count	4 (67%)	185 (89.0-305)	29 (19%)	280 (23.0-789)	0.050
Albumin (g/l)	5 (83%)	24.0 (16.0-39.0)	118 (77%)	28.0 (12.0-43.0)	0.489
Sodium (mEq/l)	5 (83%)	132 (125-138)	119 (78%)	131 (113-150)	0.692

[1]"Abnormal" refers to elevated KSHV VL, >100 copies/10^6 cells; positive K8.1 and ORF73, OD values >1 (normalised cut-off); elevated IL-6, >1.8 pg/ml; elevated CRP, >10 mg/l; low haemoglobin <12 g/dl (female) or <13g/dl (males); low white cell count <3.9; low platelet count, <186; low albumin, <35 g/l; and low sodium, <135 mEq/l. P values are by Fisher exact tests or Wilcoxon rank sum tests, as appropriate.

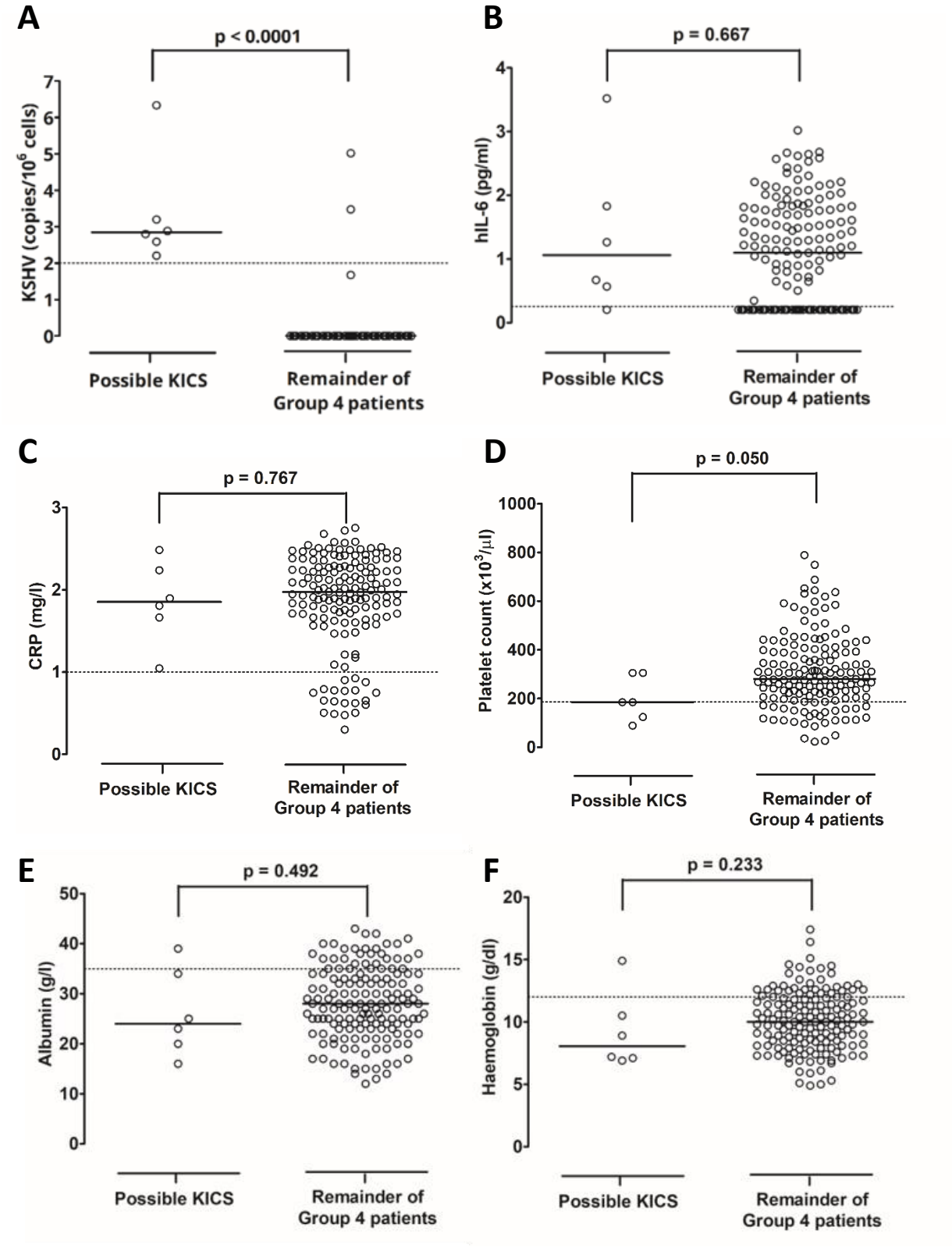

Figure 9: Selected KICS-defining parameters in "possible KICS" patients. A) KSHV VL, **B)** IL-6 levels, **C)** CRP levels, **D)** platelet count, **E)** albumin and **F)** haemoglobin in "possible KICS" patients (n=6) compared to the remainder of Group 4 patients (n=153). The dotted lines mark abnormal levels (KSHV VL >100 copies/10^6 cells; IL-6 >1.8 pg/ml [22]; CRP >10 mg/l, platelet count <186, albumin <35 g/l and haemoglobin <12 g/dl). P values are by Wilcoxon rank sum test. Data are log transformed where necessary. Each circle represents a patient.

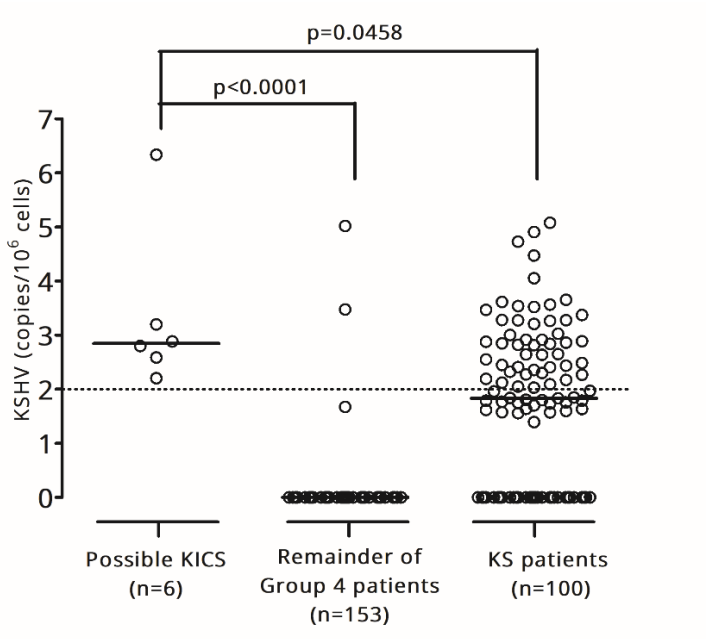

Figure 10: Comparison of KSHV VL in "possible KICS" patients with independently recruited KS patients. The dotted line marks abnormal levels (KSHV VL >100 copies/10^6 cells). P values are by Wilcoxon rank sum test. Data are log transformed. Each circle represents a patient.

Finally, the overall survival at the end of the 12-weeks study period was significantly worse in the identified "possible KICS" patients compared to the remainder of the non-proven TB patients without any other microbiologically proven co-infection, with an overall mortality of 83% (5/6) among the "possible KICS" patients (compared to 15% for the remainder of the group) and a median time to death in the "possible KICS" patients of 11 days ((95% CI: 0.00, 50.61); remainder of the group= undefined) (Figure 11), supporting previous reports of markedly elevated risk of death in KICS subjects [6]. However, this significant difference between the two survival curves should be interpreted with care as the assumption of similar percentage of censored cases between groups is not upheld due to the large discrepancy in sample size per group and the relatively short study period.

Three of the six "possible KICS" patients had KSHV-associated malignancies. One was diagnosed with KSHV-associated MCD at autopsy. This patient displayed the highest KSHV VL of the entire cohort (2,165,642 copies/10^6 cells) and was positive for K8.1 but not ORF73, indicating a highly lytically active KSHV infection. This patient was empirically treated for TB for six months with no improvement prior to admission. He presented with further deterioration after completion of TB treatment and died on the day of enrolment. His CD4 count was 328 cells/µl, and HIV VL was undetectable. The patient had evidence of systemic inflammation (CRP=304 mg/l) and cytokine activation (IL-6=3307 pg/ml), as well as severe anaemia (haemoglobin=0.9 g/dl), thrombocytopenia (platelet count=124), hypoalbuminemia (albumin=16 g/l), hyponatremia (sodium=125 mEq/l),

lymphadenopathy and hepatomegaly. KICS-associated symptoms included respiratory symptoms (cough), weight loss, nausea, body pain and weakness. Histologic examination of lymph nodes was consistent with KSHV-associated MCD (Figure 12). There was no evidence of PEL. Two other "possible KICS" patients' deaths were likely attributable to KICS in the setting of KS. One had biopsy-confirmed KS, was re-started on ART but died before assessment for chemotherapy. One patient, after deterioration on empiric anti-TB therapy, had skin KS confirmed on biopsy and features of lung KS on computed tomography scan two weeks prior to death. The other "possible KICS" patients did not have identified KSHV-associated malignancies. One was started on TB treatment empirically, deteriorated on treatment and was diagnosed with an invasive keratinising moderately differentiated SCC during evaluation of an upper gastrointestinal bleed. The other patient suffered from chronic renal failure due to an urethral stricture and was admitted with an episode of acute kidney injury. The patient was treated for suspected bacterial sepsis but died within the study period. The sixth patient was treated for suspected bacterial meningitis, improved and survived the follow-up period.

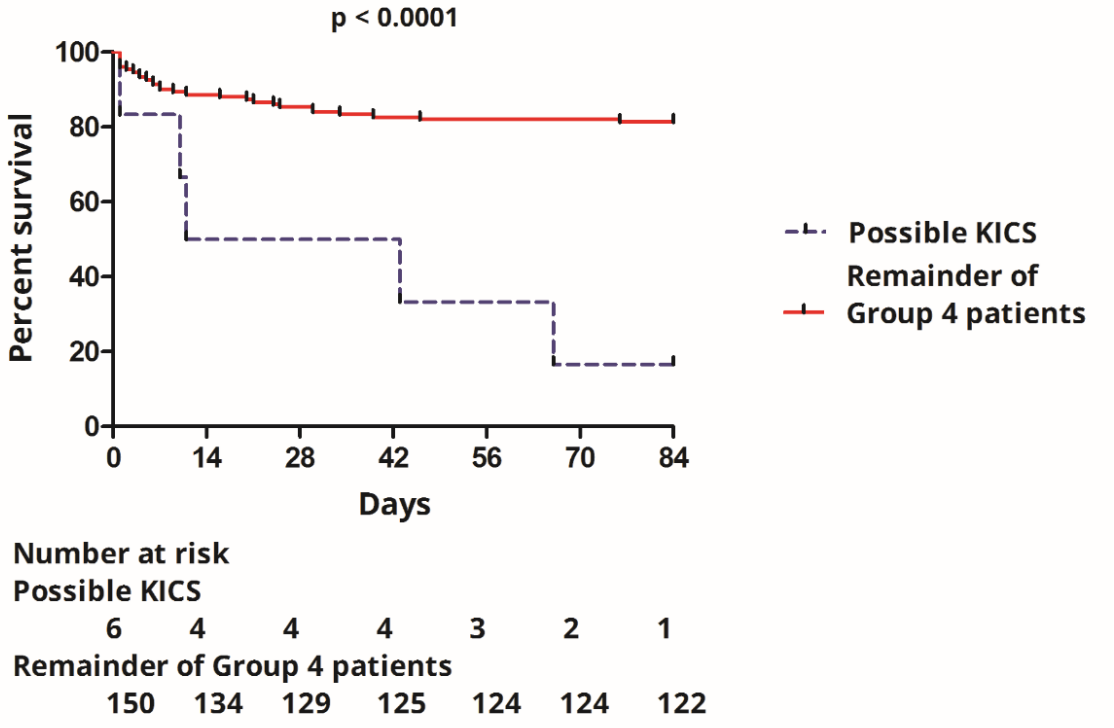

Figure 11: Overall survival at the end of the 12-weeks study period in "possible KICS" patients compared to the remainder of Group 4 patients. P value is by log-rank test.

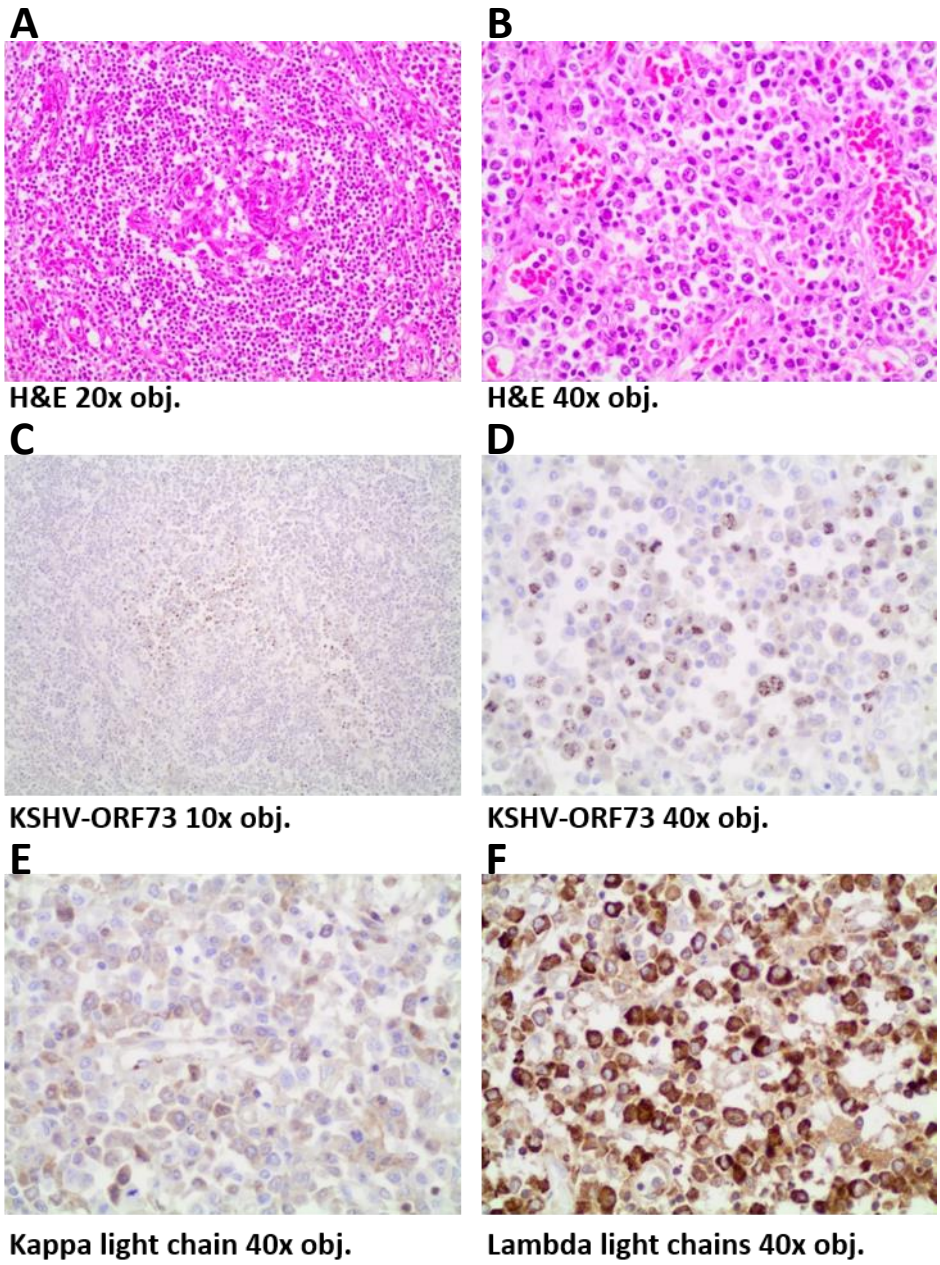

Figure 12: Histopathological assessment of post-mortem lymph node biopsies taken from a "possible KICS" patient with the highest KSHV VL of the entire patient cohort. A) Haematoxylin and eosin (H&E) stain showing a regressed germinal centre with sheets of plasma cells in the mantle zone among prominent capillaries, (20X objective magnification). **B)** Haematoxylin and eosin (H&E) stain showing an infiltrate of numerous benign plasma cells (40X objective magnification). **C)** Immunohistochemical stain of KSHV-ORF73 showing aggregates of KSHV-positive cells in the lymph node staining brown (10X objective magnification). **D)** Immunohistochemical stain showing brown granular nuclear KSHV-ORF73 positivity among the numerous background plasma cells (40X objective magnification). **E)** Immunohistochemistry for kappa light chains demonstrates few of the plasma cells in an area of ORF73-positive cells are kappa restricted (40X objective magnification). **F)** Immunohistochemistry of lambda light chains in the area ORF73-positive cells demonstrates many plasma cells are lambda restricted cells (40X objective magnification).

3.2. The genetic contribution of EPHA2 receptor variants to KSHV susceptibility and KS development

KSHV infection is necessary but insufficient for the development of KS requiring precipitating factors, such as HIV infection and related immunosuppression [67]. Even so, patients who are HIV and KSHV-positive do not strictly develop KS suggestive of a role for host factors in seroconversion after exposure to KSHV as well as in KS development [67].

EPHA2 is a key host receptor utilised by KSHV for cell entry and intracellular trafficking [36]. Moreover, EPHA2 has also been implicated in oncogenesis [36,37,307], thus potentially acting at the level of both susceptibility to KSHV infection and susceptibility to KS development. These key functional roles of EPHA2 render it a promising candidate as a host genetic factor involved in KSHV susceptibility and subsequent KS development.

3.2.1. Previously identified genetic association of EPHA2 SNVs with KSHV susceptibility and KS development

Our previous work identified SNVs in EPHA2 that were associated with susceptibility to KSHV infection or KS development, which has been published and formed my MSc thesis [34,35]. To frame the context of the current results, details of the previous study are given here.

3.2.1.1. Definition of the patient cohort

HIV-positive patients from South Africa were recruited (see 2.2) into three groups, namely:

Group 1 (KS+/KSHV+): patients with KS who were KSHV seropositive

Group 2 (KS-/KSHV+): patients without KS who were KSHV seropositive

Group 3 (KS-/KSHV-): patients without KS who were KSHV seronegative

KS was clinically diagnosed and KSHV serostatus was determined by ELISAs to KSHV lytic antigen K8.1 and latent antigen LANA.

3.2.1.2. Previous identification of EPHA2 SNVs associated with KSHV susceptibility or KS development

In our previous study, we sequenced the entire EPHA2 coding region in 150 HIV-positive patients grouped by KS and KSHV status to identify EPHA2 SNVs that were associated with KS development or KSHV susceptibility [34,35]. After removing SNVs based on linkage disequilibrium and with MAF <3% (calculated within the test group), four individual variants (Supplementary table 1) were assessed statistically for association with KSHV susceptibility by comparing their frequency in KSHV-positive patients (group 1 and 2, n=100) to KSHV-negative patients (group 3, n=50) resulting in the discovery of a novel heterozygous C>T variant in the conserved Pkinase-Tyr domain at mRNA position 2727, which was found to be significant (OR=6.4 (95% CI: 1.4, 28.4), adj. p=0.028), occurring in 21 (21%) KSHV+ patients (14 in Group 1 and 7 in Group 2) and in only 2 (4%) KSHV- (Group 3) patients. This variant was predicted to result in a non-conservative substitution of a cysteine for arginine at AA position 858.

Similarly, after removing SNVs based on linkage disequilibrium and with MAF <3% (calculated within the test group), eight individual variants (Supplementary table 2) were assessed statistically for association with KS development by comparing occurrence in KS+/KSHV+ (Group 1, n=50) patients versus KS-/KSHV+ (Group 2, n=50) patients. The variant at mRNA positions 2254 was predicted to result in a novel, non-conservative AA change from leucine to proline at AA position 700 and is in linkage disequilibrium with another SNV at mRNA position 2257 predicted to result in an AA substitution from Aspartate to alanine at the next AA position, 701, in the conserved Pkinase-Tyr domain. These variants were found to co-occur in eight (16%) KS+ patients (Group 1, with an additional Group 1 patient showing only the variant at mRNA position 2257) and not to occur at all (0%) in KS- patients in Group 2 (OR=1.2 (95% CI: 1.1, 1.3), adj. p=0.04). Additionally, several other variants occurring in the Pkinase-Tyr domain (spanning mRNA positions 1990–2766), were found to be overrepresented in the KS+ (Group 1) patients (Supplementary table 2); the most marked of these was a heterozygous G>C variant at mRNA position 2688, predicted to result in the substitution of alanine with proline at position 845 which was found to occur in 6 (12%) of KS+ (Group 1) patients and no KS-negative (Group 2) patients (OR=1.1 (95% CI: 1.0, 1.3), adj. p=0.16). A previously reported SNP at this position (rs765280326) indicated an 'A' allele while our data show a 'C' allele. Within the SAM domain, a heterozygous G>T variant at mRNA position 2990, predicted to result in a substitution of asparagine for lysine at AA position 945, was found to be significantly more frequent among KS+/KSHV+ (Group 1) patients (18%) compared to KS-/KSHV+ (Group 2) patients (0%) (OR=1.2 (95% CI: 1.1, 1.4), adj. p=0.02, Supplementary table 2).

We further assessed the occurrence of these variants in relation to detectable KSHV VL (not previously reported) amongst KSHV-positive patients (Groups 1 and 2, n=100) after removing SNVs based on linkage disequilibrium and with MAF <3% (calculated within the test group, Supplementary table 3). We discovered that the G>T variant at mRNA position 2990, also associated with KS status (Supplementary table 2), was statistically associated with KSHV VL (OR=11.7 (95% CI: 1.4, 97.3), adj. p=0.08) occurring in eight patients (18%) with detectable VL and only one patient (2%) with undetectable VL. These results are summarised in Table 23.

Table 23: Previously identified variants found to be associated with KSHV susceptibility, KS development or KSHV VL [34,35]**.** In addition to previous analyses (Supplementary table 1 and Supplementary table 2), previously identified variants were statistically tested for association with KSHV VL (not previously reported, Supplementary table 3). AA position and domain are according to the EPHA2 NCBI reference NP_004422.2 and named according to IUPAC standards. Ambiguous base notations represent heterozygous variants. P values are adjusted for multiple comparisons. SNVs that have a record on the dbSNP are indicated by their rsid numbers.

SNV /rs number	EPHA2 Domain	Predicted AA change	Associated with (Adjusted P-value)	Original analysis
2254 T>Y	Pkinase-Tyr	700 Leu>Pro	KS (0.04)	Supplementary table 2
2257 A>C	Pkinase-Tyr	701 Asp>Ala	KS (0.04)	Supplementary table 2
2688 G>S */rs765280326*	Pkinase-Tyr	845 Ala>Pro	KS (0.16)	Supplementary table 2
2727 C>Y	Pkinase-Tyr	858 Arg>Cys	KSHV (0.028)	Supplementary table 1
2990 G>K	SAM	945 Lys>Asn	KS (0.021) KSHV VL (0.08)	Supplementary table 2 Supplementary table 3

3.2.2. Aggregate association analysis of previously identified SNV data with KSHV susceptibility, KS development and KSHV VL

When aggregate variation was considered within each of the functional domains of EPHA2, it was observed that having one or more SNV in the Pkinase-Tyr domain or SAM domain was associated with increased risk of KS (OR=4.9 (95% CI: 1.9, 12.4), p=0.001 and OR=13.8 (95% CI: 1.7, 111.6), p=0.014, respectively, Table 24A). Aggregate tests did not find significant associations between EPHA2 SNVs and KSHV status. However, there was a trend indicating that having one or more Pkinase-Tyr domain SNV was associated with increased risk of KSHV infection. Specifically, 32 (32%) KSHV cases had one

Table 24: Aggregate score associations for SNV domain with A) KS status, B) KSHV status [34] **and C) KSHV VL status.** By-gene tests were restricted to SNVs with MAF <5% and were stratified by the domain in which the SNV is located (Pkinase-Tyr, SAM, 3' or 5' UTR, Fn-3 or no domain). Each study participant and category was scored based on the total number of SNVs that participant carried and categorized as having any variants (≥1) versus no variants (0). Associations were assessed using logistic regression. N=number of participants.

A

SNV domain	KS^- 0 N (%)	KS^- ≥ 1 N (%)	KS^+ 0 N (%)	KS^+ ≥ 1 N (%)	P value	OR (95% CI)
Pkinase-Tyr	42 (84%)	8 (16%)	26 (52%)	24 (48%)	0.001	4.85 (1.9, 12.38)
SAM	49 (98%)	1 (2%)	39 (78%)	11 (22%)	0.0137	13.82 (1.71, 111.6)
3'UTR	47 (94%)	3 (6%)	41 (82%)	9 (18%)	0.0777	3.44 (0.87, 13.56)
None	45 (90%)	5 (10%)	43 (86%)	7 (14%)	0.5399	1.47(0.43, 4.97)
5'UTR	49 (98%)	1 (2%)	49 (98%)	1 (2%)	1	1 (0.06, 16.44)
Fn-3	47 (94%)	3 (6%)	45 (90%)	5 (10%)	0.4655	1.74 (0.39, 7.71)

B

SNV domain	$KSHV^-$ 0 N (%)	$KSHV^-$ ≥ 1 N (%)	$KSHV^+$ 0 N (%)	$KSHV^+$ ≥ 1 N (%)	P value	OR (95% CI)
Pkinase-Tyr	41 (82%)	9 (18%)	68 (68%)	32 (32%)	0.0734	2.14 (0.93, 4.94)
SAM	48 (96%)	2 (4%)	88 (88%)	12 (12%)	0.1307	3.27 (0.7, 15.23)
3'UTR	46 (92%)	4 (8%)	88 (88%)	12 (12%)	0.4573	1.57 (0.48, 5.14)
None	43 (86%)	7 (14%)	88 (88%)	12 (12%)	0.7287	0.84 (0.31, 2.28)
5'UTR	49 (98%)	1 (2%)	98 (98%)	2 (2%)	1	1 (0.09, 11.3)
Fn-3	46 (92%)	4 (8%)	92 (92%)	8 (8%)	1	1 (0.29, 3.5)

C

SNV domain	$KSHV^-$ 0 N (%)	$KSHV^-$ ≥ 1 N (%)	$KSHV^+$ 0 N (%)	$KSHV^+$ ≥ 1 N (%)	P value	OR (95% CI)
SAM	52 (95%)	3 (5%)	36 (80%)	9 (20%)	0.036	4.33 (1.10, 17.12)
Pkinase-Tyr	42 (76%)	13 (24%)	27 (60%)	18 (40%)	0.081	2.15 (0.91, 5.10)
3'UTR	51 (93%)	4 (7%)	37 (82%)	8 (18%)	0.118	2.78 (0.77, 9.84)
None	47 (86%)	8 (14%)	41 (91%)	4 (9%)	0.391	0.57 (0.16, 2.04)
Fn-3	50 (91%)	5 (9%)	42 (93%)	3 (7%)	0.658	0.71 (0.16, 3.17)
5'UTR	54 (98%)	1 (2%)	44 (98%)	1 (2%)	0.886	1.23 (0.08, 20.19)

or more Pkinase-Tyr SNV compared to only 9 (18%) KSHV-negative controls (OR=2.1 (95% CI: 0.93, 4.9), p=0.07, Table 24B). Aggregate variation in the SAM domain was associated with detectable VL among KSHV seropositive patients (OR=4.3 (95% CI: 1.1, 17.1), p=0.036, Table 24C). These aggregate analyses indicated that the Pkinase-Tyr and SAM domains were the region of interest on which we should focus our further analyses.

3.2.3. Validation of previously identified SNVs in a newly recruited cohort

Before further analysing the SNVs presented in Table 23 (n=150, 50 patients per group) in functional assays, we wanted to increase the power of the statistical analysis by increasing the sample size (see 2.2.2.1). Sample size calculations based on our previous analyses (see 3.2.1) necessitated that we recruit n=100 patients per group (see 3.2.1.1). Due to cost constraints, it was necessary to limit this to regions of interest in EPHA2 which were identified by by-gene analysis of aggregate variation [332] stratified by EPHA2 domain (see 3.2.2, Table 24). We recruited a further 150 patients (an additional 50 per group) into our defined patient groups (see 3.2.1.1) from the same clinics.

3.2.3.1. Demographic and clinical information

Clinical and demographic information concerning the above-mentioned participant groups (see 3.2.1.1, total sample size n=300, with n=100 per group) is summarised in Table 25. All patients were HIV-infected as determined serologically prior to recruitment. Age did not differ significantly between the three groups: median age was 35, 30 and 37 for Groups 1, 2 and 3, respectively. Population group distribution was heavily skewed towards black Africans (94%) and included only a minority of mixed ancestry (5.4%) and Caucasian (0.7%) individuals which was consistent across the three patient groups. The final cohort of patients had a slight overrepresentation of males (52.3%) compared to females (47.7%) but that was particularly marked in KS patients (Group 1: males 65%, females 35%) which was different to KS-/KSHV+ Group 2 patients (p=0.007); and KSHV+ patients (Groups 1 and 2: males 57%, females 43%) vs. KSHV- Group 3 patients (p=0.05). Most recent CD4 counts were recorded at the time of patient recruitment. Median CD4 count was highest in Group 1 patients (KS+/KSHV+) and lowest in Group 3 patients (KS-/KSHV-) which is most likely a function of the proportion of patients on ART at time of recruitment: all KS+ patients (Group 1) were receiving ART or were started on ART on the day of enrolment, whereas a significantly smaller number of KS- patients (Groups 2 and 3) were on ART medication (p <0.0001) at the time of recruitment. CD4 count and ART status differed significantly between KS+/KSHV+ (Group 1) and KS-/KSHV+ (Group 2) patients and between KSHV+ (Groups 1 and 2) vs. KSHV- (Group 3) patients. Although sex ratio, CD4 count and ART status differed

between these groups, we considered them suitable for further candidate gene association analysis as these variables could not have an effect on the genetic level. Where statistical differences existed between groups tested in association analyses (Table 25 and Table 26), we performed logistic regression to control for differences in these variables.

Table 25: Clinical and demographic information of the three patient groups making up the entire cohort (n=300). Variables are assessed according to comparisons used in statistical association testing: * indicates statistical significance ($p<0.05$) for KS association test comparisons (Group 1 vs. Group 2); # for KSHV association test comparisons (Group 1 + Group 2 vs. Group 3). Age and CD4 count were assessed by Mann Whitney test. Sex, population group and ART status were assessed by Chi square or Fisher exact tests. IQR, inter-quartile range; ART, antiretroviral therapy.

	GROUP 1 KS+ KSHV+	**GROUP 2** KS- KSHV+	**GROUP 3** KS- KSHV-
Sample size	100	100	100
Age, median in years (IQR)	35 (31–41)	40 (31–47)	37 (31–45)
Sex, count (%) *#			
Male	65 (65)	48 (48)	44 (44)
Female	35 (35)	52 (52)	56 (56)
Population group, number (%)			
Black	89 (89)	95 (95)	97 (97)
Mixed ancestry	10 (10)	3 (3)	3 (3)
Caucasian	0 (0)	2 (2)	0 (0)
Unknown	1 (1)	0 (0)	0 (0)
On ART at time of blood draw *#			
Yes	99 (99)	63 (63)	64 (64)
No	1 (1)	37 (37)	36 (36)
CD4 count, median in cells/µl (IQR) *#	181 (53–332)	114 (46–225)	81 (32–204)

Table 26: Assessment of KSHV VL in patient groups. KSHV status (KSHV+/KSHV-) was determined by ELISA. KSHV VL is considered elevated if >100 copies/10^6 cells.

KSHV VL	**GROUP 1** KS+ KSHV+	**GROUP 2** KS- KSHV+	**GROUP 3** KS- KSHV-
Detectable VL, number (%)	66 (66%)	17 (17%)	0 (0%)
VL, median in copies/10^6 cells (Range)	294 (25–119,760)	199 (25–104,664)	*NA*
Elevated VL, number (%)	47 (47%)	12 (12%)	0 (0%)

3.2.3.2. KSHV VL testing

KSHV VL in the blood was assessed in all patients regardless of their KSHV serostatus by quantitative Taqman PCR (Table 26). We detected KSHV in the blood of 66 KS patients (Group 1), 47 of which had elevated VL (>100 copies/10^6 cells), and 17 KS-/KSHV+ patients, 12 of which had elevated levels. We did not detect KSHV in the blood of any of the KSHV- patients. Where detectable, VL varied over a large range with median VL of 294 copies/10^6 cells and 199 copies/10^6 cells in KS+ (Group 1) and KS-/KSHV+ (Group 2) patients, respectively. Demographic and clinical variables between KSHV VL detectable and KSHV VL non-detectable groups did not differ with the exception of sex: there was a higher proportion of males (65%) in the VL detectable group compared to the VL non-detectable group (50%, p=0.044, Table 27).

Table 27: Clinical and demographic information for patients with detectable VL vs. KSHV seropositive patients with non-detectable VL, irrespective of presence of KS (n=200). All participants were KSHV seropositive (Groups 1 and 2). * indicates statistical significance (p<0.05). Age and CD4 count were assessed by Mann Whitney test. Sex, population group and ART status were assessed by Chi square or Fisher exact tests. IQR, inter-quartile range; ART, antiretroviral therapy.

	Detectable KSHV VL	Non-detectable KSHV VL
Sample size	83	117
Age, median in years (IQR)	37 (32–42)	37 (31–45)
Sex, count (%) *		
Male	54 (65)	59 (50)
Female	29 (35)	58 (50)
Population group, number (%)		
Black	74 (90)	110 (94)
Mixed ancestry	8 (10)	5 (4)
Caucasian	0 (0)	2 (2)
On ART at time of blood draw		
Yes	71 (86)	91 (78)
No	12 (14)	26 (22)
CD4 count, median in cells/µl (IQR)	153 (55–274)	128 (44–281)

3.2.3.3. Overview of identified EPHA2 variants in the Pkinase-Tyr and SAM domains

Our original sequencing study of the entire EPHA2 coding DNA identified a total of 17 variants in the region of interest (Pkinase-Tyr and SAM domains, identified by aggregate analysis (see 3.2.2)) [34]. Additional sequencing of this region in a further 150 patients (falling into the three categories based on KS diagnosis and KSHV serology status as outlined above) resulted in a total of 18 variants, 9 of which were previously identified in our original cohort [34] and 9 of which were unique to this validation cohort (Supplementary table 4). Of the 26 variants identified across both cohorts: 20 were

missense variants and the remaining 6 were synonymous; 14 were previously reported on the SNP database while the remaining 12 were novel. For the purposes of our further analysis, we pooled the original and validation cohorts to enhance the overall statistical power.

3.2.3.4. Association testing for identified SNVs and KSHV susceptibility, KS development and detectable KSHV VL

The statistical tests previously done on the original patient cohort (selected after removing SNVs based on linkage disequilibrium and with MAF <3%; Supplementary table 1, Supplementary table 2 and Supplementary table 3) were repeated including the same SNVs within the region of interest that were previously tested as the aim was to validate the previously identified variants. Four individual variants (Supplementary table 1) were assessed statistically for association with KSHV susceptibility by comparing their frequency in KSHV-positive patients (Group 1 and 2, n=200) to KSHV-negative patients (Group 3, n=100) resulting in the validation of the previously identified C>T variant at mRNA position 2727, which was found to be significant in this larger cohort (OR=8.0 (95% CI: 1.9, 34.2), adj. p=0.004), occurring in 28 (14%) KSHV+ patients (21 in Group 1 and 7 in Group 2) and in only 2 (2%) KSHV- (Group 3) patients (Table 28).

Seven individual variants (Supplementary table 2, one variant from the original analysis of eight was outside of the region of interest) were assessed statistically for association with KS development by comparing occurrence in KS+/KSHV+ (Group 1, n=100) patients versus KS-/KSHV+ (Group 2, n=100) patients (Table 29). Variant C2727Y, associated with KSHV, was also found to be significantly associated with KS (OR=3.5 (95% CI: 1.4, 8.7), adj. p=0.0049). The variant at mRNA positions 2254 (which is in linkage disequilibrium with another SNV at mRNA position 2257), previously found to be significantly associated with KS, was validated in this larger cohort (OR undefined, adj. p=.049). The G>C variant at mRNA position 2688, which was found to be overrepresented in KS+ patients in our original analysis but not statistically significant, was found to be significantly associated with KS before adjustment for multiple comparisons but not after (OR undefined, adj. p=0.014, adj. p=0.098), occurring in 7 (7%) KS+ patients (Group 1) patients and no KS-negative (Group 2) patients. The mRNA variant at position 2990 was found to be significantly more frequent among KS+/KSHV+ (Group 1) patients (9%) compared to KS-/KSHV+ (Group 2) patients (0%) (OR undefined, adj. p=0.021).

Similarly, seven variants (Supplementary table 3) were assessed in relation to detectable KSHV VL amongst KSHV-positive patients (Groups 1 and 2, n=200, Table 30). The G>T variant at mRNA position 2990, also associated with KS status, was significantly associated with KSHV VL (OR=12.4 (95% CI: 1.5, 100.9), adj. p=0.028) occurring in 8 patients (10%) with detectable VL and only 1 patient (1%) with undetectable VL.

Table 28: Associations between EPHA2 SNVs and KSHV (n=300). [1]P values adjusted for multiple comparisons. [2]OR adjusted for logistic regression controlling for sex, ART status and CD4 count when SNV is statistically significant in univariate analysis. N=number of cases.

SNV	KSHV- n=100 N (%)	KSHV+ n=200 N (%)	p	Adjusted[1] P	OR (95% CI)	Adjusted[2] OR (95% CI)	Log reg. P
C2727Y	2 (2%)	28 (14%)	0.001	0.004	8.0 (1.9, 34.2)	6.7 (1.5, 29.2)	0.012
G2990K	2 (2%)	9 (5%)	0.347	1	2.3 (0.5, 10.9)	-	-
A2217M	2 (2%)	8 (4%)	0.505	1	2.0 (0.4, 9.7)	-	-
T2047Y	7 (7%)	12 (6%)	0.803	1	0.8 (0.3, 2.2)	-	-

Table 29: Associations between EPHA2 SNVs and KS (n=200). [1]P values adjusted for multiple comparisons. [2]OR adjusted for logistic regression controlling for sex, ART status and CD4 count when SNV is statistically significant in univariate analysis. Undefined OR is due to one group having 0 cases. N=number of cases.

SNV	KS- n=100 N (%)	KS+ n=100 N (%)	p	Adjusted[1] P	OR (95% CI)	Adjusted[2] OR (95% CI)	Log reg P
G2990K	0 (0%)	9 (9%)	0.003	0.021	Undefined	Undefined	Undefined
T2254Y	0 (0%)	8 (8%)	0.007	0.049	Undefined	Undefined	Undefined
C2727Y	7 (7%)	21 (21%)	0.007	0.049	3.5 (1.4, 8.7)	2.7 (0.9, 7.7)	0.074
G2688S	0 (0%)	7 (7%)	0.014	0.098	Undefined	Undefined	Undefined
G2325S	1 (1%)	5 (5%)	0.212	1	5.2 (0.6, 45.4)	-	-
A2217M	5 (5%)	3 (3%)	0.721	1	0.6 (0.1, 2.5)	-	-
T2047Y	5 (5%)	7 (7%)	0.76	1	1.4 (0.4, 4.7)	-	-

Table 30: Associations between EPHA2 SNVs and KSHV VL (n=200). [1]P values adjusted for multiple comparisons. [2]OR adjusted for logistic regression controlling for sex, ART status and CD4 count when SNV is statistically significant in univariate analysis. N=number of cases.

SNV	KSHV VL- n=117 N (%)	KSHV VL+ n=83 N (%)	p	Adjusted [1] P	OR (95% CI)	Adjusted[2] OR (95% CI)	Log reg P
G2990K	1 (1%)	8 (10%)	0.004	0.028	12.4 (1.5, 100.9)	11.3 (1.4, 92.8)	0.024
T2254Y	2 (2%)	6 (7%)	0.068	0.476	4.5 (0.9, 228)	-	-
G2688S	2 (2%)	5 (6%)	0.129	0.903	3.7 (0.7, 19.5)	-	-
C2727Y	13 (11%)	15 (18%)	0.214	1	1.8 (0.8, 3.9)	-	-
G2325S	3 (3%)	3 (4%)	0.694	1	1.4 (0.3, 7.2)	-	-
A2217M	5 (4%)	3 (4%)	1	1	0.8 (0.2, 3.6)	-	-
T2047Y	8 (7%)	4 (5%)	0.764	1	0.7 (0.2, 2.4)	-	-

To account for differences in demographic and clinical variables (Table 25, Table 27) that may affect our association analyses (see 3.2.3.1), logistic regression was employed for statistically significant SNVs controlling for the clinical and demographic variables that differed between the groups analysed.

3.2.3.5. Validated variants taken forward for functional analysis

SNVs that were found to be significantly associated or strongly tended toward KSHV serumpositivity (Table 28), KS (Table 29) and detectable KSHV VL (Table 30) were assessed *in silico* with the PolyPhen-2 prediction tool generating a score on a scale of 0 (benign) to 1 (probably damaging) with regard to the impact of an AA substitution on the EPHA2 protein function based on sequence homology, conserved family annotations and PDB 3D structures [330]. These scores are reported in Table 31. As a control, a conservative missense C>G variant at mRNA position 915 found within our patient cohort but not statistically associated with KSHV, KS or KSHV VL, was included and its predicted AA change of leucine to valine at position 254 was allocated a '0' score with an annotation of 'benign'. Four non-synonymous variants in the Pkinase-Tyr domain were annotated as 'probably damaging'. The SAM variant, lysine to asparagine at AA position 945 (encoded by 2990 G>T), was predicted to be 'possibly damaging'. These variants were selected for further functional assays.

Table 31: Predicted functional consequences of validated variants found to be associated with KSHV susceptibility, KS development or KSHV VL [34,35]**.** AA position and domain are according to the EPHA2 NCBI reference NP_004422.2 and named according to IUPAC standards. Ambiguous base notations represent heterozygous variants. P values are adjusted for multiple comparisons.

SNV name	Nucleotide position and change	Domain	Predicted AA position and change	PolyPhen prediction (score)	Associated with (Adjusted P-value)
SDM1	915 C>S	-6 EGF-like	254 Leu>Val	Benign (0)	-
SDM2	2257 A>M	Pkinase-Tyr	701 Asp>Ala	Probably damaging (0.965)	KS (0.0049, Table 29)
SDM3	2254 T>Y	Pkinase-Tyr	700 Leu>Pro	Probably damaging (0.998)	KS (0.0049, Table 29)
SDM4	2257 A>M + 2254 T>Y	Pkinase-Tyr	701 Asp>Ala + 700 Leu>Pro	-	KS (0.0049, Table 29)
SDM5	2688 G>S	Pkinase-Tyr	845 Ala>Pro	Probably damaging (0.991)	KS (0.098, Table 29)
SDM6	2727 C>Y	Pkinase-Tyr	858 Arg>Cys	Probably damaging (0.932)	KSHV (0.004, Table 28) KS (0.049, Table 29)
SDM7	2990 G>K	SAM	945 Lys>Asn	Possibly damaging (0.903)	KS (0.021, Table 29) KSHV VL (0.028, Table 30)

3.3. Determining the consequences of EPHA2 variants on KS development and KSHV infection

3.3.1. Establishing a relevant cell culture system to test the functional consequences of identified EPHA2 variants

To assess the functional consequences of the EPHA2 variants found within our clinical study to be associated with KS, KSHV or KSHV VL (Table 31) which were predicted to have significant functional effects *in silico,* we aimed to establish a relevant cell culture system to study the impact of EPHA2 variants on EPHA2 expression, EPHA2 steady state and KSHV-induced tyrosine phosphorylation and KSHV binding, internalisation and infection.

3.3.1.1. Assessing the EPHA2 variants in an overexpression model

Initially, we assessed endogenous EPHA2 protein expression in the HEK293 cell line, the conditionally immortalised human endothelial cell line HuARLT2 and a HuARLT2 cell line latently infected with rKSHV, HuARLT2.rKSHV, by Western blot (Figure 13). While HEK293 cells have a very low endogenous EPHA2 level, EPHA2 is expressed at significantly higher levels in HuARLT2 cells. Latent infection with rKSHV caused a slight decrease in EPHA2 expression in HuARLT2.rKSHV cells.

As HEK293 cells have relatively low endogenous expression of EPHA2 and with the rationale that the identified EPHA2 variants may have a dominant effect on function, we initially tested the identified EPHA2 variants (Table 31) in an overexpression model by transiently transfecting pCMV3-untagged negative control vector (EV), EPHA2.pCMV (WT) and its mutant EPHA2.pCMV constructs (1–7) in HEK293 cells. EPHA2 variants were introduced to the pCMV3-EPHA2 (Sino Biological Inc) by SDM, confirmed by sequencing to assess the correct mutation was introduced and no undesired changes resulted in the entire EPHA2 coding region (Supplementary figure 9). All mutant EPHA2 constructs showed EPHA2 expression comparable to that of the transfected WT (Figure 14A) indicating that the introduction of the SNVs into the EPHA2 sequence did not affect expression. Transfected cells were infected with rKSHV at MOI 10 and GFP-positive cells were counted 48 h later showing that rKSHV infection of the WT and mutant transfected cell lines did not differ significantly (Figure 14B).

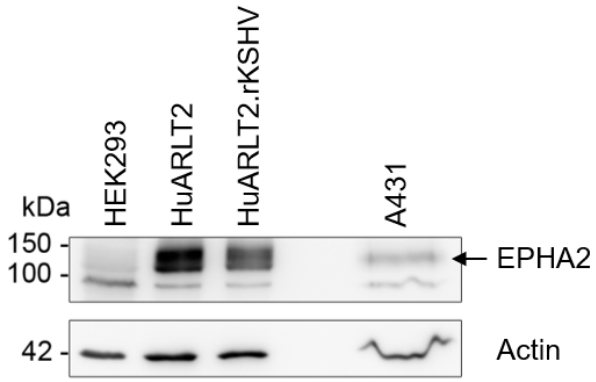

Figure 13: Endogenous expression of EPHA2 in HEK293 cells and HuARLT2 endothelial cells. HEK293, HuARLT2, HuARLT2.rKSHV and A431 (positive control, provided) cell lysates separated by SDS PAGE were probed with an anti-EphA2 antibody (clone D7 05-480, 1:500) which detects EPHA2 (140kDa) and a nonspecific band between <100 kDa [347]. Probing for actin indicates equal loading.

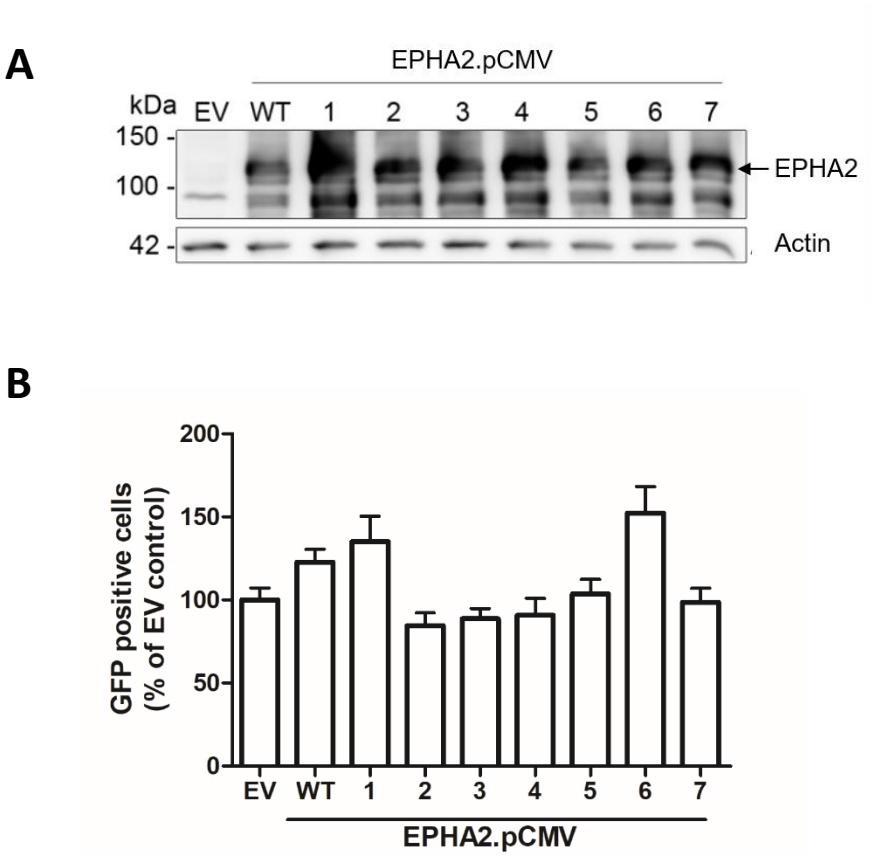

Figure 14: Transfection of WT-EPHA2 or SDM-generated mutant-EPHA2 constructs into HEK293 cells. HEK293 cells were transfected with pCMV3 negative control vector (EV), EPHA2.pCMV (WT) or mutant EPHA2.pCMV constructs 1–7. **A)** Mutant EPHA2 constructs are expression capable as shown by Western blot using an anti-EPHA2 antibody (clone D7 05-480, 1:500). EPHA2 is detected at 140 kDa, the band <100 kDa is nonspecific [347]. Actin staining serves as the loading control. **B)** Transiently transfected mutant EPHA2 cells were infected with rKSHV and infection measured by counting GFP-positive cells after 48 h. Data are pooled from two independent experiments.

3.3.1.2. CRISPR/Cas9 knockout of endogenous EPHA2 in HuARLT2 (Hu) cells

As we did not see any difference in the permissiveness to rKSHV infection upon transfection of the mutant EPHA2 constructs in HEK293 cells, we considered that the effects of our mutants may be overridden by endogenous EPHA2 expression. Moreover, we turned to HuARLT2 cells, an endothelial cell line, which is a more appropriate model system than HEK293 epithelial cells as KS develops from KSHV-infected endothelial cells. As HuARLT2 cells express endogenous EPHA2 at levels higher than HEK293 (Figure 13) which would likely interfere with our assays, we deleted the endogenous EPHA2 gene using CRISPR/Cas9. HuARLT2 cells were transduced with CRISPR/Cas9 lentiviruses containing either scrambled gRNA (control) or one of three gRNAs designed to target EPHA2 (gRNA 1, 2 and 3). Western blot analysis showed that EPHA2 expression was abolished in the cells transduced with gRNA 1 and gRNA 3 and markedly reduced in the cells transduced with gRNA 2 (Figure 15). We extracted genomic DNA from the cell lines transduced with scrambled gRNA and gRNA 1, 2 and 3 CRISPR/Cas9 lentivirus and subjected it to PCR amplification using primers designed to amplify the respective gRNA target sites followed by sequencing to confirm that the CRISPR/Cas9 system has successfully disrupted the double-stranded DNA within the expected region (Table 32). As the CRISPR/Cas9 transduced cells were not clonal, it was expected to see overlapping peaks starting within the gRNA target site, as is the case for gRNA target regions 1 and 2, when compared to the sequences generated from the HuARLT2 cells transduced with scrambled gRNA. Hu-G3 shows the introduction of a stop codon (TAA) within the gRNA target site.

We functionally compared our EPHA2 knockout cell lines, Hu-G1, Hu-G2 and Hu-G3 to two other EPHA2 knockout cell lines, SLK-KO (of epithelial origin) and LEC-KO (of LEC origin), kindly provided by Dr Frank Neipel (Institute of Clinical and Molecular Virology, University Clinic, Erlangen). As in the SLK-KO and the LEC-KO, Hu-G1 and Hu-G3 KOs had nil EPHA2 expression by Western blot (Figure 16A, top panel). Following infection with rKSHV at MOI 10 for 48 h, infection was largely reduced in Hu-G1 and Hu-G3 as well as in the SLK-KO and LEC-KO cell lines as assessed by LANA expression by Western blot (Figure 16A, bottom panel), fluorescent microscopy images of GFP+ cells (Figure 16B) and MFI of GFP as a measure of infection (Figure 16C). The greatest reduction in infection by GFP MFI between the Hu-KO cell lines compared to the control Hu-Scr cell line was seen in Hu-G3 (38% of Hu-Scr) which is comparable to the infection rates of the SLK-KO (34% of SLK) and LEC-KO (38% of LEC). Therefore, Hu-G3 was selected for future experiments.

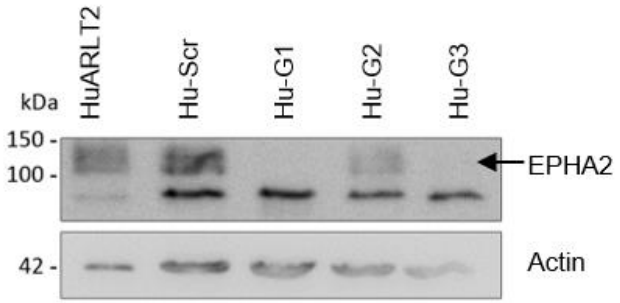

Figure 15: CRISPR/Cas9 EPHA2 KO in HuARLT2 cells. EPHA2 expression by Western blot in HuARLT2 cells and cells transduced with Scr.pLentiCRISPR v2 (Hu-Scr), G1.pLentiCRISPR v2 (Hu-G1) G2.pLentiCRISPR v2 (Hu-G2) or G3.pLentiCRISPR v2 (Hu-G3) using an anti-EPHA2 antibody (clone D7 05-480, 1:500). EPHA2 is detected at 140 kDa, while the band <100 kDa is nonspecific [347]; probing for actin indicates equal loading.

Table 32: Sequencing of the CRISPR/Cas9 cut sites in transduced cell lines shows CRISPR/Cas9 induced disruption of the double-stranded DNA. DNA extracted from Hu-Scr or Hu-KO cells was amplified and sequenced to visualise the respective gRNA cut sites (shaded in orange). The gRNA 1 and gRNA 2 cut sites show nonspecific disruption in the non-clonal KO cells while the gRNA 3 cut site shows the introduction of a stop codon (highlighted in yellow).

Region sequenced:	Cell line transduced with:	Sequencing primers:	Sequence chromatogram:
RNA1 target region	Scrambled gRNA	5' gRNA1	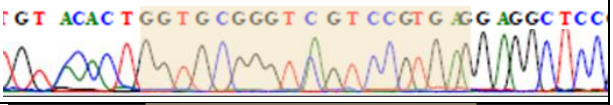
		3' gRNA1	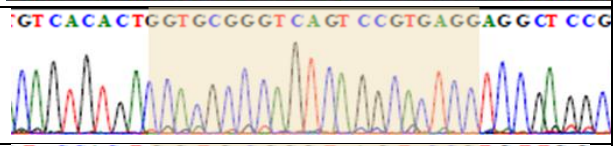
	gRNA1	5' gRNA1	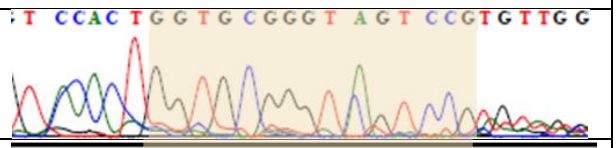
		3' gRNA1	
gRNA2 target region	Scrambled gRNA	5' gRNA2	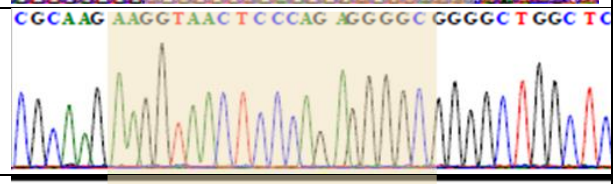
		3' gRNA2	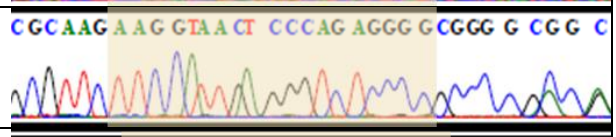
	gRNA2	5' gRNA2	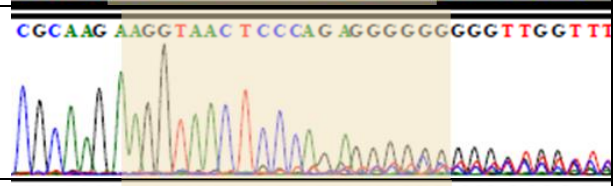
		3' gRNA2	
gRNA3 target region	Scrambled gRNA	5' gRNA3	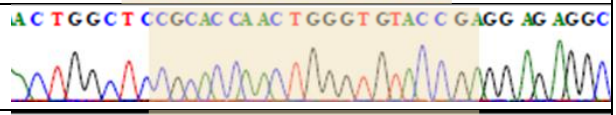
		3' gRNA3	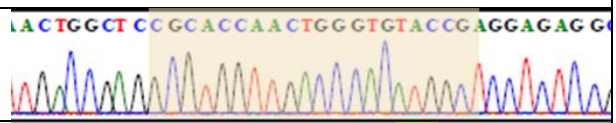
	gRNA3	5' gRNA3	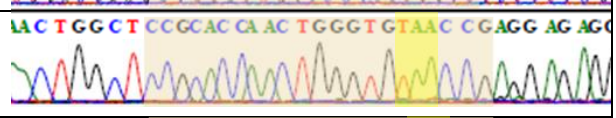
		3' gRNA3	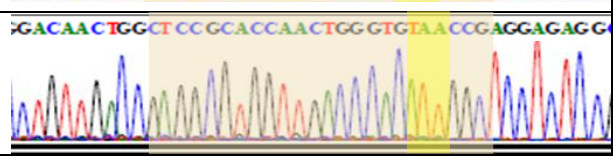

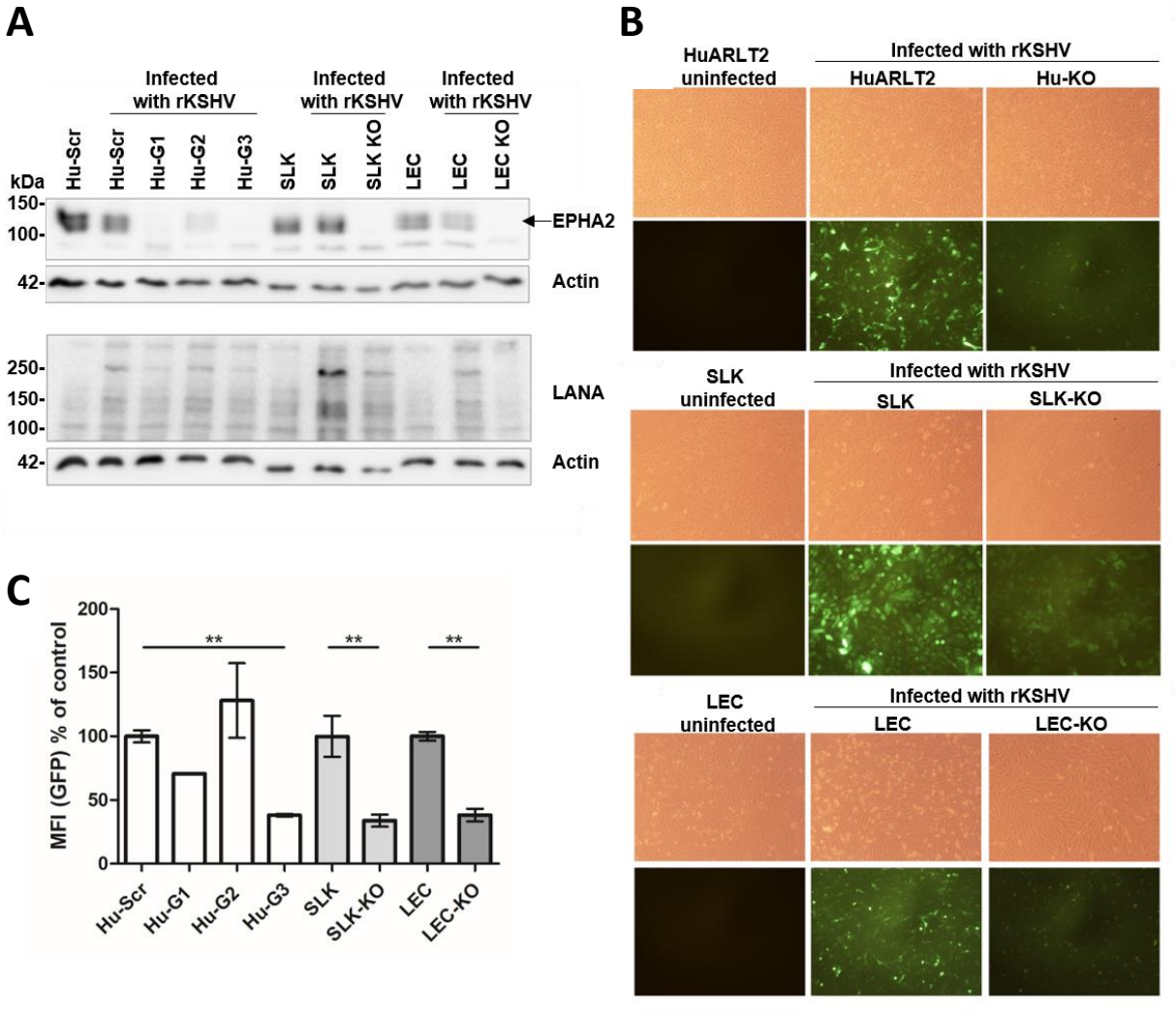

Figure 16: Evaluation of HuARLT2-KO cell lines compared to other established EPHA2 KO cell lines, SLK and LEC. A, top panel) EPHA2 expression by Western blot in Hu-G1, Hu-G2, Hu-G3, SKL-KO and LEC-KO compared to their respective control cell lines using an anti-EPHA2 antibody (clone D7 05-480, 1:500). EPHA2 is detected at 140 kDa, while the band <100 kDa is nonspecific [347]; probing for actin indicates equal loading. Subsequently to EPHA2 KO, WT and KO cells were infected with rKSHV as indicated at MOI 10 and assessed for rKSHV infection after 48 h by **A, bottom panel)** LANA Western blot (multiple bands between 100–250 kDa [348,349]) using a rat anti-LANA antibody (1:1,000), **B)** fluorescent microscopy of GFP-positive cells and **C)** MFI of GFP.

3.3.1.3. Reintroduction of synthetic EPHA2 into Hu-KO cells

Following endogenous EPHA2 knockout, reintroduction of WT and mutant EPHA2 constructs required their transduction into the generated Hu-KO cells (see 3.3.1.2). As the CRISPR/Cas9 system targeting EPHA2 was active within these cells, it was necessary to design a synthetic EPHA2 expression construct which would be resistant to the EPHA2-targeted CRISPR/Cas9. Therefore, we designed a sEPHA2 with silent mutations of the gRNA 3 target site (GeneArt, Thermo Fisher Scientific). This sEPHA2 plasmid was cloned into the lentiviral vector plasmid, RRL.SF.newMCS.i2.Zeo.pre by *Bam*HI and *Age*I restriction enzyme digestion followed by ligation. Cloning success was evaluated by restriction enzyme analysis with two sets of restriction enzymes: *Bam*HI/*Age*I and *Bam*HI/*Nde*I which were expected to yield fragments of 6564 bp/2937 bp and 9348 bp/1153 bp, respectively (see example Figure 17 in which clones 2, 4, 6 and 9 showed the expected fragment pattern on electrophoresis). Transduction of the selected clone (e.g. clone 9) into Hu-KO cells showed successful reintroduction of EPHA2 expression compared to the absence of EPHA2 in Hu-KO cells and the endogenous only expression in Hu-Scr cells (Figure 18, top panel) and further, rescued the phenotype of permissiveness to rKSHV infection as shown by Western blot to LANA (Figure 18, bottom panel). Transduced cells were selected with zeocin (400 µg/ml, determined by sensitivity experiment, Supplementary figure 13).

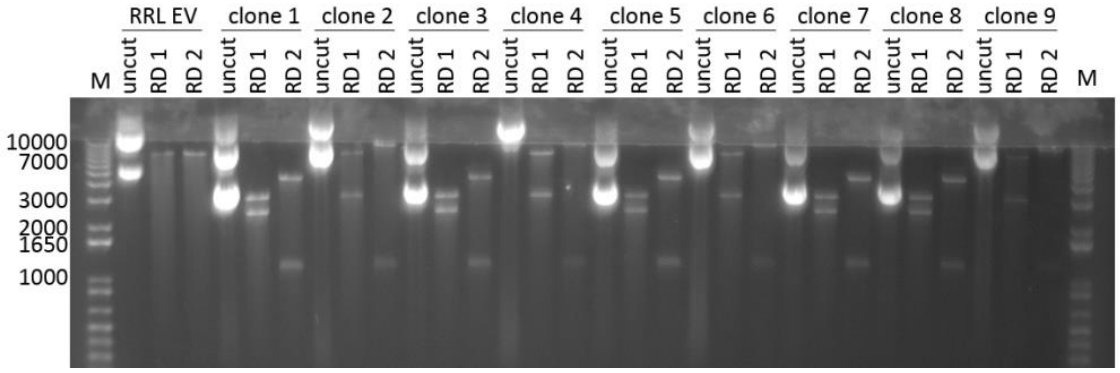

Figure 17: Restriction enzyme analysis of sEPHA2 cloned into the RRL.SF.newMCS.i2.Zeo.pre lentiviral vector. An example agarose gel showing restriction enzyme analysis with *Bam*HI and *Age*I (RD1) and *Bam*HI and *Nde*I (RD2). Expected fragments are uncut=10,501 bp (linear, nicked, circular), RD 1=6564 bp + 2937 bp; RD 2=9348 bp + 1153 bp. M=GeneRuler 1 kb DNA ladder (250-10,000 bp, Thermo Fisher Scientific).

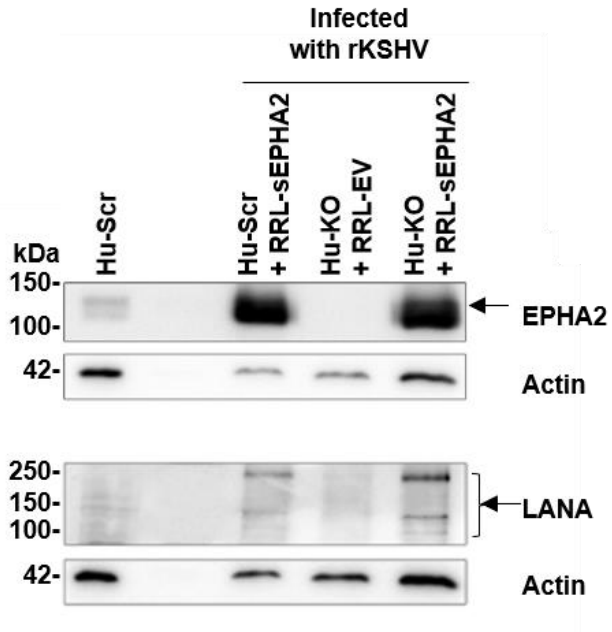

Figure 18: Transduction of sEPHA2 into control and KO cells. Empty vector (RRL-EV) and/or sEPHA2 (RRL-sEPHA2) were transduced into control cells (Hu-Scr, endogenous EPHA2 expression) or EPHA2-KO cells (Hu-KO) as indicated and EPHA2 detected by Western blot using an anti-EPHA2 antibody (clone D7 05-480, 1:500, top panel, 140 kDa). Cells were infected with rKSHV at MOI 10 and 48 h later rKSHV infection as shown by LANA expression using a rat anti-LANA antibody (1:1,000, bottom panel, 100–250 kDa [348,349]). Probing for actin indicates equal loading.

In order to determine the optimal amount of lentivirus that would achieve EPHA2 expression comparable to that of endogenous expression in Hu-Scr cells, the sEPHA2 (WT) lentivirus was titrated in HuARLT2 cells. Flow cytometry with an EPHA2-specific antibody indicated that 40 µl lentivirus yielded EPHA2 expression comparable to Hu-Scr cells transduced with EV (Figure 19) and this amount of lentivirus (40 µl) was used in further transduction experiments.

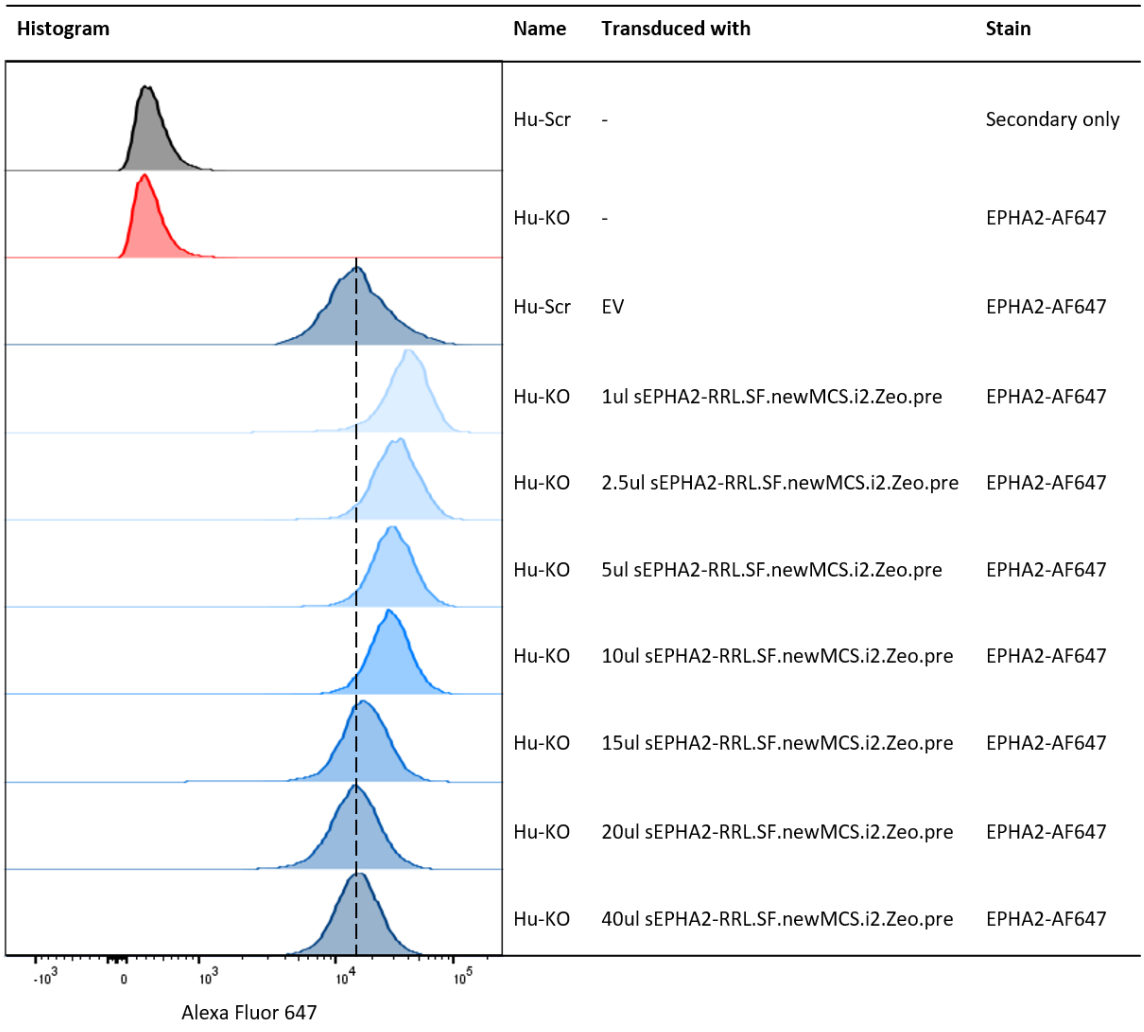

Figure 19: Lentiviral titration compared to endogenous EPHA2 expression by flow cytometry. Shown are histograms of Alexa Fluor 647 fluorescence (indicating EPHA2 expression) after gating for live cells. Dotted line indicates the MFI of Hu-Scr cells transduced with EV.

3.3.1.4. Reintroduction of mutant sEPHA2

After generating and cloning the sEPHA2 construct for stable transduction in EPHA2 knockout cell lines (see 3.3.1.3), SDM was performed on sEPHA2-RRL.SF.newMCS.i2.Zeo.pre to introduce the EPHA2 variants identified in the association study (SDM1–7, Table 31) producing sEPHA2-SDM1–7-RRL.SF.newMCS.i2.Zeo.pre lentiviral vectors. Additionally, a previously described serine phosphorylation deficient mutant (G2844A, SDM 8 [127]) was generated, producing the sEPHA2-SDM8-RRL.SF.newMCS.i2.Zeo.pre lentiviral vector. As a control, SDM with primers identical to the WT sequence (i.e. inducing no mutagenesis) was performed to generate the sEPHA2-SDM.RRL.SF.newMCS.i2.Zeo.pre lentiviral vector. The 5' LTR (Supplementary figure 10) and 3' LTR (Supplementary figure 11) regions of the lentiviral vector plasmid were sequenced to ensure integrity, as well as the sEPHA2 coding sequence to ensure that the intended mutation was introduced without any undesired mutations (Supplementary figure 12). Control and mutant EPHA2 lentiviruses were transduced in equal amounts as previously determined by titration with sEPHA2-RRL.SF.newMCS.i2.Zeo.pre (Figure 19), and flow cytometry detecting EPHA2 showed similar EPHA2 expression levels in each transduced cell line, although, slight variations did exist (Figure 20). DNA was extracted from each of these cell lines for PCR-amplification and sequencing of the respective mutated regions to confirm the successful introduction of the mutants (Figure 21).

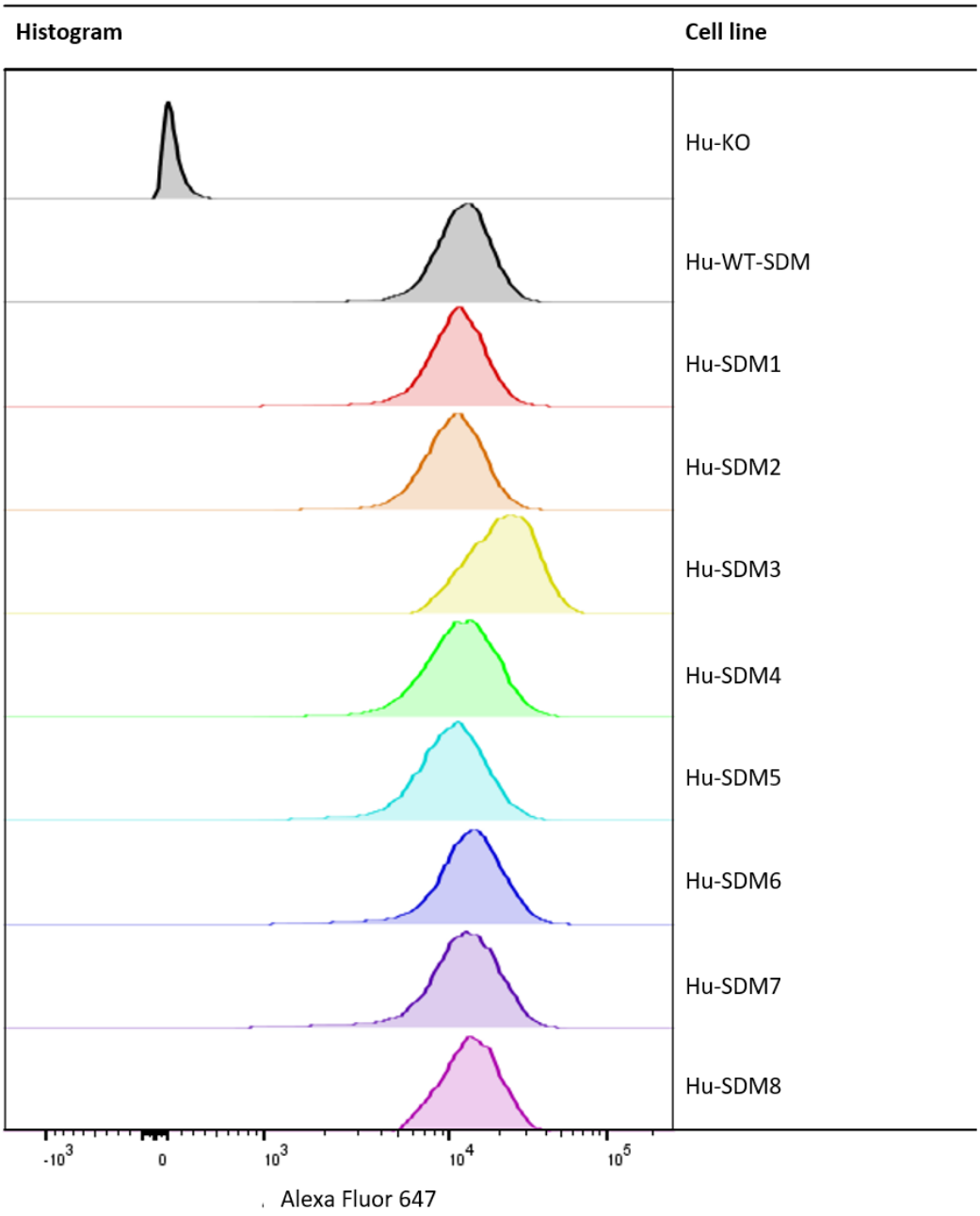

Figure 20: EPHA2 WT and mutant 1–8 expression in transduced cell lines assessed by flow cytometry. Shown are histograms of Alexa Fluor 647 fluorescence (indicating EPHA2 expression) after gating for live cells.

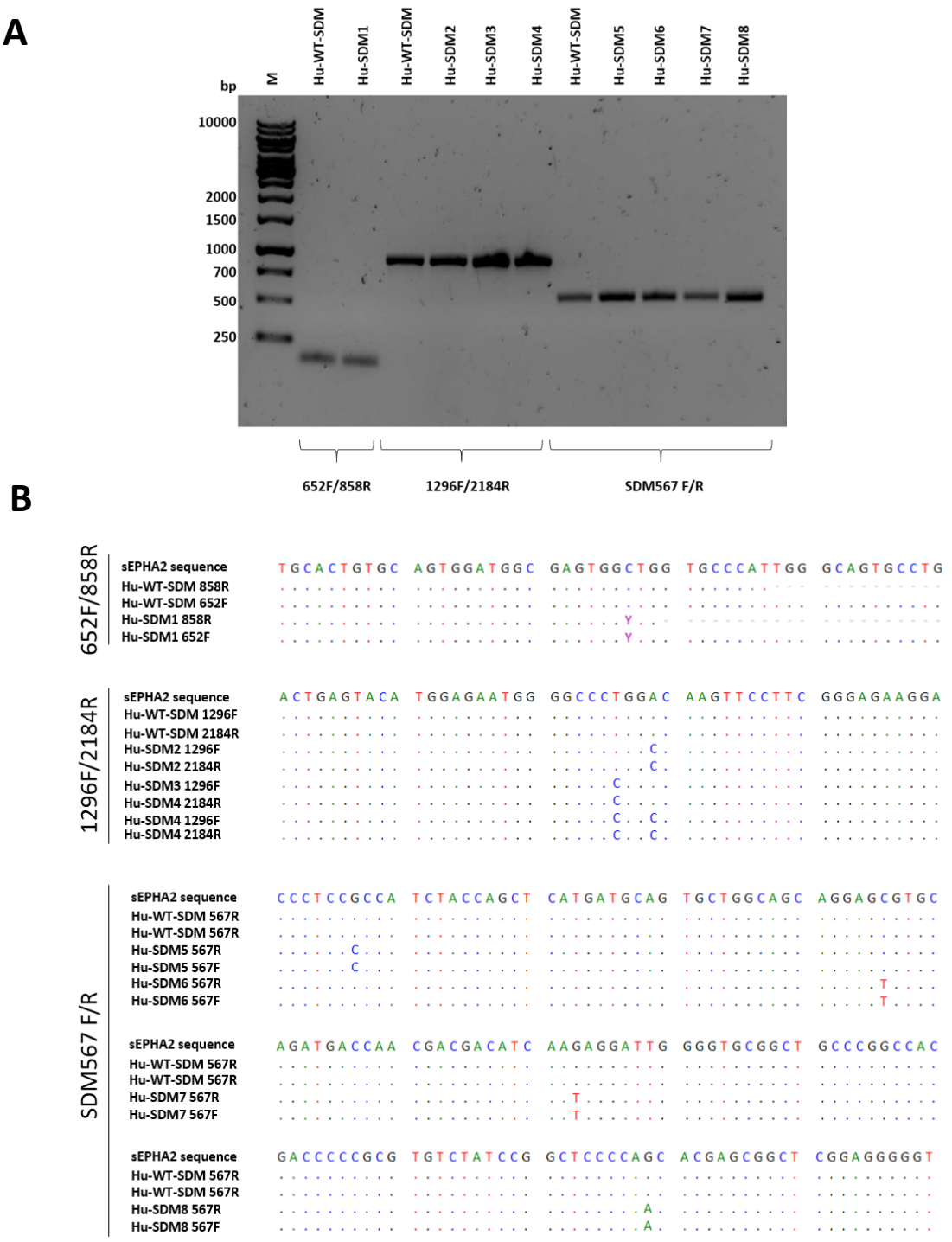

Figure 21: PCR and sequencing of transduced HuARLT2 cell lines. A) PCR with the indicated primer pairs amplified the genomic regions surrounding the introduced variants. M=GeneRuler 1 kb DNA ladder (250-10,000 bp, Thermo Fisher Scientific). **B)** Sequencing followed by alignment to the sEPHA2 reference sequence allowed for visualisation of the introduced variants. The ambiguous base 'Y' refers to a C/T as the primer pair 652F/858R amplifies both endogenous and transduced EPHA2. Primer pairs 1296F/2184R and SDM567F/R are specific to the transduced sEPHA2.

3.3.2. Assessing engineered cell lines expressing WT or variant EPHA2 in functional analyses

We next aimed to assess the functional consequences of the EPHA2 variants by expressing the WT or EPHA2 variants in the established, engineered EPHA2 KO cell lines. The expression levels of the introduced EPHA2 receptor proteins were at levels similar to endogenous expression (Figure 20). We assessed the cell viability (see 3.3.2.1), phosphorylation levels (see 3.3.2.2) and permissiveness to KSHV infection (see 3.3.2.3) in these cell lines.

3.3.2.1. Baseline characteristics of engineered cell lines

To ascertain if any of the transduced EPHA2 variants had an effect on the viability of the Hu-KO cells in which they were expressed, MTT assay was employed and cell viability was compared to that of Hu-WT-SDM cells. Cell viability in culture was not affected by the presence of any of the variants compared to HU-WT-SDM (Figure 22). Cell morphology did not differ between engineered HuARLT2 cell lines expressing EPHA2 variants (data not shown).

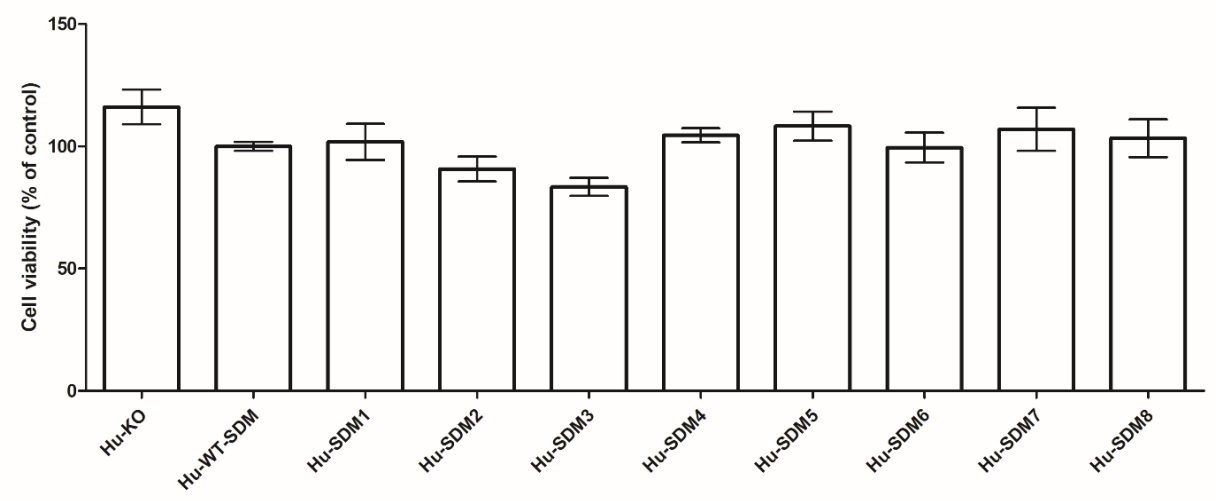

Figure 22: Cell viability does not differ between the engineered HuARLT2 cell lines expressing EPHA2 variants. MTT assay was used to quantify the cell viability of each stably transduced cell line. Presented are pooled data from two independent experiments each done in triplicate. Hu-WT-SDM was set as 100%. Means of each cell line were compared to that of Hu-WT-SDM by one-way ANOVA with *post hoc* Dunnett's test corrected for multiple comparisons.

3.3.2.2. Tyrosine phosphorylation of EPHA2

Essential to its downstream functions, tyrosine phosphorylation of EPHA2 is a measure of receptor activation. We assessed if the expression of EPHA2 variants has an effect on steady state tyrosine phosphorylation levels or the ability of EPHA2 to be phosphorylated in response to rKSHV infection. Baseline tyrosine phosphorylation levels (Figure 23), assessed by ELISA, were significantly decreased in the Hu-SDM3 and Hu-SDM4 cells lines compared to Hu-WT-SDM. As Hu-SDM4 is a double mutant of Hu-SDM2 and Hu-SDM3 (Table 31), it follows that the effect is caused by the introduction of Hu-SDM3. Conversely, Hu-SDM5 showed enhanced baseline phosphorylation levels compared to Hu-WT-SDM. The remaining mutant cell lines did not show baseline phosphorylation levels that differed significantly from Hu-WT-SDM.

We next assessed the phosphorylation response of our cell lines to rKSHV stimulation. We determined serum starvation conditions (0% FBS, 16 h) that did not affect cell viability (Figure 24A) while resulting in a significant decrease of phosphorylation levels from baseline (Figure 24B). We determined the rKSHV treatment time (20 min) that resulted in the greatest phosphorylation response empirically (Figure 24B). After serum starvation, cells were subjected to rKSHV (MOI 10) for 20 min at 37°C, before they were lysed and assayed for tyrosine phosphorylation levels. Differences in

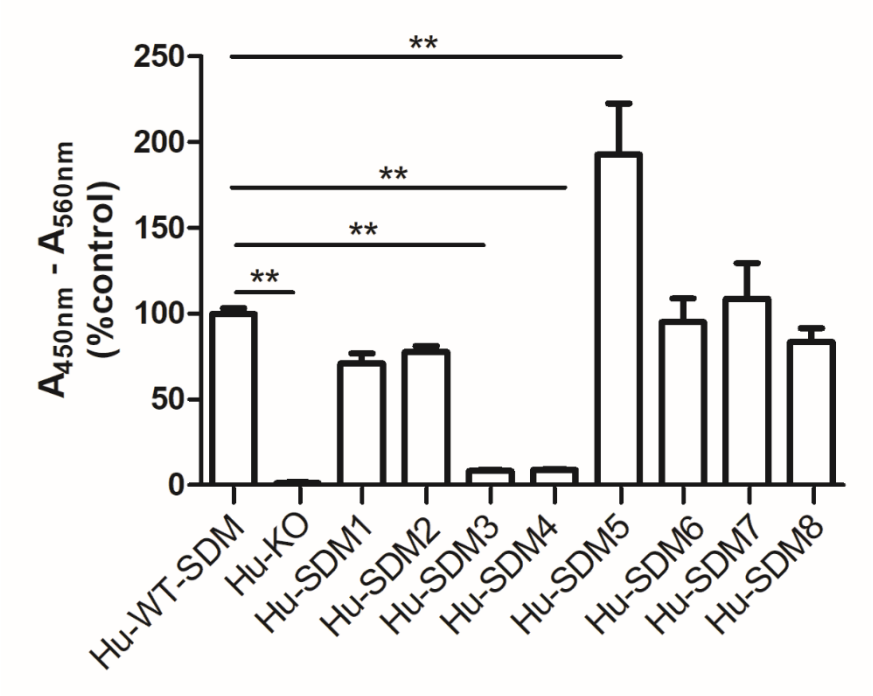

Figure 23: Baseline EPHA2 tyrosine phosphorylation levels among cell lines. EPHA2 tyrosine phosphorylation was measured by ELISA quantified by absorbance at 450nm (with reference absorbance at 560nm subtracted). Presented are pooled data from two independent experiments as a percentage of Hu-WT-SDM, which was set 100%. ** $p<0.01$ by one-way ANOVA with *post hoc* Dunnett's test corrected for multiple comparison.

phosphorylation between untreated and rKSHV-treated cells per cell line were compared between the Hu-WT-SDM cells and the mutant cell lines, none of which showed significant differences in rKSHV-induced phosphorylation (Figure 24C).

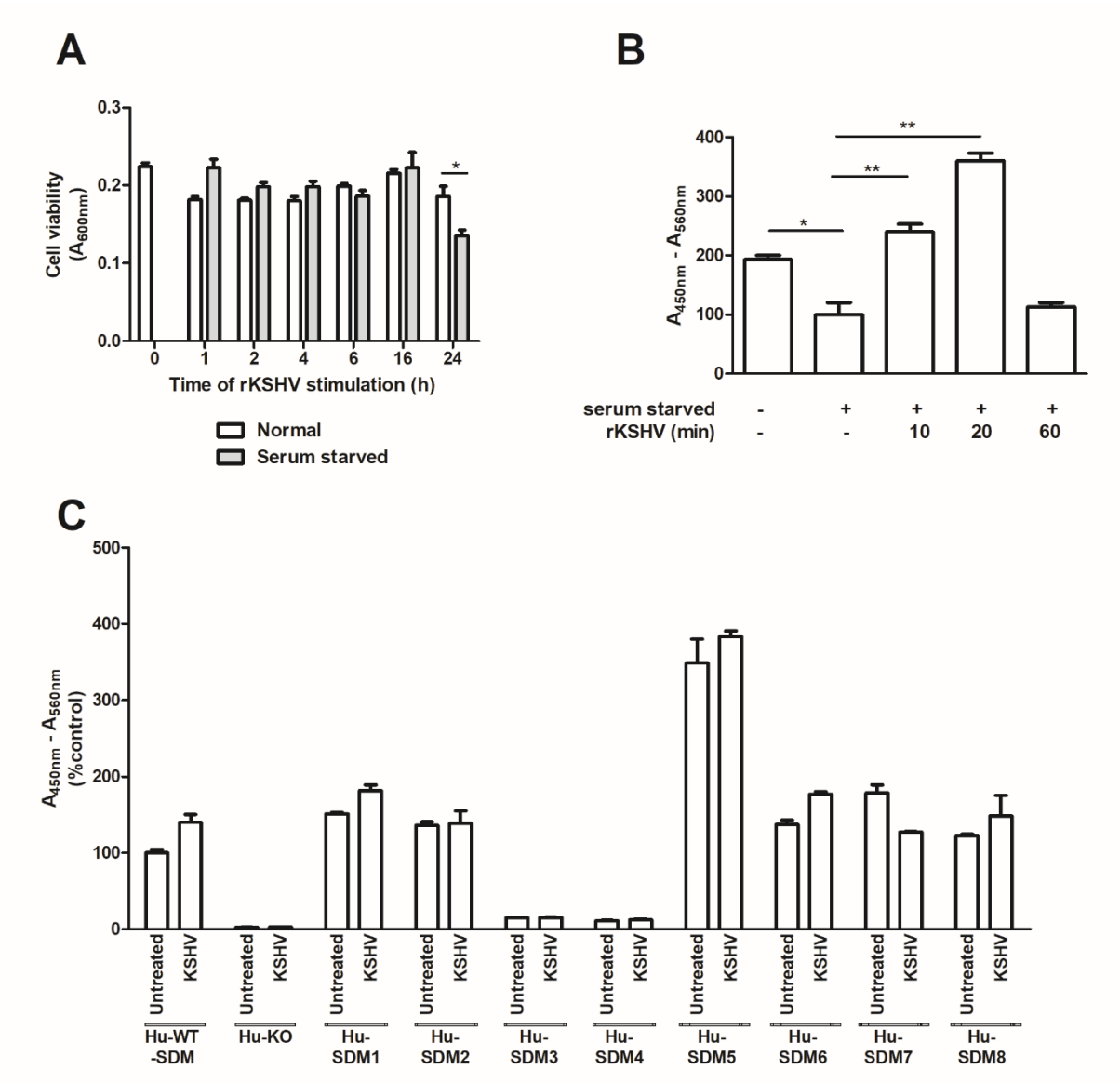

Figure 24: EPHA2 tyrosine phosphorylation response to rKSHV. A) Hu-WT-SDM cell viability when subjected to serum starvation over time was assessed by MTT assay. * $p<0.05$ was determined in a paired two-tailed t test. **B)** Time course assessing EPHA2 tyrosine phosphorylation in response to rKSHV. One-way ANOVA with *post hoc* Dunnett's multiple comparison test was done. *<0.05, **<0.01. **C)** EPHA2 tyrosine phosphorylation response to rKSHV in cell lines. Data from two independent experiments were pooled. The difference between untreated and rKSHV-treated cell lines per cell line was compared by one-way ANOVA between Hu-WT-SDM cells and mutant cell lines and no significant differences were found.

3.3.2.3. Recombinant KSHV binding, internalisation and infection

To assess the early stages of rKSHV infection (binding and internalisation), we established an experimental workflow making use of rKSHV-expressed RFP (from the viral PAN promotor) as a proxy for lytic virus that would represent these stages of infection: infection with rKHSV at 4°C for 1 h followed by two washes with PBS allowed virus to bind but not internalise (Figure 25A, top panel) while infection with rKSHV at 37°C for 1 h followed by washing resulted in bound and internalised virus (Figure 25A, bottom panel). These same procedures using virus added to empty wells (media but no plated cells) showed no visible RFP background (data not shown).

Binding did not differ significantly between the cell lines although Hu-SDM8 appeared to have slightly decreased rKSHV binding (Figure 25B). Similarly, binding and internalisation did not differ significantly between cell lines but Hu-SDM5 and Hu-SDM8 had the lowest read-out while Hu-SDM3, Hu-SDM4 and Hu-SDM6 appeared to have increased levels of bound/internalised virus (Figure 25B).

To measure the levels of rKSHV infection, we relied upon the expression of GFP as a proxy as rKSHV expresses GFP from the cellular EF-1α promoter. GFP-positive cells quantified by flow cytometry were normalised to EPHA2 expression, due to slight differences in the transduced cell lines (Figure 20). One-way Welch ANOVA with *post hoc* simple contrast testing with p-values adjusted for multiple comparison ($p<0.00625$ was considered significant) revealed that there was a significant reduction in percentage of GFP-positive cells (normalised to EPHA2 expression) of Hu-SDM3 (28.8 ± 2.8%, $p=0.001$, 45% of Hu-WT-SDM) and Hu-SDM4 (30.9 ± 9.9%; $p=0.002$, 49% of Hu-WT-SDM) compared to Hu-WT-SDM cells (63.6 ± 7.6%). In context, KO of EPHA2 resulted in reduced but not completely abolished rKSHV infection (38% of Hu-Scr, Figure 16C). The remaining cell lines did not differ significantly in infection levels from Hu-WT-SDM.

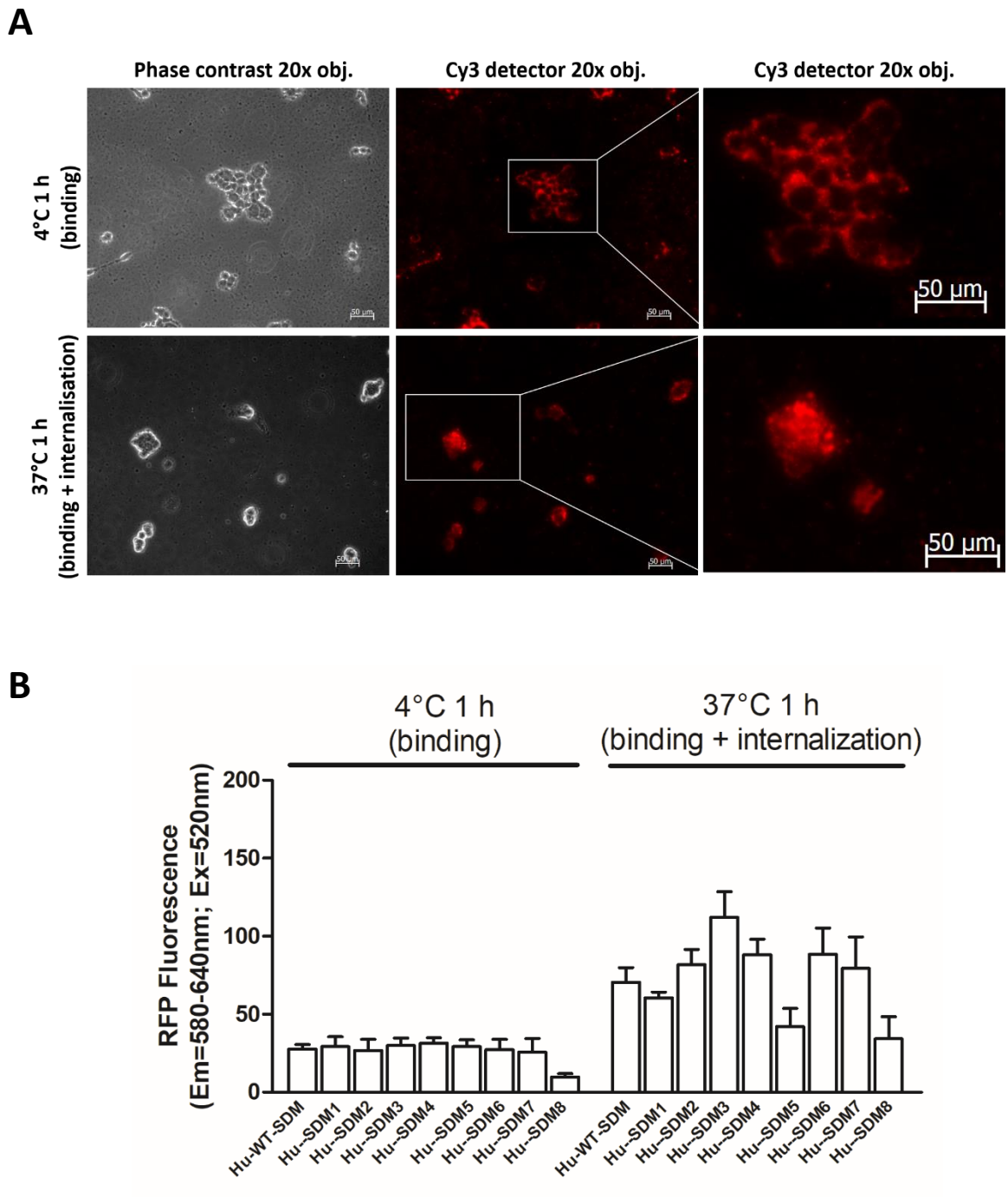

Figure 25: Early stages of rKSHV infection are not affected in engineered HuARLT2 cell lines expressing EPHA2 variants. A) Fluorescent microscopy was used to validate the conditions of internalisation and binding assays by visualising rKSHV expressed RFP (from the KSHV lytic gene PAN promoter) in Hu-WT-SDM cells using the experimental conditions for "binding" or "binding and internalisation" assays. **B)** RFP fluorescence was quantified in a fluorometer for each cell line subjected to rKSHV infection under the indicated conditions. Presented are pooled data from two independent experiments each in triplicate. Means were statistically compared by one-way ANOVA which indicated no significant differences.

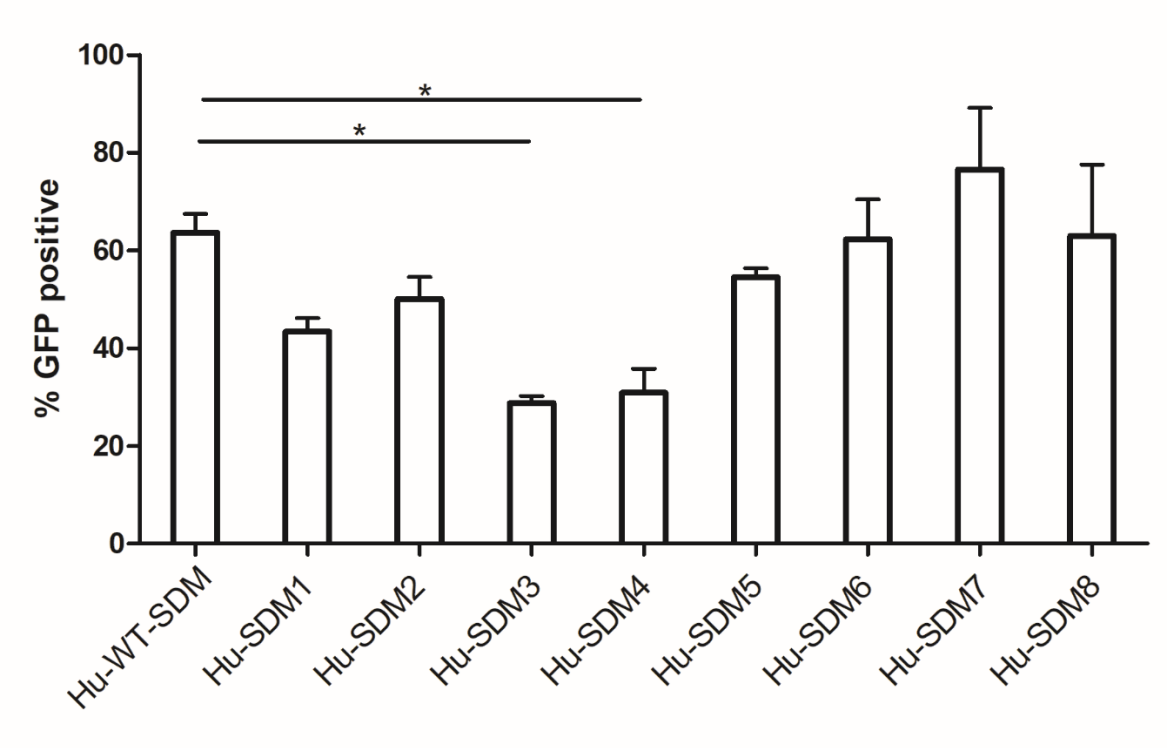

Figure 26: rKSHV infection of mutant-EPHA2 cell lines. Infection was measured by quantifying GFP-positive cells by flow cytometry. Presented are pooled data from two independent experiments each done in duplicate normalised to EPHA2 expression. One-way Welch ANOVA with simple contrasts revealed significant differences in the means of WT and SDM3 and 4, respectively when adjusting the p value for multiple comparisons. * indicates statistical significance at $p<0.00625$.

4. Discussion

While AIDS-related deaths have declined from 1.7 million in 2004 to 770,000 in 2018, due to global scale-up of ART, the majority of these (61%) occurred in SSA (see 1.1.1) [40]. With the HIV epidemiologic shift away from infectious mortality, cancer is an increasingly important cause of morbidity and mortality among people living with HIV globally [350]. KS is one of the most common AIDS-defining cancers worldwide and there is a particularly high burden of KS disease in SSA (see 1.3.1) [1]. The γ-herpesvirus, KSHV is a necessary but insufficient etiological agent of not only KS, but also PEL, KSHV-MCD [2], and the recently described KICS [6,8]. KSHV remains one of the most important oncogenic viruses in HIV-infected individuals and KSHV-associated malignancies are of particular public health significance in South Africa, and much of SSA, where both KSHV (30–50%) and HIV seroprevalence (20%) are elevated (see 1.3). Furthermore, incidence and mortality for KSHV-associated B-cell neoplasms are not well defined and therefore likely underreported. Earlier detection of progression from asymptomatic KSHV infection to tumour progression may mitigate KSHV-associated disease mortality.

Symptoms of KSHV-driven malignancies mimic TB which, despite increasing numbers of HIV-infected South Africans receiving ART, remains the leading cause of mortality [5]. However, a significant proportion of patients treated for TB have microbiologically unconfirmed diagnoses (see 1.1.2) [55]. Although KSHV and HIV co-infection are known to be particularly prevalent in SSA, the contribution of KSHV and KICS to patient mortality has not been studied in this context. We hypothesized that KSHV infection has a currently unrecognized contribution to mortality in critically ill HIV-positive South African patients who present with a suspected diagnosis of TB.

Further, genetic variants in receptors for KSHV entry and/or KSHV-driven oncogenesis are likely to have functional consequences for pathogenicity but have not been investigated in detail (see 1.6.5). We, therefore, set out to identify sequence variants in EPHA2, being both an entry receptor for KSHV [36,117] as well as being upregulated in various tumours, including KS [36,37,307–309], in South African HIV-infected patients, and to assess the functional consequences of identified EPHA2 variants associated with susceptibility to KSHV infection, KS development or elevated KSHV VL.

4.1. KSHV contributes to mortality in HIV-infected South African patients presenting with suspected but unconfirmed TB

4.1.1. Uncontrolled KSHV infection is an important contributor to mortality

South Africa has one of the highest global rates of both HIV and TB [351]. Not surprisingly, the exceptionally high burden of HIV-associated TB in South Africa causes misdiagnosis or delay of diagnosis of diseases mimicking TB symptoms (see 1.1.2). Utilising a large, well-characterized patient cohort of 682 HIV-positive critically ill patients admitted to Khayelitsha Day Hospital, South Africa, investigated for TB, and followed for 12 weeks to ascertain vital status, we retrospectively evaluated KSHV as a contributor to mortality. The patient cohort had a median CD4 count of 62 cells/µl (range: 0–526) and overall, 22% died during the 12-week follow-up period (Table 14).

In support of the reported disproportionately high KSHV seroprevalence in SSA (30–50%) compared to world prevalence rates (<10%), which has not changed significantly since the onset of the HIV/AIDS epidemic [70], we found 30.7% (95% CI, 27–34%) KSHV seroprevalence in patients presenting in Cape Town (Table 14 and Figure 6), which is in agreement with other South African estimates of 30–42% from Soweto, Johannesburg, and Kwa-Zulu Natal [67,72,73,75,98]. This is the first assessment of KSHV seroprevalence in the Western Cape Province of South Africa.

Of KSHV-seropositive patients, 18.8% (5.8% of the entire cohort, Table 14) showed detectable virus in the blood, suggestive of poor immune control of KSHV [75]. Focusing on the 33 (5%) patients with elevated (>100 copies/10^6 cells) KSHV VL, we found no higher mortality within the context of either the entire patient cohort or the cohort with confirmed TB (Table 17 and Figure 7), suggesting that KSHV does not play a significant role in potentiating TB mortality. However, 23.5% of patients had neither microbiologically proven TB nor alternative co-infection (Table 14) and, in these patients, elevated PBMC-associated KSHV VL was associated with 6.5-times higher odds (p=0.023, adjusted OR=6.5 [95% CI: 1.3, 32.4], Table 18) of mortality when adjusted for age, sex, CD4 cell count, and ART status. Moreover, KSHV VL was significantly higher in microbiologically unconfirmed TB patients who died compared to those who survived at 12-weeks follow-up (p=0.0094, Figure 7). In contrast, KSHV seropositivity alone was not associated with mortality (Table 19), suggesting that it is the burden of lytic KSHV activity that contributes to the observed association [5,8,75]. Similarly, elevated plasma KSHV VL, a marker of circulating tumour DNA, has been noted as a risk factor for death in people with established KS [215].

Although a strong association between elevated KSHV VL and mortality among microbiologically unconfirmed TB patients was identified, additional factors such as KSHV-associated malignancies, functional immune dysregulation (cytokine syndromes), or other pathological processes (e.g. co-infections or other cancers) likely also contribute to death. However, given the association of mortality with lytically active KSHV in critically ill HIV-infected patients with suspected but not microbiologically identified TB, KSHV lytic reactivation is an important consideration in the differential diagnosis of HIV-infected patients with symptoms of TB. This study is the first systematic evaluation of KSHV in HIV-infected patients presenting to hospital as TB in South Africa. Evaluation of KSHV VL in this setting is warranted to identify those patients with treatable KSHV-associated diseases [25].

4.1.2. KICS criteria and KSHV VL as biomarkers for treatable, underdiagnosed KSHV-related diseases

We further investigated whether the application of KICS criteria (Table 2 [6]) identified patients with high mortality compared to the remainder of the group and found six "possible KICS" patients, of whom five died, with a median survival of eleven days (Table 21). Only one of the six "possible KICS" patients had a pathological examination of a lymph node biopsy. While this is a limitation of our study, it is representative of a wider lack of diagnostic capacity in the African setting [17]. This was performed following death and demonstrated KSHV-MCD (Figure 12). Another had possible pulmonary KS diagnosed based on chest radiograph and confirmed cutaneous KS. It is possible that the other patients also had undiagnosed KSHV-associated diseases such as KS or MCD. Our data support that patients meeting KICS criteria should be evaluated for KSHV-MCD, visceral KS, or PEL, particularly in settings with oncology capacity to manage these treatable KSHV-associated malignancies. Although we have not definitively established that "possible KICS" patients died of KSHV-associated malignancies in most cases, elevated KSHV VL in the peripheral blood represents a parameter significantly associated with mortality (see 4.1). Although "possible KICS" patients had elevated IL-6 and CRP, these were not distinguishing features compared to other patients with TB or other critical illnesses (Table 22 and Figure 9), likely due to these patients all being critically ill with cytokine activation and systemic inflammation due to causes not investigated here. This suggests that CRP is a less useful screening tool than KSHV VL in this population in contrast to other contexts, such as the original series of KICS patients described in the USA who were distinguished by elevated CRP [6].

Previous studies identified PBMC-associated KSHV VL to be significantly higher in KSHV-MCD and KICS compared to KS patients without clinical evidence of IL-6 syndromes [25]. Similarly, in our study, KSHV VL was highest in our patients identified as "possible KICS" patients (who may have had

undiagnosed KSHV-MCD which was only confirmed in one patient at autopsy), followed by patients with KS (Figure 10) who were further distinguishable from KSHV seropositive patients without KS by elevated KSHV VL (Table 26).

KSHV viremia, rather than KSHV seropositivity, has been reported as a marker of advanced HIV disease [75]. Similarly, in our study, high KSHV VL and low CD4 count but not KSHV seropositivity were associated with mortality (Table 17). The majority of the patient cohort was anaemic (Table 14), which was significantly associated with elevated antibody levels to the KSHV lytic antigen K8.1 in KSHV-seropositive microbiologically unconfirmed TB patients but not with ORF73 (Table 20). This is consistent with results from a recent study from Uganda, which reported a link between elevated KSHV serumpositivity and anaemia in the setting of malaria [136]. A South African study found that patients with detectable KSHV viremia presented with anaemia and WHO Stage-3 or -4 defining conditions, indicative of advanced HIV disease, compared to those with undetectable KSHV VL [75]. Additional studies are required to evaluate this association. For example, anaemia may lead to reactivation of KSHV through relative tissue hypoxia [136], or KSHV reactivation may lead to anaemia or chronic inflammation mediated through IL-6.

In selected patients, KSHV VL has a strong prognostic value (Table 18). KSHV VL has been linked to an increased risk of KSHV-associated malignancies [352]; therefore, HIV-infected patients with elevated KSHV VL should be evaluated for KSHV-related malignancies. Therapeutic options exist for KS, KSHV-MCD and PEL and are most effective when employed earlier in the course of disease. In contrast, advanced KS and untreated KSHV-MCD, KICS and PEL have high mortality. Broccolo *et al.* [246] found KSHV VL to be strongly associated with progression of active KS. Jary *et al.* [25] have proposed that KSHV VL in whole blood is a useful biomarker to identify and monitor KSHV-associated diseases. Our data is consistent with this proposal and corroborates studies that propose that KSHV VL has a place in clinical practice to identify at-risk patients and monitor progression of KSHV-associated disease [25,26,246,353].

To our knowledge, this is the first systematic evaluation of KICS in South Africa and has implications for other countries with high prevalence of HIV/KSHV co-infection. In resource-limited countries of SSA, correct and timely diagnoses of KSHV-MCD, PEL and KICS are often impossible. A study from Uganda reports that three in every ten patients with HIV-associated lymphoma had a possible misdiagnosis and were treated for TB before a final diagnosis of lymphoma was made, and our data suggest that KSHV-associated diseases are important to include in the differential diagnosis of suspected TB [15]. In Malawi, and most of SSA, KSHV-MCD diagnoses is hindered by lack of availability of ancillary assays required for diagnosis (such as KSHV VL, CRP, IL-6 and vIL-6) resulting in

missed or late diagnoses and high mortality [26]. A better understanding of the spectrum of KSHV-associated diseases in the SSA context will require improved laboratory capacity. In fact, through our study, KSHV VL testing in a laboratory setting was established for the first time in South Africa.

In summary, elevated KSHV VL should be considered as an important pathology in HIV-infected patients investigated for TB, and that for those meeting other KICS criteria, evaluation for KSHV VL should be considered. Increasing implementation of PCR-based TB diagnostics should facilitate more rapid TB diagnostic workup, thereby facilitating selection of patients for whom KSHV testing may be indicated. In addition to lung cancer and lymphoma, a number of other pathologies should form part of the differential diagnosis of TB in HIV-positive patients including *Pneumocystis jirovecii* pneumonia, cytomegalovirus virus infection, Cryptococcosis and KS [58,354] or dysregulated lytic KSHV replication [62], to mitigate inappropriate TB treatment and delayed diagnosis. Appropriate implementation of KSHV VL testing offers a potential approach to improving diagnostic accuracy in HIV-infected populations with competing infectious co-morbidities. Testing for KSHV is not yet included in routine diagnostic workup but seems to claim a significant proportion of disease burden in high HIV/TB settings. We propose that a simple inexpensive test for KSHV VL could be developed and utilised in routine clinical practice throughout SSA in combination with evaluation of KICS symptoms and laboratory abnormalities to serve as an effective surveillance tool for KSHV-associated diseases in high-risk HIV-infected populations.

4.2. EPHA2 variants are associated with KSHV infection, KSHV VL and KS development in HIV-positive patients

KSHV infection is necessary but insufficient for the development of KS and other KSHV-associated pathologies. Factors, such as HIV infection and related immunosuppression precipitate oncogenesis (see 1.6.3). Regardless of the mechanism by which HIV co-infection promotes development of KSHV-associated pathologies, not all co-infected individuals develop a disease, pointing to potential underlying risk related to genetic features in KSHV and/or host factors (see 1.5). Furthermore, the geographical epidemiology of KSHV seroprevalence and population-specific incidence of KS outside the setting of HIV supports a role for genetic factors (see 1.3.1.1) [28–30,248]. The EPHA2 tyrosine kinase receptor is a promising candidate for investigation being both one of the key host receptors utilised by KSHV for endothelial cell entry and intracellular trafficking and implicated in oncogenesis (see 1.6.4 and 1.6.3). Therefore, this protein potentially acts on two levels: susceptibility to KSHV infection and susceptibility to KS development.

To elucidate a potential underlying genetic predisposition due to variants in the EPHA2 protein, we assessed aggregate variation across the entire EPHA2 coding region in a retrospective candidate gene association analysis with KSHV infectivity, KS prevalence and detectable KSHV VL in HIV-positive patients. As AIDS-related KS is by far the most common form of the KSHV-associated malignancies and particularly affects individuals in SSA due to the HIV/AIDS epidemic [67], we restricted the recruitment of patients to HIV-infected individuals within this geographical region, presenting at hospitals in the Western Cape province of South Africa. Since mother-to-child transmission via saliva is thought to be the primary route of KSHV transmission [9], the extent of later sexual transmission that could be confounding for KSHV infection is thought to be minimal [355,356]. All patients recruited to this study were adults between 19 and 73 years of age (Interquartile Range: 31–44, Table 25); therefore, it can be assumed that their exposure to and infection with KSHV has been concluded at the time of recruitment.

A number of variants previously reported on the dbSNP were identified in the entire cohort studied (n=300, 14 out of the total 26 in the region of interest including the Pkinase-Tyr and SAM domains), with a further 12 novel variants identified in our South African cohort. Large genotyping studies, such as the 1000 Genomes project and ExAc, have contributed the majority of the genetic variations stored in the dbSNP [49,50]. While these studies include African populations from Nigeria, Kenya, Gambia and Sierra Leone and people with African ancestry residing in America and the Caribbean, Southern African populations are not well represented [59]. It is thought that Southern African populations specifically have exceptionally high levels of genetic diversity due partly to the selective pressure of long term exposure to infectious diseases and due to the lack of founder effects present in populations that have migrated [357,358]. Therefore, it is expected that we would see variants in our South African population that have not yet been recorded in the dbSNP.

Based on EPHA2 variants identified in the original cohort [34], we have now validated variants within the functionally important Pkinase-Tyr and SAM domains through additional recruitment of a validation cohort. The aim of this validation was to increase the power of our study not to detect rarer variants but to improve confidence in the established associations. Specifically, 2254 T>C (in linkage disequilibrium with 2257 A>C), 2727 C>T and 2688 G>C located in the Pkinase-Tyr domain and 2990 G>T located in the SAM domain were associated with KS (Table 29). The Pkinase-Tyr variant 2727 C>T was further associated with KSHV prevalence (Table 28). The SAM domain variant 2990 G>T was also associated with having detectable KSHV VL in the blood (Table 30). Each of these variants was predicted *in silico* to result in damaging changes on the protein level when assessed for functional impact using the PolyPhen-2 prediction tool (Table 31). Interestingly, in our original analysis of the entire EPHA2 coding region, no significant sequence variation between the analysed patient groups

was found in EPHA2's ligand binding domain [34,35], supporting the hypothesis of the importance of the intracellular Pkinase-Tyr and SAM domains for KSHV-driven KS development (Table 24).

There were several limitations to our EPHA2 association analysis. Selection biases may have overestimated the association of EPHA2 variants as only HIV-positive patients presenting at clinics were recruited. The overall number of recruited patients in our original cohort was rather small (n=150), restricting the power of the analysis to only be able to detect associations of SNVs with MAF >3% with KS development and/or KSHV infection. Not all variants detected in the region of interest in the original cohort were detected in the validation cohort and vice versa (Supplementary table 4). The original cohort of KS (Group 1) patients was recruited from December 2014–February 2016 and the validation cohort of KS patients between February 2017–February 2018. The major difference between the original and validation KS cohorts was CD4 count which was significantly lower in the validation cohort recruited later in time (original: 238 cells/µl (IQR: 122-340.5); validation: 124 cells/µl (IQR: 40–232), p=0.024). This may represent KS patients with alternate risk factors or susceptibility markers. Nevertheless, the reported EPHA2 variants were statistically validated and deemed appropriate for further functional analysis.

4.3. EPHA2 variants have variable functional consequences on KS development and KSHV infection

Based on the possible functional impact of the identified EPHA2 variants (see 4.2), we proceeded to functional assessment of six EPHA2 variants associated with KS status, elevated KSHV VL and/or KSHV infection in our clinical cohort. We also included one benign variant (negative control) and one serine phosphorylation deficient variant expected to be nonpermissive to rKSHV infection [127]. These variant EPHA2s, generated by SDM and expressed in endogenous EPHA2-KO endothelial cells were compared to cells expressing the WT EPHA2 (that underwent the process of SDM with benign primers, see 3.3.1.4).

All EPHA2 WT and variant cell lines were expression capable (Figure 14), expressed EPHA2 on the cell membrane (Figure 20) and were able to bind rKSHV (Figure 25), indicating that any functional changes to the structure of the receptor that may result from the introduction of the variants did not affect the extracellular domain which was to be expected as the variants were located only in the intracellular Pkinase-Tyr and SAM domains. Moreover, neither cell viability (Figure 22) nor morphology were affected by the expression of the variant EPHA2 constructs compared to WT. On

this basis, functional characterisation of these mutants with regard to tyrosine phosphorylation and KSHV infection could be performed.

4.3.1. EPHA2 variants with altered tyrosine phosphorylation may affect KS development

Initially, we assessed tyrosine phosphorylation at steady state (Figure 23) and in response to rKSHV stimulation (Figure 24) as an indication for the receptor variants' involvement in KS development. Expectedly, there was no effect on the benign variant or the serine phosphorylation deficient variant SDM8 (p.Ser897Asn) nor SDM7 (p.Lys945Asn), located in the SAM domain. Of the remaining five variants (all affecting the Pkinase-Tyr domain), we saw a marked decrease in tyrosine phosphorylation in SDM3 (p.Leu700Pro) and SDM4 (double mutant: p.Leu700Pro+p.Asp701Ala) and enhanced tyrosine phosphorylation in SDM5 (p.Ala845Pro). We did not see an effect on phosphorylation of SDM2 (p.Asp701Ala) alone, indicating that while it is in linkage disequilibrium with p.Leu700Pro, it is p.Leu700Pro, not p.Asp701Ala, that confers the functional consequence seen in the double variant, p.Leu700Pro+p.Asp701Ala. There was also no effect on tyrosine phosphorylation in SDM6 (p.Arg858Cys) indicating that its association with KS is likely due to an alternative mechanism, potentially mediated through KSHV infection (as p.Arg858Cys is also associated with KSHV infection, see 4.3.2). Interestingly, KSHV infection did not change the mutants' baseline phosphorylation pattern (Figure 24). The effect of KSHV on EPHA2 phosphorylation as a proxy for receptor activation may be very subtle as there is likely a surplus of EPHA2 on the cell surface and in reserve inside the cell and additionally, KSHV can bind to other receptors [36,115].

The tyrosine phosphorylation deficient variant, p.Leu700Pro (which inferred the same effect in the double mutant p.Leu700Pro+p.Asp701Ala) was originally identified as being associated with KS development in our clinical cohort (Table 29). Since the tumorigenic signature of EPHA2 is defined by low levels of tyrosine phosphorylation, particularly at Tyr772, via abrogation of the canonical pathway and ligand-independent high levels of serine phosphorylation, particularly Ser897, via the noncanonical pathway (Figure 5) [283,313,314], it is likely that p.Leu700Pro promotes KS development via abrogation of the ligand- and kinase-dependent canonical EPHA2 pathway. The absence of tyrosine phosphorylation (particularly Tyr772) may lead to increased cell proliferation, migration, survival and adhesion thereby promoting oncogenesis [274,283,285,310–314]. Similar to our result, Tan *et al.* [310] identified an EPHA2 variant in the Pkinase-Tyr domain, p.Ala859Asp in genomic DNA extracted from MPM tissue which exhibited low levels of tyrosine phosphorylation and subsequently enhanced cellular proliferation and migration and resistance to cisplatin chemotherapy. Molecular dynamics

simulations identified atomic level impairment caused by the p.Ala859Asp mutant which reduced affinity of adenosine triphosphate (ATP) for the mutant, inhibiting phosphoryl transfer [310]. The mechanism by which p.Leu700Pro facilitates the lack of tyrosine phosphorylation of EPHA2 is yet to be elucidated but we speculate that this is either due to impairment of ATP-mediated cross-phosphorylation or enhancement of phosphatase activity. It is well established that EPHA2 is dephosphorylated at tyrosine residues via the phosphatase LMWPTP in cancer cells [313,315].

In contrast to p.Leu700Pro (SDM3), the variant p.Ala845Pro (SDM5) also associated with KS in our clinical cohort (before adjustment for multiple comparisons, Table 29) showed enhanced tyrosine phosphorylation at baseline (Figure 23). This effect of p.Ala845Pro on KS development might be mediated through the ligand-independent noncanonical pathway of EPHA2-mediated oncogenesis (Figure 5) which is driven predominately but not exclusively by Ser897 phosphorylation [285,286,311,316,317]. While we cannot comment of serine phosphorylation levels in this study, simultaneously increased tyrosine phosphorylation has been shown to play a kinase-independent role in the noncanonical pathway in addition to its role in the canonical pathway of EPHA2 [283]. Enhanced tyrosine phosphorylation has also been shown in breast cancer cell lines, potentially preceding a molecular switch to a highly metastatic cell programme when EPHA2 is likely dephosphorylated [283]. Faoro *et al.* [286] similarly identified an EPHA2 mutation (p.Gly391Arg) in lung SCC cell lines and patient samples that caused constitutive activation of EPHA2 indicated by enhanced baseline tyrosine phosphorylation and thereby promoted invasiveness, adhesion and survival.

Taken together, assessment of the tyrosine phosphorylation statuses of the engineered cells expressing EPHA2 variants yielded insight into the oncogenic potential of alteration to EPHA2. Particularly the mutant p.Leu700Pro alone and the double mutant p.Leu700Pro+p.Asp701Ala showed strongly impaired tyrosine phosphorylation which may have significant functional consequences for oncogenesis.

4.3.2. EPHA2 alterations with impact on KSHV infection

Having determined the effect of the EPHA2 variants on EPHA2 tyrosine phosphorylation as an indication of oncogenic potential, we next examined the direct role of EPHA2 in KSHV infection, a necessary precursor of KS development. EPHA2 is a major entry receptor for KSHV in endothelial cells, however, it is dispensable for viral attachment which is facilitated mainly by HSPGs and integrins (Figure 2) [36,105,122]. EPHA2 tyrosine phosphorylation and activation is necessary for KSHV entry [36,117]. We examined KSHV infection through binding, internalisation and infection assays making

use of purified rKSHV that expresses RFP from the lytic PAN promoter (indicating early stages of infection: binding and internalisation) and GFP from the cellular EF-1α promoter (indicating infection). As expected, binding of rKSHV was unaffected by the expression of EPHA2 variants (Figure 25A), likely mediated mostly through cellular HSPGs and integrins. Internalisation of rKSHV did not differ strikingly between EPHA2 variants compared to WT either but internalization was slightly reduced for p.Ala845Pro (SDM5) and p.Ser897Asn (SDM8) although this was not statistically significant (Figure 25B). Significantly decreased infection levels were evident in p.Leu700Pro (SDM3) and double mutant p.Leu700Pro+p.Asp701Ala (SDM4) and slightly increased infection levels were evident in p.Lys945Asn (SDM7, Figure 26). Surprisingly, p.Arg858Cys (SDM6), associated with KSHV infection in our clinical cohort (Table 28), did not have an effect on rKSHV infection into endothelial cells nor did the serine phosphorylation deficient variant (p.Ser897Asn) which had been reported to be deficient for KSHV infection in 293T cells [127].

While binding and internalisation of rKSHV to p.Leu700Pro (SDM3) and p.Leu700Pro+p.Asp701Ala (SDM4) expressing cells was unaffected (Figure 25), both cell lines showed decreased rKSHV infection (Figure 26) suggestive of non-infectious internalisation. This may be due to impaired trafficking of rKSHV to the nucleus requiring signalling pathways activated by the tyrosine phosphorylation sites [36] deficient in p.Leu700Pro and p.Leu700Pro+p.Asp701Ala. Alternatively, rKSHV may make use of other non-optimal receptors for internalisation to compensate for impaired EPHA2 activation, perhaps resulting in endocytosis into a non-permissive subcellular compartment. Even so, the remaining low level of infection suggests that other receptors besides EPHA2 such as EPHA4 or EPHA5 (as has been described in epithelial cells [119]) and EPHA5 or EPHA7 (as has been described in BJAB cells [120]) likely play a role in infectious internalisation, as has been previously suggested [107,115,116,119,120]. Both p.Leu700Pro and p.Leu700Pro+p.Asp701Ala were found to be associated with KS development in our clinical cohort (Table 29), but not with KSHV infection. While the EPHA2 variant p.Leu700Pro likely promotes oncogenesis through lack of EPHA2 phosphorylation and subsequent removal of EPHA2's canonical tumour suppressor effects (see 4.3.1), it is unclear if or how reduced rKSHV infection contributes to increased risk of KS development. We hypothesize that the lower infection rate in the presence of the tyrosine phosphorylation deficient EPHA2 might favour non-cytopathic latent infection and thereby less immune activation and chronic, ongoing KSHV infection, favouring carcinogenesis over time. Regardless of how KSHV infection is facilitated in the presence of this tyrosine phosphorylation deficient EPHA2, the effect of p.Leu700Pro is primarily on downstream oncogenesis subsequent to KSHV infection as the effect on phosphorylation is far more striking than the effect on KSHV infection. A similar dual role of a genetic marker was described for the HLA haplotype HLA-B Bw4-80I in combination with the KIR receptor haplotype KIR3DS1 which

reportedly decreases the risk of KSHV viremia, while simultaneously increasing the risk of KS development [257]. Alternatively, the interaction with HIV may play a more important role in the presence of a tyrosine phosphorylation deficient EPHA2. There is evidence that the molecular mechanisms of KS development in AIDS-KS and Classic KS differ: a SNP in the IL-8 promoter region (A-251T, rs4073) was found to decrease the risk of developing AIDS-KS in an HIV-positive, KSHV-infected cohort [251] but was overrepresented in a cohort of Classic KS patients [252]. However, given the complexity of the system, it is unlikely that the explanation can be narrowed down to a single gene effect.

Of the other variants, only p.Lys945Asn (SDM7) expression resulted in increased permissiveness to rKSHV infection (although this was not a drastic enough difference to be statistically significant (Figure 26)), although rKSHV binding and internalisation were unaffected. The variant p.Lys945Asn is located in the EPHA2 cytoplasmic SAM protein interaction domain and was found to be overrepresented among patients with KS and patients with detectable VL with "possibly damaging effects" (Table 29 and Table 30). The SAM domain binds adaptor proteins to mediate the downstream signalling events triggered by EPHA2 activation and has been reported to play a role in activation itself [287–289]. Although likely attenuated by other effects in our cell culture system, we can speculate that p.Lys945Asn may contribute to oncogenesis or enhanced KSHV lytic activity by altering the coupling of the SAM to an adaptor protein and regulating downstream signalling pathways. It is interesting that p.Lys945Asn is overrepresented in males (8/11) in our clinical cohort and of these, the majority (7/8) had KS and detectable (6/8), even elevated (5/8), VL. Indeed, males were overrepresented in our KS cohort as well as in patients with detectable KSHV VL compared to KSHV-positive patients in which VL is undetectable. This supports numerous previous reports [67,127,185,359] that KS risk is higher in males and gives further evidence suggesting that the mechanism for this is mediated via increased KSHV lytic activity (detectable VL in the blood) [360]. Wang *et al.* [127] suggest that this disproportionate risk of KS in males is due to the interaction of EPHA2 with the AR which leads to increased phosphorylation on Ser897, essential for KSHV infection in epithelial cells. AR recruits Src and RSK1 to mediate this phosphorylation of EPHA2 and thereby enhance rKSHV infection [127]. This suggests a potential role for p.Lys945Asn EPHA2 SAM domain variant in potentiating the interaction of EPHA2 with AR to enhance KSHV lytic activity.

Interestingly, p.Ser897Asn (SDM8), reported to abolish rKSHV infection in 293T cells due to a loss of function mutation of Ser897 to Asn [127], showed reduced binding and internalisation although the reduced levels were not statistically significant (Figure 25). While this mutant was included as a KSHV-infection deficient control, we observed infection rates of HuARLT2 cells expressing p.Ser897Asn to be comparable to that of WT. This could be attributed to the use of a different cell line. KSHV enters

endothelial cells (such as HuARLT2) via actin-dependent macropinocytosis [129] and epithelial cells (such as 293T) via clathrin-independent endocytosis [131] (Table 1). Ser897 phosphorylation may mediate endocytosis of KSHV in epithelial cells but not affect macropinocytosis of KSHV in endothelial cells.

In contrast to p.Leu700Pro (SDM3) and p.Leu700Pro+p.Asp701Ala (SDM4), p.Ala845Pro (SDM5) did not have an effect on rKSHV internalisation (Figure 25) or permissiveness to rKSHV infection (Figure 26) despite enhanced tyrosine phosphorylation levels (Figure 23). This is fitting as p.Ala845Pro was found to be associated with KS development (although not after adjustment for multiple comparisons, Table 29), but not KSHV infection in our clinical cohort.

The variant p.Arg858Cys (SDM6) was identified as being associated with increased susceptibility to KSHV infection (Table 28) and KS development (Table 29) in the clinical cohort. However, in functional assays, we did not see an effect of this variant on rKSHV infection (Figure 26). This suggests that the effect of this EPHA2 variant is tempered in our cell culture system. Other EPH receptors have previously been shown to compensate for EPHA2 in overexpression systems [107,115,116,120] and similarly, in our model, EPHA2 KO reduced rKSHV infection (38% of Hu-Scr, Figure 16C) but did not abolish it, indicating that other receptors are used in compensation. We can speculate that p.Arg858Cys mediates KSHV infection through a mechanism not accounted for in our cell culture system.

In summary, EPHA2 variants identified within a clinical KS cohort were assessed in functional assays to determine their effects in mediating KS oncogenesis and KSHV infection. While the molecular mechanisms of some variants are yet to be elucidated, alteration in EPHA2, in particular p.Leu700Pro expressed alone or as a double mutant (p.Leu700Pro+p.Asp701Ala), was linked to functional outcomes validating their association with KS in the clinical association study. This may have consequences for clinical applications and our data supports this claim by linking EPHA2 variants found in KS patients with functional roles in oncogenesis which may have implications for treatment strategies. EPHA2 inhibitors have been suggested as a potential therapeutic avenue for further investigation in patients who have EPHA2 alterations resulting in increased oncogenic potential [310]. Studies have shown that EPHA2 mutants can confer differing drug sensitivities. For example, the p.Gly391Arg EPHA2 mutant showed increased sensitivity to rapamycin [286,310] and low dose resistance to cisplatin [310] in human lung epithelial cells while the p.Ala859Asp mutant showed resistance to doxazosin in HEK293 cells [310]. EPHA2 variants in patients with KS warrant further investigation to ascertain their therapeutic importance.

However, care should be taken when validating isolated aspects on genetic variations in a cell culture model as it cannot capture the complexities of an *in vivo* biochemical system. We established a cell culture model that relevantly approximated the scenario of KSHV infection of endothelial cells, the major cell type in KS, however, it is likely that our model does not recapitulate the complex *in vivo* scenario or that an alternative cell line may produce different effects. The signalling pathways mediating internalisation and infection after receptor activation are complex to interpret and further investigation is warranted. The markedly differing profile of phosphorylation, internalisation and infection seen in p.Leu700Pro (and the double mutant p.Leu700Pro+p.Asp701Ala) versus p.Ala845Pro, which both are associated with KS in our clinical cohort, indicated that these variants affect different downstream pathways to enact their function. To further elucidate the functional effects of EPHA2 variants, our future work will delve into the signalling pathways induced by rKSHV binding to EPHA2 and address the trafficking and fusion kinetics of EPHA2 entry through analysis of transport of capsids to the nucleus or co-localization of capsid with cellular markers. Moreover, investigation of the serine phosphorylation status of the variant-expressing EPHA2 cell lines will better inform the oncogenic potential of the cellular microenvironment.

Taken together, these results link the discovery of EPHA2 variants associated with KS development in a clinical cohort to functional roles in the molecular pathways of KS development.

5. Conclusion

The data presented in this thesis provide important and novel findings on 1) the contribution of KSHV to mortality in HIV-infected South African patients presenting with suspected but unconfirmed TB, and 2) the genetic contribution of EPHA2 receptor variants to KSHV susceptibility, KSHV lytic activity and KS development, respectively.

While KS has been well established as an independent risk factor for death in HIV-infected people, a broader and more heterogeneous range of KSHV-associated diseases, particularly in the SSA context of high HIV burden, likely plays a yet under-recognized role in HIV-associated morbidity and mortality. We have shown that elevated KSHV VL is an important cause of mortality in HIV-infected patients presenting with suspected TB that is not microbiologically confirmed. Furthermore, KICS criteria identified patients at high risk of mortality with untreated or undiagnosed KSHV-associated malignancies. This study is an important first step in describing the clinical spectrum and epidemiology of KSHV infection and KICS in the South African context. Based on these data, including tests for KSHV lytic reactivation in the diagnostic work-up of hospitalised HIV-infected patients (once TB has been ruled out) should be considered. KSHV-associated malignancies are treatable, and earlier diagnosis may improve survival. Inclusion of KSHV VL testing in screening, diagnostic and prognostic pathways may lead to earlier detection and improved monitoring of KSHV-associated diseases, and ultimately more timely and targeted therapeutic intervention in resource-limited countries.

On a genetic level, we identified sequence variants in the host EPHA2 tyrosine kinase receptor pivotal to KSHV infection and KS oncogenesis that are significantly associated with KS development, KSHV infection and KSHV lytic activity in the blood and validated their functional impact for KSHV infection and/or KS oncogenesis on a molecular level. Importantly, the Pkinase-Tyr domain variant p.Leu700Pro, associated with KS development, was found to be deficient in tyrosine phosphorylation, known to promote oncogenesis, and resulted in non-infectious internalisation of viral particles likely due to impairment of rKSHV trafficking which may interact with downstream signalling pathways and immune-modulatory molecules to further promote carcinogenesis. This study provides the basis for further investigation into the impact and functional relevance of EPHA2 variants on KSHV infection, lytic activity and KS development which may have clinical implications in terms of identifying KSHV-infected patients who are susceptible to KS development and highlighting EPHA2 as a novel biomarker to predict KSHV-associated diseases and as a potential therapeutic target.

6. References

1 Thakker, S. and Verma, S. C. (**2016**) Co-infections and pathogenesis of KSHV-associated malignancies. Front. Microbiol. 7, 1–14.

2 Goncalves, P. H., Uldrick, T. S. and Yarchoan, Y. (**2017**) HIV-associated Kaposi Sarcoma and Related Diseases. AIDS 31, 1903–1916.

3 Chang, Y., Cesarman, E., Pessin, M. S., Lee, F., Culpepper, J., Knowles, M., Moore, P. S. and Knowles, D. M. (**1994**) Identification of Herpesvirus-Like DNA Sequences in AIDS-Associated Kaposi's Sarcoma. Science 266, 1865–1869.

4 Cesarman, E., Chang, Y., Moore, P., Said, J. and Knowles, D. M. (**1995**) Kaposi's sarcoma-associated herpesvirus-like DNA sequences in aids-related body-cavity-based lymphomas. N. Engl. J. Med. 1186–1191.

5 Oksenhendler, E., Carcelain, G., Aoki, Y., Boulanger, E., Maillard, A., Clauvel, J. and Agbalika, F. (**2000**) High levels of human herpesvirus 8 viral load, human interleukin-6, interleukin-10, and C reactive protein correlate with exacerbation of multicentric Castleman disease in HIV-infected patients. Blood 96, 2069–2073.

6 Polizzotto, M. N., Uldrick, T. S., Wyvill, K. M., Aleman, K., Marshall, V., Wang, V., Whitby, D., Pittaluga, S., Jaffe, E. S., Millo, C., et al. (**2015**) Clinical Features and Outcomes of Patients with Symptomatic Kaposi Sarcoma Herpesvirus (KSHV)-associated Inflammation: Prospective Characterization of KSHV Inflammatory Cytokine Syndrome (KICS). Clin. Infect. Dis. 62, 730–738.

7 Polizzotto, M. N., Uldrick, T. S., Hu, D. and Yarchoan, R. (**2012**) Clinical manifestations of Kaposi sarcoma herpesvirus lytic activation: Multicentric Castleman disease (KSHV-MCD) and the KSHV inflammatory cytokine syndrome. Front. Microbiol. 3, 1–9.

8 Uldrick, T. S., Wang, V., O'Mahony, D., Aleman, K., Wyvill, K. M., Marshall, V., Steinberg, S. M., Pittaluga, S., Maric, I., Whitby, D., et al. (**2010**) An Interleukin-6-related systemic inflammatory syndrome in patients co-infected with Kaposi sarcoma-associated herpesvirus and HIV but without Multicentric Castleman disease. Clin. Infect. Dis. 51, 350–358.

9 Plancoulaine, S., Abel, L., Beveren, M. Van, Trégouët, D., Joubert, M., Tortevoye, P., Thé, G. De and Gessain, A. (**2000**) Human herpesvirus 8 transmission from mother to child and between siblings in an endemic population. Lancet 356, 1062–1065.

10 Schäfer, G., Blumenthal, M. J. and Katz, A. A. (**2015**) Interaction of Human Tumor Viruses with Host Cell Surface Receptors and Cell Entry. Viruses 7, 2592–2617.

11 Farahani, M., Mulinder, H., Farahani, A. and Marlink, R. (**2017**) Prevalence and distribution of non-AIDS causes of death among HIV-infected individuals receiving antiretroviral therapy: a systematic review and meta-analysis. Int. J. STD AIDS 28, 636–650.

12 Blumenthal, M. J., Ujma, S., Katz, A. A. and Schäfer, G. (**2017**) The role of type 2 diabetes for the development of pathogen-associated cancers in the face of the HIV/AIDS epidemic. Front. Microbiol. 8.

13 Gupta, R. K., Lucas, S. B., Fielding, K. L. and Lawn, S. D. (**2015**) Prevalence of tuberculosis in post-mortem studies of HIV-infected adults and children in resource-limited settings: A systematic review and meta-analysis. AIDS 29, 1987–2002.

14 Puvaneswaran, B. and Shoba, B. (**2013**) Misdiagnosis of tuberculosis in patients with lymphoma. South African Med. J. 103, 32–33.

15 Buyego, P., Nakiyingi, L., Ddungu, H., Walimbwa, S., Nalwanga, D., Reynolds, S. J. and Parkes-Ratanshi, R. (**2017**) Possible misdiagnosis of HIV associated lymphoma as tuberculosis among patients attending Uganda Cancer Institute. AIDS Res. Ther. 14, 10–15.

16 Bhatt, M. L. B., Kant, S. and Bhaskar, R. (**2012**) Pulmonary tuberculosis as differential diagnosis of lung cancer. South Asian J. Cancer 1, 36–42.

17 Masamba, L. P. L., Jere, Y., Brown, E. R. S. and Gorman, D. R. (**2016**) Tuberculosis Diagnosis Delaying Treatment of Cancer: Experience From a New Oncology Unit in Blantyre, Malawi. J. Glob. Oncol. 2, 26–29.
18 Staskus, K. A., Sun, R., Miller, G., Racz, P., Jaslowski, A., Metroka, C., Brett-Smith, H. and Haase, A. T. (**1999**) Cellular tropism and viral interleukin-6 expression distinguish human herpesvirus 8 involvement in Kaposi's sarcoma, primary effusion lymphoma, and multicentric Castleman's disease. J. Virol. 73, 4181–7.
19 Sitas, F. and Newton, R. (**2000**) Kaposi's Sarcoma in South Africa. JNCI Monogr. 2000, 1–4.
20 Uldrick, T. S., Wang, V., O'Mahony, D., Aleman, K., Wyvill, K. M., Marshall, V., Steinberg, S. M., Pittaluga, S., Maric, I., Whitby, D., et al. (**2010**) An Interleukin-6–Related Systemic Inflammatory Syndrome in Patients Co-Infected with Kaposi Sarcoma–Associated Herpesvirus and HIV but without Multicentric Castleman Disease. Clin. Infect. Dis. 51, 350–358.
21 Della Bella, S., Taddeo, A., Calabrò, M. L. L., Brambilla, L., Bellinvia, M., Bergamo, E., Clerici, M. and Villa, M. L. L. (**2008**) Peripheral blood endothelial progenitors as potential reservoirs of Kaposi's sarcoma-associated herpesvirus. PLoS One 3, 1–8.
22 Ye, F., Lei, X. and Gao, S. J. (**2011**) Mechanisms of Kaposi's sarcoma-associated herpesvirus latency and reactivation. Adv. Virol. 1–19.
23 Burbelo, P., Issa, A. T., Ching, K. H., Wyvill, K. M., Little, R. F., Iadarola, M. J., Kovacs, J. A. and Yarchoan, R. (**2010**) Distinct Profiles of Antibodies to Kaposi Sarcoma-Associated Herpesvirus Antigens in Patients with Kaposi Sarcoma, Multicentric Castlemen's Disease, and Primary Effusion Lymphoma. J Infect Dis 201, 1919–1922.
24 Parravicini, C., Chandran, B., Corbellino, M., Berti, E., Paulli, M., Moore, P. S. and Chang, Y. (**2000**) Differential viral protein expression in Kaposi's sarcoma-associated herpesvirus-infected diseases: Kaposi's sarcoma, primary effusion lymphoma, and multicentric Castleman's disease. Am. J. Pathol. 156, 743–749.
25 Jary, A., Leducq, V., Palich, R., Gothland, A., Descamps, D., Joly, V., Lambert-Niclot, S., Amiel, C., Canestri, A., Mirand, A., et al. (**2018**) Usefulness of kaposi's sarcoma-Associated herpesvirus (KSHV) DNA viral load in whole blood for diagnosis and monitoring of KSHV-Associated diseases. J. Clin. Microbiol. 56, 1–4.
26 Gopal, S., Liomba, N. G., Montgomery, N. D., Moses, A., Kaimila, B., Nyasosela, R., Chikasema, M., Dhungel, B. M., Kampani, C., Sanders, M. K., et al. (**2015**) Characteristics and survival for HIV-associated multicentric Castleman disease in Malawi. J. Int. AIDS Soc. 18, 1–6.
27 Cronin, D. M. P. and Warnke, R. A. (**2009**) Castleman disease: An update on classification and the spectrum of associated lesions. Adv. Anat. Pathol. 16, 236–246.
28 Cavallin, L. E., Goldschmidt-Clermont, P. and Mesri, E. a. (**2014**) Molecular and Cellular Mechanisms of KSHV Oncogenesis of Kaposi's Sarcoma Associated with HIV/AIDS. PLoS Pathog. 10, 5–8.
29 Hengge, U. R., Ruzicka, T., Tyring, S. K., Stuschke, M., Roggendorf, M., Schwartz, R. A. and Seeber, S. (**2002**) Review Update on Kaposi's sarcoma and other HHV8 associated diseases. Part 1: epidemiology, environmental predispositions, clinical manifestations, and therapy. Lancet Infect. Dis. 2, 281–292.
30 Plancoulaine, S., Gessain, A., Beveren, M. Van, Tortevoye, P. and Abel, L. (**2003**) Evidence for a Recessive Major Gene Predisposing to Human Herpesvirus 8 (HHV-8) Infection in a Population in Which HHV-8 Is Endemic. J. Infect. Dis. 8, 1944–1950.
31 Aissani, B., Boehme, A. K., Wiener, H. W., Shrestha, S., Jacobson, L. P. and Kaslow, R. a. (**2014**) SNP screening of central MHC-identified HLA-DMB as a candidate susceptibility gene for HIV-related Kaposi's sarcoma. Genes Immun. 15, 424–429.
32 Foster, C. B., Lehrnbecher, T., Samuels, S., Stein, S., Mol, F., Metcalf, J. A., Wyvill, K., Steinberg, S. M., Kovacs, J., Blauvelt, A., et al. (**2000**) An IL6 promoter polymorphism is associated with a lifetime risk of development of Kaposi sarcoma in men infected with human immunodeficiency virus. Blood 96, 2562–2567.

33 Lehrnbecher, T. L., Foster, C. B., Zhu, S., Venzon, D., Steinberg, S. M., Wyvill, K., Metcalf, J. A., Cohen, S. S., Kovacs, J., Yarchoan, R., et al. (**2000**) Variant genotypes of FcγRIIIA influence the development of Kaposi's sarcoma in HIV-infected men. Blood 95, 2386–2390.
34 Blumenthal, M. J., Schutz, C., Meintjes, G., Mohamed, Z., Mendelson, M., Ambler, J. M., Whitby, D., Mackelprang, R. D., Carse, S., Katz, A. A., et al. (**2018**) EPHA2 sequence variants are associated with susceptibility to Kaposi's sarcoma-associated herpesvirus infection and Kaposi's sarcoma prevalence in HIV-infected patients. Cancer Epidemiol. 56, 133–139.
35 Blumenthal, M. J. (**2016**) The impact of EPHA2 polymorphism on KSHV infectivity and KS prevalence among HIV/AIDS patients in South Africa, University of Cape Town.
36 Hahn, A. S., Kaufmann, J. K., Wies, E., Naschberger, E., Panteleev-Ivlev, J., Schmidt, K., Holzer, A., Schmidt, M., Chen, J., König, S., et al. (**2012**) The ephrin receptor tyrosine kinase A2 is a cellular receptor for Kaposi's sarcoma–associated herpesvirus. Nat. Med. 18, 961–6.
37 Thaker, P. H., Deavers, M., Celestino, J., Thornton, A., Fletcher, M. S., Landen, C. N., Kinch, M. S., Kiener, P. A. and Sood, A. K. (**2004**) EphA2 expression is associated with aggressive features in ovarian carcinoma. Clin. Cancer Res. 10, 5145–5150.
38 Zelinski, D. P., Zantek, N. D., Walker-Daniels, J., Peters, M. A., Taparowsky, E. J. and Kinch, M. S. (**2002**) Estrogen and Myc negatively regulate expression of the EphA2 tyrosine kinase. J. Cell. Biochem. 85, 714–720.
39 The Joint United Nations Programme on HIV/AIDS (UNAIDS). (**2009**) 2008 UNAIDS Annual Report: Towards Universal Access.
40 The Joint United Nations Programme on HIV/AIDS (UNAIDS). (**2019**) Global HIV statistics.
41 Palmisano, L. and Vella, S. (**2011**) A brief history of antiretroviral therapy of HIV infection : success and challenges. Ann 1st Super Sanita 47, 44–48.
42 Nixon, S. A., Hanass-Hancock, J., Whiteside, A. and Barnett, T. (**2011**) The increasing chronicity of HIV in sub-Saharan Africa: Re-thinking "HIV as a long-wave event" in the era of widespread access to ART. Global. Health 7, 1–5.
43 Grulich, A. E., Leeuwen, M. T. Van, Falster, M. O. and Vajdic, C. M. (**2007**) Incidence of cancers in people with HIV/AIDS compared with immunosuppressed transplant recipients: a meta-analysis. Lancet 370, 59–67.
44 Frisch, M. (**2001**) Association of Cancer With AIDS-Related Immunosuppression in Adults. JAMA 285, 1736.
45 Coghill, A. E., Newcomb, P. A., Madeleine, M. M., Richardson, B. A., Mutyaba, I., Okuku, F., Phipps, W., Wabinga, H., Orem, J. and Casper, C. (**2013**) Contribution of HIV infection to mortality among cancer patients in Uganda. AIDS 27, 2933–42.
46 Stein, L., Urban, M. I., O'Connell, D., Xue, Q. Y., Beral, V., Newton, R., Ruff, P., Donde, B., Hale, M., Patel, M., et al. (**2008**) The spectrum of human immunodeficiency virus-associated cancers in a South African black population: Results from a case-control study, 1995-2004. Int. J. Cancer 122, 2260–2265.
47 Sasco, A. J., Jaquet, A., Boidin, E., Ekouevi, D. K., Thouillot, F., LeMabec, T., Forstin, M. A., Renaudier, P., N'Dom, P., Malvy, D., et al. (**2010**) The challenge of AIDS-related malignancies in sub-Saharan Africa. PLoS One 5.
48 Casper, C. (**2011**) The increasing burden of HIV-associated malignancies in resource-limited regions. Annu. Rev. Med. 62, 157–70.
49 The Joint United Nations Programme on HIV/AIDS (UNAIDS). (**2019**) UNAIDS Data 2019.
50 Mills, E. J., Bärnighausen, T. and Negin, J. (**2012**) HIV and aging - Preparing for the challenges ahead. N. Engl. J. Med. 366, 1270–1273.
51 Bloomfield, G. S., Khazanie, P., Morris, A., Rabadán-Diehl, C., Benjamin, L. A., Murdoch, D., Radcliff, V. S., Velazquez, E. J. and Hicks, C. (**2014**) HIV and noncommunicable cardiovascular and pulmonary diseases in low-and middle-income countries in the art era: What we know and best directions for future research. J. Acquir. Immune Defic. Syndr. 67.
52 Dave, J. A., Lambert, E. V., Badri, M., West, S., Maartens, G. and Levitt, N. S. (**2011**) Effect of

nonnucleoside reverse transcriptase inhibitor-based antiretroviral therapy on dysglycemia and insulin sensitivity in South African HIV-Infected Patients. J. Acquir. Immune Defic. Syndr. 57, 284–289.

53 Levitt, N. S., Peer, N., Steyn, K., Lombard, C., Maartens, G., Lambert, E. V. and Dave, J. A. (**2016**) Increased risk of dysglycaemia in South Africans with HIV; especially those on protease inhibitors. Diabetes Res. Clin. Pract. 119, 41–47.

54 Low, A., Gavriilidis, G., Larke, N., B-Lajoie, M. R., Drouin, O., Stover, J., Muhe, L. and Easterbrook, P. (**2016**) Incidence of Opportunistic Infections and the Impact of Antiretroviral Therapy among HIV-Infected Adults in Low- and Middle-Income Countries: A Systematic Review and Meta-analysis. Clin. Infect. Dis. 62, 1595–1603.

55 Kyeyune, R., Den Boon, S., Cattamanchi, A., Davis, J. L., Worodria, W., Yoo, S. D. and Huang, L. (**2010**) Causes of early mortality in HIV-infected TB suspects in an East African referral hospital. J. Acquir. Immune Defic. Syndr. 55, 446–450.

56 Subbarao, S., Wilkinson, K. A., Van Halsema, C. L., Rao, S. S., Boyles, T., Utay, N. S., Wilkinson, R. J. and Meintjes, G. (**2015**) Raised venous lactate and markers of intestinal translocation are associated with mortality among in-patients with HIV-associated TB in rural South Africa. J. Acquir. Immune Defic. Syndr. 70, 406–413.

57 Meintjes, G., Kerkhoff, A. D., Burton, R., Schutz, C., Boulle, A., Van Wyk, G., Blumenthal, L., Nicol, M. P. and Lawn, S. D. (**2015**) HIV-related medical admissions to a South African district hospital remain frequent despite effective antiretroviral therapy scale-up. Med. (United States) 94, 1–10.

58 Schutz, C., Barr, D., Andrade, B. B., Shey, M., Ward, A., Janssen, S., Burton, R., Wilkinson, K. A., Sossen, B., Fukutani, K. F., et al. (**2019**) Clinical, microbiologic, and immunologic determinants of mortality in hospitalized patients with HIV-associated tuberculosis: A prospective cohort study. PLOS Med. 16, e1002840.

59 The 1000 Genomes Project Consortium. (**2015**) A global reference for human genetic variation. Nature 526, 68–74.

60 Peter, J. G., Zijenah, L. S., Chanda, D., Clowes, P., Lesosky, M., Gina, P., Mehta, N., Calligaro, G., Lombard, C. J., Kadzirange, G., et al. (**2016**) Effect on mortality of point-of-care, urine-based lipoarabinomannan testing to guide tuberculosis treatment initiation in HIV-positive hospital inpatients: A pragmatic, parallel-group, multicountry, open-label, randomised controlled trial. Lancet 387, 1187–1197.

61 Gupta-Wright, A., Corbett, E. L., van Oosterhout, J. J., Wilson, D., Grint, D., Alufandika-Moyo, M., Peters, J. A., Chiume, L., Flach, C., Lawn, S. D., et al. (**2018**) Rapid urine-based screening for tuberculosis in HIV-positive patients admitted to hospital in Africa (STAMP): a pragmatic, multicentre, parallel-group, double-blind, randomised controlled trial. Lancet 392, 292–301.

62 Blumenthal, M. J., Schutz, C., Barr, D., Locketz, M., Marshall, V., Whitby, D., Katz, A. A., Uldrick, T., Meintjes, G. and Schäfer, G. (**2019**) The Contribution of Kaposi's Sarcoma-Associated Herpesvirus to Mortality in Hospitalized Human Immunodeficiency Virus-Infected Patients Being Investigated for Tuberculosis in South Africa. J. Infect. Dis. 220, 841–851.

63 The Joint United Nations Programme on HIV/AIDS (UNAIDS). (**2019**) Tuberculosis and HIV.

64 World Health Organization. (**2019**) TB disease burden. Global Tuberculosis Report.

65 Martin, J. N. (**2007**) The epidemiology of KSHV and its association with malignant disease. In Human Herpesviruses: Biology, Therapy, and Immunoprophylaxis (Arvin, A., Campadelli-Fiume, G., Mocarski, E., Moore, P. S., Roizman, B., Whitley, R., and Yamanishi, K., eds.), pp 960–985, Cambridge University Press, Cambridge.

66 de Sanjose, S., Mbisa, G., Perez-Alvarez, S., Benavente, Y., Sukvirach, S., Hieu, N. T., Shin, H., Anh, P. T. H., Thomas, J., Lazcano, E., et al. (**2009**) Geographic Variation in the Prevalence of Kaposi Sarcoma–Associated Herpesvirus and Risk Factors for Transmission. J. Infect. Dis. 199, 1449–1456.

67 Mesri, E. A., Cesarman, E. and Boshoff, C. (**2010**) Kaposi's sarcoma and its associated

herpesvirus. Nat. Rev. Cancer 10, 707–19.
68 Martin, J. N., Ganem, D. E., Osmond, D. H., Page-Schafer, K. A., Macrae, D. and Kedes, D. H. (**1998**) Sexual Transmission and the Natural History of Human. N. Engl. J. Med. 338, 948–954.
69 Goudsmit, J., Renwick, N., Dukers, N. H. T. M., Coutinho, R. A., Heisterkamp, S., Bakker, M., Schulz, T. F., Cornelissen, M. and Weverling, G. J. (**2000**) Human herpesvirus 8 infections in the Amsterdam Cohort Studies (1984-1997): Analysis of seroconversions to ORF65 and ORF73. Proc. Natl. Acad. Sci. USA 97, 4838–4843.
70 Dedicoat, M. and Newton, R. (**2003**) Review of the distribution of Kaposi's sarcoma-associated herpesvirus (KSHV) in Africa in relation to the incidence of Kaposi's sarcoma. Br. J. Cancer 88, 1–3.
71 Labo, N., Miley, W., Benson, C. A., Campbell, T. B. and Whitby, D. (**2015**) Epidemiology of Kaposi's sarcoma-associated herpesvirus in HIV-1-infected US persons in the era of combination antiretroviral therapy. AIDS 29, 1217–1225.
72 Sitas, F., Carrara, H., Beral, V., Newton, R., Reeves, G., Bull, D., Jentsch, U., Pacella-Norman, R., Bourboulia, D., Whitby, D., et al. (**1999**) Antibodies against Human Herpesvirus 8 in Black South African Patients With Cancer. N. Engl. J. Med. 340, 1863–71.
73 Wilkinson, D., Sheldon, J., Gilks, C. F. and Schulz, T. F. (**1999**) Prevalence of infection with human herpesvirus 8/Kaposi's sarcoma herpesvirus in rural South Africa. South African Med. J. 89, 3–6.
74 Human Sciences Research Council. (**2018**) The fifth South African national HIV prevalence, incidence, behavious and communication survey, 2017 (SABSSM V).
75 Maskew, M., MacPhail, A., Whitby, D., Egger, M., Wallis, C. L. and Fox, M. P. (**2011**) Prevalence and predictors of kaposi sarcoma herpes virus seropositivity: A cross-sectional analysis of HIV-infected adults initiating ART in Johannesburg, South Africa. Infect. Agent. Cancer 6, 1–8.
76 Moore, P. S., Gao, S. J., Dominguez, G., Cesarman, E., Lungu, O., Knowles, D. M., Garber, R., Pellett, P. E., McGeoch, D. J. and Chang, Y. (**1996**) Primary characterization of a herpesvirus agent associated with Kaposi's sarcomae. J. Virol. 70, 549–558.
77 Renne, R., Zhong, W., Herndier, B., McGrath, M., Abbey, N., Kedes, D. and Ganem, D. (**1996**) Lytic growth of Kaposi's sarcoma-associated herpesvirus (human herpesvirus 8) in culture. Nat. Med. 2, 342–346.
78 Dezube, B. J., Zambela, M., Sage, D. R., Wang, J. F. and Fingeroth, J. D. (**2002**) Characterization of Kaposi sarcoma-associated herpesvirus/human herpesvirus-8 infection of human vascular endothelial cells: early events. Blood 100, 888–896.
79 Whitley, R. J. (**1996**) Herpesviruses. In Medical Microbiology (Baron, S., ed.), University of Texas Medical Branch at Galveston, Galveston (TX).
80 Neipel, F., Albrecht, J. C. and Fleckenstein, B. (**1997**) Cell-homologous genes in the Kaposi's sarcoma-associated rhadinovirus human herpesvirus 8: Determinants of its pathogenicity? J. Virol. 71, 4187–4192.
81 Gong, D., Dai, X., Xiao, Y., Du, Y., Chapa, T. J., Johnson, J. R., Li, X., Krogan, N. J., Deng, H., Wu, T.-T., et al. (**2017**) Virus-Like Vesicles of Kaposi's Sarcoma-Associated Herpesvirus Activate Lytic Replication by Triggering Differentiation Signaling. J. Virol. 91, 1–18.
82 Bechtel, J. T., Winant, R. C. and Ganem, D. (**2005**) Host and Viral Proteins in the Virion of Kaposi's Sarcoma-Associated Herpesvirus. J. Virol. 79, 4952–4964.
83 Zhu, F. X., Chong, J. M., Wu, L. and Yuan, Y. (**2005**) Virion Proteins of Kaposi's Sarcoma-Associated Herpesvirus. J. Virol. 79, 800–811.
84 Neipel, F., Albrecht, J. C. and Fleckenstein, B. (**1998**) Human herpesvirus 8- the first human Rhadinovirus. J. Natl. Cancer Inst. Monogr. 8, 73–77.
85 Russo, J. J., Bohenzky, R. A., Chien, M., Chen, J., Yan, M., Maddalena, D., Parry, J. P., Peruzzi, D., Edelman, I. S., Chang, Y., et al. (**1996**) Nucleotide sequence of the Kaposi sarcoma- associated herpesvirus (HHV8). Microbiology 93, 14862–14867.
86 Wang, F., Akula, S., Pramod, N., Zeng, L. and Chandran, B. (**2001**) Human herpesvirus 8

envelope glycoprotein K8.1A interaction with the target cells involves heparan sulfate. J. Virol. 75, 7517–7527.

87 Birkmann, A., Mahr, K., Ensser, A., Yag, S., Titgemeyer, F., Fleckenstein, B. and Neipel, F. (**2001**) Cell Surface Heparan Sulfate Is a Receptor for Human Herpesvirus 8 and Interacts with Envelope Glycoprotein K8.1. J. Virol. 75, 11583–11593.

88 Hayward, G. S. and Zong, J. C. (**2006**) Modern Evolutionary History of the Human KSHV Genome. In Current Topics in Microbiology and Immunology, pp 1–42.

89 Hayward, G. S. (**1999**) KSHV strains: the origins and global spread of the virus. Semin. Cancer Biol. 9, 187–99.

90 Fouchard, N., Lacoste, V., Couppie, P., Develoux, M., Mauclere, P., Michel, P., Herve, V., Pradinaud, R., Bestetti, G., Huerre, M., et al. (**2000**) Detection and genetic polymorphism of human herpes virus type 8 in endemic or epidemic Kaposi's sarcoma from West and Central Africa, and South America. Int. J. Cancer 85, 166–170.

91 Meng, Y. X., Spira, T. J., Bhat, G. J., Birch, C. J., Druce, J. D., Edlin, B. R., Edwards, R., Gunthel, C., Newton, R., Stamey, F. R., et al. (**1999**) Individuals from North America, Australasia, and Africa are infected with four different genotypes of human herpesvirus 8. Virology 261, 106–119.

92 Zong, J., Ciufo, D. M., Viscidi, R., Alagiozoglou, L., Tyring, S., Rady, P., Orenstein, J., Boto, W., Kalumbuja, H., Romano, N., et al. (**2002**) Genotypic analysis at multiple loci across Kaposi's sarcoma herpesvirus (KSHV) DNA molecules: Clustering patterns, novel variants and chimerism. J. Clin. Virol. 23, 119–148.

93 Kajumbula, H., Wallace, R. G., Zong, J. C., Hokello, J., Sussman, N., Simms, S., Rockwell, R. F., Pozos, R., Hayward, G. S. and Boto, W. (**2006**) Ugandan Kaposi's sarcoma-associated herpesvirus phylogeny: Evidence for cross-ethnic transmission of viral subtypes. Intervirology 49, 133–143.

94 Bourboulia, D., Whitby, D., Boshoff, C., Newton, R., Beral, V., Carrara, H., Lane, A. and Sitas, F. (**1998**) Serologic Evidence for Mother-to-Child Transmission of Kaposi Sarcoma-Associated Herpesvirus Infection. J. Am. Med. Assoc. 280, 31–32.

95 He, J., Bhat, G., Kankasa, C., Chintu, C., Mitchell, C., Duan, W. and Wood, C. (**1998**) Seroprevalence of human herpesvirus 8 among Zambian women of childbearing age without Kaposi's sarcoma (KS) and mother-child pairs with KS. J. Infect. Dis. 178, 1787–1790.

96 Davidovici, B., Karakis, I., Bourboulia, D., Ariad, S., Zong, J., Benharroch, D., Dupin, N., Weiss, R., Hayward, G., Sarov, B., et al. (**2001**) Seroepidemiology and molecular epidemiology of Kaposi's sarcoma-associated herpesvirus among Jewish population groups in Israel. J. Natl. Cancer Inst. 93, 194–202.

97 Duus, K. M., Lentchitsky, V., Wagenaar, T., Grose, C. and Webster-cyriaque, J. (**2004**) Wild-Type Kaposi's Sarcoma-Associated Herpesvirus Isolated from the Oropharynx of Immune-Competent Individuals Has Tropism for Cultured Oral Epithelial Cells. J. Virol. 78, 4074–4084.

98 Dedicoat, M., Newton, R., Alkharsah, K. R., Sheldon, J., Szabados, I., Ndlovu, B., Page, T., Casabonne, D., Gilks, C. F., Cassol, S. A., et al. (**2004**) Mother-to-child transmission of human herpesvirus-8 in South Africa. J Infect Dis 190, 1068–1075.

99 Matteoli, B., Broccolo, F., Scaccino, A., Cottoni, F., Angeloni, A., Faggioni, A. and Ceccherini-Nelli, L. (**2012**) In Vivo and In Vitro Evidence for an Association Between the Route-Specific Transmission of HHV-8 and the Virus Genotype. J. Med. Virol. 84, 786–791.

100 Koelle, D. M., Huang, M. L., Chandran, B., Vieira, J., Piepkorn, M. and Corey, L. (**1997**) Frequent detection of Kaposi's sarcoma-associated herpesvirus (human herpesvirus 8) DNA in saliva of human immunodeficiency virus-infected men: clinical and immunologic correlates. J. Infect. Dis. 176, 94–102.

101 Vieira, J., Huang, M. L., Koelle, D. M. and Corey, L. (**1997**) Transmissible Kaposi's sarcoma-associated herpesvirus (human herpesvirus 8) in saliva of men with a history of Kaposi's sarcoma. J. Virol. 71, 7083–7087.

102 Pauk, J., Huang, M., Brodie, S. J., Wald, A., Koelle, D. M., Schacker, T., Celum, C., Selke, S. and

Corey, L. (**2000**) Mucosal shedding of human herpesvirus 8 in men. N. Engl. J. Med. 343, 1369–1377.
103 Minhas, V. and Wood, C. (**2014**) Epidemiology and Transmission of Kaposi's Sarcoma-Associated Herpesvirus. Viruses 6, 4178–4194.
104 Akula, S. M., Pramod, N. P., Wang, F. Z. and Chandran, B. (**2001**) Human herpesvirus 8 envelope-associated glycoprotein B interacts with heparan sulfate-like moieties. Virology 284, 235–249.
105 Dollery, S. J., Santiago-Crespo, R. J., Chatterjee, D. and Berger, E. A. (**2018**) Glycoprotein K8.1A of Kaposi's Sarcoma-Associated Herpesvirus Is a Critical B Cell Tropism Determinant Independent of Its Heparan Sulfate Binding Activity. J. Virol. 93, 1–13.
106 Veettil, M. V., Sadagopan, S., Sharma-Walia, N., Wang, F.-Z., Raghu, H., Varga, L. and Chandran, B. (**2008**) Kaposi's sarcoma-associated herpesvirus forms a multimolecular complex of integrins (αVβ5, αVβ3, and α3β1) and CD98-xCT during infection of human dermal microvascular endothelial cells, and CD98-xCT is essential for the postentry stage of infection. J. Virol. 82, 12126–12144.
107 Dollery, S. J. (**2019**) Towards Understanding KSHV Fusion and Entry. Viruses 11, 1–17.
108 Akula, S. M., Pramod, N. P., Wang, F. and Chandran, B. (**2002**) Integrin α3β1 (CD 49c/29) Is a Cellular Receptor for Kaposi's Sarcoma-Associated Herpesvirus (KSHV/HHV-8) Entry into the Target Cells. Cell 108, 407–419.
109 Garrigues, H. J., Rubinchikova, Y. E., Dipersio, C. M. and Rose, T. M. (**2008**) Integrin αVβ3 Binds to the RGD motif of glycoprotein B of Kaposi's sarcoma-associated herpesvirus and functions as an RGD-dependent entry receptor. J. Virol. 82, 1570–1580.
110 Garrigues, H. J., DeMaster, L. K., Rubinchikova, Y. E. and Rose, T. M. (**2014**) KSHV attachment and entry are dependent on αVβ3 integrin localized to specific cell surface microdomains and do not correlate with the presence of heparan sulfate. Virology 464–465, 118–133.
111 Garrigues, H. J., DeMaster, L. K., Rubinchikova, Y. E. and Rose, T. M. (**2018**) Corrigendum to: "KSHV attachment and entry are dependent on αVβ3 integrin localized to specific cell surface microdomains and do not correlate with the presence of heparan sulfate." Virology 515, 264–265.
112 Kerur, N., Veettil, M. V., Sharma-Walia, N., Sadagopan, S., Bottero, V., Paul, A. G. and Chandran, B. (**2010**) Characterization of entry and infection of monocytic THP-1 cells by Kaposi's sarcoma associated herpesvirus (KSHV): Role of heparan sulfate, DC-SIGN, integrins and signaling. Virology 406, 103–116.
113 Rappocciolo, G., Jenkins, F. J., Hensler, H. R., Piazza, P., Jais, M., Borowski, L., Watkins, S. C. and Rinaldo, C. R. (**2006**) DC-SIGN is a receptor for human herpesvirus 8 on dendritic cells and macrophages. J. Immunol. 176, 1741–1749.
114 Rappocciolo, G., Hensler, H. R., Jais, M., Reinhart, T. A., Pegu, A., Jenkins, F. J. and Rinaldo, C. R. (**2008**) Human Herpesvirus 8 Infects and Replicates in Primary Cultures of Activated B Lymphocytes through DC-SIGN. J. Virol. 82, 4793–4806.
115 Großkopf, A. K., Ensser, A., Neipel, F., Jungnickl, D., Schlagowski, S., Desrosiers, R. C. and Hahn, A. S. (**2018**) A conserved Eph family receptor-binding motif on the gH/gL complex of Kaposi's sarcoma-associated herpesvirus and rhesus monkey rhadinovirus. PLoS Pathog. 14, 1–26.
116 Hahn, A. S. and Desrosiers, R. C. (**2013**) Rhesus Monkey Rhadinovirus Uses Eph Family Receptors for Entry into B Cells and Endothelial Cells but Not Fibroblasts. PLoS Pathog. 9, 1–14.
117 Dutta, D., Chakraborty, S., Bandyopadhyay, C., Valiya Veettil, M., Ansari, M. A., Singh, V. V. and Chandran, B. (**2013**) EphrinA2 Regulates Clathrin Mediated KSHV Endocytosis in Fibroblast Cells by Coordinating Integrin-Associated Signaling and c-Cbl Directed Polyubiquitination. PLoS Pathog. 9, 1–22.
118 Chen, J., Zhang, X., Schaller, S., Jardetzky, T. S. and Longnecker, R. (**2019**) Ephrin receptor A4 (EphA4) is a new Kaposi's sarcoma-associated herpesvirus virus entry receptor. MBio 10, 1–29.
119 TerBush, A. A., Hafkamplwan, F., Lee, H. J. and Coscoy, L. (**2018**) A Kaposi's Sarcoma-Associated Herpesvirus Infection Mechanism Is Independent of Integrins α3β1, αVβ3, and αVβ5. J. Virol.

92, 1–22.
120 Großkopf, A. K., Schlagowski, S., Hörnich, B. F., Fricke, T., Desrosiers, R. C. and Hahn, A. S. (**2019**) EphA7 Functions as Receptor on BJAB Cells for Cell-to-Cell Transmission of the Kaposi's Sarcoma-Associated Herpesvirus and for Cell-Free Infection by the Related Rhesus Monkey Rhadinovirus. J. Virol. 93, 1–19.
121 Hahn, A., Birkmann, A., Wies, E., Dorer, D., Mahr, K., Stürzl, M., Titgemeyer, F. and Neipel, F. (**2009**) Kaposi's sarcoma-associated herpesvirus gH/gL: glycoprotein export and interaction with cellular receptors. J. Virol. 83, 396–407.
122 Chakraborty, S., Veettil, M. V., Bottero, V. and Chandran, B. (**2012**) Kaposi's sarcoma-associated herpesvirus interacts with EphrinA2 receptor to amplify signaling essential for productive infection. Proc. Natl. Acad. Sci. USA 109, E1163-72.
123 Kaleeba, J. A. R. and Berger, E. (**2006**) Kaposi's Sarcoma-Associated Herpesvirus Fusion-Entry Receptor: Cysteine Transporter xCT. Science 311, 1921–1925.
124 Pan, H., Xie, J., Ye, F. and Gao, S.-J. (**2006**) Modulation of Kaposi's Sarcoma-Associated Herpesvirus Infection and Replication by MEK/ERK, JNK, and p38 Multiple Mitogen-Activated Protein Kinase Pathways during Primary Infection. J. Virol. 80, 5371–5382.
125 Xie, J., Pan, H., Yoo, S. and Gao, S.-J. (**2005**) Kaposi's Sarcoma-Associated Herpesvirus Induction of AP-1 and Interleukin 6 during Primary Infection Mediated by Multiple Mitogen-Activated Protein Kinase Pathways. J. Virol. 79, 15027–15037.
126 Sharma-Walia, N., Krishnan, H. H., Naranatt, P. P., Zeng, L., Smith, M. S. and Chandran, B. (**2005**) ERK1/2 and MEK1/2 Induced by Kaposi's Sarcoma-Associated Herpesvirus (Human Herpesvirus 8) Early during Infection of Target Cells Are Essential for Expression of Viral Genes and for Establishment of Infection. J. Virol. 79, 10308–10329.
127 Wang, X., Zou, Z., Deng, Z., Liang, D., Zhou, X., Sun, R. and Lan, K. (**2017**) Male hormones activate EphA2 to facilitate Kaposi's sarcoma-associated herpesvirus infection: Implications for gender disparity in Kaposi's sarcoma. PLoS Pathog. 13, 1–23.
128 Kumar, B. and Chandran, B. (**2016**) KSHV Entry and Trafficking in Target Cells—Hijacking of Cell Signal Pathways, Actin and Membrane Dynamics. Viruses 8, 1–23.
129 Raghu, H., Sharma-Walia, N., Veettil, M. V., Sadagopan, S. and Chandran, B. (**2009**) Kaposi's sarcoma-associated herpesvirus utilizes an actin polymerization-dependent macropinocytic pathway to enter human dermal microvascular endothelial and human umbilical vein endothelial cells. J. Virol. 83, 4895–4911.
130 Akula, S. M., Naranatt, P. P., Walia, N., Wang, F., Fegley, B. and Chandran, B. (**2003**) Kaposi's Sarcoma-Associated Herpesvirus (Human Herpesvirus 8) Infection of Human Fibroblast Cells Occurs through Endocytosis. J. Virol. 77, 7978–7990.
131 Inoue, N., Winter, J., Lal, R. B., Offermann, M. K. and Koyano, S. (**2003**) Characterization of Entry Mechanisms of Human Herpesvirus 8 by Using an Rta-Dependent Reporter Cell Line. J. Virol. 77, 10177–10177.
132 Boshoff, C. (**2012**) Ephrin receptor: a door to KSHV infection. Nat. Med., Nature Publishing Group 18, 861–863.
133 Weed, D. J., Dollery, S. J., Komala Sari, T. and Nicola, A. V. (**2018**) Acidic pH Mediates Changes in Antigenic and Oligomeric Conformation of Herpes Simplex Virus gB and Is a Determinant of Cell-Specific Entry. J. Virol. 92, 1–11.
134 Ballestas, M. E. and Kaye, K. M. (**2001**) Kaposi's Sarcoma-Associated Herpesvirus Latency-Associated Nuclear Antigen 1 Mediates Episome Persistence through cis-acting Terminal Repeat (TR) Sequence and Specifically Binds TR DNA. J. Virol. 75, 3250–3258.
135 Chen, J., Ueda, K., Sakakibara, S., Okuno, T., Parravicini, C., Corbellino, M. and Yamanishi, K. (**2001**) Activation of latent Kaposi's sarcoma-associated herpesvirus by demethylation of the promoter of the lytic transactivator. Proc. Natl. Acad. Sci. USA 98, 4119–24.
136 Nalwoga, A., Cose, S., Nash, S., Miley, W., Asiki, G., Kusemererwa, S., Yarchoan, R., Labo, N., Whitby, D. and Newton, R. (**2018**) Relationship between anemia, malaria coinfection, and

Kaposi sarcoma-associated herpesvirus seropositivity in a population-based study in rural Uganda. J. Infect. Dis. 218, 1061–1065.

137 Bihl, F., Mosam, A., Henry, L. N., Chisholm, J. V, Dollard, S., Gumbi, P., Cassol, E., Page, T., Mueller, N., Kiepiela, P., et al. (**2007**) Kaposi's sarcoma-associated herpesvirus-specific immune reconstitution and antiviral effect of combined HAART/chemotherapy in HIV clade C-infected individuals with Kaposi's sarcoma. AIDS 21, 1245–52.

138 Aoki, Y. and Tosato, G. (**2004**) HIV-1 Tat enhances Kaposi sarcoma–associated herpesvirus (KSHV) infectivity. Blood 104, 810–815.

139 Damania, B. (**2004**) Oncogenic γ-herpesviruses: Comparison of viral proteins involved in tumorigenesis. Nat. Rev. 2, 656–669.

140 Dupin, N., Fisher, C., Kellam, P., Ariad, S., Tulliez, M., Franck, N., van Marck, E., Salmon, D., Gorin, I., Escande, J. P. P., et al. (**1999**) Distribution of human herpesvirus-8 latently infected cells in Kaposi's sarcoma, multicentric Castleman's disease, and primary effusion lymphoma. Proc. Natl. Acad. Sci. USA 96, 4546–4551.

141 Gao, S. J., Boshoff, C., Jayachandra, S., Weiss, R. a, Chang, Y. and Moore, P. S. (**1997**) KSHV ORF K9 (vIRF) is an oncogene which inhibits the interferon signaling pathway. Oncogene 15, 1979–85.

142 Shin, Y. C., Nakamura, H., Liang, X., Feng, P., Chang, H., Kowalik, T. F. and Jung, J. U. (**2006**) Inhibition of the ATM/p53 Signal Transduction Pathway by Kaposi's Sarcoma-Associated Herpesvirus Interferon Regulatory Factor 1. J. Virol. 80, 2257–2266.

143 Esteban, M., Garcı, M. A., Arroyo, J., Nombela, C. and Rivas, C. (**2003**) The latency protein LANA2 from Kaposi's sarcoma-associated herpesvirus inhibits apoptosis induced by dsRNA-activated protein kinase but not RNase L activation. J. Gen. Virol. 84, 1463–1470.

144 Rivas, C., Thlick, A., Parravicini, C., Moore, P. S. and Chang, Y. (**2001**) Kaposi's Sarcoma-Associated Herpesvirus LANA2 Is a B-Cell-Specific Latent Viral Protein That Inhibits p53. J. Virol. 75, 429–438.

145 Fuld, S., Cunningham, C., Klucher, K., Davison, A. J. and Blackbourn, D. J. (**2006**) Inhibition of Interferon Signaling by the Kaposi's Sarcoma-Associated Herpesvirus Full-Length Viral Interferon Regulatory Factor 2 Protein. J. Virol. 80, 3092–3097.

146 Lee, H., Dog, S., Chung, B., Toth, Z., Brulois, K., Lee, S., Kanketayeva, Z., Feng, P., Ha, T. and Jung, J. U. (**2014**) Kaposi's Sarcoma-Associated Herpesvirus Viral Interferon Regulatory Factor 4 (vIRF4) Targets Expression of Cellular IRF4 and the Myc. J. Virol. 88, 2183–2194.

147 Ma, Q., Cavallin, L. E., Leung, H. J., Chiozzini, C., Goldschmidt-Clermont, P. J. and Mesri, E. a. (**2013**) A role for virally induced reactive oxygen species in Kaposi's sarcoma herpesvirus tumorigenesis. Antioxid. Redox Signal. 18, 80–90.

148 Bais, C., Santomasso, B., Coso, O., Arvanitakis, L., Raaka, E. G., Gutkind, J. S., Asch, A. S., Cesarman, E., Gershengorn, M. C., Mesri, E. A., et al. (**1998**) G-protein-coupled receptor of Kaposi's sarcoma-associated herpesvirus is a viral oncogene and angiogenesis activator. Nature 391, 86–9.

149 Vart, R. J., Nikitenko, L. L., Lagos, D., Trotter, M. W. B., Cannon, M., Bourboulia, D., Gratrix, F., Takeuchi, Y. and Boshoff, C. (**2007**) Kaposi's sarcoma-associated herpesvirus-encoded interleukin-6 and G-protein-coupled receptor regulate angiopoietin-2 expression in lymphatic endothelial cells. Cancer Res. 67, 4042–4051.

150 Schwarz, M. and Murphy, P. M. (**2001**) Kaposi's Sarcoma-Associated Herpesvirus G Protein-Coupled Receptor Constitutively Activates NF-kB and Induces Proinflammatory Cytokine and Chemokine Production Via a C-Terminal Signaling Determinant. J. Immunol. 167, 505–513.

151 Swanton, C., Mann, D. J., Fleckenstein, B., Neipel, F., Peters, G. and Jones, N. (**1997**) Herpes viral cyclin/Cdk6 complexes evade inhibition by CDK inhibitor proteins. Nature 390, 184–7.

152 Radkov, S. a, Kellam, P. and Boshoff, C. (**2000**) The latent nuclear antigen of Kaposi sarcoma-associated herpesvirus targets the retinoblastoma-E2F pathway and with the oncogene Hras transforms primary rat cells. Nat. Med. 6, 1121–1127.

153 Guasparri, I., Keller, S. a and Cesarman, E. (**2004**) KSHV vFLIP is essential for the survival of infected lymphoma cells. J. Exp. Med. 199, 993–1003.
154 Sun, Q., Matta, H., Lu, G. and Chaudhary, P. M. (**2006**) Induction of IL-8 expression by human herpesvirus 8 encoded vFLIP K13 via NF-kappaB activation. Oncogene 25, 2717–26.
155 Grossmann, C., Podgrabinska, S., Skobe, M. and Ganem, D. (**2006**) Activation of NF-kappaB by the latent vFLIP gene of Kaposi's sarcoma-associated herpesvirus is required for the spindle shape of virus-infected endothelial cells and contributes to their proinflammatory phenotype. J. Virol. 80, 7179–85.
156 Zeng, Y., Zhang, X., Huang, Z., Cheng, L., Yao, S., Qin, D., Chen, X., Tang, Q., Lv, Z., Zhang, L., et al. (**2007**) Intracellular Tat of Human Immunodeficiency Virus Type 1 Activates Lytic Cycle Replication of Kaposi's Sarcoma-Associated Herpesvirus: Role of JAK/STAT Signaling. J. Virol. 81, 2401–2417.
157 Varthakavi, V., Smith, R. M., Deng, H., Sun, R. and Spearman, P. (**2002**) Human immunodeficiency virus type-1 activates lytic cycle replication of Kaposi's sarcoma-associated herpesvirus through induction of KSHV Rta. Virology 297, 270–280.
158 Fiorelli, V., Gendelman, R., Sirianni, M. C., Chang, H. K., Colombini, S., Markham, P. D., Monini, P., Sonnabend, J., Pintus, A., Gallo, R. C., et al. (**1998**) γ-Interferon produced by CD8+ T cells infiltrating Kaposi's sarcoma induces spindle cells with angiogenic phenotype and synergy with human immunodeficiency virus-1 Tat protein: An immune response to human herpesvirus-8 infection? Blood 91, 956–967.
159 Albini, A., Soldi, R., Giunciuglio, D., Giraudo, E., Benelli, R., Primo, L., Noonan, D., Salio, M., Camussi, G., Rockl, W., et al. (**1996**) The angiogenesis induced by HIV-1 Tat protein is mediated by the Flk-1/KDR receptor on vascular endothelial cells. Nat. Med. 2, 1371–1375.
160 Ensoli, B., Barillari, G., Salahuddin, S. Z., Gallo, R. C. and Wong-Staal, F. (**1990**) Tat protein of HIV-1 stimulates growth of cells derived from Kapoi's sarcoma lesions of AIDS patients. Nature 344, 84–86.
161 Yao, S., Hu, M., Hao, T., Li, W., Xue, X., Xue, M., Zhu, X., Zhou, F., Qin, D., Yan, Q., et al. (**2015**) MiRNA-891a-5p mediates HIV-1 Tat and KSHV Orf-K1 synergistic induction of angiogenesis by activating NF-κB signaling. Nucleic Acids Res. 43, 9362–9378.
162 Xue, M., Yao, S., Hu, M., Li, W., Hao, T., Zhou, F., Zhu, X., Lu, H., Qin, D., Yan, Q., et al. (**2014**) HIV-1 Nef and KSHV oncogene K1 synergistically promote angiogenesis by inducing cellular miR-718 to regulate the PTEN/AKT/mTOR signaling pathway. Nucleic Acids Res. 42, 9862–9879.
163 Barillari, G., Gendelman, R., Gallo, R. C. and Ensoli, B. (**1993**) The Tat protein of human immunodeficiency virus type 1, a growth factor for AIDS Kaposi sarcoma and cytokine-activated vascular cells, induces adhesion of the same cell types by using integrin receptors recognizing the RGD amino acid sequence. Proc. Natl. Acad. Sci. USA 90, 7941–7945.
164 Barillari, G., Sgadari, C., Fiorelli, V., Samaniego, F., Colombini, S., Manzari, V., Modesti, A., Nair, B. C., Cafaro, A., Stürzl, M., et al. (**1999**) The Tat protein of human immunodeficiency virus type-1 promotes vascular cell growth and locomotion by engaging the α5β1 and αvβ3 integrins and by mobilizing sequestered basic fibroblast growth factor. Blood 94, 663–672.
165 Guo, H., Pati, S., Sadowska, M., Charurat, M. and Reitz, M. (**2004**) Tumorigenesis by Human Herpesvirus 8 vGPCR Is Accelerated by Human Immuodeficiency Virus Type 1 Tat. J. Virol. 78, 9336–9342.
166 Pati, S., Foulke, J. S., Barabitskaya, O., Kim, J., Nair, B. C., Hone, D., Smart, J., Feldman, R. A. and Reitz, M. (**2003**) Human Herpesvirus 8-Encoded vGPCR Activates Nuclear Factor of Activated T Cells and Collaborates with Human Immunodeficiency Virus Type 1 Tat. J. Virol. 77, 5759–5773.
167 Hanahan, D. and Weinberg, R. (**2000**) The Hallmarks of Cancer. Cell 100, 57–70.
168 Ramos da Silva, S. and Elgui de Oliveira, D. (**2011**) HIV, EBV and KSHV: Viral cooperation in the pathogenesis of human malignancies. Cancer Lett., Elsevier Ireland Ltd 305, 175–185.
169 Wang, Q. J., Jenkins, F. J., Jacobsen, L. P., Kingsley, L. A., Day, R. D., Zhang, Z. W., Meng, Y. X., Pellet, P. E., Kousoulas, K. G., Baghian, A., et al. (**2001**) Primary human herpesvirus 8 infection

generates a broadly specific CD8+ T-cell response to viral lytic cycle proteins. Blood 97, 2366–2373.
170 Gregory, S. M., West, J. A., Dillon, P. J., Hilscher, C., Dittmer, D. P. and Damania, B. (**2009**) Toll-like receptor signaling controls reactivation of KSHV from latency. Proc. Natl. Acad. Sci. USA 106, 11725–11730.
171 Kaposi, M. (**1872**) Idiopathisches multiples Pigmentsarcom der Haut. Arch. Derm. Syph. 4, 2675–2678.
172 Soulier, J., Grollet, L., Oksenhendler, E., Cacoub, P., Cazals-Hatem, D., Babinet, P., D'Agay, M. F., Clauvel, J. P., Raphael, M., Degos, L., et al. (**1995**) Kaposi's sarcoma-associated herpesvirus-like DNA sequences in multicentric Castleman's disease. Blood 86, 1276–1280.
173 Guillet, S., Gérard, L., Meignin, V., Agbalika, F., Cuccini, W., Denis, B., Katlama, C., Galicier, L. and Oksenhendler, E. (**2016**) Classic and extracavitary primary effusion lymphoma in 51 HIV-infected patients from a single institution. Am. J. Hematol. 91, 233–237.
174 Mularoni, A., Gallo, A., Riva, G., Barozzi, P., Miele, M., Cardinale, G., Vizzini, G., Volpes, R., Grossi, P., Di Carlo, D., et al. (**2017**) Successful Treatment of Kaposi Sarcoma–Associated Herpesvirus Inflammatory Cytokine Syndrome After Kidney–Liver Transplant: Correlations With the Human Herpesvirus 8 miRNome and Specific T Cell Response. Am. J. Transplant. 17, 2963–2969.
175 Teruya-Feldstein, J., Zauber, P., Setsuda, J. E., Berman, E. L., Sorbara, L., Raffeld, M., Tosato, G. and Jaffe, E. S. (**1998**) Expression of human herpesvirus-8 oncogene and cytokine homologues in an HIV-seronegative patient with multicentric Castleman's disease and primary effusion lymphoma. Lab. Investig. 78, 1637–1642.
176 Cook-Mozaffari, P., Newton, R., Beral, V. and Burkitt, D. P. (**1998**) The geographical distribution of Kaposi's sarcoma and of lymphomas in Africa before the AIDS epidemic. Br. J. Cancer 78, 1521–8.
177 Torre, L. A., Bray, F., Siegel, R. L., Ferlay, J., Lortet-tieulent, J. and Jemal, A. (**2015**) Global Cancer Statistics, 2012. CA a cancer J. Clin. 65, 87–108.
178 Iscovich, J., Boffetta, P., Franceschi, S., Azizi, E. and Sarid, R. (**2000**) Classic Kaposi Sarcoma Epidemiology and risk factors. Cancer 88, 500–517.
179 Harwood, A. R., Osoba, D., Hofstader, S. L., Goldstein, M. B., Cardella, C. J., Holecek, M. J., Kunynetz, R. and Giammarco, R. A. (**1979**) Kaposi's sarcoma in recipients of renal transplants. Am. J. Med. 67, 759–765.
180 Andreoni, M., Goletti, D., Pezzotti, P., Pozzetto, A., Monini, P., Sarmati, L., Farchi, F., Tisone, G., Piazza, A., Pisani, F., et al. (**2001**) Prevalence, incidence and correlates of HHV-8/KSHV infection and Kaposi's Sarcoma in renal and liver transplant recipients. J. Infect. 43, 195–199.
181 Orenstein, J. M. (**2008**) Ultrastructure of Kaposi sarcoma. Ultrastruct. Pathol. 32, 211–220.
182 International collaboration on HIV and Cancer. (**2000**) Highly Active Antiretroviral Therapy and Incidence of Cancer in Human Immunodeficiency Virus-Infected Adults. J. Natl. cancer Inst. 92, 1823–1830.
183 Ferlay, J., Soerjomataram, I., Ervik, M., Dikshit, R., Eser, S., Mathers, C., Rebelo, M., Parkin, D., Forman, D. and Bray, F. (**2013**) GLOBOCAN 2012 v1.0, Cancer Incidence and Mortality Worldwide: IARC CancerBase No. 11. Lyon, Fr. Int. Agency Res. Cancer Available online http//globocan.iarc.fr [accessed 2017/02/25].
184 Mosam, A., Carrara, H., Shaik, F., Uldrick, T., Berkman, A., Aboobaker, J. and Coovadia, H. M. (**2009**) Increasing incidence of Kaposi's sarcoma in black South Africans in KwaZulu-Natal, South Africa (1983-2006). Int. J. STD AIDS 20, 553–6.
185 Bray, F., Ferlay, J., Soerjomataram, I., Siegel, R. L., Torre, L. A. and Jemal, A. (**2018**) Global cancer statistics 2018: GLOBOCAN estimates of incidence and mortality worldwide for 36 cancers in 185 countries. CA. Cancer J. Clin. 68, 394–424.
186 Ferlay, J., Ervik, M., Lam, F., Colombet, M., Mery, L., Piñeros, M., Znaor, A., Soerjomataram, I. and Bray, F. (**2018**) Global Cancer Observatory: Cancer Today. Lyon, Fr. Int. Agency Res. Cancer.

187 Semeere, A., Wenger, M., Busakhala, N., Buziba, N., Bwana, M., Muyindike, W., Amerson, E., Maurer, T., Mccalmont, T., Leboit, P., et al. (**2016**) A prospective ascertainment of cancer incidence in sub-Saharan Africa: The case of Kaposi sarcoma. Cancer Med. 5, 914–928.
188 Martin, J. N. (**2011**) Kaposi Sarcoma-Associated Herpesvirus/Human Herpesvirus 8 and Kaposi Sarcoma. Adv Dent Res 23, 76–78.
189 O'Brien, T. R., Kedes, D., Ganem, D., Macrae, D. R., Rosenberg, P. S., Molden, J. and Goedert, J. J. (**1999**) Evidence for Concurrent Epidemics of Human Herpesvirus 8 and Human Immunodeficiency Virus Type 1 in US Homosexual Men: Rates, Risk Factors, and Relationship to Kaposi's Sarcoma. J. Infect. Dis. 180, 1010–7.
190 Centers for Disease Control. (**1992**) 1993 Revised Classification System for HIV Infection and Expanded Surveillance Case Definition for AIDS Among Adolescents and Adults. Morb Mortal Wkly Rep 41, 1–19.
191 Beral, V., Peterman, T. A., Berkelman, R. L. and Jaffe, H. W. (**1990**) Kaposi's sarcoma among persons with AIDS: a sexually transmitted infection? Lancet 335, 123–128.
192 Bohlius, J., Valeri, F., Maskew, M., Prozesky, H., Garone, D., Sengayi, M., Fox, M. P., Davies, M.-A. and Egger, M. (**2014**) Kaposi's Sarcoma in HIV-infected patients in South Africa: Multicohort study in the antiretroviral therapy era. Int. J. Cancer 135, 2644–2652.
193 Hiatt, K. M., Nelson, A. M., Lichy, J. H. and Fanburg-Smith, J. C. (**2008**) Classic Kaposi Sarcoma in the United States over the last two decades: a clinicopathologic and molecular study of 438 non-HIV-related Kaposi Sarcoma patients with comparison to HIV-related Kaposi Sarcoma. Mod. Pathol. 21, 572–82.
194 Donato, V., Guarnaccia, R., Dognini, J., Pascalis, G. D. E., Caruso, C., Bellagamba, R. and Morrone, A. (**2013**) Radiation Therapy in the Treatment of HIV-related Kaposi's Sarcoma. Anticancer Res. 33, 2153–2157.
195 Crum, N. F., Riffenburgh, R. H., Wegner, S., Agan, B. K., Tasker, S. a, Spooner, K. M., Armstrong, A. W., Fraser, S. and Wallace, M. R. (**2006**) Comparisons of Causes of Death and Mortality Rates Among HIV-infected persons. Analysis of the pre-, Early, and Late HAART (Highly Active Retroviral Therapy) Eras. J. Acquir. Immune Defic. Syndr. 41, 194–200.
196 Nguyen, H. Q., Magaret, A. S., Kitahata, M. M., Van Rompaey, S. E., Wald, A. and Casper, C. (**2008**) Persistent Kaposi sarcoma in the era of HAART: characterizing the predictors of clinical response. AIDS 22, 937–945.
197 Whitby, D., Howard, M. R., Tenant-Flowers, M., Brink, N. S., Copas, A., Boshoff, C., Hatzioannou, T., Suggett, F. E., Aldam, D. M. and Denton, A. S. (**1995**) Detection of Kaposi sarcoma associated herpesvirus in peripheral blood of HIV-infected individuals and progression to Kaposi's sarcoma. Lancet 346, 799–802.
198 Moore PS, C. Y. (**1995**) Detection of herpesvirus-like DNA sequences in Kaposi's sarcoma in patients with and those without HIV infection. N. Engl. J. Med. 332, 1181–1185.
199 Boshoff, C., Whitby, D., Hatzioannou, T., Fisher, C., van der Walt, J., Hatzakis, A., Weiss, R. and Schulz, T. F. (**1995**) Kaposi's-sarcoma-associated herpesvirus in HIV-negative Kaposi's sarcoma. Lancet 345, 1043–4.
200 Dupin, N., Grandadam, M., Calvez, V., Gorin, I., Aubin, J. T., Harvard, S., Lamy, F., Leibowitch, M., Huraux, J. M., Escande, J. P., et al. (**1995**) Herpesvirus-like DNA sequences in patients with Mediterranean Kaposi's sarcoma. Lancet 345, 761–762.
201 Schalling, M., Eckman, M., Kaaya, E. E., Linde, A. and Biberfeld, P. (**1995**) A role for a new herpes virus (KSHV) in different forms of Kaposi's sarcoma. Nat. Med. 1, 707–708.
202 Collandre, H., Ferris, S., Grau, O., Montagnier, L. and Blanchard, A. (**1995**) Kaposi's sarcoma and new herpesvirus. Lancet 345, 1043.
203 Cathomas, G., Mcgandy, C. E., Terracciano, L. M., Itin, P. H., De Rosa, G. and Gudat, F. (**1996**) Detection of herpesvirus-like DNA by nested PCR on archival skin biopsy specimens of various forms of Kaposi sarcoma. J Clin Pathol 49, 631–633.
204 Ciufo, D., Cannon, J. and Poole, L. (**2001**) Spindle cell conversion by Kaposi's sarcoma-

associated herpesvirus: formation of colonies and plaques with mixed lytic and latent gene expression in infected. J. Virol. 75, 5614–5626.
205 Flore, O., Rafii, S., Ely, S. and O'Leary, J. (**1998**) Transformation of primary human endothelial cells by Kaposi's sarcoma-associated herpesvirus. Nature 394, 588–592.
206 Moses, A. V, Fish, K. N., Ruhl, R., Smith, P. P., Strussenberg, J. G., Zhu, L., Chandran, B. and Nelson, J. a. (**1999**) Long-term infection and transformation of dermal microvascular endothelial cells by human herpesvirus 8. J. Virol. 73, 6892–6902.
207 Wang, L. and Damania, B. (**2008**) Kaposi's sarcoma-associated herpesvirus confers a survival advantage to endothelial cells. Cancer Res. 68, 4640–4648.
208 An, F., Folarin, H. M., Compitello, N., Roth, J., Gerson, S. L., Mccrae, K. R., Fakhari, F. D., Dittmer, D. P. and Renne, R. (**2006**) Long-Term-Infected Telomerase-Immortalized Endothelial Cells: a Model for Kaposi's Sarcoma-Associated Herpesvirus Latency In Vitro and In Vivo. J. Virol. 80, 4833–4846.
209 IARC Working Group on the Evaluation of Carcinogenic Risks to Humans. (**2012**) Biological Agents. Volume 100 B. A Review of Human Carcinogens. IARC Monogr. Eval. Carcinog. risks to humans 100, 169–214.
210 Gramolelli, S. and Schulz, T. F. (**2015**) The role of Kaposi sarcoma-associated herpesvirus in the pathogenesis of Kaposi sarcoma. J. Pathol. 235, 368–380.
211 Lee, S., Abrahamian, F. and Stroger, J. H. (**2012**) Gastrointestinal Kaposi's sarcoma. Am J Gastroenterol 107, 2012.
212 Patel, R. M., Goldblum, J. R. and Hsi, E. D. (**2004**) Immunohistochemical detection of human herpes virus-8 latent nuclear antigen-1 is useful in the diagnosis of Kaposi sarcoma. Mod. Pathol. 17, 456–460.
213 Mosam, A., Shaik, F., Uldrick, T. S., Esterhuizen, T., Friedland, G. H., Scadden, D. T., Aboobaker, J. and Coovadia, H. M. (**2012**) A randomized controlled trial of HAART versus HAART and chemotherapy in therapy-naïve patients with HIV-associated Kaposi sarcoma in South Africa. J Acquir Immune Defic Syndr 60, 150–157.
214 Bower, M., Weir, J., Francis, N., Newsom-Davis, T., Powles, S., Crook, T., Boffito, M., Gazzard, B. and Nelson, M. (**2009**) The effect of HAART in 254 consecutive patients with AIDS-related Kaposi's sarcoma. AIDS 23, 1701–1706.
215 Letang, E., Lewis, J. J., Bower, M., Mosam, A., Borok, M., Campbell, T. B., Naniche, D., Newsom-Davis, T., Shaik, F., Fiorillo, S., et al. (**2013**) Immune reconstitution inflammatory syndrome associated with Kaposi sarcoma: Higher incidence and mortality in Africa than in the UK. AIDS 27, 1603–1613.
216 Simonelli, C., Spina, M., Cinelli, R., Talamini, R., Tedeschi, R., Gloghini, A., Vaccher, E., Carbone, A. and Tirelli, U. (**2003**) Clinical features and outcome of primary effusion lymphoma in HIV-infected patients: A single-institution study. J. Clin. Oncol. 21, 3948–3954.
217 Ota, Y., Hishima, T., Mochizuki, M., Kodama, Y., Moritani, S., Oyaizu, N., Mine, S., Ajisawa, A., Tanuma, J., Uehira, T., et al. (**2014**) Classification of AIDS-related lymphoma cases between 1987 and 2012 in Japan based on the WHO classification of lymphomas, fourth edition. Cancer Med. 3, 143–153.
218 Lurain, K., Polizzotto, M. N., Aleman, K., Bhutani, M., Wyvill, K. M., Gonçalves, P. H., Ramaswami, R., Marshall, V. A., Miley, W., Steinberg, S. M., et al. (**2019**) Viral, immunologic, and clinical features of primary effusion lymphoma. Blood 133, 1–8.
219 Carbone, A., Gloghini, A., Vaccher, E., Zagonel, V., Pastore, C., Palma, P. D., Branz, F., Saglio, G., Volpe, R., Tirelli, U., et al. (**1996**) Kaposi's sarcoma-associated herpesvirus DNA sequences in AIDS-related and AIDS-unrelated lymphomatous effusions. Br. J. Haematol.
220 Banks, P. M. and Warnke, R. A. (**2001**) Primary effusion lymphoma. In World Health Organization Classification of Tumours, Pathology and Genetics of Tumours of Haematopoietic and Lymphoid Tissues (Jaffe, E. S., Harris, N. L., Stein, H., and Vardiman, J. W., eds.), pp 179–180, IARC Press, Lyon.

221 Gaidano, G., Gloghini, A., Gattei, V., Rossi, M. F., Cilia, A. M., Godeas, C., Degan, M., Perin, T., Canzonieri, V., Aldinucci, D., et al. (**1997**) Association of Kaposi's sarcoma-associated herpesvirus-positive primary effusion lymphoma with expression of the CD138/syndecan-1 antigen. Blood 90, 4894–4900.
222 Powles, T., Stebbing, J., Bazeos, A., Hatzimichael, E., Mandalia, S., Nelson, M., Gazzard, B. and Bower, M. (**2009**) The role of immune suppression and HHV-8 in the increasing incidence of HIV-associated multicentric Castleman's disease. Ann. Oncol. 20, 775–779.
223 Engels, E. A., Mbulaiteye, S. M., Othieno, E., Gomez, M., Mathew, S., Cesarman, E., Knowles, D. M. and Chadburn, A. (**2007**) Kaposi sarcoma-associated herpesvirus in non-Hodgkin lymphoma and reactive lymphadenopathy in Uganda. Hum. Pathol. 38, 308–314.
224 Lazzi, S., Bellan, C., Amato, T., Palummo, N., Cardone, C., D'Amuri, A., De Luca, F., Beyanga, M., Facchetti, F., Tosi, P., et al. (**2006**) Kaposi's sarcoma-associated herpesvirus/human herpesvirus 8 infection in reactive lymphoid tissues: A model for KSHV/HHV-8-related lymphomas? Hum. Pathol. 37, 23–31.
225 Chinula, L., Moses, A. and Gopal, S. (**2017**) HIV-associated malignancies in sub-Saharan Africa: progress, challenges, opportunities. Curr Opin HIV AIDS 12, 89–95.
226 Uldrick, T. S., Polizzotto, M. N., Aleman, K., O'Mahony, D., Wyvill, K. M., Wang, V., Marshall, V., Pittaluga, S., Steinberg, S. M., Tosato, G., et al. (**2011**) High-dose zidovudine plus valganciclovir for Kaposi sarcoma herpesvirus-associated multicentric Castleman disease: A pilot study of virus-activated cytotoxic therapy. Blood 117, 6977–6986.
227 Uldrick, T. S., Polizzotto, M. N., Aleman, K., Wyvill, K. M., Marshall, V., Whitby, D., Wang, V., Pittaluga, S., O'Mahony, D., Steinberg, S. M., et al. (**2014**) Rituximab plus liposomal doxorubicin in HIV-infected patients with KSHV-associated multicentric Castleman disease. Blood 124, 3544–3552.
228 Yamasaki, S., Iino, T., Nakamura, M., Henzan, H., Ohshima, K., Kikuchi, M., Otsuka, T. and Harada, M. (**2003**) Detection of human herpesvirus-8 in peripheral blood mononuclear cells from adult Japanese patients with multicentric Castleman's disease. Br. J. Haematol. 120, 471–477.
229 Suda, T., Katano, H., Delsol, G., Kakiuchi, C., Nakamura, T., Shiota, M., Sata, T., Higashihara, M. and Mori, S. (**2001**) HHV-8 infection status of AIDS-unrelated and AIDS-associated multicentric Castleman ' s disease 8, 671–679.
230 Kikuta, H., Itakura, O., Taneichi, K. and Kohno, M. (**1997**) Tropism of human herpesvirus 8 for peripheral blood lymphocytes in patients with Castleman's disease. Br. J. Haematol. 99, 790–793.
231 Oksenhendler, E., Duarte, M., Soulier, J., Cacoub, P., Welker, Y., Cadranel, J., Cazals-Hatem, D., Autran, B., Clauvel, J. and Raphael, M. (**1996**) Multicentric Castleman's disease in HIV infection: a clinical and pathological study of 20 patients. AIDS 10, 61–67.
232 Oksenhendler, E., Boutboul, D., Beldjord, K., Meignin, V., de Labarthe, A., Fieschi, C., Dossier, A., Agbalika, F., Parravicini, C., Tosato, G., et al. (**2013**) Human herpesvirus 8+ polyclonal IgMλ B-cell lymphocytosis mimicking plasmablastic leukemia/lymphoma in HIV-infected patients. Eur. J. Haematol. 91, 497–503.
233 Marcelin, A., Aaron, L., Mateus, C., Gyan, E., Gorin, I., Viard, J.-P., Calvez, V. and Dupin, N. (**2003**) Rituximab therapy for HIV-associated Castleman disease. Blood 102, 2786–2788.
234 Gérard, L., Bérezné, A., Galicier, L., Meignin, V., Obadia, M., De Castro, N., Jacomet, C., Verdon, R., Madelaine-Chambrin, I., Boulanger, E., et al. (**2007**) Prospective study of rituximab in chemotherapy-dependent human immunodeficiency virus-associated multicentric Castleman's disease: ANRS 117 CastlemaB trial. J. Clin. Oncol. 25, 3350–3356.
235 Pantanowitz, L., Früh, K., Marconi, S., Moses, A. V. and Dezube, B. J. (**2008**) Pathology of rituximab-induced Kaposi sarcoma flare. BMC Clin. Pathol. 8, 1–5.
236 Gopal, S., Wood, W. A., Lee, S. J., Shea, T. C., Naresh, K. N., Kazembe, P. N., Casper, C., Hesseling, P. B. and Mitsuyasu, R. T. (**2012**) Meeting the challenge of hematologic malignancies in sub-

Saharan Africa. Blood 119, 5078–5087.
237 Ray, A., Marshall, V., Uldrick, T., Leighty, R., Labo, N., Wyvill, K., Aleman, K., Polixxotto, M. N., Little, R. F., Yarchoan, R., et al. (**2012**) Sequence Analysis of KSHV microRNAs in patients with Multicentric Castleman Disease and KSHV-associated Inflammatory Cytokine Syndrome. J. Infect. Dis. 1–19.
238 Clark-Coller, M. P., Kuhn, B. T., Rashidi, H. H. and Avdalovic, M. V. (**2019**) Kaposi's Sarcoma-Associated Herpesvirus Inflammatory Cytokine Syndrome - Diagnostic and Management Dilemmas in the Critically Ill Patient with KICS. Am. J. Respir. Crit. Care Med., p A4591.
239 Martin, D. F., Kuppermann, B. D., Wolitz, R. A., Palestine, A. G., Li, H., Robinson, C. A. and The Roche Ganciclovir Study Group. (**1999**) Oral Ganciclovir for Patients with Cytomegalovirus Retinitis Treated with a Ganciclovir Implant. N. Engl. J. Med. 1063–1070.
240 Mazzi, R., Parisi, S. G., Sarmati, L., Uccella, I., Nicastri, E., Carolo, G., Gatti, F., Concia, E. and Andreoni, M. (**2001**) Efficacy of cidofovir on human herpesvirus 8 viraemia and Kaposi's sarcoma progression in two patients with AIDS [1]. AIDS 15, 2061–2062.
241 Löw, P., Neipel, F., Rascu, A., Steininger, H., Manger, B., Fleckenstein, B., Kalden, J. R. and Harrer, T. (**1998**) Suppression of HHV-8 viremia by foscarnet in an HIV-infected patient with Kaposi's sarcoma and HHV-8 associated hemophagocytic syndrome. Eur. J. Med. Res. 3, 461–464.
242 Luppi, M., Barozzi, P., Rasini, V., Riva, G., Re, A., Rossi, G., Setti, G., Sandrini, S., Facchetti, F. and Torelli, G. (**2002**) Severe pancytopenia and hemophagocytosis after HHV-8 primary infection in a renal transplant patient successfully treated with foscarnet. Transplantation 74, 131–133.
243 Casper, C., Nichols, W. G., Huang, M. L., Corey, L. and Wald, A. (**2004**) Remission of HHV-8 and HIV-associated multicentric Castleman disease with ganciclovir treatment. Blood 103, 1632–1634.
244 Marcelin, A., Motol, J., Guihot, A., Caumes, E., Viard, J., Dussaix, E., Cadranel, J., Francès, C., Carcelain, G., Calvez, V., et al. (**2007**) Relationship between the Quantity of Kaposi Sarcoma–Associated Herpesvirus (KSHV) in Peripheral Blood and Effusion Fluid Samples and KSHV-Associated Disease. J. Infect. Dis. 196, 1163–1166.
245 Laney, A. S., Cannon, M. J., Jaffe, H. W., Offermann, M. K., Ou, C. Y., Radford, K. W., Patel, M. M., Spira, T. J., Gunthel, C. J., Pellett, P. E., et al. (**2007**) Human herpesvirus 8 presence and viral load are associated with the progression of AIDS-associated Kaposi's sarcoma. AIDS 21, 1541–1545.
246 Broccolo, F., Din, C. T., Viganò, M. G., Rutigliano, T., Esposito, S., Lusso, P., Tambussi, G. and Malnati, M. S. (**2016**) HHV-8 DNA replication correlates with the clinical status in AIDS-related Kaposi's sarcoma. J. Clin. Virol., Elsevier B.V. 78, 47–52.
247 Tedeschi, R., Enbom, M., Bidoli, E., Linde, A., De Paoli, P. and Dillner, J. (**2001**) Viral load of human herpesvirus 8 in peripheral blood of human immunodeficiency virus-infected patients with Kaposi's sarcoma. J. Clin. Microbiol. 39, 4269–4273.
248 Guttman-Yassky, E., Cohen, A., Kra-Oz, Z., Friedman-Birnbaum, R., Sprecher, E., Zaltzman, N., Friedman, E., Silbermann, M., Rubin, D., Linn, S., et al. (**2004**) Familial clustering of classic Kaposi sarcoma. J. Infect. Dis. 189, 2023–2026.
249 Pedergnana, V., Gessain, A., Tortevoye, P., Byun, M., Bacq-daian, D., Boland, A., Casanova, J., Abel, L. and Plancoulaine, S. (**2012**) A major locus on chromosome 3p22 conferring predisposition to human herpesvirus 8 infection. Eur. J. Hum. Genet. 20, 690–695.
250 Gazouli, M., Zavos, G., Papaconstantinou, I., Lukas, J. C., Zografidis, A., Boletis, J. and Kostakis, A. (**2004**) The Interleukin-6-174 Promoter Polymorphism is Associated with a Risk of Development of Kaposi's Sarcoma in Renal Transplant Recipients. Anticancer Res. 24, 1311–1314.
251 van der Kuyl, A. C., Polstra, A. M., Jan Weverling, G., Zorgdrager, F., van der Burg, R. and Cornelissen, M. (**2004**) An IL-8 gene promoter polymorphism is associated with the risk of the development of AIDS-related Kaposi's sarcoma: a case–control study. AIDS 18, 1203–1216.

252 Brown, E. E., Fallin, D., Ruczinski, I., Hutchinson, A., Staats, B., Vitale, F., Lauria, C., Serraino, D., Rezza, G., Mbisa, G., et al. (**2006**) Associations of classic Kaposi sarcoma with common variants in genes that modulate host immunity. Cancer Epidemiol. Biomarkers Prev. 15, 926–934.
253 Alkharsah, K. R., Alzahrani, A. J. and Obeid, O. E. (**2014**) Vascular endothelial growth factor A polymorphism and risk of Kaposi's sarcoma herpesvirus viremia in kidney allograft recipients. Transpl. Infect. Dis. 16, 783–789.
254 Gonçales, J. P., Silva Júnior, J. V. J., Lopes, T. R. R., Tozetto-Mendoza, T. R., de Farias Guimarães, D., de Morais, V. M. S. and Coêlho, M. R. C. D. (**2019**) Association of polymorphisms in NFκB1 promoter and NFκBIA gene with the development of antibodies against HHV-8 in HIV-infected individuals. Virology, Elsevier Inc. 535, 255–260.
255 De Morais, V. M. S., De Lima, E. L. S., Cahú, G. G. D. O. M., Lopes, T. R. R., Gonçales, J. P., Muniz, M. T. C. and Coêlho, M. R. C. D. (**2018**) MBL2 gene polymorphisms in HHV-8 infection in people living with HIV/AIDS. Retrovirology 15, 1–9.
256 Guerini, F. R., Mancuso, R., Agostini, S., Agliardi, C., Zanzottera, M., Hernis, A., Tourlaki, A., Calvo, M. G., Bellinvia, M., Brambilla, L., et al. (**2012**) Activating KIR/HLA complexes in classic Kaposi's Sarcoma. Infect Agent Cancer 7, 1–5.
257 Goedert, J. J., Martin, M. P., Vitale, F., Lauria, C., Whitby, D., Qi, Y., Gao, X. and Carrington, M. (**2016**) Risk of classic kaposi sarcoma with combinations of killer immunoglobulin-like receptor and human leukocyte antigen loci: A population-based case-control study. J. Infect. Dis. 213, 432–438.
258 Cornejo Castro, E. M., Morrison, B. J., Marshall, V. A., Labo, N., Miley, W. J., Clements, N., Nelson, G., Ndom, P., Stolka, K., Hemingway-Foday, J. J., et al. (**2019**) Relationship between human leukocyte antigen alleles and risk of Kaposi's sarcoma in Cameroon. Genes Immun. 20, 684–689.
259 Dorak, M. T., Yee, L. J., Tang, J., Shao, W., Lobashevsky, E. S., Jacobson, L. P. and Kaslow, R. A. (**2005**) HLA-B, -DRB1/3/4/5, and -DQB1 gene polymorphisms in human immunodeficiency virus-related Kaposi's sarcoma. J. Med. Virol. 76, 302–310.
260 Azmandian, J., Lessan-Pezeshki, M., Alipour Abedi, B., Mahdavi-Mazdeh, M., Nafar, M. and Farhangi, S. (**2007**) Posttransplant malignancies and their relationship with human leukocyte antigens in kidney allograft recipients. Iran. J. Kidney Dis. 1, 98–101.
261 Masala, M. V., Carcassi, C., Cottoni, F., Mulargia, M., Contu, L. and Cerimele, D. (**2005**) Classic Kaposi's sarcoma in Sardinia: HLA positive and negative associations. Int. J. Dermatol. 44, 743–745.
262 Gaya, A., Esteve, A., Casabona, J., McCarthy, J., Martorell, J., Schulz, T. and Whitby, D. (**2004**) Amino acid residue at position 13 in HLA-DR beta chain plays a critical role in the development of Kaposi's sarcoma in AIDS patients. AIDS 18, 199–204.
263 Aissani, B., Wiener, H. W., Zhang, K., Kaslow, R. a., Ogwaro, K. M., Shrestha, S. and Jacobson, L. P. (**2014**) A candidate gene approach for virally induced cancer with application to HIV-related Kaposi's sarcoma. Int. J. Cancer 134, 397–404.
264 Miles, S. A., Rezai, A. R., Salazar-González, J. F., Vander Meyden, M., Stevens, R. H., Logan, D. M., Mitsuyasu, R. T., Taga, T., Hirano, T. and Kishimoto, T. (**1990**) AIDS Kaposi sarcoma-derived cells produce and respond to interleukin 6. Proc. Natl. Acad. Sci. USA 87, 4068–72.
265 Koene, H. R., Kleijer, M., Algra, J., Roos, D., von dem Borne, A. E. G. K. and de Haas, M. (**1997**) FcgRIIIa-158V/F Polymorphism Influences the Binding of IgG by Natural Killer Cell FcgRIIIa, Independently of the FcgRIIIa-48L/R/H Phenotype. Blood 90, 1109–1114.
266 Matthews, N. C., Goodier, M. R., Robey, R. C., Bower, M. and Gotch, F. M. (**2011**) Killing of Kaposi's sarcoma-associated herpesvirus-infected fibroblasts during latent infection by activated natural killer cells. Eur. J. Immunol. 41, 1958–1968.
267 Wykosky, J. and Debinski, W. (**2008**) The EphA2 receptor and ephrinA1 ligand in solid tumors: function and therapeutic targeting. Mol. Cancer Res. 6, 1795–1806.
268 Zhou, R. (**1998**) The Eph family receptors and ligands. Pharmacol. Ther. 77, 151–181.

269 Hafner, C., Schmitz, G., Meyer, S., Bataille, F., Hau, P., Langmann, T., Dietmaier, W., Landthaler, M. and Vogt, T. (**2004**) Differential Gene Expression of Eph Receptors and Ephrins in Benign Human Tissues and Cancers. Clin. Chem. 50, 490–499.
270 Davis, B. C. B., Dikic, I., Unutmaz, D., Hill, C. M., Arthos, J., Siani, M. A., Thompson, D. A., Schlessinger, J. and Littman, D. R. (**1997**) Signal transduction due to HIV-1 envelope interactions wih Chemokine Receptors CXCR4 or CCR5. J. Exp. Med. 186, 1793–1798.
271 Holland, S. J., Gale, N. W., Mbamalu, G., Yancopoulos, G. D., Henkemeyer, M. and Pawson, T. (**1996**) Bidirectional signalling through the EPH-family receptor Nuk and its transmembrane ligands. Nature 383.
272 Bruckner, K., Pasquale, E. B. and Klein, R. (**1997**) Tyrosine Phosphorylation of Transmembrane Ligands for Eph Receptors. Science 275, 1640–1644.
273 Pasquale, E. B. (**2005**) Eph receptor signalling casts a wide net on cell behaviour. Nat. Rev. Mol. Cell Biol. 6, 462–475.
274 Barquilla, A. and Pasquale, E. B. (**2015**) Eph Receptors and Ephrins: Therapeutic Opportunities. Annu. Rev. Pharmacol. Toxicol. 55, 465–487.
275 Pasquale, E. B. (**2008**) Eph-Ephrin Bidirectional Signaling in Physiology and Disease. Cell 133, 38–52.
276 Lindberg, R. A. and Hunter, T. (**1990**) cDNA cloning and characterization of eck, an epithelial cell receptor protein-tyrosine kinase in the eph/elk family of protein kinases. Mol. Cell. Biol. 10, 6316–6324.
277 Gale, N. W., Holland, S. J., Valenzuela, D. M., Flenniken, A., Pan, L., Ryan, T. E., Henkemeyer, M., Strebhardt, K., Hirai, H., Wilkinson, D. G., et al. (**1996**) Eph Receptors and Ligands Comprise Two Major Specificity Subclasses and Are Reciprocally Compartmentalized during Embryogenesis. Neuron 17, 9–19.
278 Himanen, J. and Nikolov, D. B. (**2003**) Eph signaling: a structural view. TRENDS Neurosci. 26, 46–51.
279 Shiels, A., Bennett, T. M., Knopf, H. L. S., Maraini, G., Li, A., Jiao, X. and Hejtmancik, J. F. (**2008**) The EPHA2 gene is associated with cataracts linked to chromosome 1p. Mol. Vis. 14, 2042–2055.
280 Schmucker, D. and Zipursky, S. L. (**2001**) Signaling downstream of Eph receptors and ephrin ligands. Cell 105, 701–704.
281 Miao, H., Burnett, E., Kinch, M., Simon, E. and Wang, B. (**2000**) Activation of EphA2 kinase suppresses integrin function and causes focal-adhesion-kinase dephosphorylation. Nat. Cell Biol. 2, 62–69.
282 Fang, W. Bin, Brantley-Sieders, D. M., Hwang, Y., Ham, A.-J. L. and Chen, J. (**2008**) Identification and Functional Analysis of Phosphorylated Tyrosine Residues within EphA2 Receptor Tyrosine Kinase. J. Biol. Chem. 283, 16017–16026.
283 Locard-Paulet, M., Lim, L., Veluscek, G., McMahon, K., Sinclair, J., van Weverwijk, A., Worboys, J. D., Yuan, Y., Isacke, C. M. and Jørgensen, C. (**2016**) Phosphoproteomic analysis of interacting tumor and endothelial cells identifies regulatory mechanisms of transendothelial migration. Sci. Signal. 9, 1–35.
284 Singh, D. R., Pasquale, E. B. and Hristova, K. (**2016**) A small peptide promotes EphA2 kinase-dependent signaling by stabilizing EphA2 dimers. Biochim. Biophys. Acta, Elsevier B.V. 1860, 1922–1928.
285 Zhou, Y. and Sakurai, H. (**2017**) Emerging and diverse functions of the EphA2 noncanonical pathway in cancer progression. Biol. Pharm. Bull. 40, 1616–1624.
286 Faoro, L., Singleton, P. A., Cervantes, G. M., Lennon, F. E., Choong, N. W., Kanteti, R., Ferguson, B. D., Husain, A. N., Tretiakova, M. S., Ramnath, N., et al. (**2010**) EphA2 mutation in lung squamous cell carcinoma promotes increased cell survival, cell invasion, focal adhesions, and mammalian target of rapamycin activation. J. Biol. Chem. 285, 18575–18585.
287 Schultz, J., Ponting, C. P., Hofmann, K. and Bork, P. (**1997**) SAM as a protein interaction domain

involved in developmental regulation. Protein Sci. 6, 249–53.
288 Smalla, M., Schmieder, P., Kelly, M., Ter Laak, A., Krause, G., Ball, L., Wahl, M., Bork, P. and Oschkinat, H. (**1999**) Solution structure of the receptor tyrosine kinase EphB2 SAM domain and identification of two distinct homotypic interaction sites. Protein Sci. 8, 1954–1961.
289 Shi, X., Hapiak, V., Zheng, J., Muller-Greven, J., Bowman, D., Lingerak, R., Buck, M., Wang, B. C. and Smith, A. W. (**2017**) A role of the SAM domain in EphA2 receptor activation. Sci. Rep., Nature Publishing Group 7, 1–12.
290 Brantley-Sieders, D. M., Caughron, J., Hicks, D., Pozzi, A., Ruiz, J. C. and Chen, J. (**2004**) EphA2 receptor tyrosine kinase regulates endothelial cell migration and vascular assembly through phosphoinositide 3-kinase-mediated Rac1 GTPase activation. J. Cell Sci. 117, 2037–2049.
291 Shao, H., Pandey, A., O'Shea, K. S., Seldin, M. and Dixit, V. M. (**1995**) Characterization of B61, the Ligand for the Eck Receptor Protein-Tyrosine Kinase. J. Biol. Chem. 270, 5636–5641.
292 Son, A. I., Cooper, M. A., Sheleg, M., Sun, Y., Kleiman, N. J. and Zhou, R. (**2013**) Further analysis of the lens of ephrin-A5-/- mice: development of postnatal defects. Mol. Vis. 19, 254–66.
293 Shi, Y., de Maria, A., Bennett, T., Shiels, A. and Bassnett, S. (**2012**) A role for Epha2 in cell migration and refractive organization of the ocular lens. Investig. Ophthalmol. Vis. Sci. 53, 551–559.
294 Jun, G., Guo, H., Klein, B. E. K., Klein, R., Jie, J. W., Mitchell, P., Miao, H., Lee, K. E., Joshi, T., Buck, M., et al. (**2009**) EPHA2 is associated with age-related cortical cataract in mice and humans. PLoS Genet. 5, 1–19.
295 Sundaresan, P., Ravindran, R. D., Vashist, P., Shanker, A., Nitsch, D., Talwar, B., Maraini, G., Camparini, M., Nonyane, B. A. S., Smeeth, L., et al. (**2012**) EPHA2 polymorphisms and age-related cataract in India. PLoS One 7, e33001.
296 Tan, W., Hou, S., Jiang, Z., Hu, Z., Yang, P. and Ye, J. (**2011**) Association of EPHA2 polymorphisms and age-related cortical cataract in a Han Chinese population. Mol. Vis. 17, 1553–8.
297 Kaul, H., Riazuddin, S. A., Shahid, M., Kousar, S., Butt, N. H., Zafar, A. U., Khan, S. N., Husnain, T., Akram, J., Hejtmancik, J. F., et al. (**2010**) Autosomal recessive congenital cataract linked to EPHA2 in a consanguineous Pakistani family. Mol. Vis. 16, 511–517.
298 Zhang, T., Hua, R., Xiao, W., Burdon, K. P., Bhattacharya, S. S., Craig, J. E., Shang, D., Zhao, X., Mackey, D. A., Moore, A. T., et al. (**2009**) Mutations of the EPHA2 receptor tyrosine kinase gene cause autosomal dominant congenital cataract. Hum. Mutat. 30, 603–610.
299 Saeger, B. M., Suhm, M. and Neubüser, A. (**2011**) Ephrin/ephrin receptor expression during early stages of mouse inner ear development. Dev. Dyn. 240, 1578–1585.
300 Vaught, D., Chen, J. and Brantley-Sieders, D. M. (**2009**) Regulation of Mammary Gland Branching Morphogenesis by EphA2 Receptor Tyrosine Kinase. Mol. Biol. Cell 20, 2572–2581.
301 Miao, H., Nickel, C. H., Cantley, L. G., Bruggeman, L. A., Bennardo, L. N. and Wang, B. (**2003**) EphA kinase activation regulates HGF-induced epithelial branching morphogenesis. J. Cell Biol. 162, 1281–1292.
302 Sharfe, N., Nikolic, M., Cimpeon, L., Van De Kratts, A., Freywald, A. and Roifman, C. M. (**2008**) EphA and ephrin-A proteins regulate integrin-mediated T lymphocyte interactions. Mol. Immunol. 45, 1208–1220.
303 Park, J. E., Son, A. I. and Zhou, R. (**2013**) Roles of EphA2 in development and disease. Genes 4, 334–357.
304 Baldwin, C., Chen, Z. W., Bedirian, A., Yokota, N., Nasr, S. H., Rabb, H. and Lemay, S. (**2006**) Upregulation of EphA2 during in vivo and in vitro renal ischemia-reperfusion injury: role of Src kinases. Am. J. Physiol. Renal Physiol. 291, F960-71.
305 Zhang, G., Njauw, C. N., Jong, M. P., Naruse, C., Asano, M. and Tsao, H. (**2008**) EphA2 is an essential mediator of UV radiation-induced apoptosis. Cancer Res. 68, 1691–1696.
306 Irie, N., Takada, Y., Watanabe, Y., Matsuzaki, Y., Naruse, C., Asano, M., Iwakura, Y., Suda, T. and Matsuo, K. (**2009**) Bidirectional signaling through EphrinA2-EphA2 enhances osteoclastogenesis and suppresses osteoblastogenesis. J. Biol. Chem. 284, 14637–14644.

307 Zelinski, D. P., Zantek, N. D., Stewart, J. C., Irizarry, A. R. and Kinch, M. S. (**2001**) EphA2 Overexpression Causes Tumorigenesis of Mammary Epithelial Cells 1. Cancer Res. 61, 2301–2306.
308 Walker-Daniels, J., Coffman, K., Azimi, M., Rhim, J. S., Bostwick, D. G., Snyder, P., Kerns, B. J., Waters, D. J. and Kinch, M. S. (**1999**) Overexpression of the EphA2 tyrosine kinase in prostate cancer. Prostate 41, 275–280.
309 Hess, A. R., Seftor, E. A., Gardner, L. M. G., Carles-Kinch, K., Schneider, G. B., Seftor, R. E. B., Kinch, M. S. and Hendrix, M. J. C. (**2001**) Molecular regulation of tumor cell vasculogenic mimicry by tyrosine phosphorylation: Role of epithelial cell kinase (Eck/EphA2). Cancer Res. 61, 3250–3255.
310 Tan, Y. H. C., Srivastava, S., Won, B. M., Kanteti, R., Arif, Q., Husain, A. N., Li, H., Vigneswaran, W. T., Pang, K. M., Kulkarni, P., et al. (**2019**) EPHA2 mutations with oncogenic characteristics in squamous cell lung cancer and malignant pleural mesothelioma. Oncogenesis, Springer US 8.
311 Miao, H., Li, D. Q., Mukherjee, A., Guo, H., Petty, A., Cutter, J., Basilion, J. P., Sedor, J., Wu, J., Danielpour, D., et al. (**2009**) EphA2 Mediates Ligand-Dependent Inhibition and Ligand-Independent Promotion of Cell Migration and Invasion via a Reciprocal Regulatory Loop with Akt. Cancer Cell, Elsevier Ltd 16, 9–20.
312 Nasreen, N., Mohammed, K. A., Lai, Y. and Antony, V. B. (**2007**) Receptor EphA2 activation with ephrinA1 suppresses growth of malignant mesothelioma (MM). Cancer Lett. 258, 215–222.
313 Chiarugi, P., Taddei, M. L., Schiavone, N., Papucci, L., Giannoni, E., Fiaschi, T., Capaccioli, S., Raugei, G. and Ramponi, G. (**2004**) LMW-PTP is a positive regulator of tumor onset and growth. Oncogene 23, 3905–3914.
314 Zantek, N. D., Azimi, M., Fedor-Chaiken, M., Wang, B., Brackenbury, R. and Kinch, M. S. (**1999**) E-cadherin regulates the function of the EphA2 receptor tyrosine kinase. Cell Growth Differ. 10, 629–638.
315 Kikawa, K. D., Vidale, D. R., Van Etten, R. L. and Kinch, M. S. (**2002**) Regulation of the EphA2 kinase by the low molecular weight tyrosine phosphatase induces transformation. J. Biol. Chem. 277, 39274–39279.
316 Zhou, Y., Yamada, N., Tanaka, T., Hori, T., Yokoyama, S., Hayakawa, Y., Yano, S., Fukuoka, J., Koizumi, K., Saiki, I., et al. (**2015**) Crucial roles of RSK in cell motility by catalysing serine phosphorylation of EphA2. Nat. Commun., Nature Publishing Group 6, 1–12.
317 Barquilla, A., Lamberto, I., Noberini, R., Heynen-genel, S. and Lidke, D. (**2016**) Protein kinase A can block EphA2 receptor – mediated cell repulsion by increasing EphA2 S897 phosphorylation. Mol. Biol. Cell 27, 2757–2770.
318 Singh, D. R., Ahmed, F., King, C., Gupta, N., Salotto, M., Pasquale, E. B. and Hristova, K. (**2015**) EphA2 Receptor Unliganded Dimers Suppress EphA2 Pro-tumorigenic Signalling. J. o Biol. Chem. 290, 27271–27279.
319 Hafner, C., Becker, B., Landthaler, M. and Vogt, T. (**2006**) Expression profile of Eph receptors and ephrin ligands in human skin and downregulation of EphA1 in nonmelanoma skin cancer 1369–1377.
320 Herath, N. I., Doecke, J., Leggett, B. A. and Boyd, A. W. (**2009**) Epigenetic silencing of EphA1 expression in colorectal cancer is correlated with poor survival 1095–1102.
321 Hahn, A. S. and Desrosiers, R. C. (**2014**) Binding of the Kaposi's Sarcoma-Associated Herpesvirus to the Ephrin Binding Surface of the EphA2 Receptor and Its Inhibition by a Small Molecule. J. Virol. 88, 8724–8734.
322 Lupberger, J., Zeisel, M. B., Xiao, F., Thumann, C., Fofana, I., Zona, L., Davis, C., Mee, C. J., Turek, M., Gorke, S., et al. (**2011**) EGFR and EphA2 are host factors for hepatitis C virus entry and possible targets for antiviral therapy. Nat. Med. 17, 589–594.
323 Keppler, S., Weißbach, S., Langer, C., Knop, S., Pischimarov, J., Kull, M., Stühmer, T., Steinbrunn, T., Bargou, R., Einsele, H., et al. (**2016**) Rare SNPs in receptor tyrosine kinases are negative outcome predictors in multiple myeloma. Oncotarget 7, 38762–38774.

324 Mbisa, G. L., Miley, W., Gamache, C. J., Gillette, W. K., Esposito, D., Hopkins, R., Busch, M. P., Schreiber, G. B., Little, R. F., Yarchoan, R., et al. (**2010**) Detection of antibodies to Kaposi's sarcoma-associated herpesvirus: A new approach using K8.1 ELISA and a newly developed recombinant LANA ELISA. J. Immunol. Methods, Elsevier B.V. 356, 39–46.
325 De Sanjosé, S., Marshall, V., Solà, J., Palacio, V., Almirall, R., Goedert, J. J., Bosch, F. X. and Whitby, D. (**2002**) Prevalence of Kaposi's sarcoma-associated herpesvirus infection in sex workers and women from the general population in Spain. Int. J. Cancer 98, 155–158.
326 Yuan, C. C., Miley, W. and Waters, D. (**2001**) A quantification of human cells using an ERV-3 real time.pdf. J. Virol. Methods 91 91, 109–117.
327 Box, A. G. E. P. and Tidwell, P. W. (**1962**) Transformation of the Independent Variables. Technometrics 4, 531–550.
328 Rice, P., Longden, I. and Bleasby, A. (**2000**) EMBOSS: The European Molecular Biology Open Software Suite. Trends Genet. 16, 276–277.
329 Larkin, M. A., Blackshields, G., Brown, N. P., Chenna, R., Mcgettigan, P. A., McWilliam, H., Valentin, F., Wallace, I. M., Wilm, A., Lopez, R., et al. (**2007**) Clustal W and Clustal X version 2.0. Bioinformatics 23, 2947–2948.
330 Adzhubei, I. A., Schmidt, S., Peshkin, L., Ramensky, V. E., Gerasimova, A., Bork, P., Kondrashov, A. S. and Sunyaev, S. R. (**2010**) A method and server for predicting damaging missense mutations. Nat. Methods, Nature Publishing Group 7, 248–249.
331 Sherry, S., Ward, M., Kholodov, M., Baker, J., Phan, L., Smigielski, E. and Sirotkin, K. (**2001**) dbSNP: the NCBI database of genetic variation. Nucleic Acids Res. Nucleic Acids Res. 29, 308–11.
332 Mackelprang, R. D., Bamshad, M. J., Chong, J. X., Hou, X., Buckingham, K. J., Shively, K., DeBruyn, G., Mugo, N. R., Mullins, J. I., McElrath, M. J., et al. (**2017**) Whole genome sequencing of extreme phenotypes identifies variants in CD101 and UBE2V1 associated with increased risk of sexually acquired HIV-1o Title. PLoS Pathog. 13, e1006703.
333 Morris, A. P. A. and Zeggini, E. (**2010**) An evaluation of statistical approaches to rare variant analysis in genetic association studies. Genet. Epidemiol. 34, 188–93.
334 Clarke, G. M., Anderson, C. a, Pettersson, F. H., Cardon, L. R., Morris, A. P. and Zondervan, K. T. (**2011**) Basic statistical analysis in genetic case-control studies. Nat. Protoc. 6, 121–133.
335 Kati, S., Hage, E., Mynarek, M., Ganzenmueller, T., Indenbirken, D., Grundhoff, A. and Schulz, T. F. (**2015**) Generation of high-titre virus stocks using BrK.219 ,a B-cell line infected stably with recombinant Kaposi's sarcoma-associated herpesvirus. J. Virol. Methods 217, 79–86.
336 Vieira, J. and O'Hearn, P. M. (**2004**) Use of the red fluorescent protein as a marker of Kaposi's sarcoma-associated herpesvirus lytic gene expression. Virology 325, 225–240.
337 May, T., Butueva, M., Bantner, S., Markusic, D., Seppen, J., MacLeod, R. A. F., Weich, H., Hauser, H. and Wirth, D. (**2010**) Synthetic gene regulation circuits for control of cell expansion. Tissue Eng. - Part A 16, 441–452.
338 Montague, T. G., Cruz, J. M., Gagnon, J. A., Church, G. M. and Valen, E. (**2014**) CHOPCHOP: A CRISPR/Cas9 and TALEN web tool for genome editing. Nucleic Acids Res. 42, 401–407.
339 Labun, K., Montague, T. G., Gagnon, J. A., Thyme, S. B. and Valen, E. (**2016**) CHOPCHOP v2: a web tool for the next generation of CRISPR genome engineering. Nucleic Acids Res. 44, W272–W276.
340 Shalem, O., Sanjana, N. E., Hartenian, E., Shi, X., Scott, D. A., Heckl, D., Ebert, B. L., Root, D. E. and Doench, J. G. (**2014**) Genome-Scale CRISPR-Cas9 Knockout Screening in Human Cells. Science 343, 84–87.
341 Sanjana, N. E., Shalem, O. and Zhang, F. (**2015**) Improved vectors and genome-wide libraries for CRISPR screening. Nat. Methods 11, 783–784.
342 Gramolelli, S., Weidner-Glunde, M., Abere, B., Viejo-Borbolla, A., Bala, K., Rückert, J., Kremmer, E. and Schulz, T. F. (**2015**) Inhibiting the Recruitment of PLCγ1 to Kaposi's Sarcoma Herpesvirus K15 Protein Reduces the Invasiveness and Angiogenesis of Infected Endothelial Cells. PLoS

Pathog. 11, 1–28.
343 Dallas, P. B., Yaciuk, P. and Moran, E. (**1997**) Characterization of monoclonal antibodies raised against p300: Both p300 and CBP are present in intracellular TBP complexes. J. Virol. 71, 1726–1731.
344 Guadalupe, M., Flahive, Y., Westbrook, S., Redding, S., Bullock, D., Sankar, V., Agan, B., Barbieri, S., Yeh, C., Dang, H., et al. (**2009**) KSHV seroprevalence, and blood and saliva viral loads in the HIV-infected population of south Texas. Infect. Agent. Cancer 4, 95.
345 Brown, E. E., Whitby, D., Vitale, F., Fei, P. C., Del Carpio, C., Marshall, V., Alberg, A. J., Serraino, D., Messina, A., Gafa, L., et al. (**2005**) Correlates of Human Herpesvirus-8 DNA detection among adults in Italy without Kaposi sarcoma. Int. J. Epidemiol. 34, 1110–1117.
346 Borges, Á. H., Connor, J. L. O., Phillips, A. N., Rönsholt, F. F., Pett, S. and Vjecha, M. J. (**2015**) Factors Associated With Plasma IL-6 Levels During HIV Infection. J. Infect. Dis. 212, 585–595.
347 Taddei, M. L., Parri, M., Angelucci, A., Onnis, B., Bianchini, F., Giannoni, E., Raugei, G., Calorini, L., Rucci, N., Teti, A., et al. (**2009**) Kinase-dependent and -independent roles of EphA2 in the regulation of prostate cancer invasion and metastasis. Am. J. Pathol. 174, 1492–1503.
348 Abere, B., Mamo, T. M., Hartmann, S., Samarina, N., Hage, E., Rückert, J., Hotop, S. K., Büsche, G. and Schulz, T. F. (**2017**) The Kaposi's sarcoma-associated herpesvirus (KSHV) non-structural membrane protein K15 is required for viral lytic replication and may represent a therapeutic target. PLoS Pathog.
349 Weidner-Glunde, M., Mariggiò, G. and Schulz, T. F. (**2017**) Kaposi's Sarcoma-Associated Herpesvirus Latency-Associated Nuclear Antigen: Replicating and Shielding Viral DNA during Viral Persistence. J. Virol. 91, 1–10.
350 Yarchoan, R. and Uldrick, T. S. (**2018**) HIV-Associated Cancers and Related Diseases. N. Engl. J. Med. 378, 1029–1041.
351 Karim, S. S. A., Churchyard, G. J., Karim, Q. A. and Lawn, S. D. (**2009**) HIV infection and tuberculosis in South Africa: an urgent need to escalate the public health response. Lancet, Elsevier Ltd 374, 921–933.
352 Campbell, T. B., Borok, M., Gwanzura, L., MaWhinney, S., White, I. E., Ndemera, B., Gudza, I., Fitzpatrick, L. and Schooley, R. T. (**2000**) Relationship of human herpesvirus 8 peripheral blood virus load and Kaposi's sarcoma clinical stage. AIDS 14, 2109–2116.
353 Stebbing, J., Pantanowitz, L., Dayyani, F., Sullivan, R. J., Bower, M. and Dezube, B. J. (**2008**) HIV-associated multicentric Castleman's disease. Am. J. Hematol. 83, 498–503.
354 Davies, P. D. O. and Pai, M. (**2008**) The diagnosis and misdiagnosis of tuberculosis. Int. J. Tuberc. Lung Dis. 12, 1226–1234.
355 Malope, B. I., MacPhail, P., Mbisa, G., MacPhail, C., Stein, L., Ratshikhopha, E. M., Ndhlovu, L., Sitas, F. and Whitby, D. (**2008**) No evidence of sexual transmission of Kaposi's sarcoma herpes virus in a heterosexual South African population. AIDS 22, 519–526.
356 Butler, L. M., Were, W. A., Balinandi, S., Downing, R., Dollard, S., Neilands, T. B., Gupta, S., Rutherford, G. W. and Mermin, J. (**2011**) Human herpesvirus 8 infection in children and adults in a population-based study in rural Uganda. J. Infect. Dis. 203, 625–634.
357 Campbell, M. M. C. and Tishkoff, S. a. (**2008**) African genetic diversity: implications for human demographic history, modern human origins, and complex disease mapping. Annu. Rev. Genomics Hum. Genet. 9, 403–433.
358 Gomez, F., Hirbo, J. and Tishkoff, S. A. (**2014**) Genetic variation and adaptation in Africa : Implications for human evolution and disease. Cold Spring Harb Perspect Biol. 6, 1–21.
359 Begré, L., Rohner, E., Mbulaiteye, S. M., Egger, M. and Bohlius, J. (**2016**) Is human herpesvirus 8 infection more common in men than in women? Systematic review and meta-analysis. Int. J. Cancer 139, 776–783.
360 Shebl, F. M., Emmanuel, B., Bunts, L., Biryahwaho, B., Kiruthu, C., Huang, M.-L., Pfeiffer, R. M., Casper, C. and Mbulaiteye, S. M. (**2013**) Population-Based Assessment of Kaposi Sarcoma-Associated Herpesvirus DNA in Plasma Among Ugandans. J. Med. Virol. 85, 1602–1610.

7. Appendix

7.1. Solution recipes

1X PBS-Tween

8 g NaCl

0.2 g KCl

1.44 g Na_2HPO_4

0.24 g KH_2PO_4

2 ml Tween 20

pH 7.2, in 1 l dH_2O

1X SDS sample buffer

62.5 mM Tris-HCl pH 6.8

2% (w/v) SDS

10% (v/v) Glycerol

50 mM Dithiothreitol

0.01% (v/v) β-Mercaptoethanol

0.01% (w/v) Bromophenol Blue

10X Electrophoresis buffer

72 g Glycine

19 g Trisaminomethane

Up to 500 ml with dH_2O

1X Running buffer

50 ml 10X Electrophoresis buffer

10 ml 10% SDS

Up to 500 ml dH_2O

1X Transfer buffer

700 ml dH_2O

200 ml Methanol

100 ml 10X Electrophoresis buffer

Luria Bertani Agar

2.5 g Tryptone

1.25 g Yeast extract

2.5 g NaCl

3.75 g Agar

Luria Bertani media

5 g Tryptone

2.5 g Yeast extract

2.5 g NaCl

Up to 500 ml dH_2O

50X Tris-acetate-EDTA (TAE)

242 g Trisaminomethane

57.1 ml Glacial Acetic Acid

100 ml 0.5M EDTA (pH 8.0)

In 1 l dH_2O

KSHV ELISA Assay buffer

2.5% Bovine Serum Albumin (BSA)

2.5% Normal Donor Goat serum (Equitech-Bio cat# SG-0500)

0.005% Tween 20

0.005% Triton X-100 (3%)

In 1X PBS

KSHV ELISA Wash buffer

0.05% Tween 20

In 1X PBS

KSHV ELISA Stop buffer

3M NaOH

In dH_2O

MTT reagent

0.1 g MTT

20 ml 1X PBS

Flow cytometry block solution

5% BSA

5 mM EDTA

2 mM NaN_3

In 1X PBS

Flow cytometry wash solution

0.5% BSA

5 mM EDTA

2 mM NaN_3

In 1X PBS

Flow cytometry fix solution

0.5% BSA

1% Formaldehyde

5mM EDTA

2mM NaN_3

In 1X PBS

7.2. Plasmid maps

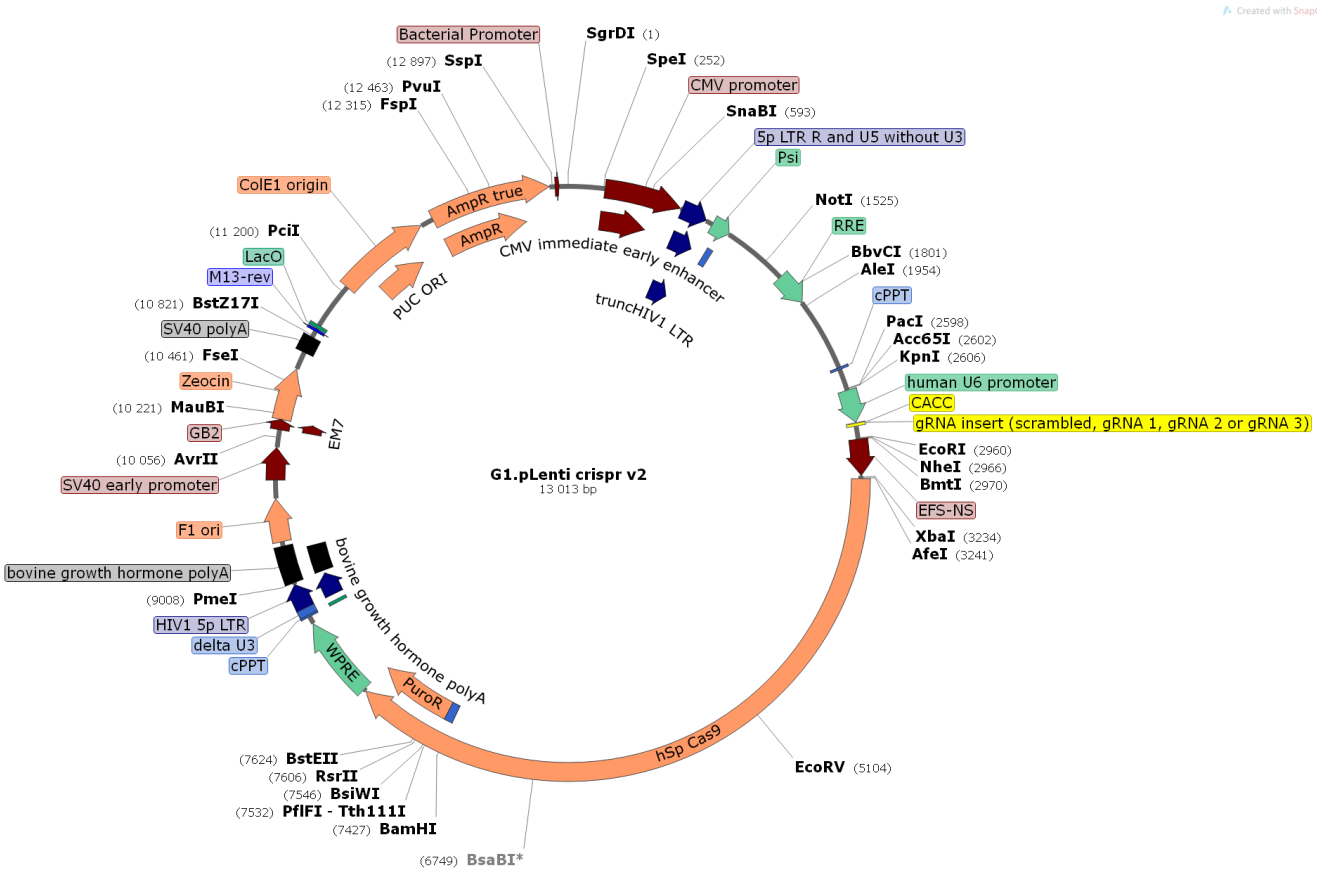

Supplementary figure 1: pLentiCRISPR v2 plasmid map. The plasmid was engineered to carry gRNA at the site indicated in yellow.

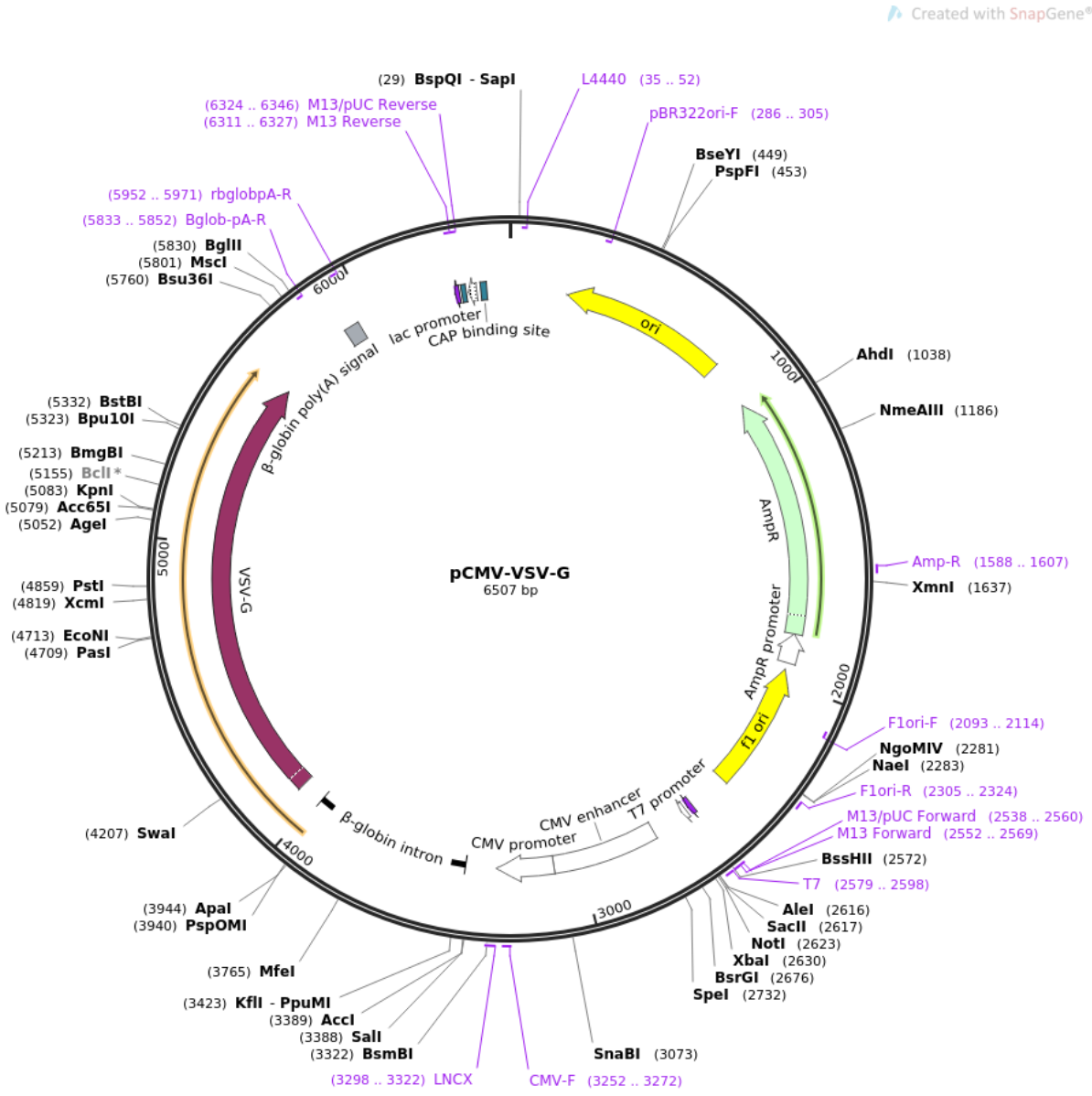

Supplementary figure 2: pCMV-VSV-G plasmid map.

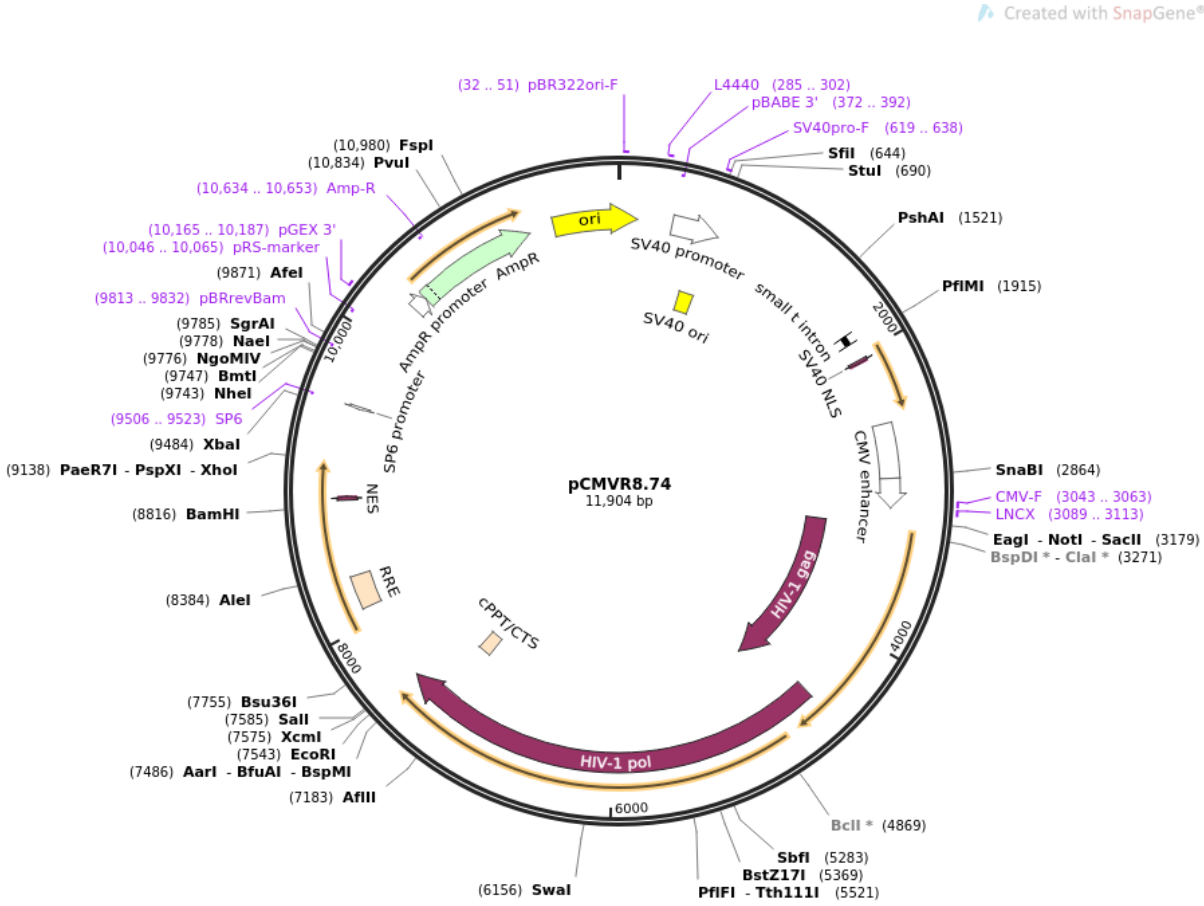

Supplementary figure 3: pCMVR8.74 plasmid map.

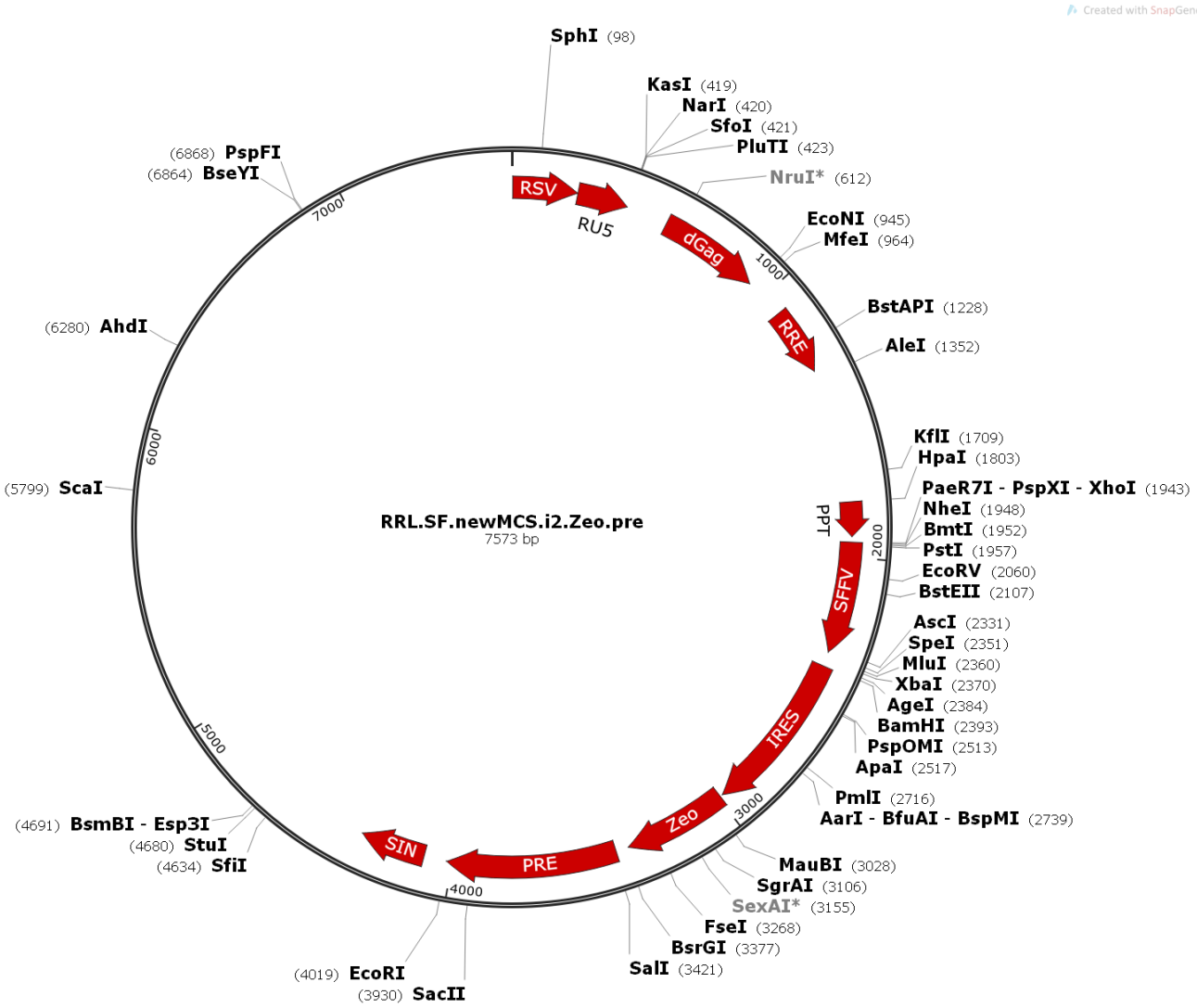

Supplementary figure 4: RRL.SF.newMCS.i2.Zeo.pre plasmid map.

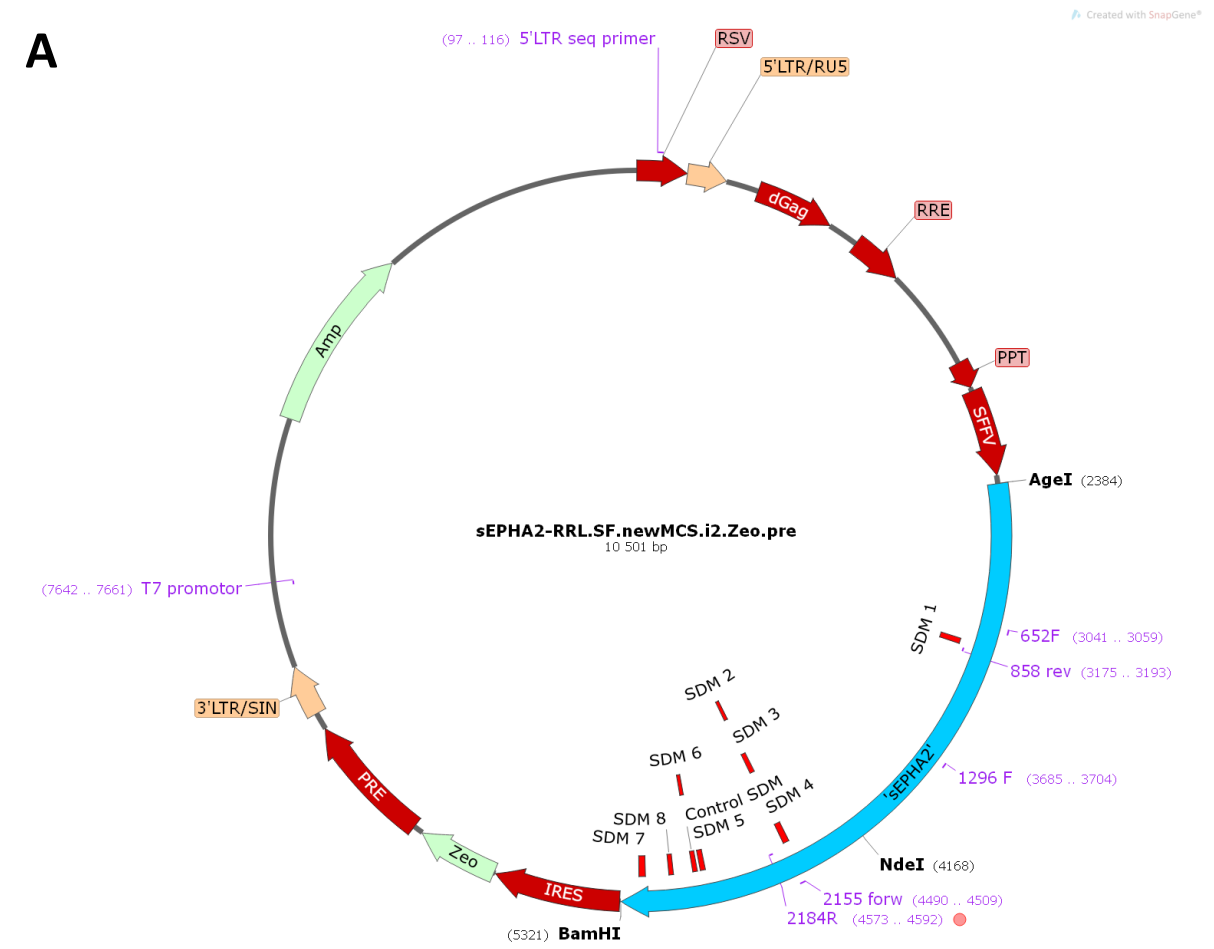

B

```
EPHA2 cdDNA          TGTGCAACGTGATGTCTGGCGACCAGGACAACTGGCTCCGCACCAACTGGGTGTACCGAGGAGAGGCTGAGCGTATCTTCATTGAGCTCAAGTTTACTGTACG
gRNA EPHA2 3         ....................                                                                                    
EPHA2 cdDNA mutated  ....................A.A..T..T.....A..TA....................................................................
```

Supplementary figure 5: Cloned sEPHA2-RRL-SF.newMCS.i2.Zeo.pre vector. A) Plasmid map showing the position of SDM primers indicated as red features; sequencing primers indicated in purple. **B)** Alignment indicating the silent mutations made to the gRNA 3 binding site in sEPHA2 compared to EPHA2 cDNA to avoid knockout by targeted CRISPR/Cas9.

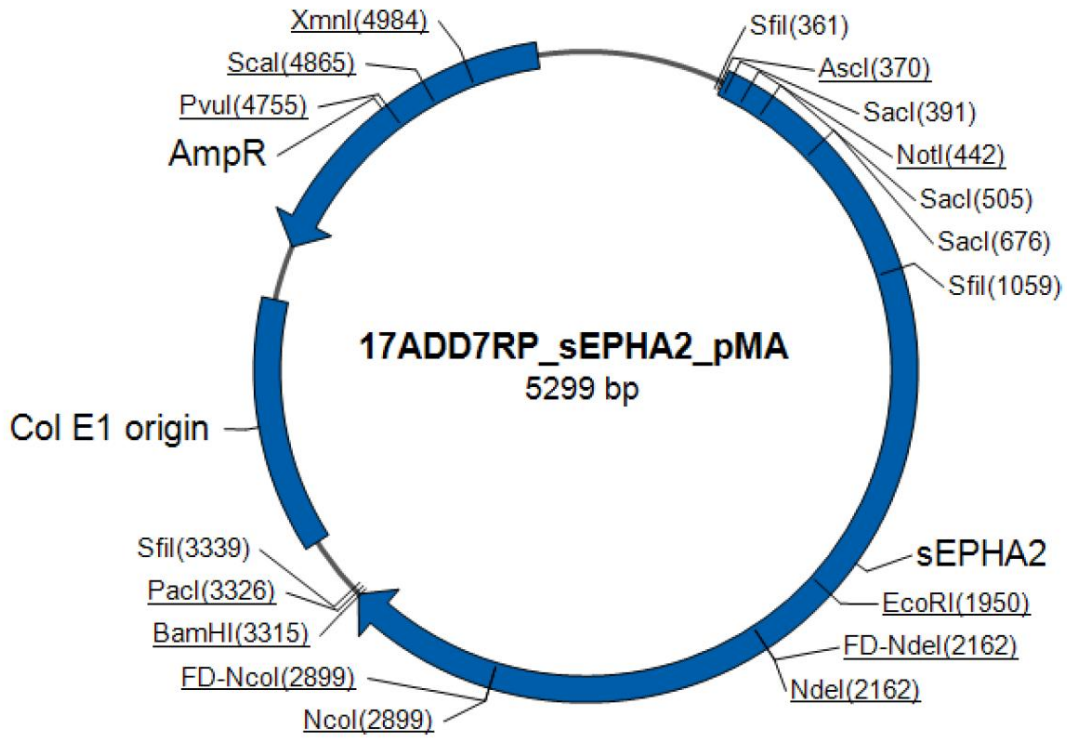

Supplementary figure 6: 177ADD7RP_sEPHA2_pMA plasmid map.

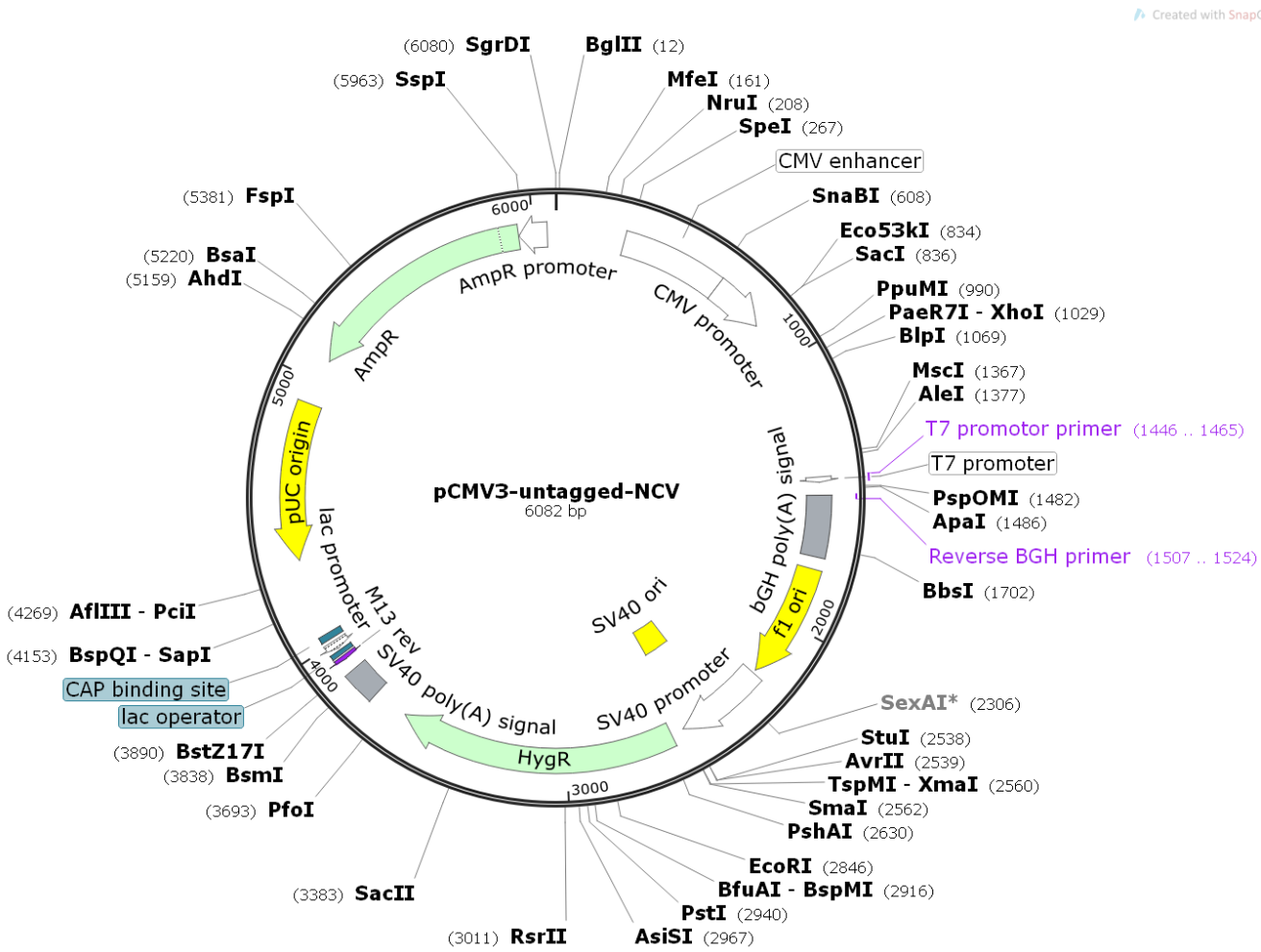

Supplementary figure 7: pCMV3-untagged negative control vector plasmid map.

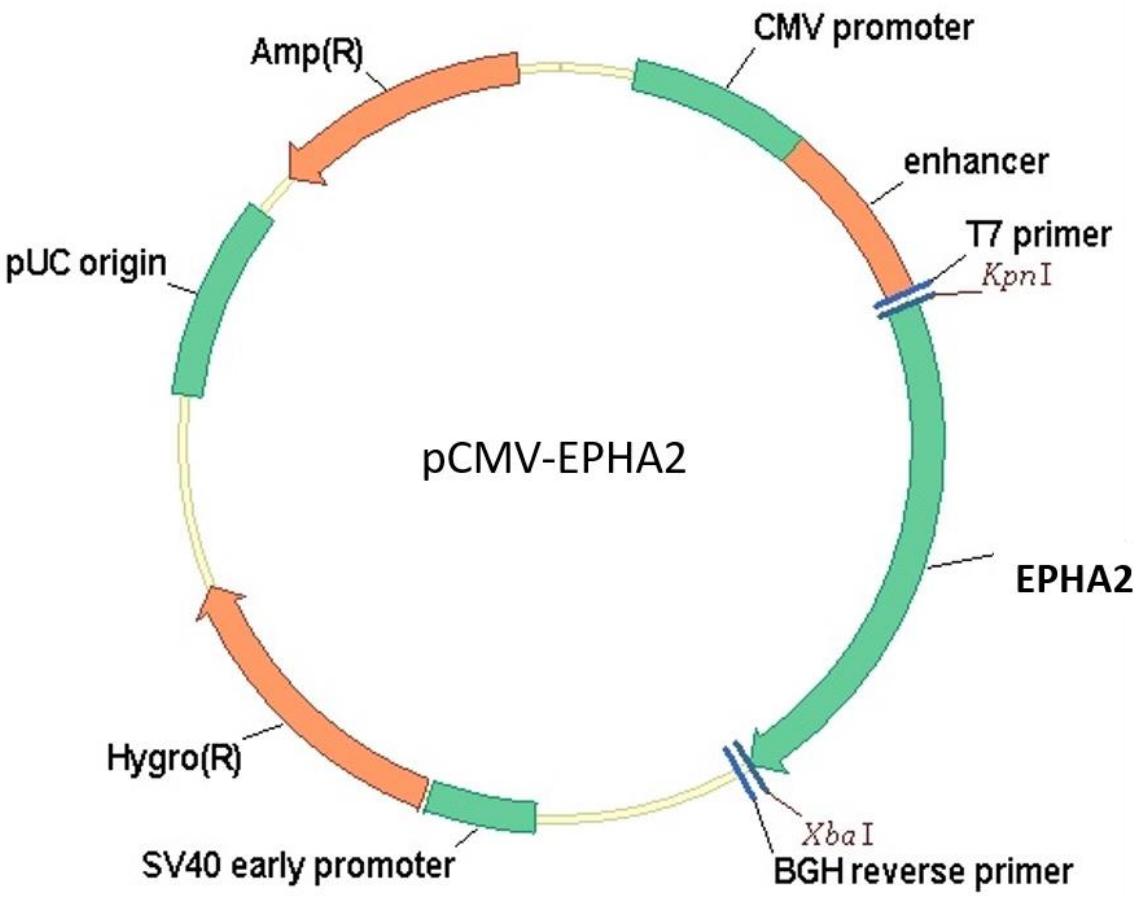

Supplementary figure 8: pCMV-EPHA2 plasmid map.

7.3. Additional material

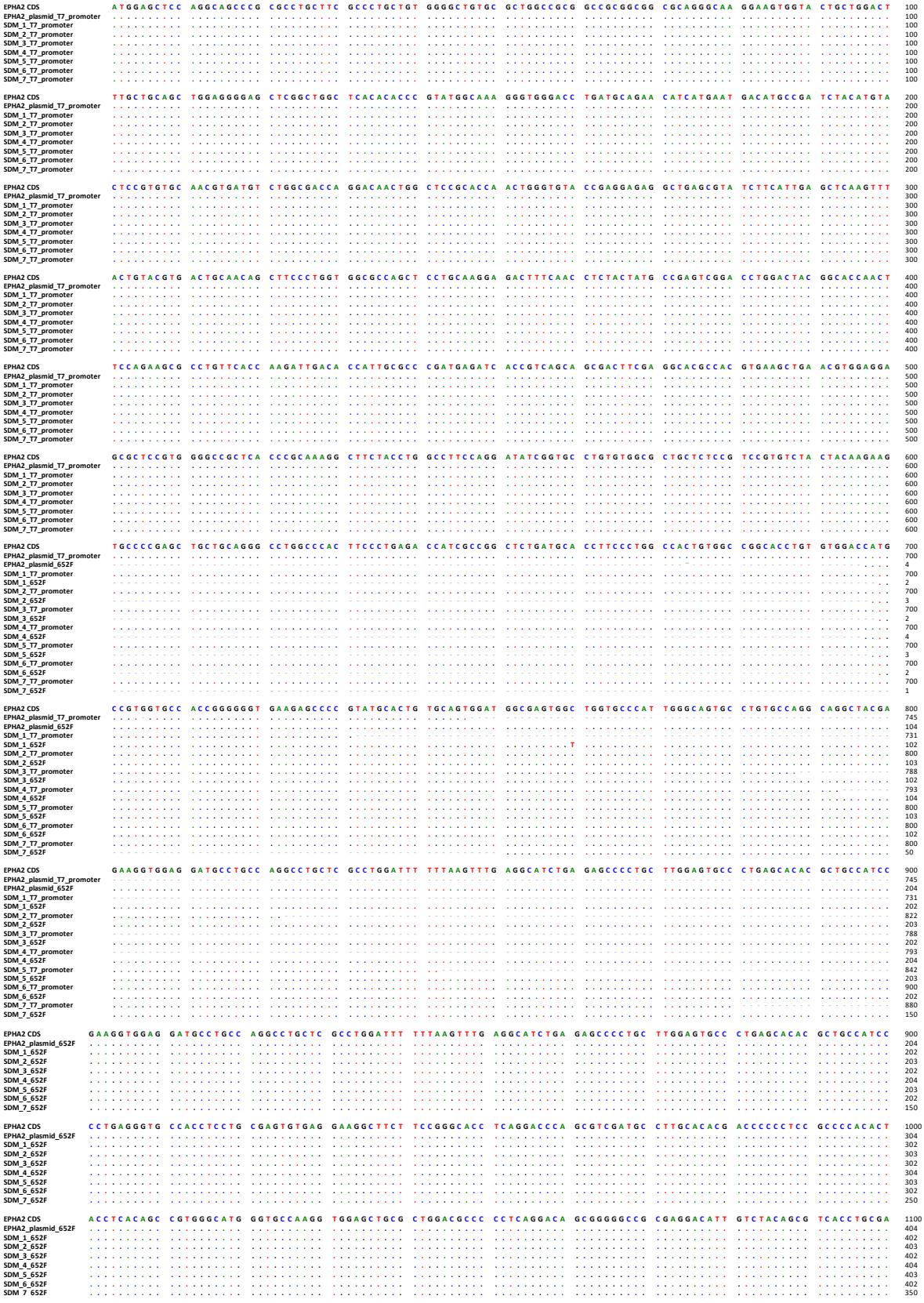

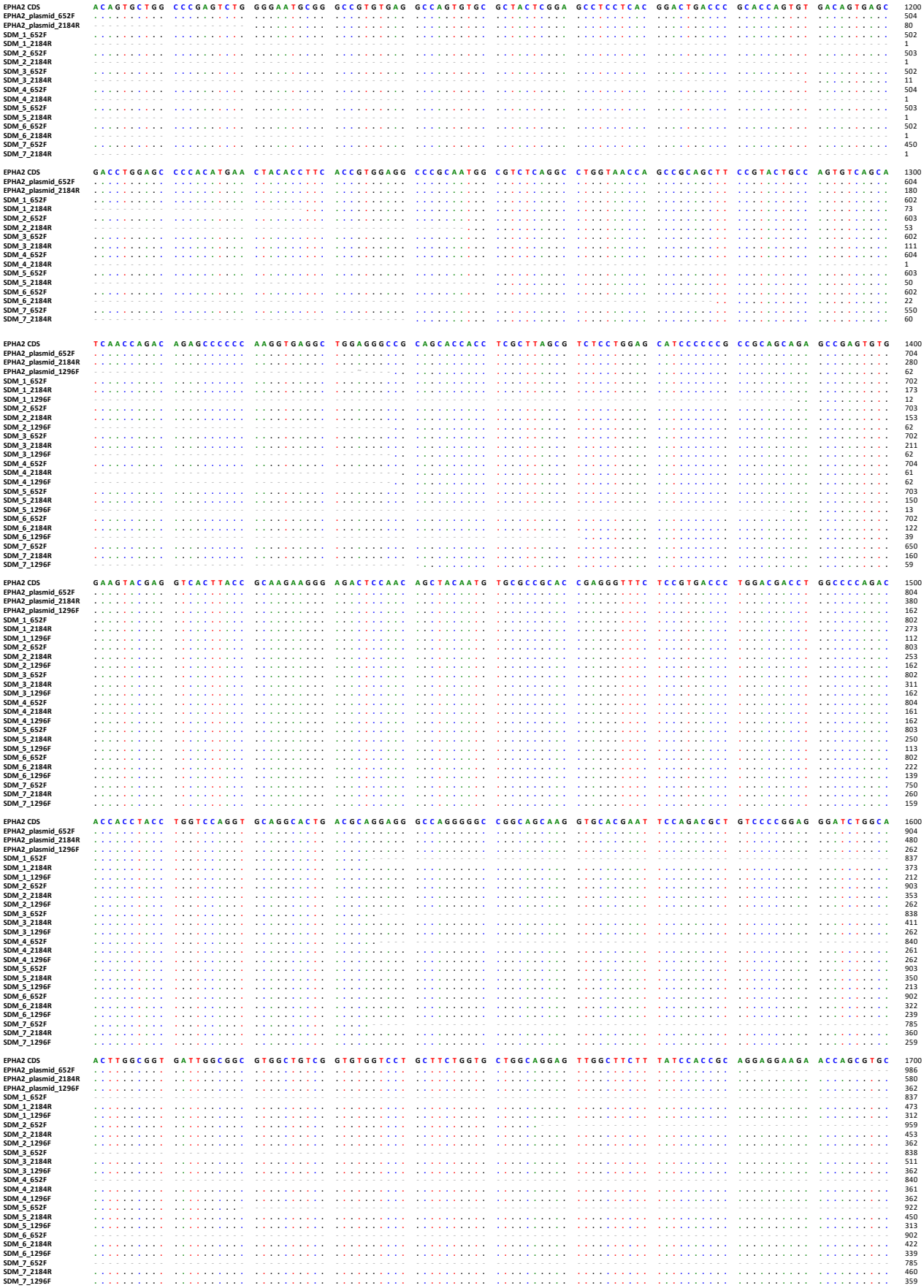
EPHA2 CDS
EPHA2_plasmid_652F
EPHA2_plasmid_2184R
EPHA2_plasmid_1296F
SDM_1_652F
SDM_1_2184R
SDM_1_1296F
SDM_2_652F
SDM_2_2184R
SDM_2_1296F
SDM_3_652F
SDM_3_2184R
SDM_3_1296F
SDM_4_652F
SDM_4_2184R
SDM_4_1296F
SDM_5_652F
SDM_5_2184R
SDM_5_1296F
SDM_6_652F
SDM_6_2184R
SDM_6_1296F
SDM_7_652F
SDM_7_2184R
SDM_7_1296F

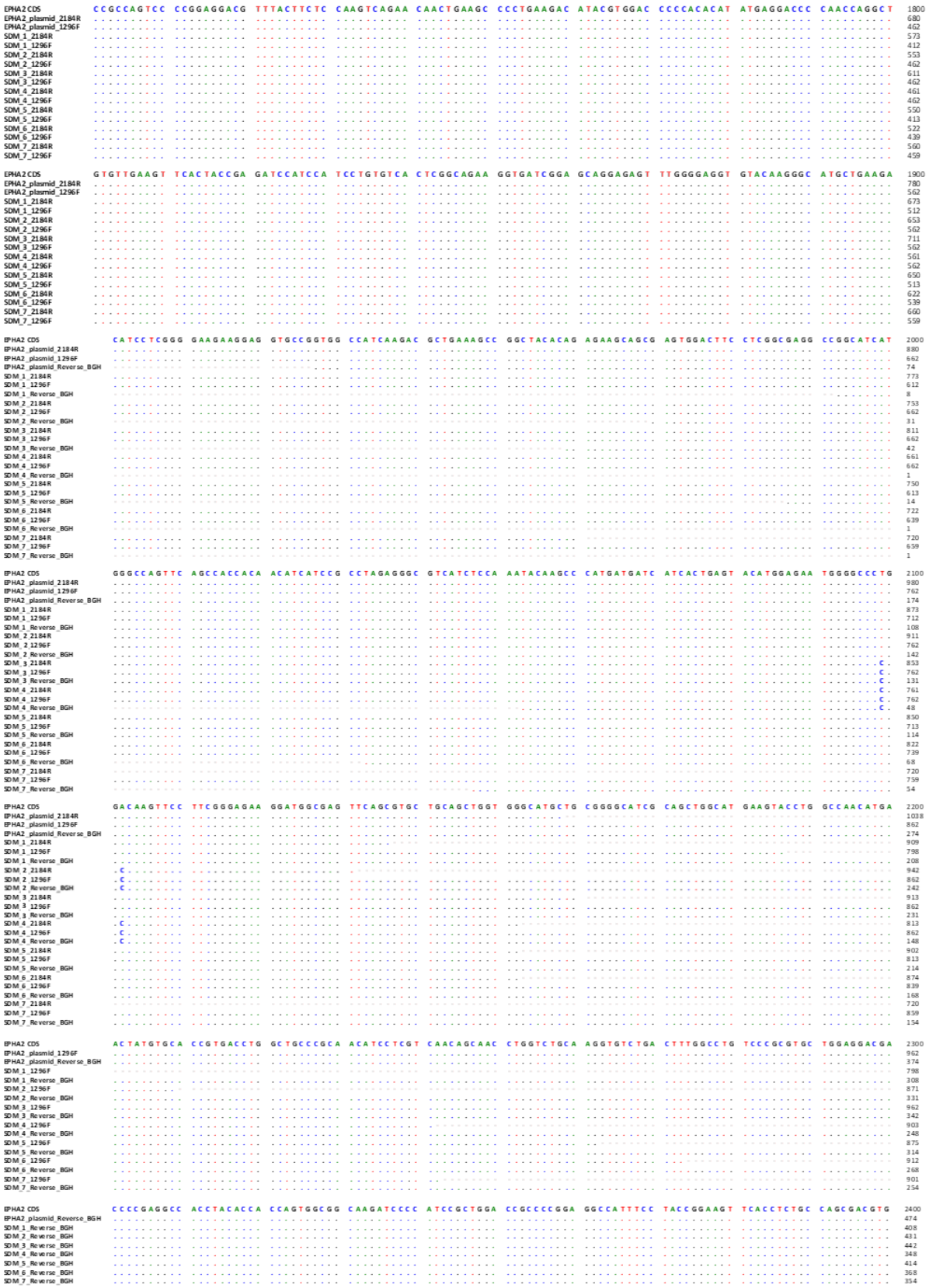

Supplementary figure 9: Sequence alignment of pCMV-EPHA2 WT and SDM vectors showing the integrity of the entire EPHA2 cDNA.

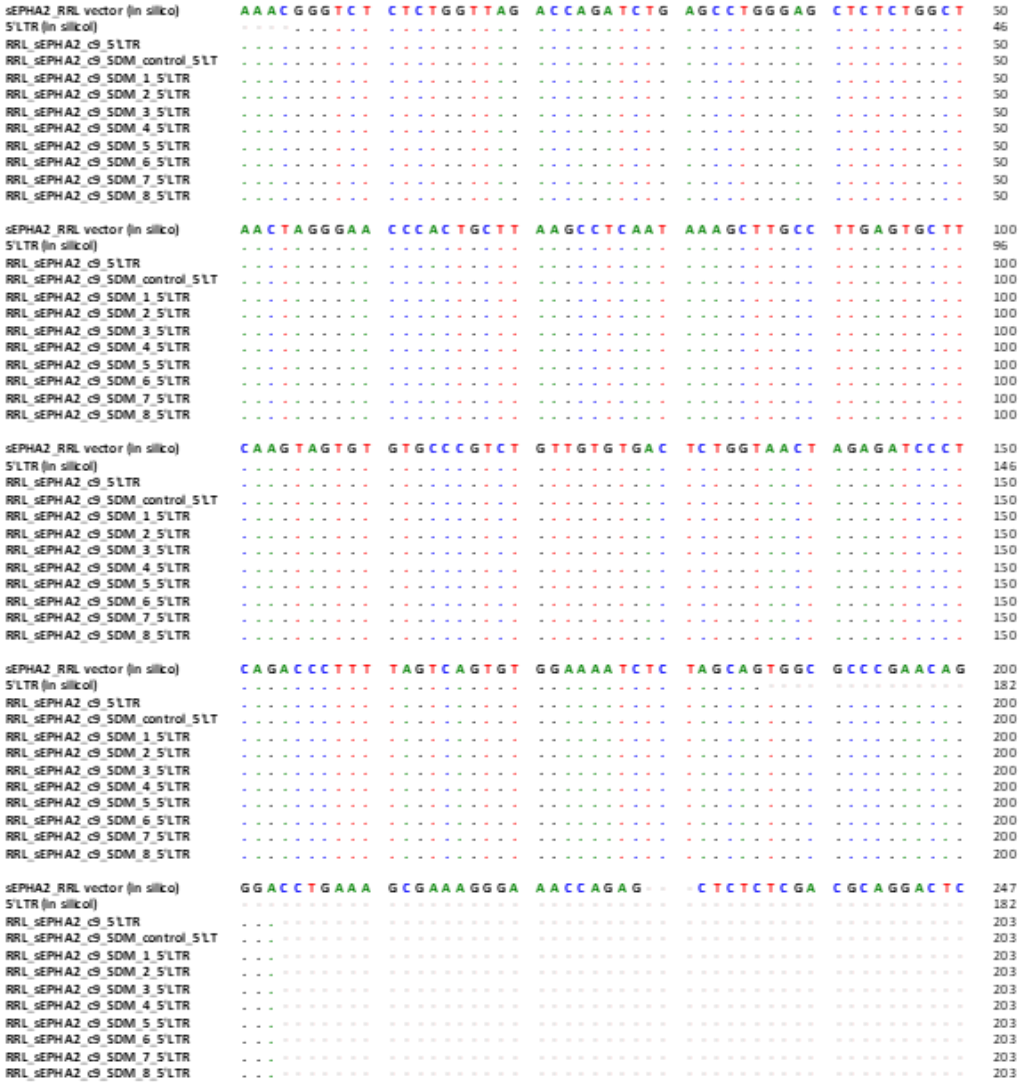

Supplementary figure 10: 5'LTR of the lentiviral vector is unchanged after undergoing SDM and transformation.

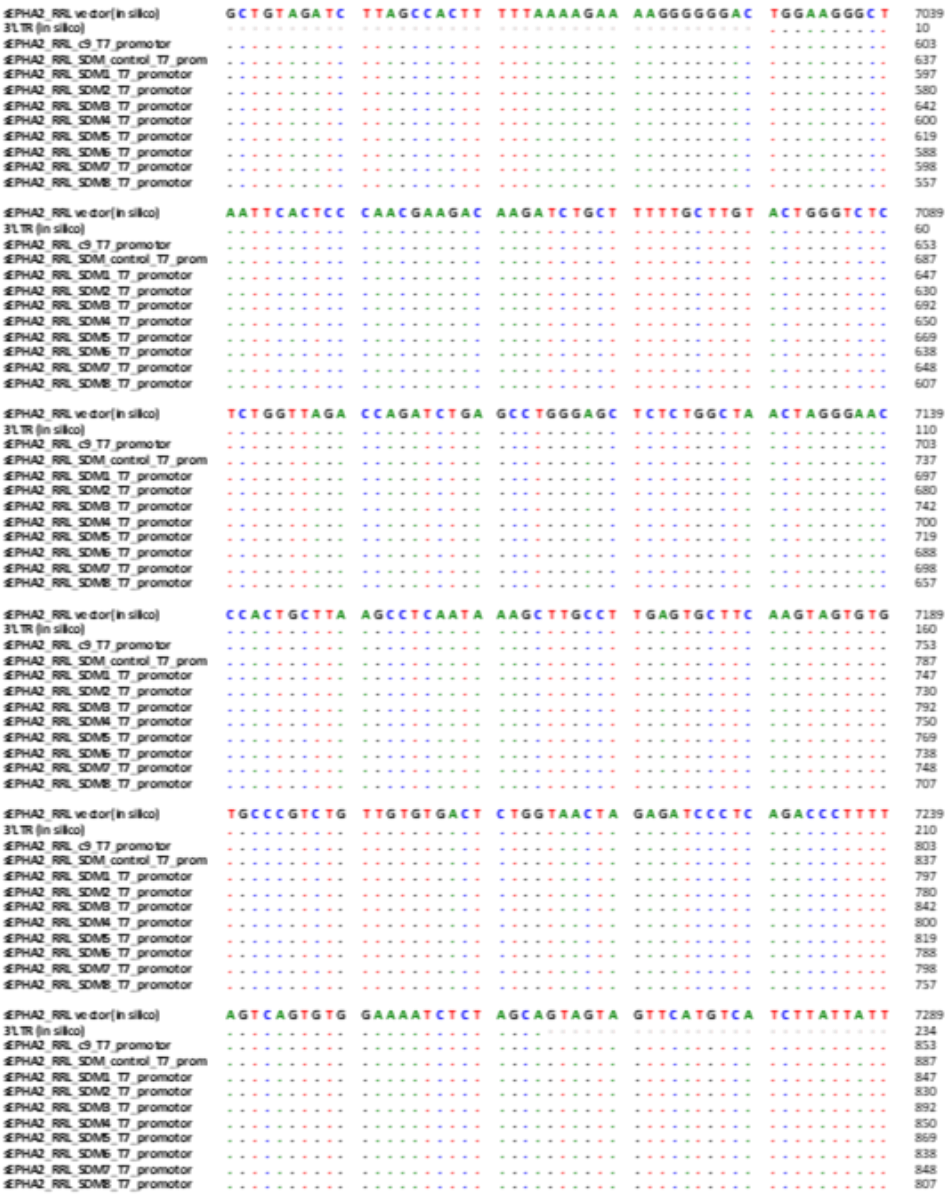

Supplementary figure 11: 3' LTR of the lentiviral vector is unchanged after undergoing SDM and transformation.

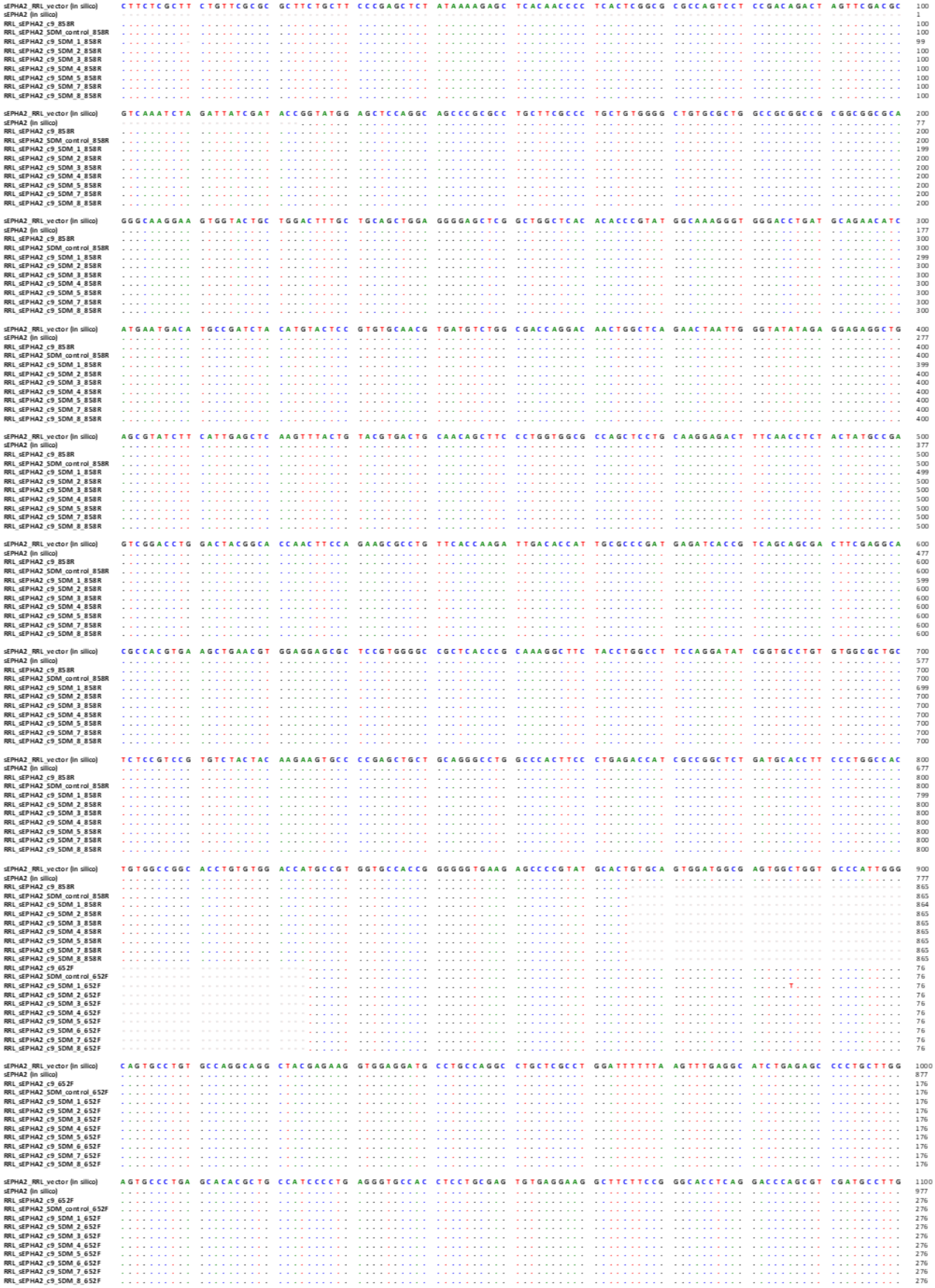
sEPHA2_RRL_vector (in silico)
sEPHA2 (in silico)
RRL_sEPHA2_c9_858R
RRL_sEPHA2_SDM_control_858R
RRL_sEPHA2_c9_SDM_1_858R
RRL_sEPHA2_c9_SDM_2_858R
RRL_sEPHA2_c9_SDM_3_858R
RRL_sEPHA2_c9_SDM_4_858R
RRL_sEPHA2_c9_SDM_5_858R
RRL_sEPHA2_c9_SDM_7_858R
RRL_sEPHA2_c9_SDM_8_858R
RRL_sEPHA2_SDM_control_652F
RRL_sEPHA2_c9_SDM_1_652F
RRL_sEPHA2_c9_SDM_2_652F
RRL_sEPHA2_c9_SDM_3_652F
RRL_sEPHA2_c9_SDM_4_652F
RRL_sEPHA2_c9_SDM_5_652F
RRL_sEPHA2_c9_SDM_6_652F
RRL_sEPHA2_c9_SDM_7_652F
RRL_sEPHA2_c9_SDM_8_652F

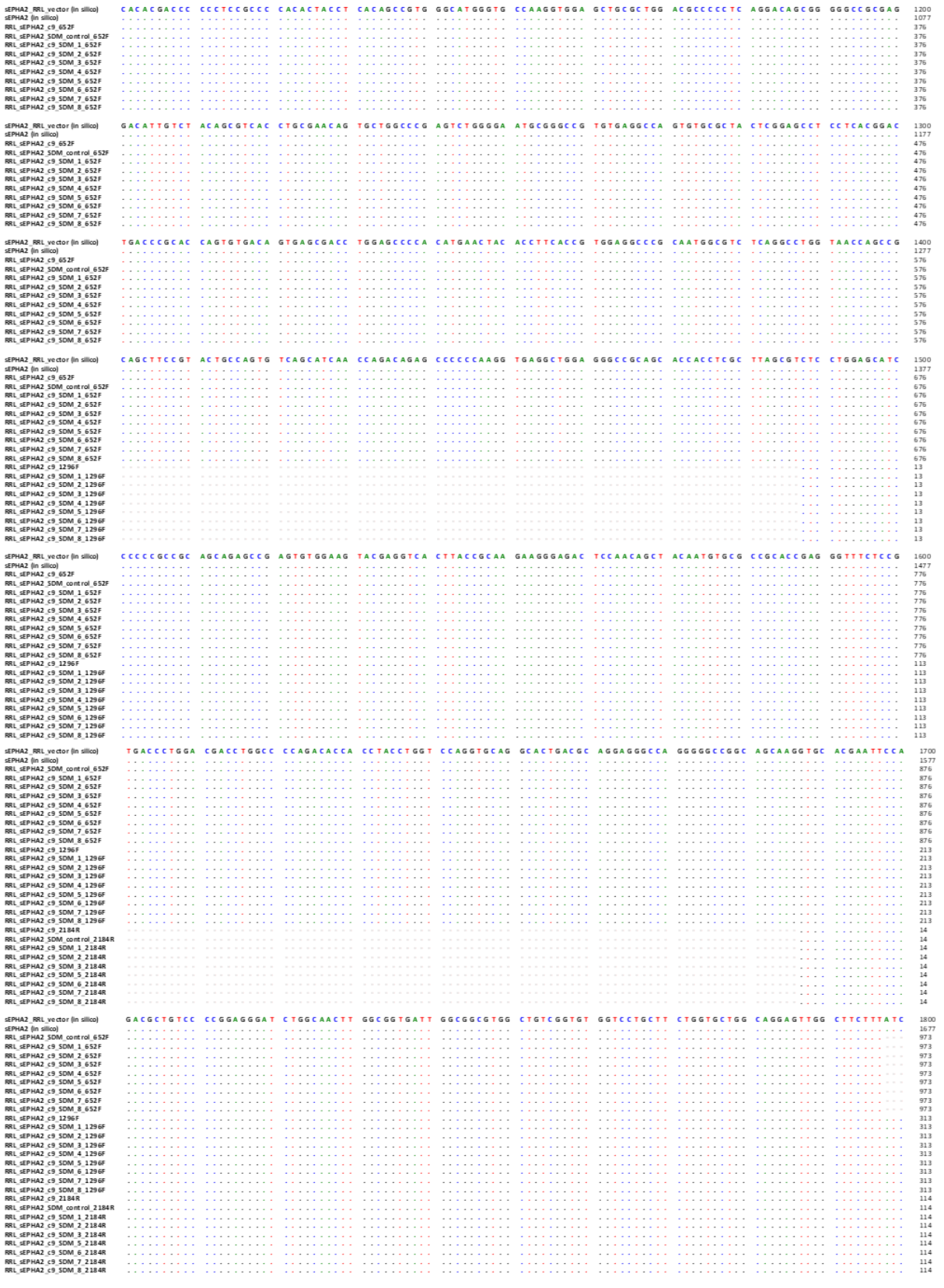
sEPHA2_RRL vector (in silico)
sEPHA2 (in silico)
RRL sEPHA2 c9 652F
RRL sEPHA2 SDM control 652F
RRL sEPHA2 c9 SDM 1 652F
RRL sEPHA2 c9 SDM 2 652F
RRL sEPHA2 c9 SDM 3 652F
RRL sEPHA2 c9 SDM 4 652F
RRL sEPHA2 c9 SDM 5 652F
RRL sEPHA2 c9 SDM 6 652F
RRL sEPHA2 c9 SDM 7 652F
RRL sEPHA2 c9 SDM 8 652F
RRL sEPHA2 c9 1296F
RRL sEPHA2 c9 SDM 1 1296F
RRL sEPHA2 c9 SDM 2 1296F
RRL sEPHA2 c9 SDM 3 1296F
RRL sEPHA2 c9 SDM 4 1296F
RRL sEPHA2 c9 SDM 5 1296F
RRL sEPHA2 c9 SDM 6 1296F
RRL sEPHA2 c9 SDM 7 1296F
RRL sEPHA2 c9 SDM 8 1296F
RRL sEPHA2 c9 2184R
RRL sEPHA2 SDM control 2184R
RRL sEPHA2 c9 SDM 1 2184R
RRL sEPHA2 c9 SDM 2 2184R
RRL sEPHA2 c9 SDM 3 2184R
RRL sEPHA2 c9 SDM 5 2184R
RRL sEPHA2 c9 SDM 6 2184R
RRL sEPHA2 c9 SDM 7 2184R
RRL sEPHA2 c9 SDM 8 2184R

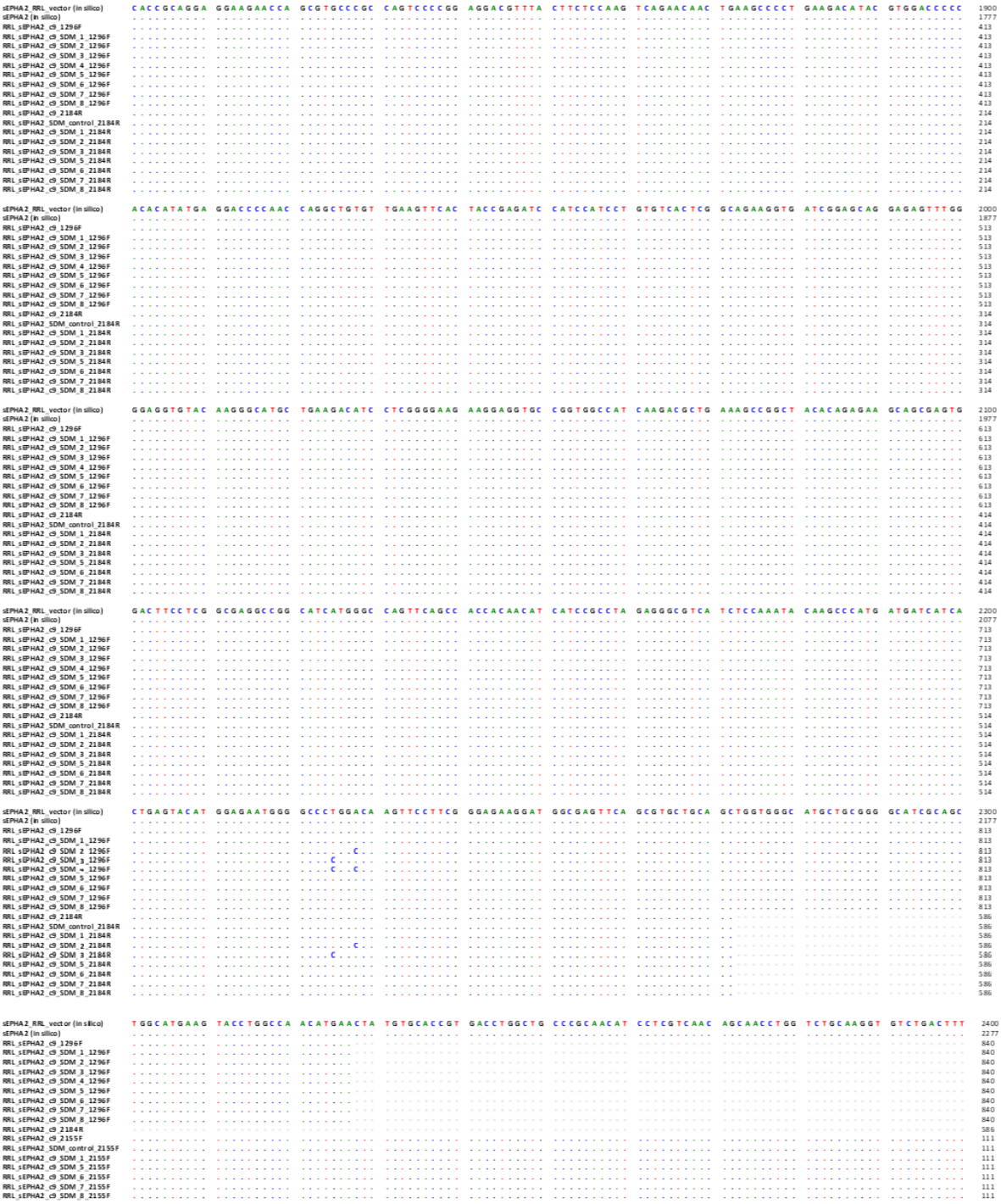

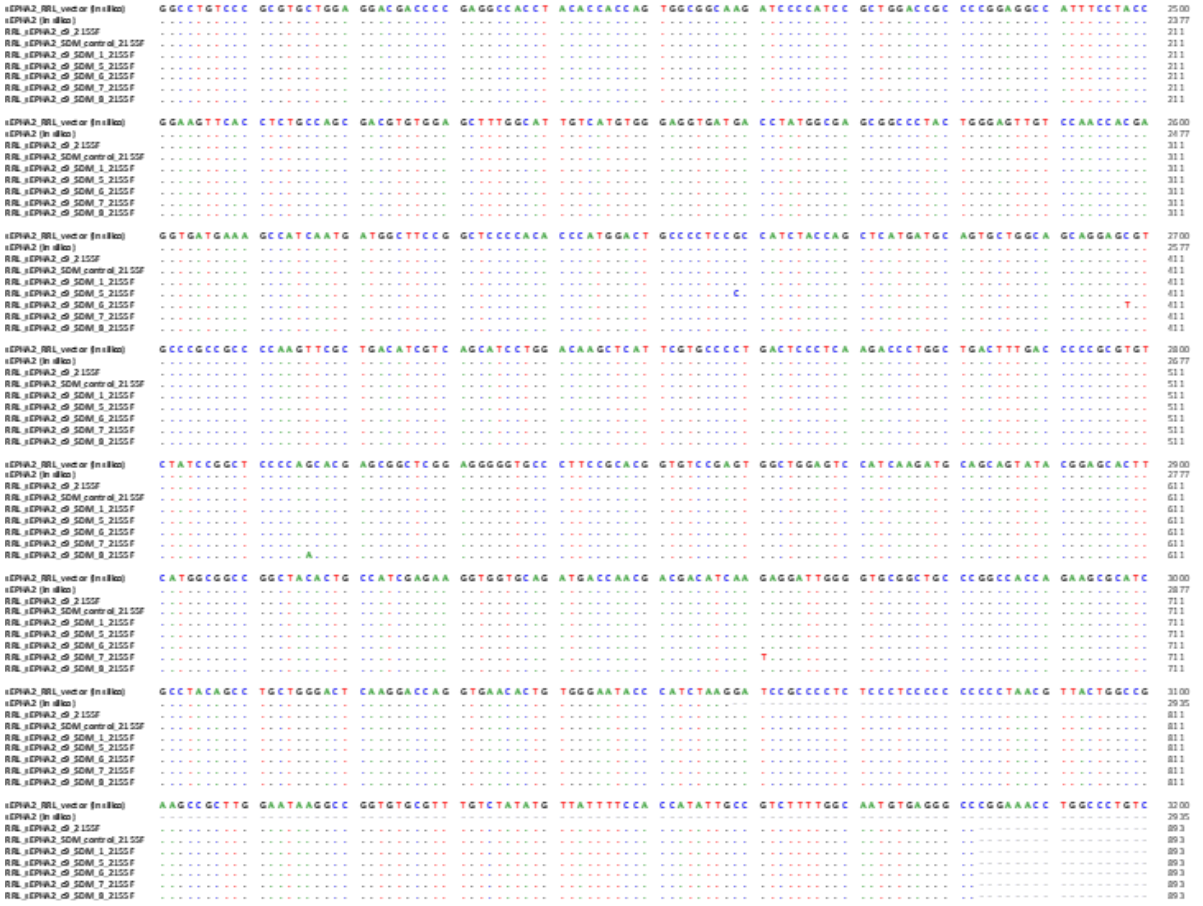

Supplementary figure 12: EPHA2 cDNA of lentiviral vectors showing SDM-introduced mutants while there were no undesired changes to the EPHA2 cDNA sequence.

Supplementary table 1: Associations between EPHA2 SNVs and KSHV (n=150). Ambiguous base notations represent heterozygous variants. N=number of cases.

SNV	KSHV- N(%)	KSHV+ N(%)	OR (95% CI)	p	adj. p	MAF
C2727Y	2 (4%)	21 (21%)	6.4 (1.4, 28.4)	0.007	0.028	0.077
G2990K	2 (4%)	9 (9%)	2.4 (0.5, 11.4)	0.338	1	0.037
A2217M	2 (4%)	7 (7%)	1.8 (0.4, 9)	0.718	1	0.03
T2047Y	7 (14%)	12 (12%)	0.8 (0.3, 2.3)	0.796	1	0.067

Supplementary table 2: Associations between EPHA2 SNVs and KS (n=100). Ambiguous base notations represent heterozygous variants. N=number of cases.

SNV	KS- N(%)	KS+ N(%)	OR (95% CI)	p	adj. p	MAF
G2990K	0 (0%)	9 (18%)	1.2 (1.1, 1.4)	0.003	0.021	0.045
T2254Y	0 (0%)	8 (16%)	1.2 (1.1, 1.3)	0.006	0.04	0.04
G2688S	0 (0%)	6 (12%)	1.1 (1.0, 1.3)	0.027	0.16	0.03
C2727Y	7 (14%)	14 (28%)	2.4 (0.9, 6.6)	0.14	0.698	0.105
G2325S	1 (2%)	5 (10%)	5.4 (0.6, 48.4)	0.204	0.818	0.03
A2217M	5 (10%)	2 (4%)	0.4 (0.1, 2)	0.436	1	0.035
C915S	5 (10%)	2 (4%)	0.4 (0.1, 2)	0.436	1	0.035
T2047Y	5 (10%)	7 (14%)	1.5 (0.4, 5)	0.76	1	0.065

Supplementary table 3: EPHA2 SNVs and KSHV VL (n=100). Ambiguous base notations represent heterozygous variants. N=number of cases.

SNV	KSHV VL- N(%)	KSHV VL+ N(%)	OR (95% CI)	P	adj. p	MAF
G2990K	1 (2%)	8 (18%)	11.7 (1.4, 97.3)	0.01	0.08	0.05
T2254Y	2 (4%)	6 (13%)	4.1 (0.8, 21.3)	0.135	1	0.04
G2688S	2 (4%)	4 (9%)	2.6 (0.5, 14.8)	0.404	1	0.03
C2727Y	10 (18%)	11 (24%)	1.5 (0.6, 3.8)	0.469	1	0.11
G2325S	3 (6%)	3 (7%)	1.2 (0.2, 6.5)	1	1	0.03
A2217M	5 (9%)	2 (4%)	0.6 (0.1, 2.5)	0.453	1	0.04
T2047Y	8 (15%)	4 (9%)	0.6 (0.2, 2.0)	0.539	1	0.06
C915S	5 (9%)	2 (4%)	0.47 (0.1, 2.5)	0.453	1	0.04

Supplementary table 4: Overview of identified EPHA2 variants in the Pkinase-Tyr and SAM domains in the entire cohort. Variants found to be statistically associated with KS development, KSHV susceptibility and/or detectable KSHV VL are indicated in yellow.

mRNA position	Change (zygosity)	Group 1 (KS+/KSHV+)		Group 2 (KS-/KSHV+)		Group 3 (KS-/KSHV-)		Validation Group 1 (KS+/KSHV+)		Validation Group 2 (KS-/KSHV+)		Validation Group 3 (KS-/KSHV-)
2217	A>C (Het)	2	KS025, KS029	5	MB005, MB007, MB008, MB009, MB011	2	MB006, MB010	1	KS059	0		0
2218	T>C (Het)	1	KS025	0		0		0		0		0
2254	T>C (Het)	8	KS022, KS023, KS024, KS025, KS026, KS027, KS028, KS029	0		0		0		0		0
2257	A>C (Het)	9	KS022, KS023, KS024, KS025, KS026, KS027, KS028, KS029, KS040	0		0		0		0		0
2269	G>A (Het)	0		0		0		8	KS052, KS053, KS058, KS059, KS060, KS062, KS063, KS064	0		0
2325	G>C (Het)	5	KS014, KS015, KS-017, KS018, KS-021	1	TB033	0		0		0		0
2369	T>G (Het)	0		0		0		2	KS052, KS053	1	TB112	0
2394	G>A (Het)	0		0		0		1	KS057	0		0
2397	A>C (Het)	3	KS013, KS014, KS-015	0		0		0		0		0
2412	T>A (Het)	0		0		0		4	KS087, KS091, KS092, KS094	0		0

2472	A>C (Het)	3	KS020, KS045, KS-046	1	TB033	1	TB061	0		0		0	
2478	A>G (Het)	0		0		0		2	KS069, KS070	11	TB140, TB171, TB185, TB201, TB204, TB216, TB223, TB236, TB237, TB240, TB265	9	TB118, TB109, TB116, TB119, TB123, TB125, TB139, TB146, TB147
2507	C>T (Het)	1	KS001	0		2	TB044, MB032	2	KS078, KS091	3	TB172, TB178, TB192	2	TB89, TB149
2529	C>A (Het)	1	KS028	0		1	TB052	0		2	TB154, TB203	1	TB082
2603	G>C (Het)	1	KS001	0		0		0		1	TB112	2	TB083, TB118
2627	C>T (Het)	3	KS013, KS042, KS-043	3	TB070, TB086, MB011	5	TB052, TB069, TB011, TB102, MB001	3	KS056, KS067, KS069, KS091	4	TB042, TB097, TB192, TB223,	0	
2669	A>G (Het)	7	KS008, KS010, K-S015, KS023, KS-029, KS038, KS-047	5	TB033, TB070, TB-088, TB105, MB026	7	TB004, TB027, TB-045, TB046, TB048, MB004, MB032	7	KS053, KS061, KS070, KS072, KS073, KS097*	12	TB060, TB087, TB117, TB128, TB133, TB134, TB172, TB192, TB215, TB216, TB254, TB259,	13	TB032, TB083, TB090, TB124, TB125, TB126, TB129, TB132, TB135, TB136, TB144, TB145, TB149
	A>G (Hom)	0		0		0		1	KS068	0		0	
2688	G>C (Het)	6	KS015, KS016, KS-017, KS018, KS-020, KS021	0		0		1	KS086	0		1	TB136
2709	C>A (Het)	0		0		0		3	KS051, KS058, KS059	0		0	
2727	C>T (Het)	14	KS017, KS018, KS-021, KS022, KS-023, KS024, KS-025, KS020, KS-	7	TB078, TB088, MB009, MB013, MB015, MB024, MB027	2	MB030, MB035	7	KS052, KS053, KS058, KS059, KS063, KS062, KS067,	0		0	

			015, KS016, KS-014, KS026, KS-027, KS029										
2737	G>C (Het)	0		0		0		5	KS063, KS060, KS059, KS058, KS052	1	TB128	2	TB136, TB056
2859	G>A (Het)	3	KS014, KS046, KS-050	0		0		0		0		0	
2990	G>T (Het)	9	KS003, KS014, KS020, KS029, KS033, KS035, KS036, KS043, MB002	0		2	TB013, MB004	0		0		0	
3029	C>T (Het)	13	KS004, KS006, KS-009, KS012, KS-016, KS017, KS-024, KS027, KS-034, KS035, KS-040, KS041, KS-050	20	TB008, TB010, TB014, TB015, TB-039, TB041, TB-063, TB071, TB-078, TB079, TB-080, TB088, TB095, TB099, TB-103, MB005, MB-007, MB024, MB-025, MB029	20	TB002, TB004, TB 006, TB017, TB-022, TB023, TB-030, TB044, TB-076, TB065, TB-069, TB098, TB-100, TB102, MB-006, MB018, MB-028, MB030, MB-032, MB036	1	KS097*	0		0	
	C>T (Hom)	2	KS005, KS047	4	TB028, TB033, MB020, MB027	11	TB019, TB027, TB-031, TB035, TB-052, TB061, TB-064, TB046, MB-022, MB031, MB-034	2	KS058, KS092,	0		0	
3030	G>C (Het)	0		1	KDHTB020	0		0		0		0	

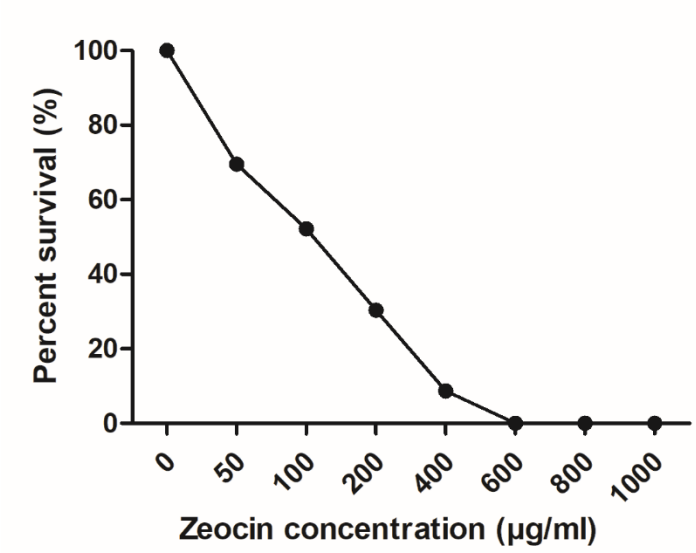

Supplementary figure 13: Zeocin sensitivity curve for HuARLT2 cells. Cells were treated with the indicated concentrations of zeocin for 10 days at which point live cells were counted after staining with trypan blue and presented as a percentage of the number of live, untreated cells.

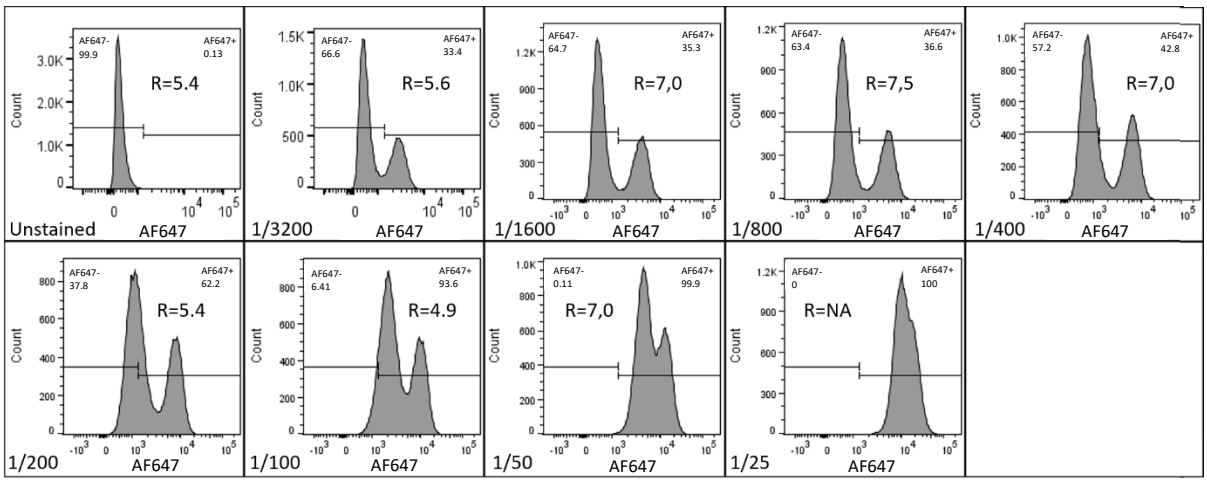

Supplementary figure 14: Secondary antibody titration with a mixture of Hu-KO (EPHA2-negative) and Hu-WT (EPHA2-positive) cells.

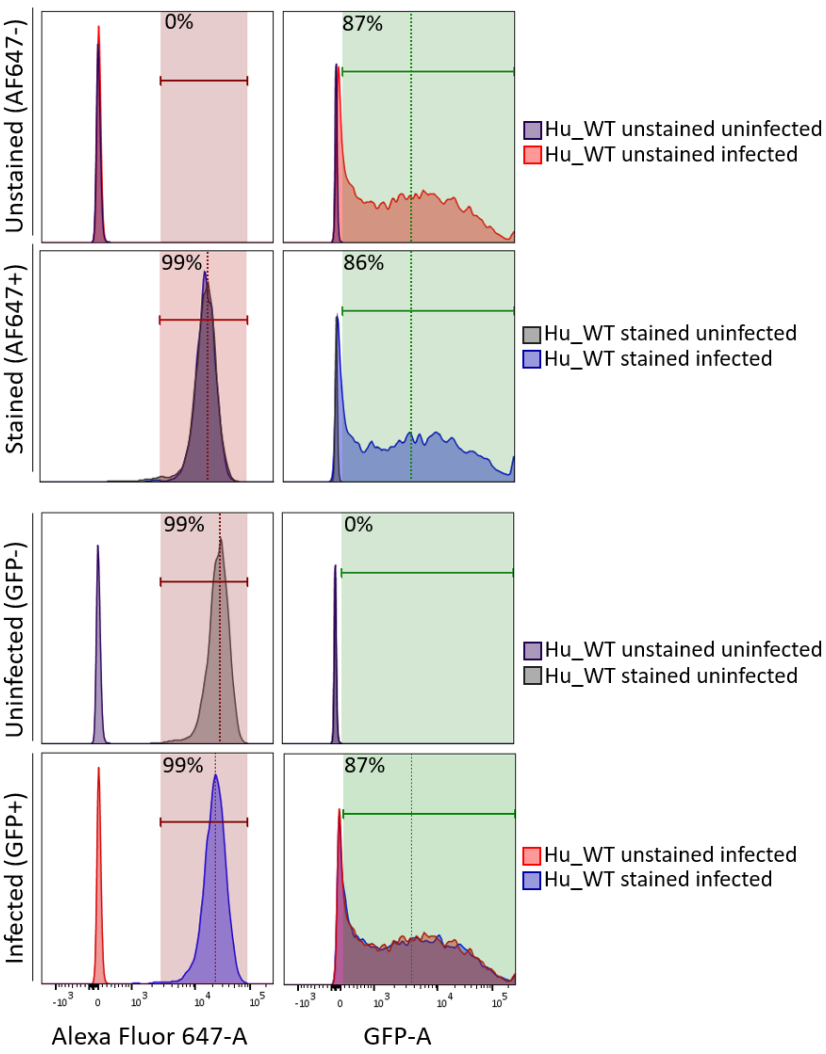

Supplementary figure 15: Compensation study to detect GFP and AF647. Detection of GFP does not change when co-stained for AF647 and vice versa therefore compensation is not required when using the two channels.